The Dissertation Committee for Abhishek Kumar Gupta
certifies that this is the approved version of the following dissertation:

Association and Spectrum Sharing in Cellular Networks

Committee:

Jeffrey G. Andrews, Supervisor

Robert W. Heath Jr, Supervisor

François Baccelli

Sanjay Shakkottai

Haris Vikalo

Eugene Visotsky

Association and Spectrum Sharing in Cellular Networks

by

Abhishek Kumar Gupta, B.Tech. M.Tech.

DISSERTATION

Presented to the Faculty of the Graduate School of

The University of Texas at Austin

in Partial Fulfillment

of the Requirements

for the Degree of

DOCTOR OF PHILOSOPHY

THE UNIVERSITY OF TEXAS AT AUSTIN

December 2016

Dedicated to my parents and family.

Acknowledgments

I would first like to express my gratitude to my dissertation advisors Prof. Jeffrey G. Andrews and Prof. Robert W. Heath Jr for their invaluable guidance and support. Working with them has been a wonderful experience for many reasons. Their help at each step of my PhD whether in formulating meaningful research problems or in providing me technical inputs when I got stuck, was very crucial for me throughout my stay here. I learnt how to write and present my ideas effectively from their comments and feedback. Moreover, they taught me how to be a good advisor and how to treat the students by providing me the most ideal experience.

I would also like to thank my committee members Prof. François Baccelli, Prof. Sanjay Shakkottai, Prof. Haris Vikalo and Dr. Eugene Visotsky for their insightful comments and discussions. I would like to take this opportunity to thank Prof. Sanjay Shakkottai for supporting me at all times and for being a great teacher to me. During my stay in Wireless Networking and Communications Group (WNCG), I have been fortunate to foster collaboration with some wonderful researchers. My special thanks to Prof. Harpreet S. Dhillon for being a mentor and motivator. His guidance was invaluable in getting me started with my graduate research. I would like to thank my collaborators Somsubhra Barik, Mandar Kulkarni, Ahmed Alkhateeb, Dr. Xinchen Zhang, Dr. Tianyang Bai for the countless discussions we have had on various topics.

I thank Cockrell school of engineering at UT Austin and National Science Foundation (NSF) grant CIF- 1514275 for supporting my research. I was also fortunate to gain some useful industry experience during my stay here. I would like to thank Dr. Leonard Piazzi for hosting me at Huawei Technologies, NJ, during summer 2013 and 2014. I would like to thank Dr. Amitava Ghosh and Dr. Eugene Visotsky for hosting me at Nokia Networks, IL, during summer 2015. I would like to thank Dr. Arunabha Ghosh at AT&T Research, TX for providing various valuable inputs throughout my mmWave spectrum sharing work.

My stay at UT would not have been so memorable without the friends that I have made along the way. I would like to thank Somsubhra, Ananya, Harpreet, Ahmed, Saumik and Rebal for being great friends and keeping me sane. I would like to thank my WNCG colleagues Deepjyoti, Talha, Ankit, Sarabjot, Mandar , Kiran, Mohammed, Amir, Jianhua, Anam, Derya, Yingzhe, Preeti for some wonderful discussions. I take this opportunity to thank Melanie Gulick from ECE office, and Karen Little from WNCG office, for taking care of all the paperwork and other logistics.

I will never be able to thank my family enough. I would like to dedicate my dissertation to my parents Sri Basant Prasad and Smt. Damayanti Gupta for their unconditional love and support. Their high values and emphasis on simple life and quality education have shaped me. I also thank my sisters Rashmi, Gunjan and Sonali Di and their significant ones for always being there for me.

Association and Spectrum Sharing in Cellular Networks

Publication No. _____

Abhishek Kumar Gupta, Ph.D.
The University of Texas at Austin, 2016

Supervisors: Jeffrey G. Andrews
Robert W. Heath Jr

Many models have been proposed to evaluate performance of cellular communication systems. However, the emergence of new technologies have changed cellular systems significantly, and requires new modeling and analysis approaches. This dissertation studies network level optimization concerning cell association and spectrum sharing. As the first contribution, the dissertation presents a framework to investigate downlink multi-antenna heterogeneous networks with flexible cell selection and shows that a simple selection bias-based cell selection criterion closely approximates more complex selection rules to maximize mean the signal-to-interference-plus-noise-ratio (SINR). Under this simpler cell selection rule, the exact expressions for coverage probability and achievable rate of a typical user are derived along with an approximation of the coverage optimal cell selection bias. In the second contribution, the dissertation considers a cellular system where users are simultaneously connected to multiple base stations (BSs) to decrease blockage sensitivity and proposes a framework to analyze the correlation in blocking among multiple links. It evaluates the

gains of macro-diversity in the presence of random blockages along with the impact of the blockage size.

In the third contribution, the dissertation considers spectrum sharing among millimeter wave (mmWave) operators. A two-level architecture is proposed to model a mmWave multi-operator system and the SINR and per-user rate distribution are derived in the presence of spectrum and infrastructure sharing. It is shown that due to narrow beams, license sharing among operators improves system performance by increasing the per-user rate, even when there is no explicit coordination. In the fourth contribution, this analysis is extended to include static coordination among operators in the form of secondary licensing. A framework is developed to model a mmWave cellular system with a primary operator that has an "exclusive-use" license with a provision to sell a restricted secondary license to another operator that has a maximum allowable interference threshold. This licensing approach provides a way of differentiating the spectrum access for the different operators. Results show that compared to uncoordinated sharing, a reasonable gain can be achieved using the proposed secondary licensing, especially for edge rates.

Table of Contents

List of Tables

List of Figures

Chapter 1

Introduction

The modeling and analysis of various types of wireless systems including cellular and ad hoc systems has been a focus in wireless communication research. In the past, researchers have proposed many analytical and simulation based models to evaluate the performance of cellular systems. However, cellular systems have evolved significantly over time and will continue to do so. The emergence of new technologies increasingly drives older models to obsolescence, thus requiring new modeling approaches for their analysis. This introductory chapter will briefly provide some background on cellular analysis and key modeling approaches in Section 1.1. Section 1.2 and 1.3 introduce some of new emergent technologies expected to be important in future generation cellular systems and overview various issues related to these technologies. Finally, Section 1.4 summarizes the key contributions of this dissertation.

1.1 Analysis and Modeling of Cellular Systems

A conventional cellular system consists of a network of base stations (BSs) deployed over a land area and a set of subscriber users with each user connected to a BS. This association can be as simple as connecting to the nearest BS or can be based on a complicated criteria to achieve a global best performance. Due to this

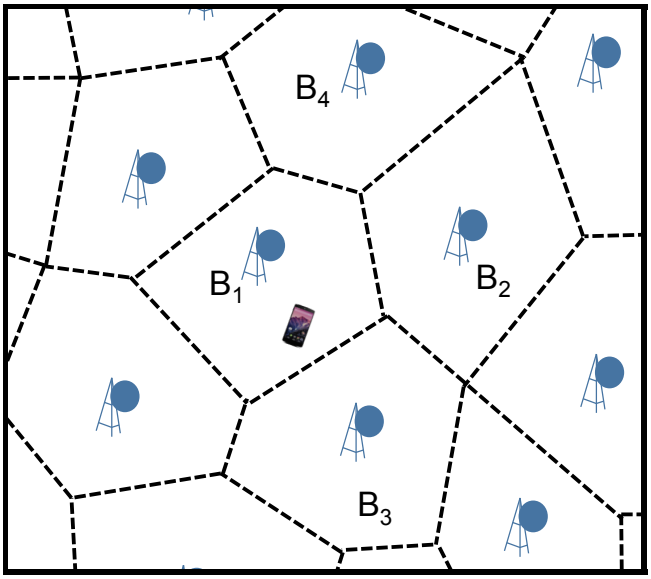

Figure 1.1: A cellular system consisting of a network of BSs ($\mathbf{B}_i$'s) and a user associated with BS $\mathbf{B}_1$. The area is divided into coverage areas or cell of each BS.

association, the whole area can be divided into coverage areas or cells around the BSs. A cellular system is generally owned by a cellular operator and can be used to provide voice or data services to fixed or mobile users. The BSs are connected to the core network and possibly to each other using a wired or wireless back-haul infrastructure.

Let us consider a cellular system as shown in Fig. 1.1 consisting of N BSs $\mathbf{B}_i$'s ($i = 1, 2, \cdots, N$). A user is connected to the BS $\mathbf{B}_1$, located at distance r_1. The signal transmitted from the ith BS $\mathbf{B}_i$ undergoes an attenuation in power due to the channel. Therefore, the received power at the user is given as $P_{ri} = Ph_i r_i^{-\alpha}$. Here, P is the BS transmit power, α is the path-loss exponent, r_i is the distance of the BS $\mathbf{B}_i$ from the user and h_i denotes the random attenuation present in the channel

which includes fading and shadowing. Hence, the signal-to-interference-plus-noise ratio (SINR) at the user is given as

$$\text{SINR} = \frac{Ph_1 r_1^{-\alpha}}{\sigma^2 + \sum_{i=2}^{N} Ph_i r_i^{-\alpha}} \tag{1.1}$$

where σ^2 is the noise present at the receiver. The distribution and various statistics of the SINR can be used to determine the performance of this system. One metric that can be used to evaluate a system's performance is the SINR coverage probability (also known as the coverage probability). It is defined as the probability that the SINR at the user from its associated BS is above a threshold τ and is equivalently the CCDF (complementary cumulative distribution function) of the SINR.

While the SINR represents the serving link quality, the per-user rate represents the data bits received per second per user and is given as $R = W \log_2(1+\text{SINR})$ where W is the amount of frequency-time resource allocated to the user. The CCDF of the rate is another important performance metric, and also called the rate coverage which is defined as the probability of the rate of a user being greater than the threshold ρ.

There are various other performance metrics including latency, average throughput, and spectral efficiency. Determining which metric is the most appropriate is subjective and depends largely on the supported applications and user requirements. Due to the large number of variables and randomness present in the channel, evaluating the performance of a cellular system is not a trivial problem and various approaches are proposed in the past to model and analyze cellular systems.

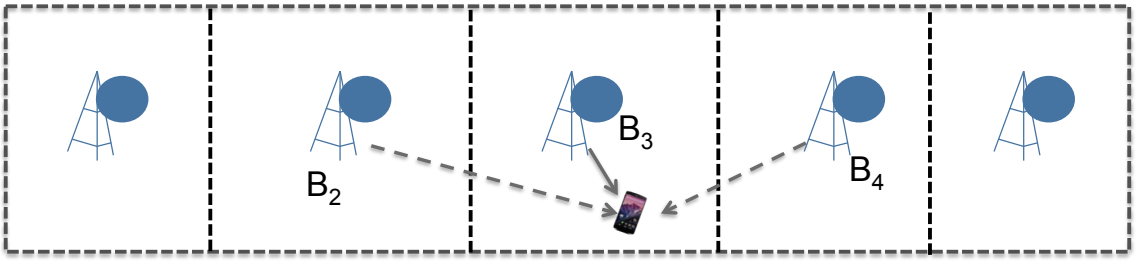

Figure 1.2: A 1-D Wyner model.

1.1.1 Hexagonal Grid Model

The hexagonal grid model is one of the widely used models to evaluate the performance of cellular systems. In this model, BS locations are modeled as cell centers in a hexagonal grid. It is often limited to 1 or 2 layers of BSs around the origin resulting in a 7 BSs grid or 19 BSs grid system. This model is in general not tractable. Therefore, most of the studies are performed via simulations only and may fail to provide insights into systems.

1.1.2 Wyner Model

The Wyner model [2] provides a simplistic approach to model cellular systems. In this model, BSs are assumed to be located in a line at a fixed distance R with square coverage regions as shown in Fig. 1.2. This model assumes that a user located in the coverage cell of a BS faces interference only from its neighboring cells which is scaled by a factor termed as interference intensity. Although the Wyner model is tractable, it is overly simplistic.

1.1.3 Stochastic Geometry Based Model

Due to the increasing heterogeneity in cellular infrastructure and irregularity in BS locations, random spatial models are proposed to model the inherent randomness in such networks. Modeling the BS locations as a Poisson Point Process (PPP) further lends tractability and allows to compute simple expressions for key metrics, such as coverage and rate. The field of stochastic geometry provides the relevant tools necessary to analyze most of the wireless systems [3]. This dissertation focuses on stochastic geometry, therefore, we have summarized some key concepts of stochastic geometry in Appendix A.

Due to the emergence of new technologies, increase in data usage and the introduction of new applications, wireless systems have evolved significantly. In the next section, we will discuss some of these technologies that are expected to be important in next generation systems.

1.2 New Emergent Technologies

Since the current generation of cellular systems is reaching its maturity and limits, researchers have started looking into new approaches for the next generation cellular communication. The growing number of new applications and devices such as wearables, smart phones and development of Internet-of-Things have increased the sheer volume of data and data-rate requirements in last years and will continue to do the same in the upcoming years [4]. The expectations from next generation systems have been set to very high to meet these requirements. It is clear that there must be non-trivial differences and improvements over the current generation to achieve these

expectations [5]. In this section, we will discuss some of the technologies which will be the key factors in bridging this gap.

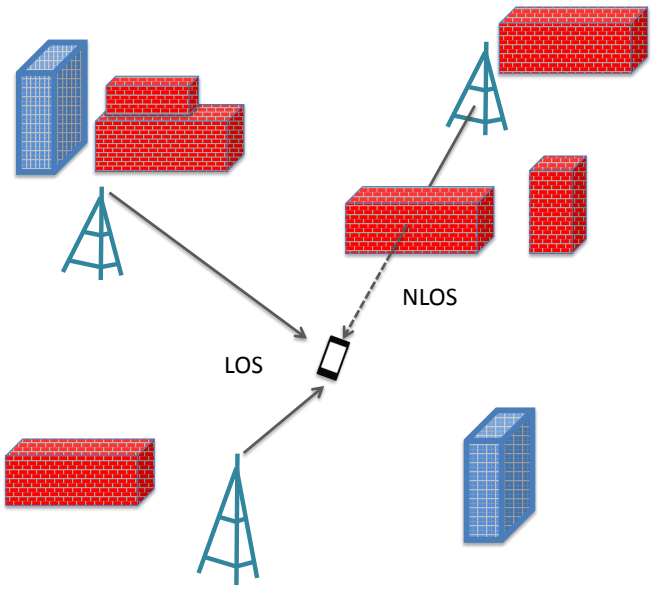

Figure 1.3: A mmWave cellular system with random blockages. A link can be blocked by one or more blockages to become NLOS.

1.2.1 Use of Millimeter Wave Bands

One of the proposed feature of future cellular systems will be the inclusion of bands from the mmWave spectrum (30GHz-300GHz). Until now, cellular communication was restricted to the bands less than 6 GHz, known as conventional cellular frequencies (CCF) or sub 6 GHz. As these bands are almost fully occupied, the only way to acquire more spectrum is by going up towards higher frequencies (6-100GHz). Many recent studies have focused on characterizing the mmWave channel [6, 7], modeling and evaluating the system performance [8] and making the communication work

at mmWave. The signal propagation at higher frequencies suffers from various issues such as higher atmospheric absorption and sensitivity to blockages due to reduced diffraction and penetration. However, due to smaller antenna sizes at mmWave frequencies, a large number of antennas can be accommodated in the same aperture size which makes communication at mmWave highly directional and helps reduce some of the propagation issues mentioned before. Also, blockages present in the channel severely impact the performance of a mmWave system. This necessitates the separate modeling of line-of-sight (LOS) and non-LOS (NLOS) links for mmWave systems (see Fig. 1.3). Random shape theory can be used to model the effect of blocking in cellular systems [9] where buildings are modeled as random shapes such as lines, rectangles or circles.

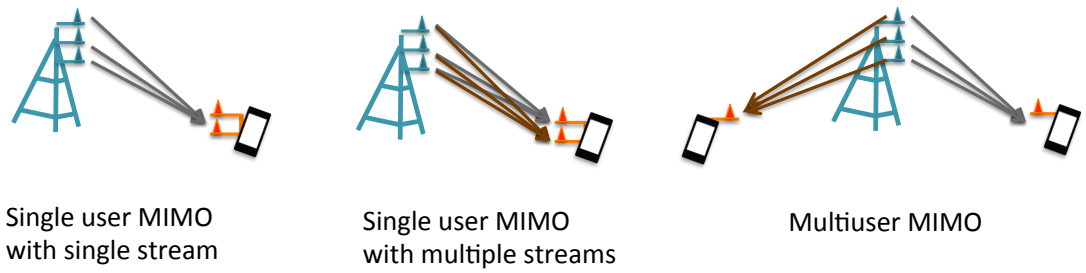

Figure 1.4: MIMO technology: Multiple antennas can be used for single user or multiple users to enhance the link reliability and system throughput.

1.2.2 Multiple Input Multiple Output Systems

Multiple input multiple output (MIMO) refers to the use of multiple antennas at the transmitters and/or receivers in a wireless system. MIMO systems have

become key part of present wireless communication systems by offering significant performance improvement. The use of multiple antennas provides multiple transmission paths and can increase the diversity order. Higher diversity order reduces the effect of fading and increases the overall capacity of the system. Depending on the pre-coding used at the antennas, MIMO can be used to increase link reliability and/or the data throughput. For example, for a single user, multiple antennas can help beamform the desired signal to the user, reducing the intercell interference and increasing the data throughput. Using space time codes with MIMO, the same signal can be sent over multiple paths increasing the link reliability and reducing the impact of fading.

MIMO can also be used with multiple users, which is termed *multiuser MIMO*. Using a zeroforcing pre-coder and spatial multiplexing, a single BS with multiple antennas can transmit data simultaneously to multiple users with single or multiple antennas. It is expected that the limit on number of antennas in systems will increase by the order of magnitude, leading to massive MIMO [10]. The idea is to have hundreds or even thousands of antennas serve tens of users simultaneously in each resource block which leads to very high theoretical gains in the throughput.

As discussed above, directional communication is crucial for mmWave systems. Fortunately, it is possible to accommodate a large number of antennas at mmWave frequencies which will enable very narrow beams in mmWave systems. The high cost and power consumption of mixed signal components prevent dedicating a separate radio frequency (RF) chain for each antenna and using traditional MIMO baseband pre-coding schemes. To reduce the power consumption, a hybrid analog-digital pre-

coding architecture is proposed [11] where precoding processing is divided between analog and digital domains. The number of complete RF chains required is lower than the number of antennas and hence, the performance of hybrid pre-coding is limited by the number of RF chains.

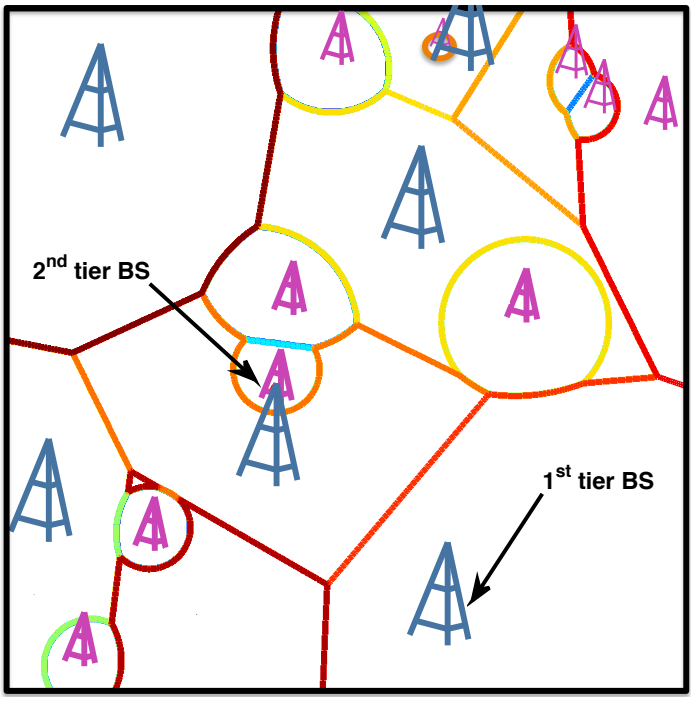

Figure 1.5: A two tier HetNet showing coverage area of each BS. Due to difference in the transmit power of BSs, the coverage areas are no longer Voronoi cells.

1.2.3 Heterogeneous Networks

Cellular systems have gone through a great deal of densification over time. As the signal-to-interference ratio (SIR) is invariant to the BS density [12], increasing the BS density will decrease user load on each BS, and hence, increase achievable per-user data rate. As the distance between BSs and users decreases, the conven-

tional high power macro BSs do not make sense. In addition, some of the BSs may be deployed by users to increase their own data rate in the form of small cells such as femetocells, picocells, WiFi access points. This leads to additional heterogeneity among BSs. MmWave BSs will also be small cells and deployed densely. To increase their reliability, they are expected to be deployed in the presence of UHF/LTE network [13,14]. Such a cellular system which consists of multiple classes of base stations (BSs) is known as a heterogeneous networks (HetNets) which already exists in current cellular systems. These classes (or tiers) of BSs may differ in terms of transmit power, deployment density, number of transmit antennas, number of users served, transmission scheme, and path loss exponent [15]. Since BSs are no longer homogeneous and most of the small cells are deployed randomly as per the user requirements, coverage areas are no longer regular (see Fig. 1.5). Therefore, conventional cellular models are no longer relevant to the analysis of HetNets and random spatial models are more accurate to model these systems. A PPP based model was first introduced for multi-tier cellular networks in [16, 17], and generalized further in [18–21] to study various cell selection rules for single-antenna HetNets.

1.3 Technical Issues in Next Generation Systems

In the previous section, we have discussed some of the new technologies that are expected to be present in next generation systems. These new technologies have been studied in recent work in isolation, however, their interplay has not been well investigated. When these technologies are implemented together in future systems, there can be various network level issues due to their interplay. In this section, we

will discuss few of these issues.

1.3.1 Association Issues

In cellular systems, each user associates itself to a BS (termed 'serving BS') based on a cell selection rule. A usual cell selection criterion in cellular systems is to connect to the BS that provides maximum average received power [18]. Since the channel from a BS in a single antenna system exhibits same statistical properties regardless of it acting as a serving link or an interfering link [22], the BS providing the highest average received power will also cause highest average interference if not selected as the serving BS. Therefore, in a HetNet where each tier has only a single antenna, this cell selection criterion is also the one that maximizes the SINR and the coverage probability. However, in a HetNet where each tier has a different number of antennas and/or uses different MIMO technique, the channel from a BS exhibits different statistical properties based on its role as a serving link or an interfering link [22]. Hence, the conventional average received power based association is no longer the coverage maximizing association. Therefore, it is important to understand which cell selection rule should be adopted such that each user can maximize its coverage probability.

Another issue arises when we consider association in mmWave systems. As discussed above, blockages may result in significant drop in signal strengths or even outages for some users [8]. In addition, a user can block desired signals from its serving BS due to its own body causing sudden outages [23, 24]. Therefore, conventional single BS-association rules will not be able to ensure connectivity in mmWave cellular

systems. To increase link reliability, macro diversity can be leveraged where a user is connected to multiple BSs simultaneously so that when one link is blocked, there can be other BSs available to the user immediately [13,25–27]. However, the presence of large blockages will result in correlation among different links which need to be investigated to accurately characterize gains obtained by macro-diversity.

1.3.2 Load Balancing and Offloading

Since in a single tier network, all BSs have the same transmit power and resources, a simple received power based association results in almost equal number of users at each BS on an average [28]. However, in multi-tier networks, different tiers may have different transmit power and amount of resources. In this case, the conventional association rule may end up in congested macro cells and under-utilized small cells which creates a load imbalance among tiers. In [28–31], a simple cell selection rule was proposed to tackle load balancing issue in HetNets where each tier is assigned a certain bias value for association. This rule helps the system offload users from a congested tier to idle tiers. The use of multiple antennas can increase communication range and accommodate more users in the same amount of resources. Hence, the load imbalance issue becomes more complicated when HetNets with multiple antennas are considered. Combining load balancing with the earlier discussion on optimal cell selection rule raises an interesting question if there is an optimal cell selection which can provide optimal rate coverage in multi-tier networks.

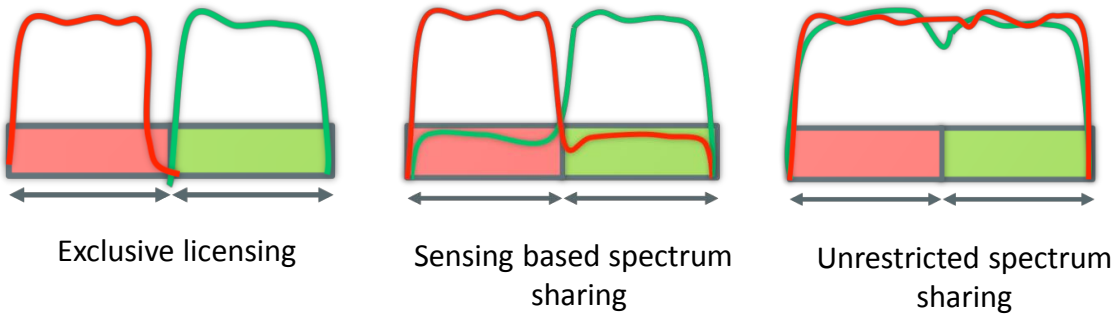

Figure 1.6: Various spectrum sharing mechanism for mmWave cellular systems.

1.3.3 Efficient Spectrum Utilization for MmWave Spectrum

MmWave communication causes less interference to neighboring BSs operating in the same frequency bands compared to communication at conventional cellular frequencies [6,8,14], which requires us to rethink how mmWave spectrum should be licensed. In conventional cellular licensing, commercial operators buy exclusive licenses which give each of them exclusive and complete control over a band of spectrum. This conventional exclusive licensing is not efficient for mmWave due to the lower level of interference and it seems evident that spectrum sharing should be implemented for mmWave systems [32]. There are two main ways to share the spectrum: one way is to share the spectrum without any coordination among the operators and another way is to implement some type of sensing or coordination to avoid transmission conflicts [33–35] (see Fig. 1.6). Currently, there are no regulatory framework for cellular services in the mmWave bands. Therefore, these different types of sharing mechanisms should be evaluated in advance to understand the behavior of multi-operator mmWave systems and increase spectrum utilization.

1.4 Contributions

Although there is a significant amount of recent work dealing with the aforementioned technologies present in new generation systems, they are studied in isolation and therefore, their interplay is not well investigated. It is evident that studies focused on analysis and optimization of systems incorporating these technologies are needed to enable their full potential. This dissertation focuses on some of the network level optimization issues related to users association and resource sharing for systems embodying these technologies and divided into four parts. The first part of this dissertation focuses on interplay between MIMO and HetNets to study optimal users association and load balancing among different classes of BSs. The second part considers association in mmWave BSs where each user is simultaneously connected to multiple BSs. The third part changes the focus to the spectrum sharing issues in a multi-operator mmWave system to study feasibility of uncoordinated sharing of spectrum and infrastructure among operators. The fourth part extends this to include some kind of static coordination among the operators. The main contributions of this dissertation can be summarized as follows:

Chapter 2: Cell selection and load balancing in downlink multi-antennas heterogeneous cellular network: We model and analyze heterogeneous cellular networks with multiple antenna BSs (multi-antenna HetNets) with K classes or tiers of base stations (BSs), which may differ in terms of transmit power, deployment density, number of transmit antennas, number of users served, transmission scheme, and path loss exponent. We show that the cell selection rules in multi-antenna HetNets may differ significantly from the single-antenna HetNets due

to the possible differences in multi-antenna transmission schemes across tiers. While it is challenging to derive exact cell selection rules even for maximizing signal-to-interference-plus-noise-ratio (SINR) at the receiver, we show that adding an appropriately chosen tier-dependent cell selection bias in the received power yields a close approximation. Assuming arbitrary selection bias for each tier, simple expressions for downlink coverage and rate are derived. For coverage maximization, the required selection bias for each tier is given in closed form. Due to this connection with biasing, multi-antenna HetNets may balance load more naturally across tiers in certain regimes compared to single-antenna HetNets, where a large cell selection bias is often needed to offload traffic to small cells.

Chapter 3: Macro-diversity in mmWave cellular networks with random blockages: Transmission at mmWave frequencies is significantly impacted by various blockages in the form of buildings or foliage. To reduce the chances of users to be in complete outage, they can be allowed to connect to multiple BSs simultaneously which increases the reliability of communication links. We evaluate the benefits of macro-diversity for a mmWave cellular system in presence of random blockages. We present a framework to analyze the correlation among blocking of multiple links in a cellular system and compute the average probability of having at least one line-of-sight communication link out of all connected links at any user. We also study the impact of size of blockages on the reliability and show that diversity gains are higher when blockages are small. We also show that the BS density must scale as the square of the blockage density to maintain the same level of reliability.

Chapter 4: Uncoordinated sharing of spectrum licenses in mmWave

cellular systems: The reduced level of interference in mmWave systems owing to highly directional antennas opens up the possibility of uncoordinated sharing of spectrum licenses between commercial cellular operators. There are several advantages to sharing including a reduction in license costs and an increase in spectrum utilization. We establish the theoretical feasibility of spectrum license sharing among mmWave cellular operators. We consider a heterogeneous multi-operator system containing multiple independent cellular networks, each owned by an operator. We then compute the SINR and rate distribution for downlink mobile users of each network. Using the analysis, we compare systems with fully shared licenses and exclusive licenses for different access rules and explore the trade-offs between system performance and spectrum cost. We show that sharing spectrum licenses increases the per-user rate when antennas have narrow beams and is also favored when there is a low density of users. We also consider a multi-operator system where BSs of all the networks are co-located to show that the simultaneous sharing of spectrum and infrastructure is also feasible. We show that all networks can share licenses with less bandwidth and still achieve the same per-user median rate as if they each had an exclusive license to spectrum with more bandwidth.

Chapter 5: Restricted secondary licensing in mmWave cellular systems: We extend the results of previous contribution to include static coordination between operators in a primary-secondary framework. We model a mmWave cellular system where an operator that primarily owns an exclusive-use license of a certain band can sell a restricted secondary license of the same band to another operator. This secondary network has a restriction on the maximum interference it can cause

to the original network. Using stochastic geometry, we derive expressions for the coverage and rate of both networks, and establish the feasibility of secondary licensing in licensed mmWave bands. To explain economic trade-offs, we consider a revenue-pricing model for both operators in the presence of a central licensing authority. Our results show that the original operator and central network authority can benefit from secondary licensing when the maximum interference threshold is properly adjusted. This means that the original operator and central licensing authority have an incentive to permit a secondary network to restrictively share the spectrum. Our results also illustrate that the spectrum sharing gains increase with narrow beams and when the network densifies.

Chapter 2

Cell Selection and Load Balancing in Downlink Multi-Antenna Heterogeneous Cellular Network

Current cellular networks are undergoing a significant transformation due to the capacity-driven opportunistic deployment of small cells [36]. The resulting cell splitting gain due to increased infrastructure, along with the possibility of multi-antenna transmission, provides one of the most promising solutions to handle current data deluge [37]. Due to the relative maturity of both HetNets [38] and multi-antenna transmission techniques in cellular standards [39], their coexistence in future networks is almost inevitable. However, quite remarkably, this synergy is not reflected in the current HetNet research efforts using tools from stochastic geometry, e.g., see [40] for a survey. These two strategies are mostly studied in isolation, thereby missing important interplay between them, especially in the cases where one can complement the other's shortcomings. In this chapter,[1] we take a step towards bridging this gap. In particular, we focus on developing simple yet useful cell selection rules for multi-antenna HetNets, which highlight certain natural connections with current standardization activities, most importantly cell range expansion and load balancing [43].

[1] This work has appeared in [41] and [42] in parts. I am the first author of both of these articles.

2.1 Related Work

The stochastic geometry model was first introduced for multi-tier cellular networks in [16,17], and generalized further in [18–21] to study various cell selection rules for single-antenna HetNets. Interested readers can refer to [40] for a detailed survey and to [44–47] for a subset of prior work on cell selection. The PPP-based HetNet model of [17] was generalized to multi-antenna HetNets in [48], where an upper bound on downlink coverage probability was derived using tools from stochastic geometry, and in [22], where stochastic orders were used to order the performance of various multi-antenna transmission schemes in a general multi-antenna HetNet. A key difference between these works and the current paper is that they all assume maximum instantaneous SINR based cell selection, whereas this paper assumes average-SINR based cell selection with an additional flexibility of per-tier cell selection bias. Another relevant prior work is [49], which studies a hybrid multi-antenna HetNet with a fixed size "typical" cell. In this paper, we extend the multi-antenna HetNet model of [22, 48], with a special emphasis on cell selection and its impact on downlink coverage probability and average rate.

It should be noted that while there is a limited prior work on general multi-antenna HetNets besides [22,48,49], the special case of two-tier multi-antenna HetNets has been investigated fairly thoroughly. For example, [50] compares single and multi-user linear beamforming in a two-tier network under perfect channel state information (CSI), [51], [52], respectively study random orthogonal beamforming with max-rate scheduling and coordinated beamforming for two-tier networks, and [53] studies the effect of channel uncertainty in linear beamforming. Additionally, it is worth men-

tioning that multi-antenna transmission schemes have been investigated extensively in the context of ad-hoc networks, see e.g., [54–56]. Some of the tools developed there can be extended to HetNets.

2.2 Contributions

In this chapter, we focus on the cell selection rules for a multi-antenna HetNet and compute its performance in terms of coverage probability and rate coverage. The main contributions of this chapter are following:

Cell selection rules for multi-antenna HetNets: We investigate cell selection rules for a multi-antenna HetNet consisting of K different classes of BSs, which may differ in terms of transmit power, deployment density, number of transmit antennas, number of users served, transmission scheme, and path loss exponent. This is motivated by the fact that, unlike single-antenna HetNet, connecting with the BS that provides maximum received power may not always maximize the received SINR in a multi-antenna HetNet. Building upon this observation, we show that although it is challenging to derive exact cell selection rule to maximize average received SINR, a simpler selection rule based on adding an appropriately chosen per-tier selection bias in the received power yields a surprisingly close approximation. We also derive this approximate per-tier selection bias in closed form for coverage probability maximization. One key observation is that the bias value depends only on the number of antennas at the BS and the number of users served in each resource block, which makes it easier to implement it in practice. Assuming a general cell selection bias for each tier, we derive exact expressions for downlink SINR distribution,

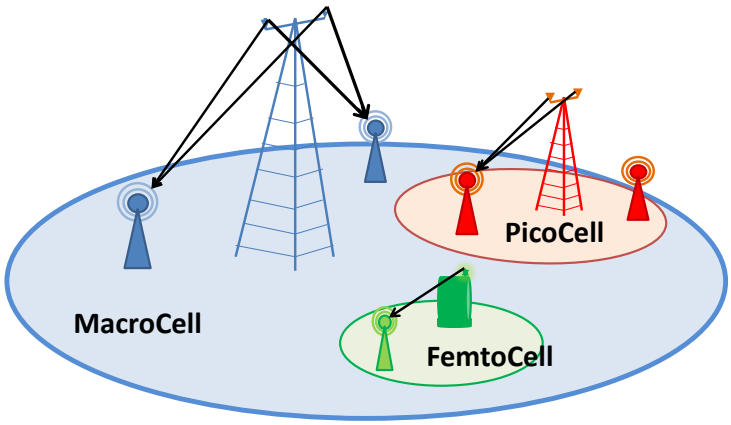

Figure 2.1: A three-tier HetNet consisting of macro, pico and femtocells, with different number of transmit antennas and different transmission schemes across tiers.

from which we study downlink rate achievable at a typical user.

Connections with biasing and load balancing: An important interpretation of our results is in terms of *load balancing* in HetNets. It is well known that the load in HetNets is unbalanced due to differences in transmit powers of macro and small cells [57]. An artificial bias is generally introduced to expand the coverage regions of small cells in order to *offload* more users from macrocells [28, 58, 59]. However, as discussed above, multi-antenna HetNets may need selection bias even for SINR, and hence coverage, maximization. Therefore, in certain cases, the selection bias that maximizes coverage, may naturally balance load across tiers compared to single-antenna HetNets. We characterize such regimes in this paper and validate our intuition through extensive simulations.

2.3 System Model

We consider a K-tier HetNet consisting of K different tiers or classes of BSs. For notational ease we denote $\mathcal{K} = \{1, 2, \dots K\}$. The BSs across tiers differ in terms of the transmit power P_k (to each user), deployment density λ_k, number of transmit antennas M_k, number of users served in each resource block Ψ_k, transmission scheme, and the path-loss exponent α_k. The locations of each tier are assumed to be sampled from an independent homogeneous PPP Φ_k of density λ_k. This model is the same as the one introduced in [22], except for some key differences in cell selection, which will be clarified later in this section. Although the PPP model is likely more accurate for the opportunistic deployment of small cells, it has also been verified for the planned tiers, such as macrocells, both by empirical evidence [60] and theoretical validation [61] under sufficient channel randomness. For easier exposition later in the paper, we denote the locations of all the BSs by $\Phi = \cup_{k \in \mathcal{K}} \Phi_k$. A particular realization of Φ will be denoted by ϕ. Each user is assumed to have a single receive antenna. Note that since each BS serves multiple users and the channel from a BS to each user is multiple-input single-output (MISO), the current setup can be precisely defined as a K-tier multi-user MISO HetNet. The temporal evolution of the system is not studied in this paper.

For multiple access, we assume orthogonal resource partitioning, e.g., orthogonal frequency division multiple access (OFDMA), with a provision that multiple users can be scheduled on a given resource block if the BS has sufficient degrees of freedom to orthogonalize them in space. In terms of the notation introduced above, this leads to the constraint $\Psi_k \leq M_k$ for all $k \in \mathcal{K}$. The users are assumed to form

Table 2.1: Summary of Notation

Notation	Description
$\mathcal{K}$	Indices of the tiers, where $\mathcal{K} = \{1, 2, \ldots, K\}$
$\Phi_k, \Phi; \phi$	A PPP modeling the locations of k^{th} tier BSs, $\Phi = \cup_{k\in\mathcal{K}}\Phi_k$; a realization of Φ
Φ_u	An independent PPP modeling user locations
$\mathbb{1}(e), \mathbb{1}_e$	Indicator function for logic e
P_k, λ_k, α_k	Downlink transmit power to each user, deployment density, path loss exponent of the k^{th} tier BSs
M_k, Ψ_k, Δ_k	Number of transmit antennas, number of users served in each resource block by a k^{th} tier BS, $\Delta_k = M_k - \Psi_k + 1$
$h_{x_k k}$	Channel power distribution of the direct link from a BS at $x_k \in \Phi_k$ to a typical user, $h_{x_k k} \sim \Gamma(\Delta_k; 1)$
$g_{y_j j}$	Channel power distribution of the interference link from a BS $y_j \in \Phi_j$ to a typical user, $g_{y_j j} \sim \Gamma(\Psi_j; 1)$
$\widehat{(\cdot)}_j$	Ratio of a j^{th} parameter to the same parameter of the serving tier, e.g., if k^{th} tier is serving, $\widehat{P}_j = \frac{P_j}{P_k}$
B_k, A_k	Cell selection bias, selection probability for k^{th} tier
γ_k, P_c	Instantaneous SINR, coverage probability
R_k, R_c	Instantaneous rate conditional on serving BS being in k^{th} tier, rate coverage
$W_k, \mathcal{O}_k, N_k$	Total time frequency resource, e.g., bandwidth, for each k^{th} tier BS, fraction of resources allocated to each user served by k^{th} tier, average load over a k^{th} tier BS

an independent PPP Φ_u of density λ_u. Note that more sophisticated user location models can in principle be considered, e.g., by using tools from [62], but are out of the scope of this paper. The downlink analysis will be performed at a typical user, which is assumed to be at the origin. This is facilitated by Slivnyak's theorem, which states that the properties observed by a typical point of the point process Φ_u are the same as those observed by the origin in the point process $\Phi_u \cup \{0\}$ [63].

In this paper, we will restrict our discussion to zero-forcing precoding, which is general enough to encompass important transmission schemes such as beamforming and spatial division multiple access (SDMA), while being tractable enough to provide important system design guidelines. Note that due to precoding at the BS, the effective channel gain to a given user depends upon whether that BS acts as a serving BS or an interferer for that user. For example, if a multi-antenna transmitter beamforms to a given user, the effective channel gain would be much higher than when it simply acts as an interferer. Therefore, we denote the effective channel power gain from a k^{th} tier BS located at $x_k \in \Phi_k$ to a typical user by $h_{x_k k}$ when it acts as a serving BS, and by $g_{x_k k}$ when it acts as an interferer. We also assume perfect CSI at the transmitter, although as argued in [22] the tools developed in this paper can also be used to study the effect of imperfect CSI on the network performance. For zero-forcing precoding with perfect CSI under Rayleigh fading, $h_{x_k k} \sim \Gamma(\Delta_k, 1)$ and $g_{x_k k} \sim \Gamma(\Psi_k, 1)$, where $\Delta_i = M_i - \Psi_i + 1$ as discussed in detail in [22]. More general precoding techniques are left for future work. The received power at a typical user from a serving BS located at $x_k \in \Phi_k$ is

$$P(x_k) = P_k h_{x_k k} \|x_k\|^{-\alpha_k}, \tag{2.1}$$

where $\|x_k\|^{-\alpha_k}$ is a standard power-law path-loss with exponent α_k, which may be different for different tiers. Also recall that P_k is the transmit power to each user. The resulting SINR $\gamma_k(x_k)$ is

$$\gamma_k(x_k) = \frac{P_k h_{x_k k} \|x_k\|^{-\alpha_k}}{I + N}, \tag{2.2}$$

where N is the noise power, and I is the interference power given by

$$I = \sum_{j \in \mathcal{K}} I_j = \sum_{j \in \mathcal{K}} \sum_{x \in \Phi_j \setminus x_k} P_j g_{xj} \|x\|^{-\alpha_j}. \tag{2.3}$$

For cleaner exposition in the next section, we denote the average received power from a k^{th} tier BS by $P_{rk}(x_k)$, which can be expressed as

$$P_{rk}(x_k) = P_k \Delta_k \|x_k\|^{-\alpha_k}. \tag{2.4}$$

For this setup, we discuss cell selection for multi-antenna HetNets in the next section. As evident from the following discussion, the cell selection principles for multi-antenna HetNets have some fundamental differences compared to their counterparts in single-input single-output (SISO) HetNets, mainly because of the precoding at the transmitter.

2.4 Cell Selection

Recall that a usual cell selection criterion in SISO HetNets is to connect to the BS that provides the maximum average received power, possibly with a certain bias value for load balancing [28]. In the case when there is no bias, this cell selection criterion is also the one that maximizes the SINR. Therefore, to maximize coverage probability, a typical user simply connects to the BS that provides the highest received power, as discussed in [18]. However, it is easy to construct a simple toy example showing that this is not the case in multi-antenna HetNets.

Example 1. *Consider two BSs at the same distance from a typical user, one having* 4 *antennas serving a single user, which with a slight overloading of the notation*

implies $M_1 = 4, \Psi_1 = 1, \Delta_1 = 4$*, and the other serving* 4 *users with* 6 *antennas, i.e.,* $M_2 = 6, \Psi_2 = 4, \Delta_2 = 3$*. Since* $\Delta_1 > \Delta_2$*, a typical user should be served by the first BS to maximize average received power. However, since* $\Psi_2 > \Psi_1$*, the interference from second BS is larger than the first and it should be served by the second to minimize the received interference power. Further, since* $\frac{\Delta_2}{\Psi_1} > \frac{\Delta_1}{\Psi_2}$*, it should be served by the second BS to maximize its received SINR.*

We first discuss cell selection with the goal of maximizing the average received SINR conditional on the point process Φ. Note that to maximize both the average received power and average SINR, it is strictly suboptimal for a typical user to connect to any BS except the ones that are closest to it in each tier. We denote by γ_k the instantaneous SINR when a typical user connects to the closest k^{th} tier BS. Under maximum average SINR cell selection rule, k^{th} tier is selected if

$$k = \arg\max_{j \in \mathcal{K}} \mathbb{E}[\gamma_j | \Phi = \phi], \tag{2.5}$$

where the selection rule clearly depends upon the distances of the BSs to a typical mobile due to conditioning on the realization of the point process. As will be evident in the sequel, it is quite challenging to derive an exact selection rule from (2.5). We take several alternate routes in the following subsections. Our eventual goal is to come up a simple and practical cell selection rule that works well across wide range of system parameters.

2.4.1 Results from Stochastic Orders

Put simply, stochastic orders are binary relations defined to compare random variables, see [64] for details. Ideas from stochastic orders were used in [22] to compare the coverage probability and downlink rate for various multi-antenna transmission schemes. Using tools developed in [22], it is possible to derive a sufficient condition for the selection rule that is slightly stronger than the average SINR maximization. The idea is to condition on the locations of the BSs and then find a condition under which the conditional cumulative distribution function (CCDF) of SINR from the chosen tier dominates the conditional CCDF of SINR for all other choices. More formally, the k^{th} tier is selected if

$$k = \arg\max_{j \in \mathcal{K}} \mathbb{P}(\gamma_j > z | \Phi = \phi), \forall z. \tag{2.6}$$

In stochastic ordering terms, this means that conditional on the point process Φ, γ_k (first order) stochastically dominates γ_j for all $j \in \mathcal{K}$, which is denoted by $\gamma_k \geq_{st} \gamma_j \forall j \in \mathcal{K} \setminus \{k\}$. Clearly, (2.6) $\Rightarrow$ (2.5). Now let us rewrite γ_k and γ_j as

$$\gamma_k(x_k) = \frac{P_k h_{x_k k} \|x_k\|^{-\alpha_k}}{P_j g_{x_j j} \|x_j\|^{-\alpha_j} + W} = \frac{h_{x_k k} a_k}{g_{x_j j} a_j + W} \tag{2.7}$$

$$\gamma_j(x_j) = \frac{P_j h_{x_j j} \|x_j\|^{-\alpha_j}}{P_k g_{x_k k} \|x_k\|^{-\alpha_k} + W} = \frac{h_{x_j j} a_j}{g_{x_k k} a_k + W}, \tag{2.8}$$

where $a_i = P_i \|x_i\|^{-\alpha_i}$ and W is a random variable representing thermal noise plus interference from all the BSs except $x_k \in \Phi_k$ and $x_j \in \Phi_j$. For $a_k \geq a_j$, using [22, Lemma 3], it can be shown that conditional on the locations of the BSs, $\gamma_k \geq_{st} \gamma_j, \forall j \in \mathcal{K}$, if $\Delta_k \geq \Delta_j$ and $\Psi_k \geq \Psi_j$. This leads to the following set of sufficient conditions

for (2.6) to hold:

$$P_k\|x_k\|^{-\alpha_k} \geq P_i\|x_i\|^{-\alpha_i} \quad \forall i \neq k \tag{2.9}$$

$$\Delta_k \geq \Delta_i \quad \forall i \neq k \tag{2.10}$$

$$\Psi_k \geq \Psi_i \quad \forall i \neq k. \tag{2.11}$$

Clearly, these conditions are also sufficient for the selection of k^{th} tier to maximize the average received SINR. Since first order stochastic dominance is a stronger notion than the ordering of the means required in (2.5), it is possible that none of the tiers satisfy the above set of conditions simultaneously, which limits the applicability of this selection rule. In the pursuit of a more useful cell selection rule, we explore two more directions below.

2.4.2 Results from Jenson's Inequality Approximation

In this section, we approximate the mean SINR using Jenson's inequality. For any realization of point process ϕ, the mean of SINR over fading distribution is given by

$$\mathbb{E}[\gamma_k(x_k)|\phi] = \mathbb{E}\left[\frac{h_{x_k k}a_k}{g_{x_j j}a_j + W}|\phi\right] \tag{2.12}$$

$$= a_k\Delta_k\mathbb{E}\left[\frac{1}{g_{x_j j}a_j + W}|\phi\right] \tag{2.13}$$

$$\geq a_k\Delta_k\frac{1}{\mathbb{E}[g_{x_j j}a_j + W|\phi]} = \frac{a_k\Delta_k}{\Psi_j a_j + \mathbb{E}[W|\phi]}. \tag{2.14}$$

Using this lower bound, the conditions for (2.5) to hold are

$$P_k\Delta_k\|x_k\|^{-\alpha_k} \geq P_i\Delta_i\|x_i\|^{-\alpha_i} \quad \forall i \neq k \tag{2.15}$$

$$P_k \Psi_k \|x_k\|^{-\alpha_k} \geq P_i \Psi_i \|x_i\|^{-\alpha_i} \quad \forall i \neq k. \tag{2.16}$$

Although this approximation has reduced the number of simultaneous conditions from three to two compared to the previous subsection, it is still possible that none of the tiers satisfy these new conditions simultaneously. We construct an example below to highlight this point. The same example is also true for the conditions (2.9) (2.10) and (2.11) discussed in the previous subsection in the context of stochastic orders.

Example 2. *Consider a two-tier network such that the distance of the typical user to the nearest BS in each tier is the same, i.e.,* $\|x_1\| = \|x_2\|$. *Further assume that the transmit powers for the two tiers are also the same. Fixing* $\Delta_1 = 2, \Delta_2 = 1, \Psi_1 = 2, \Psi_2 = 3$, *it is easy to check that neither* $k = 1$ *nor* $k = 2$ *satisfy* (2.15) *and* (2.16) *simultaneously.*

As discussed above, although there is no guarantee that the conditions given by (2.15) and (2.16) would provide a solution, it is possible to derive a simpler but more useful condition for the selection of k^{th} tier by combining (2.15) and (2.16). The new selection law is

$$P_k \sqrt{\Delta_k \Psi_k} \|x_k\|^{-\alpha_k} \geq P_i \sqrt{\Delta_i \Psi_i} \|x_i\|^{-\alpha_i} \quad \forall i \neq k. \tag{2.17}$$

It is easy to verify that there always exists a $k \in \mathcal{K}$ for which the selection law (2.17) holds and is equal to solution of (2.15) and (2.16) if the solution of latter pair exists. We now remark on an interesting connection between this cell selection criterion and the idea of cell selection bias used for load balancing.

Remark 1 (Connections with biasing)**.** *Note that* (2.17) *can be equivalently expressed as:*

$$\sqrt{\frac{\Psi_k}{\Delta_k}} P_k \Delta_k \|x_k\|^{-\alpha_k} \geq \sqrt{\frac{\Psi_i}{\Delta_i}} P_i \Delta_i \|x_i\|^{-\alpha_i} \quad \forall i \neq k, \tag{2.18}$$

where recall that $P_{rk}(x_k) = P_k \Delta_k \|x_k\|^{-\alpha_k}$ *is the average received power from a* k^{th} *tier BS located at* $x_k \in \Phi_k$*. The selection criterion can now be expressed in terms of the average received power as:*

$$\sqrt{\frac{\Psi_k}{\Delta_k}} P_{rk}(x_k) \geq \sqrt{\frac{\Psi_i}{\Delta_i}} P_{ri}(x_i) \quad \forall i \neq k, \tag{2.19}$$

where $B_k = \sqrt{\frac{\Psi_k}{\Delta_k}}$ *can be perceived as a "cell selection bias". Note that since* $\Psi_k = \Delta_k = 1 \; \forall k \in \mathcal{K}$ *in the SISO case, the above rule reduces to selecting the BS providing highest received power, which is also the SINR maximizing rule in the SISO case.*

Although (2.17) will be shown to be a more useful cell selection rule, it is in principle possible to derive other candidate laws, e.g., by adding the inequalities (2.15) and (2.16), we get:

$$P_k \left(\Delta_k + \Psi_k\right) \|x_k\|^{-\alpha_k} \geq P_i \left(\Delta_i + \Psi_i\right) \|x_i\|^{-\alpha_i} \quad \forall i \neq k, \tag{2.20}$$

which is also consistent with the biasing interpretation discussed in Remark 1. The bias that needs to be added to the received power (in dB) in this case is $B_k = 1 + \frac{\Psi_k}{\Delta_k}$. We will comment more on this alternate cell selection law in the numerical results section. After gaining these insights, we now investigate the cell selection criterion using the mean SINR expression in the following subsection.

2.4.3 Results from Mean SINR Expression

We first present an exact expression for the mean SINR. Using this expression, we will argue that the general form of the cell selection criterion given by (2.17) is possibly the more appropriate one to maximize the average SINR, which will further be validated in the numerical results section.

Lemma 1. *Given a realization ϕ of point process Φ, mean SINR at typical user (at origin) associated with a k^{th} tier BS situated at x_k is given as*

$$\mathbb{E}[\gamma_k|\phi] = \frac{P_k \Delta_k}{\|x_k\|^{\alpha_k}} \int_0^\infty \frac{e^{-NT}}{\prod_{y\in\phi\setminus x_k}(1+\frac{TP_j}{\|y\|^{\alpha_j}})^{\Psi_j}} \mathrm{d}T. \tag{2.21}$$

Proof.

$$\begin{aligned}\mathbb{E}[\gamma_k|\phi] &= \mathbb{E}\left[\frac{P_k h_{x_k k}\|x_k\|^{-\alpha_k}}{N+\sum_{j\in\mathcal{K}}\sum_{y\in\phi_j\setminus x_k} P_j g_{yj}\|y\|^{-\alpha_j}}\right] \\ &= \frac{P_k \mathbb{E}[h_{x_k k}]}{\|x_k\|^{\alpha_k}} \mathbb{E}\left[\frac{1}{N+\sum_{j\in\mathcal{K}}\sum_{y\in\phi_j\setminus x_k}\frac{P_j g_{yj}}{\|y\|^{\alpha_j}}}\right]\end{aligned}$$

Let F be an independent exponential random variable with mean 1, then the last term in the expression can be written as

$$\begin{aligned}\mathbb{E}\left[\frac{\mathbb{E}_F[F]}{N+\sum_{j\in\mathcal{K}}\sum_{y\in\phi_j\setminus x_k}\frac{P_j g_y}{\|y\|^{\alpha_j}}}\right] &= \mathbb{E}\left[\mathbb{E}_F\left[\frac{F}{N+\sum_{j\in\mathcal{K}}\sum_{y\in\phi_j\setminus x_k}\frac{P_j g_y}{\|y\|^{\alpha_j}}}\right]\right] \\ &= \int_0^\infty \mathbb{P}\left[\frac{F}{N+\sum_{j\in\mathcal{K}}\sum_{y\in\phi_j\setminus x_k}\frac{P_j g_{yj}}{\|y\|^{\alpha_j}}} > T\right]\mathrm{d}T \\ &= \int_0^\infty \mathbb{E}[e^{-NT-T\sum_{j\in\mathcal{K}}\sum_{y\in\phi_j\setminus x_k} P_j g_{yj}\|y\|^{-\alpha_j}}]\mathrm{d}T \\ &= \int_0^\infty e^{-NT}\prod_{j\in\mathcal{K}}\prod_{y\in\phi_j\setminus x_k}\mathbb{E}[e^{-TP_j g_{yj}\|y\|^{-\alpha_j}}]\mathrm{d}T\end{aligned}$$

$$= \int_0^{\infty} e^{-NT} \prod_{j\in\mathcal{K}} \prod_{y\in\phi_j\setminus x_k} \frac{1}{\left(1+TP_j\|y\|^{-\alpha_j}\right)^{\Psi_j}} \mathrm{d}T.$$

Note that the insertion of random variable F makes the calculation simple and does not change the integral due to independence assumption. □

Using the same setup as Section 2.4.1, where we focused on the selection of two BSs $x_k \in \Phi_k$ and $x_j \in \Phi_j$, and represented to thermal noise plus interference from all the other BSs except x_k and x_j by W, we can argue that a simple selection criterion very similar to the one given by (2.17) can be derived directly form the expressions of the mean SINR. The result is given in the following Lemma.

Lemma 2. *The mean SINR of a k^{th} tier BS at x_k at typical user at origin is greater than the mean SINR of a j^{th} tier BS at x_j if*

$$\frac{P_{rk}e^{-\frac{W\Delta_k}{P_{rk}}}\left(\frac{P_{rk}}{\Delta_k}\right)^{\Psi_k}}{W^{\Psi_k-1}\Gamma(1-\Psi_k,\frac{W\Delta_k}{P_{rk}})} > \frac{P_{rj}e^{-\frac{W\Delta_j}{P_{rj}}}\left(\frac{P_{rj}}{\Delta_j}\right)^{\Psi_j}}{W^{\Psi_j-1}\Gamma(1-\Psi_j,\frac{W\Delta_j}{P_{rj}})} \tag{2.22}$$

with the assumption that the interference from all other BSs and noise is fixed and denoted by residue W. Here $P_{ri} = P_{ri}(x_i)$ is the average received power from i^{th} tier BS situated at x_i for $i = j, k$ and $\Gamma(\cdot,\cdot)$ is the incomplete Gamma function. With the further assumption $W = 0$, the above selection criterion can be simplified to

$$P_{rk}\sqrt{\frac{(\Psi_k-1)}{\Delta_k}} > P_{rj}\sqrt{\frac{(\Psi_j-1)}{\Delta_j}}. \tag{2.23}$$

Proof. Using a similar idea as Lemma 1, the mean SINR for BS at x_k conditional on BS locations for the assumed case is given as

$$\mathbb{E}[\gamma_k|\phi] = P_{rk}\int_0^{\infty} e^{-WT}\frac{1}{\left(1+TP_j\|x_j\|^{-\alpha_j}\right)^{\Psi_j}}\mathrm{d}T.$$

Substituting $W(1+P_j\|x_j\|^{-\alpha_j}T) = P_j\|x_j\|^{-\alpha_j}y = P_{rj}y/\Delta_j$, the above expression simplifies to

$$\begin{aligned}\mathbb{E}[\gamma_k|\phi] &= P_{rk}e^{W\Delta_j/P_{rj}}\frac{W^{\Psi_j-1}}{(P_{rj}/\Delta_j)^{\Psi_j}}\int\limits_{W\Delta_j/P_{rj}}^{\infty} e^{-y}\frac{1}{y^{\Psi_j}}\mathrm{d}y \\ &= P_{rk}e^{W\Delta_j/a_j}\frac{W^{\Psi_j-1}}{(P_{rj}/\Delta_j)^{\Psi_j}}\Gamma\left(1-\Psi_j,\frac{W\Delta_j}{P_{rj}}\right),\end{aligned}$$

which leads to the first rule in the lemma. Further taking the limit $W\to 0$, and using the fact that $\lim_{x\to 0}\frac{\Gamma(-a,x)}{x^a} = \frac{1}{a}; a>0$, we get

$$\begin{aligned}\mathbb{E}[\gamma_k] &= P_{rk}e^{\frac{W\Delta_j}{P_{rj}}}\lim_{W\to 0}\frac{W^{\Psi_j-1}}{(P_{rj}/\Delta_j)^{\Psi_j}}\Gamma\left(1-\Psi_j,\frac{W\Delta_j}{P_{rj}}\right) \\ &= \Delta_j\frac{P_{rk}}{P_{rj}}\lim_{W\to 0}\left(\frac{W\Delta_j}{P_{rj}}\right)^{\Psi_j-1}\Gamma\left(1-\Psi_j,\frac{W\Delta_j}{P_{rj}}\right) \\ &= \frac{\Delta_j}{\Psi_j-1}\frac{P_{rk}}{P_{rj}}\end{aligned}$$

which leads to the second rule. □

The above discussions provide enough evidence that a selection-bias based criterion is a meaningful option for cell selection in multi-antenna HetNets. Although in the previous lemma, we have taken W to be a fixed constant which is generally not the case, still it indicates that taking the multiplicative form of sufficient conditions, i.e., (2.17) is a better candidate function. As validated in the numerical results section, the bias value of $B_k = \sqrt{\frac{\Psi_k}{\Delta_k}}$ is surprisingly accurate for SINR, and hence coverage, maximization. Note, however, that this choice of selection bias is not necessarily optimal for other metrics considered in this paper, e.g., rate coverage. Therefore, to maintain generality, we derive all the results in terms of an arbitrary cell-selection

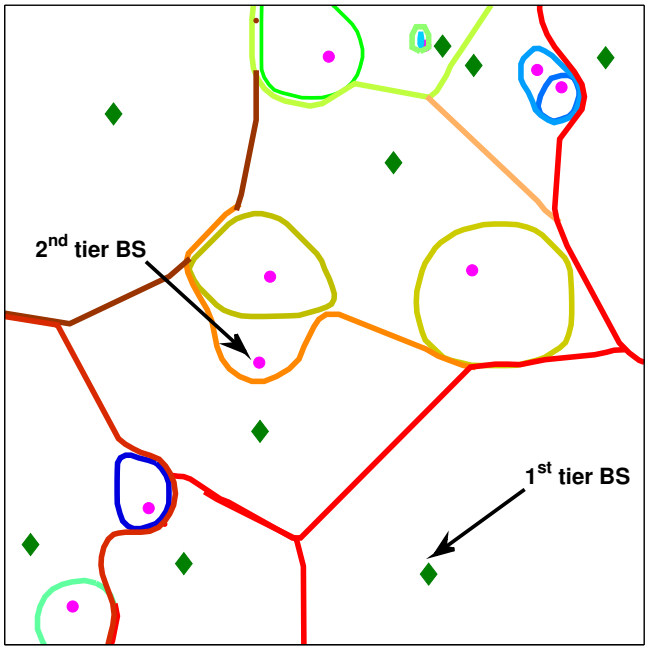

(a)

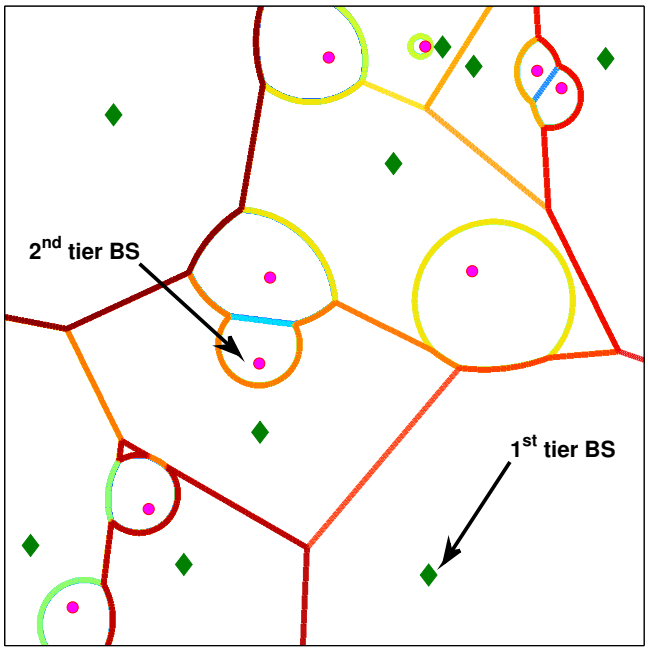

(b)

Figure 2.2: Cell Selection region for $P_1 = 5P_2, \lambda_1 = \lambda_2, \Psi = [3, 2], \Delta = [2, 1]$: (a) from simulation, where selection is based on highest mean SINR, and (b) from theory, where selection is based on Lemma 2.

bias term B_k, i.e., a user selects a nearest BS of k^{th} tier if

$$k = \arg\max_{j \in \mathcal{K}} B_j P_j \Delta_j \|x_j\|^{-\alpha_j}. \tag{2.24}$$

2.4.4 Association Region

Under the selection rule discussed in the previous section, a typical user selects a BS that provides the maximum "biased" received power, where the bias values are tuned according to the metric that is being maximized. This creates exclusion regions around a typical user in which the interfering BSs can not lie. These exclusion regions are characterized in the following Lemma.

Lemma 3. *A typical user selects k^{th} tier BS located at a distance d_k if the closest BSs of all the other tiers, located at distance $d_j, j \neq k$, satisfy the following condition*

$$d_j \;\geq\; \left(\widehat{P}_j \widehat{B}_j \widehat{\Delta}_j\right)^{\frac{1}{\alpha_j}} {d_k}^{\frac{1}{\widehat{\alpha}_j}}, \tag{2.25}$$

where $\widehat{P}_j = P_j/P_k$ and similarly for $\widehat{B}_j, \widehat{\Delta}_j$ and $\widehat{\alpha}_j$.

Proof. A user is associated with tier k^{th} if other tier BS distances d_j satisfies following relation for all j,

$$\begin{aligned} P_{rj} B_j &\leq P_{rk} B_k \\ P_j \Delta_j (d_j)^{-\alpha_j} B_j &\leq P_k \Delta_k (d_k)^{-\alpha_k} B_k \\ d_j &\geq \left(\widehat{P_j}\widehat{\Delta_j}\widehat{B_j}\right)^{1/\alpha_j} {d_k}^{1/\widehat{\alpha_j}}, \end{aligned}$$

where $\widehat{f_j} = f_j/f_k$. □

Due to the nature of the cell selection rule, all the interfering BSs will satisfy (2.25). Lemma 3 shows that association regions are weighted Voronoi regions where weights are not just equal to the received power but also include a bias term which accounts for minimizing the interference. To justify our model, we compare it with a simulated mean SINR based selection model. First, the locations of the BSs are sampled from a PPP over a small spatial window. Then, the received SINR from each BS is computed for every point (on a grid) in the space according to appropriate fading distribution. Fig. 2.2(a) shows the simulated coverage area where the user connects to the BS having best mean SINR (averaged over fading) conditioned on the given realization of BSs' positions whereas Fig. 2.2(b) shows the coverage area based on approximate modified bias association region for the same realization of BSs' locations. For this particular realization, the error region where the above two regions do not match is 0.3 percentage of the total simulated area which is surprisingly accurate given the simple biasing-based approach used for the second plot.

Fig. 2.3 compares the coverage regions of a SISO and multi-antenna HetNet with the same BS locations. For the multi-antenna HetNet, we consider two different cell selection rules: i) based on max received power, ii) based on max mean SINR. For the SISO HetNet, both these selection rules are exactly the same. As it can be seen that using multiple antennas and SDMA at the small cells includes a natural bias for these cells and therefore results in expansion of their coverage regions. This expansion naturally balances load across tiers and hence reduces the need for artificial bias to offload sufficient traffic to small cells compared to SISO HetNets. In the following example, we provide a useful insight into the selection of multi-antenna techniques

for maximum expansion of the coverage regions of small cells with no external bias.

Example 3 (Coverage expansion)**.** *Consider a two-tier SISO HetNet consisting of macrocells and femtocells. Owing to their smaller transmit powers, femtocells have smaller coverage regions, which results in imbalanced load and degrades performance, especially in terms of rate [58]. However, the coverage regions of the femtocells can be naturally expanded by using multi-antenna transmission. For the sake of argument, assume that the number of antennas per femtocell in the new setup is* $M = 8$*, while the macrocells still have* 1 *antenna per BS. If cell-selection is based on maximum received power, optimal strategy is to maximize* Δ*, which is achieved by single-user beamforming, i.e.,* $\Delta = 8$ *and* $\Psi = 1$*. On the other hand, if the goal is to maximize the average SINR, the optimal strategy is the one that maximizes* $\sqrt{\Delta\Psi}$*. This is achieved under SDMA with* $\Delta = 5$ *and* $\Psi = 4$*. The sub-optimality of single-user beamforming for SINR maximization is counter-intuitive since single-user beamforming is mostly associated with range expansion of wireless links.*

With these insights, we now derive the cell selection or cell association probability, which is the probability with which a typical user selects a k^{th} tier BS.

Lemma 4. *The probability that a typical user is associated with a* k^{th} *tier BS is given as*

$$A_k \;=\; 2\pi\lambda_k \int_0^{\infty} e^{-\pi \sum_j \lambda_j \left(\widehat{P}_j \widehat{\Delta}_j \widehat{B}_j\right)^{\frac{2}{\alpha_j}} r^{\frac{2}{\alpha_j}}} r \mathrm{d}r.$$

If $\alpha_j = \alpha \; \forall j$*, the above can be simplified to*

$$A_k \;=\; \frac{\lambda_k}{\sum_j \lambda_j \left(\widehat{P}_j \widehat{\Delta}_j \widehat{B}_j\right)^{\frac{2}{\alpha}}}.$$

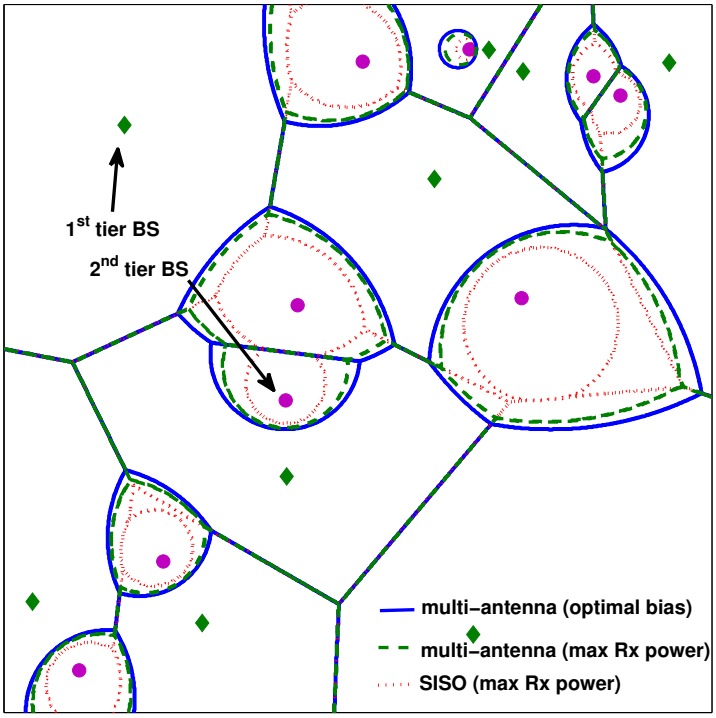

Figure 2.3: The expanding of the coverage regions due to inherent biasing in two-tier multi-antenna HetNet with $\Psi_1 = 1; \Psi_2 = 6; P = [30; 1]; \Delta = [1; 3]$. In this hypothetical case, small cells (denoted by filled circle) use 8 antennas and schedule 3 users per resource block per BS. Macrocell BS (denoted by diamonds) have single antenna per BS.

Proof. The proof is the same as [18, Lemma 1], hence skipped. □

2.5 Coverage Probability

In this section, we will compute the coverage probability of a typical user. Recall that the coverage probability is the probability that SINR at a typical user from the associated tier is above some threshold T and can be given for a heterogeneous

multi-tier network as

$$\mathrm{P_c} = \sum_{k=1}^{K} \mathbb{P}[\gamma_k > T, k = \text{associated tier}]. \tag{2.26}$$

For the mean SINR association model, the coverage probability is given as

$$\mathrm{P_c} = \sum_{k=1}^{K} \mathbb{E}_{\Phi_k}\left[\mathbb{1}_{(\gamma(x_k)>T)}\mathbb{1}_{(S_{x_k,\phi}\geq S_{y,\phi}\ \forall y\in\phi\setminus x_k)}\right] \tag{2.27}$$

where γ_k and $\mathbb{E}[\gamma_k|\phi]$ are given by (2.2) and (2.21) and $S_{y,\phi} = \mathbb{E}[\gamma(y)|\phi]$.

The above expression is quite complicated and will need the higher order factorial moments of a PPP. For the rest of this discussion, we will assume the selection bias-based model discussed in previous section. For this model, $S_k = P_{rk}B_k$ and we can further simplify the expression (2.27) using iterative conditioning and get

$$\mathrm{P_c} = \quad 2\pi\sum_{k=1}^{K}\lambda_k\int_0^{\infty}\mathbb{P}\left(P_k h_{xk}\|x\|^{-\alpha_k} > T(N + I_{\Phi'})\right)e^{-\sum_{j=1}^{K}\lambda_j\pi(\widehat{P}_j\widehat{\Delta}_j\widehat{B}_j)^{\frac{2}{\alpha_j}}x^{\frac{2}{\widehat{\alpha}_j}}}x\mathrm{d}x, \tag{2.28}$$

where $\Phi^{'}$ is

$$\Phi^{'} = \cup_{k=1}^{K}\Phi_k \cap B\left(0, (\widehat{P}_j\widehat{\Delta}_j\widehat{B}_j)^{\frac{1}{\alpha_j}}x^{\frac{1}{\widehat{\alpha}_j}}\right)^c, \tag{2.29}$$

where $B(0,r)$ is open ball around origin with radius r and $(.)^c$ denotes the set complement. The Proof of (2.28) is given as follows:

Proof. For notational simplicity, let

$$\begin{aligned} e_k(x_k, \phi\setminus x_k) &= \mathbb{1}(S_{x_k} \geq S_y\ \forall y \in \phi\setminus x_k) \\ &= \mathbb{1}\left(\|y\| \geq (\widehat{P}_j\widehat{\Delta}_j\widehat{B}_j)^{\frac{1}{\alpha_j}}\|x_k\|^{\frac{2}{\widehat{\alpha}_j}}\ \forall y \in \phi\setminus x_k\right), \end{aligned}$$

then

$$
\begin{aligned}
\mathrm{P_c} &= \sum_{k=1}^{K} \mathbb{E}_{\Phi_k}\left[\mathbb{1}\left(\frac{P_k h_{x_k k}}{\|x_k\|^{\alpha_k}} > T(N + I_{\Phi\setminus x_k})\right) e_k(x_k,\phi)\right] \\
&\overset{(a)}{=} \sum_{k=1}^{K} \lambda_k \int_0^{\infty} \mathbb{P}\left[\frac{P_k h_{x_k k}}{\|x_k\|^{\alpha_k}} > T(N + I_{\Phi}), e_k(x_k,\phi)\right] \mathrm{d}x_k \\
&= \sum_{k=1}^{K} \lambda_k \int_0^{\infty} \mathbb{P}\left(\frac{P_k h_{x_k k}}{\|x_k\|^{\alpha_k}} > T(N + I_{\Phi}) | e_k(x_k,\phi)\right) \cdot \\
&\quad \mathbb{P}\left(\|y\| \geq (\widehat{P}_j \widehat{\Delta}_j \widehat{B}_j)^{\frac{1}{\alpha_j}} \|x_k\|^{\frac{1}{\widehat{\alpha}_j}} \ \forall y \in \Phi\right) \mathrm{d}x_k \\
&\overset{(b)}{=} \sum_{k=1}^{K} \lambda_k \int_0^{\infty} \mathbb{P}\left(P_k h_{x_k k} \|x_k\|^{-\alpha_k} > T(N + I_{\Phi'})\right) e^{-\sum_{j=1}^{K} \lambda_j \pi (\widehat{P}_j \widehat{\Delta}_j \widehat{B}_j)^{\frac{2}{\alpha_j}} \|x_k\|^{\frac{2}{\widehat{\alpha}_j}}} \mathrm{d}x_k \\
&\overset{(c)}{=} 2\pi \sum_{k=1}^{K} \lambda_k \int_0^{\infty} \mathbb{P}\left(P_k h_{x k} \|x\|^{-\alpha_k} > T(N + I_{\Phi'})\right) e^{-\sum_{j=1}^{K} \lambda_j \pi (\widehat{P}_j \widehat{\Delta}_j \widehat{B}_j)^{\frac{2}{\alpha_j}} x^{\frac{2}{\widehat{\alpha}_j}}} x \mathrm{d}x,
\end{aligned}
$$

where $\Phi^{'}$ is

$$
\Phi^{'} = \cup_{k=1}^{K} \Phi_k \cap B\left(0, (\widehat{P}_j \widehat{\Delta}_j \widehat{B}_j)^{\frac{1}{\alpha_j}} x^{\frac{1}{\widehat{\alpha}_j}}\right)^{c}, \tag{2.30}
$$

where $B(0,r)$ is open ball around origin with radius r and $(.)^c$ denotes the set complement. Here (a) is due to Cambell-Mecke's formula [63] and Slivnyak's theorem, (b) follows from the basic properties of a PPP, and (c) by converting to polar coordinates: $\|x_k\| \to x$. This completes the proof. □

In the following subsections, we will compute the probability term inside the integral in (2.28), which can be interpreted as the CCDF of SINR at a typical user associated with a k^{th} tier BS located at $x_k \in \Phi_k$. Before going into further details, it is important to understand the resulting form of this term. Since SINR at a typical user depends only on the magnitude of x_k, i.e., the distance of BS $x_k \in \Phi_k$ from

the origin, we will denote SINR by $\gamma_k(x_k) = \gamma_k(\|x_k\|)$ with slight abuse of notation. Letting $\|x_k\| = x$, the CCDF of SINR can be expressed as

$$\begin{aligned}
\mathbb{P}[\gamma_k(x) > T] &= \mathbb{P}[P_k h_{xk} x^{-\alpha_k} > T(I+N)] \\
&= \mathbb{P}[h_{xk} > T P_k^{-1} x^{\alpha_k}(I+N)] \\
&= \sum_{i=0}^{\Delta_k - 1} \frac{1}{i!} \mathbb{E}\left[[-s(I+N)]^i e^{[-s(I+N)]}\right] \\
&= \sum_{i=0}^{\Delta_k - 1} \frac{1}{i!} (-s)^i \frac{\mathrm{d}^i}{\mathrm{d}s^i} \left[\mathbb{E}\left[e^{-s(I+N)}\right]\right], \qquad (2.31)
\end{aligned}$$

with $s = T P_k^{-1} x^{\alpha_k}$. As is clear from (2.31), we will not only need the Laplace transform of the interference but also its derivatives, which we compute in the following subsections.

2.5.1 Laplace Transform of Noise Plus Interference

Since the typical user is associated with a k^{th} tier BS located at x_k with $\|x_k\| = x$, all the other BSs satisfy (2.25) and are therefore located outside the ball of radius r_j, where

$$r_j = \left(\widehat{P}_j \widehat{\Delta}_j \widehat{B}_j\right)^{\frac{1}{\alpha_j}} x^{\frac{1}{\widehat{\alpha}_j}}.$$

for all $j = 1, 2, \cdots K$.

Theorem 1. *The Laplace transform of the noise plus interference from all BSs at a typical user associated with a k^{th} tier BS located at a distance $x = \|x_k\|, x_k \in \Phi_k$, is given by*

$$\mathcal{L}_{IN}(s) = e^{-sN} \exp\left[-2\pi \sum_{j=1}^{K} \frac{\lambda_j}{\alpha_j} (sP_j)^{\frac{2}{\alpha_j}} \sum_{m=1}^{\Psi_j} \binom{\Psi_j}{m}\right.$$

$$B'\left(\Psi_j - m + \frac{2}{\alpha_j}, m - \frac{2}{\alpha_j}, \frac{1}{1+\frac{sP_j x^{-\alpha_k}}{\left(\widehat{P}_j\widehat{\Delta}_j\widehat{B}_j\right)}}\right)\Bigg], \tag{2.32}$$

where $B'(a,b,c)$ is the complementary incomplete Beta function defined as

$$B'(a,b,z) \;=\; \int_z^1 u^{a-1}(1-u)^{b-1}\mathrm{d}u.$$

Proof. Laplace transform of the sum interference caused by j^{th} tier BSs is due to all j^{th} tier BSs outside the ball $B(0,r_j)$ where $r_j = \left(\widehat{P}_j\widehat{\Delta}_j\widehat{B}_j\right)^{1/\alpha_j} x^{1/\widehat{\alpha_j}}$ is given by $\mathcal{L}_j(s) = \mathbb{E}[e^{-sI_j}] =$

$$\begin{aligned}
&\mathbb{E}\left[\exp\left\{-s\sum_{y\in\Phi_j\setminus B(0,r_j)} P_j g_{yj}||y||^{-\alpha_j}\right\}\right]\\
&=\exp\left[-\lambda_j\int_{\mathbb{R}^2\setminus B(0,r_j)} 1-E_{g_{yj}}[e^{-sP_j g_{yj}||y||^{-\alpha_j}}]dy\right]\\
&=\exp\left[-2\pi\lambda_j\int_{r_j}^{\infty} 1-E_{g_{rj}}[e^{-sP_j g_{rj}r^{-\alpha_j}}]rdr\right]\\
&=\exp\left[-2\pi\lambda_j\int_{r_j}^{\infty}\left(1-\frac{1}{(1+sP_j r^{-\alpha_j})^{\Psi_j}}\right)rdr\right]\\
&\overset{(a)}{=}\exp\left[-2\pi\lambda_j(sP_j)^{\frac{2}{\alpha_j}}\int_{t_j}^{\infty}\left(1-\frac{1}{(1+t^{-\alpha_j})^{\Psi_j}}\right)tdt\right]\\
&\overset{(b)}{=}\exp\left[-2\pi\lambda_j(sP_j)^{\frac{2}{\alpha_j}}\sum_{m=1}^{\Psi_j}\binom{n}{k}\int_{t_j}^{\infty}\left(\frac{t^{-\alpha_j m}}{(1+t^{-\alpha_j})^{\Psi_j}}\right)tdt\right]\\
&\overset{(c)}{=}\exp\left[-2\pi\frac{\lambda_j}{\alpha_j}(sP_j)^{\frac{2}{\alpha_j}}\sum_{m=1}^{\Psi_j}\binom{n}{k}\int_{u_j}^{1} u^{\Psi_j-1-m+\frac{2}{\alpha_j}}(1-u)^{m-\frac{2}{\alpha_j}-1}\mathrm{d}u\right]
\end{aligned}$$

$$\stackrel{(d)}{=} \exp\left[-2\pi\frac{\lambda_j}{\alpha_j}(sP_j)^{\frac{2}{\alpha_j}}\sum_{m=1}^{\Psi_j}\binom{n}{k}B'\left(\Psi_j-m+\frac{2}{\alpha_j},m-\frac{2}{\alpha_j},u_j\right)\right]$$

with limits as

$$t_j = (sP_j)^{-1/\alpha_j}r_j$$
$$u_j = \frac{1}{1+t_j^{-\alpha_j}} = \frac{1}{1+sP_j\left(\widehat{P}_j\widehat{\Delta}_j\widehat{B}_j\right)^{-1}x^{-\alpha_k}},$$

where (a) follows from substituting $(sP_j)^{-1/\alpha_j}r \to t$, (b) follows from binomial expansion and (c) follows from $1/(1+t^{-\alpha}) \to u$. In (d), we defined $B'(a,b,c)$ as the complimentary incomplete Beta function as

$$B'(a,b,z) = \int_z^1 u^{a-1}(1-u)^{b-1}\mathrm{d}u.$$

The Laplace transform of sum of aggregate interference from all BS and noise is equal to

$$\mathcal{L}_{IN}(s) = E[e^{-s(I+N)}] = e^{-sN}\mathbb{E}\left[e^{-\sum_{j=1}^{K}I_j}\right] \stackrel{(e)}{=} e^{sN}\prod_{j=1}^{K}\mathbb{E}\left[e^{-I_j}\right],$$

where (e) follows from independence of BS point processes among tiers. □

Corollary 1. *The Laplace transform of the noise plus interference at $s = TP_k^{-1}x^{\alpha_k}$ is given as*

$$\mathcal{L}_{IN}(TP_k^{-1}x^{\alpha_k}) \;=\; e^{-TP_k^{-1}x^{\alpha_k}N}e^{\left[-\sum_{j=1}^{K}\lambda_j(T\widehat{P}_j)^{\frac{2}{\alpha_j}}x^{\frac{2}{\widehat{\alpha}_j}}\mathcal{C}_j\right]},$$

where $\mathcal{C}_j$ is defined as

$$\mathcal{C}_j \stackrel{\Delta}{=} \frac{2\pi}{\alpha_j}\sum_{m=1}^{\Psi_j}\binom{\Psi_j}{m}B'\left(\Psi_j-m+\frac{2}{\alpha_j},m-\frac{2}{\alpha_j},\frac{1}{1+\frac{T}{\widehat{\Delta}_j\widehat{B}_j}}\right).$$

Further, if $\alpha_j = \alpha \ \forall j$, the Laplace transform of the noise plus interference at $s = TP_k^{-1}x^{\alpha}$ is

$$\mathcal{L}_{IN}(TP_k^{-1}x^{\alpha}) \ = \ e^{-TP_k^{-1}Nx^{\alpha}-\left[\sum_{j=1}^{K}\lambda_j(T\widehat{P}_j)^{\frac{2}{\alpha}}\mathcal{C}_j\right]x^2}.$$

2.5.2 Derivatives of the Laplace Transform

We now provide an expression for the derivative of the Laplace transform along with a brief sketch of the proof. The proof is based on the tools developed in [22].

Theorem 2. *The n^{th} derivative of the Laplace transform of noise plus interference (computed in section III-A) is given as*

$$\frac{\mathrm{d}^n}{\mathrm{d}s^n}\mathcal{L}_{IN}(s) = \mathcal{L}_{IN}(s)\sum_{\bar{m}\in M}C(\bar{m})\cdot\prod_{l=1}^{n}\left(-N\mathbb{1}_{l=1}+2\pi\sum_{j=1}^{K}(-1)^l D_j(l)P_j^l(sP_j)^{\frac{2}{\alpha_j}-l}\right)^{m_l},$$

where

$$\begin{aligned}
M(n) &= \{\bar{m}=(m_1,m_2,\cdots m_n)^T : \sum_{i=1}^{n} i m_i = n\} \\
C(\bar{m}) &= \frac{n!}{\prod_i (m_i!(i!)^{m_i})} \\
D_j(l) &= \frac{\lambda_j}{\alpha_j}\frac{(\Psi_j+l-1)!}{(\Psi_j-1)!}B'\left(\Psi_j+\frac{2}{\alpha_j}, l-\frac{2}{\alpha_j}, u_j\right) \\
u_j &= \frac{1}{1+\frac{sP_jx^{-\alpha_k}}{(\widehat{P}_j\widehat{\Delta}_j\widehat{B}_j)}}.
\end{aligned}$$

Proof. The Laplace transform of noise plus interference $\mathcal{L}_{IN}(s)$ can be written as $f(g(s))$ where $f(x) = \exp(x)$ and $g(s) =$

$$-sN + 2\pi\sum_{j=1}^{K}\lambda_j\int_{r_j}^{\infty}\left(-1+\frac{1}{(1+sP_jr^{-\alpha_j})^{\Psi_j}}\right)r\mathrm{d}r. \tag{2.33}$$

Using Faà di Bruno lemma, n^{th} derivative can be written as $\frac{d^n\mathcal{L}_{IN}(s)}{ds^n} =$

$$\frac{\mathrm{d}^n f(g(s))}{\mathrm{d}s^n} = \sum_{\bar{m}\in M} C(\bar{m}) f^{1^T\bar{m}}(g(s)) \prod_{l=1}^{n} \left(g^{(l)}(s)\right)^{m_l}. \tag{2.34}$$

The l^{th} derivatives of $g(s)$ can be computed as

$$\begin{aligned} g^{(l)}(s) &= -N\mathbb{1}_{l=1} + 2\pi \sum_{j=1}^{K} \lambda_j (-1)^l \frac{(\Psi_j + l - 1)!}{(\Psi_j - 1)!} P_j^l \int_{r_j}^{\infty} \frac{r^{1-l\alpha_j}}{\left(1 + sP_j r^{-\alpha_j}\right)^{\Psi_j + l}} \mathrm{d}r \\ &\overset{(a)}{=} -N\mathbb{1}_{l=1} + 2\pi \sum_{j=1}^{K} (-1)^l D_j(l) P_j^l (sP_j)^{\frac{2}{\alpha_j} - l} \end{aligned}$$

where (a) can be computed using the similar transformations as used in computing Laplace transform of noise plus interference as in the proof of the Theorem 1. □

For the interference limited case, the above expression can be simplified further and is given in the following Corollary.

Corollary 2. *If $\alpha_j = \alpha\ \forall j$ and noise $N = 0$, for $s = TP_k^{-1}x^{\alpha}$,*

$$\frac{\mathrm{d}^n\mathcal{L}_I(s)}{\mathrm{d}s^n} = e^{-\left[\sum_{j=1}^{K} \lambda_j (T\widehat{P}_j)^{\frac{2}{\alpha}} \mathcal{C}_j\right] x^2} \sum_{\bar{m}\in M} C(\bar{m}) x^{-n\alpha + 2\sum m_l} (-1)^n F(\bar{m}), \tag{2.35}$$

where

$$F(\bar{m}) \triangleq \frac{(2\pi)^{\sum m_l}}{\left(TP_k^{-1}\right)^{-\frac{2}{\alpha}\sum m_l + n}} \prod_{l=1}^{n} \left(\sum_{j=1}^{K} D_j(l) P_j^{\frac{2}{\alpha}} \right)^{m_l}$$

with $u_j = \frac{1}{1 + \frac{T}{\widehat{\Delta}_j \widehat{B}_j}}$.

Proof. The result follows simply by substituting $\alpha_j = \alpha, \widehat{\alpha}_j = 1, N = 0$, taking terms containing x out of the product and using the fact that $\prod_{l=1}^{n} \left(x^{t-l}\right)^{m_l} = x^{t(\sum m_l) - n}$. □

2.5.3 SINR Distribution

Using (2.31) and the results derived in the previous two subsections, we can now compute the CCDF of SINR, which is given by the following Lemma.

Lemma 5. *The CCDF of SINR at a typical user associated with the k^{th} tier BS located at a distance x from the user is* $\mathbb{P}[\gamma_k(x) > T] =$

$$\sum_{n=0}^{\Delta_k-1} \frac{(-1)^n T^n x^{n\alpha_k}}{n! P_k^n} e^{-\frac{Tx^{\alpha_k} N}{P_k}} \cdot$$
$$e^{-\sum_{j=1}^{K} \lambda_j (T\widehat{P}_j)^{\frac{2}{\alpha_j}} x^{\frac{2}{\widehat{\alpha}_j}} \mathcal{C}_j} \sum_{\bar{m}\in M} C(\bar{m}) \prod_{l=1}^{n} \left(N\mathbb{1}_{l=1} + 2\pi \sum_{j=1}^{K} (-1)^l D_j(l) P_j^l (T\widehat{P}_j)^{\frac{2}{\alpha_j}-l} \frac{x^{\frac{2}{\widehat{\alpha}_j}}}{x^{l\alpha_k}} \right)^{m_l} \tag{2.36}$$

with $u_j = \frac{1}{1+\frac{T}{\widehat{\Delta}_j \widehat{B}_j}}$.

Proof. Using expressions of $\mathcal{L}_{IN}$ and its derivatives, we can write (2.31) as

$$P[\gamma_k(x) > T] = \sum_{n=0}^{\Delta_k-1} \frac{1}{n!}(-s)^n \frac{\mathrm{d}^n}{\mathrm{d}s^n} \mathbb{E}\left[e^{-s(I+N)}\right]$$
$$= \sum_{n=0}^{\Delta_k-1} \frac{1}{n!}(-s)^n \mathcal{L}_{IN}(s) \sum_{\bar{m}\in M} C(\bar{m}) \prod_{j=1}^{n} \left(N\mathbb{1}_{l=1} + 2\pi \sum_{j=1}^{K} (-1)^l D_j(l) (sP_j)^{\frac{2}{\alpha_j}-l} \right)^{m_j}$$

with $s = TP_k^{-1} x^{\alpha_k}$. □

Corollary 3. *If we assume $\alpha_j = \alpha \ \forall j$ and interference limited case ($N = 0$), the CCDF of SINR at typical user is given by* $P[\gamma_k(x) > T] =$

$$\sum_{n=0}^{\Delta_k-1} \frac{1}{n!}(-TP_k^{-1}x^{\alpha})^n e^{-\left[\sum_{j=1}^{K} \lambda_j (T\widehat{P}_j)^{\frac{2}{\alpha}} \mathcal{C}_j\right] x^2} \sum_{\bar{m}\in M} C(\bar{m}) x^{-n\alpha+2\sum m_l} (-1)^n F(\bar{m})$$
$$= \sum_{n=0}^{\Delta_k-1} \frac{1}{n!}(TP_k^{-1})^n \sum_{\bar{m}\in M} C(\bar{m}) F(\bar{m}) e^{-\left[\sum_{j=1}^{K} \lambda_j (T\widehat{P}_j)^{\frac{2}{\alpha}} \mathcal{C}_j\right] x^2} x^{2\sum m_l}.$$

2.5.4 Coverage Probability

Substituting the SINR CCDF given by Theorem 5 in (2.28), we can compute the coverage probability, which is given by the following Theorem.

Theorem 3. *Coverage probability of a typical user is* $\mathrm{P_c} =$

$$\sum_{k=1}^{K} 2\pi\lambda_k \int_0^{\infty} \sum_{n=0}^{\Delta_k-1} \frac{1}{n!}(-TP_k^{-1}x^{\alpha_k})^n e^{-TP_k^{-1}x^{\alpha_k}N} e^{-\sum_{j=1}^{K}\lambda_j(T\widehat{P}_j)^{\frac{2}{\alpha_j}}x^{\frac{2}{\alpha_j}}\mathcal{C}_j} \sum_{\bar{m}\in M} C(\bar{m})\cdot$$
$$\prod_{l=1}^{n}\left(N\mathbb{1}_{l=1} + 2\pi\sum_{j=1}^{K}(-1)^l D_j(l) P_j^l (T\widehat{P}_j)^{\frac{2}{\alpha_j}-l} \frac{x^{\frac{2}{\widehat{\alpha}_j}}}{x^{l\alpha_k}}\right)^{m_l} x e^{-\pi\sum_{j=1}^{K}\lambda_j(\widehat{P}_j\widehat{\Delta}_j\widehat{B}_j)^{\frac{2}{\alpha_j}}x^{\frac{2}{\widehat{\alpha}_j}}}\mathrm{d}x$$

with $u_j = \frac{1}{1+\frac{T}{\widehat{\Delta}_j\widehat{B}_j}}$.

Corollary 4. *If we assume* $\alpha_j = \alpha\ \forall j$ *and interference limited case* ($N = 0$)*, the coverage probability of a typical user is given as* $\mathrm{P_c} =$

$$\sum_{k=1}^{K}\pi\lambda_k \sum_{n=0}^{\Delta_k-1}\frac{1}{n!}(TP_k^{-1})^n \sum_{\bar{m}\in M}\frac{C(\bar{m})F(\bar{m})\Gamma(\sum m_l+1)}{\left[\sum_{j=1}^{K}\lambda_j(T\widehat{P}_j)^{\frac{2}{\alpha}}\mathcal{C}_j + \pi\sum_{j=1}^{K}\lambda_j(\widehat{P}_j\widehat{\Delta}_j\widehat{B}_j)^{\frac{2}{\alpha}}\right]^{\sum m_l+1}} \tag{2.37}$$

Proof. For this case, the coverage probability is

$$\begin{aligned}
P_c =& 2\pi\lambda_k \int_0^{\infty}\sum_{n=0}^{\Delta_k-1}\frac{1}{n!}(TP_k^{-1})^n\cdot \\
&\sum_{\bar{m}\in M} C(\bar{m})F(\bar{m}) e^{-\left[\sum_{j=1}^{K}\lambda_j(T\widehat{P_j})^{\frac{2}{\alpha}}\mathcal{C}_j\right]x^2} x^{2\sum m_l} x e^{-\pi\sum_{j=1}^{K}\lambda_j(\widehat{P_j}\widehat{\Delta_j}\widehat{B_j})^{2/\alpha}x^2}\mathrm{d}x \\
=& 2\pi\lambda_k \sum_{n=0}^{\Delta_k-1}\frac{1}{n!}(TP_k^{-1})^n \\
&\sum_{\bar{m}\in M} C(\bar{m})F(\bar{m}) \int_0^{\infty} e^{-\left[\sum_{j=1}^{K}\lambda_j(T\widehat{P_j})^{\frac{2}{\alpha}}\mathcal{C}_j\right]x^2} e^{-\left[\pi\sum_{j=1}^{K}\lambda_j(\widehat{P_j}\widehat{\Delta_j}\widehat{B_j})^{2/\alpha}\right]x^2} x^{1+2\sum m_l}\mathrm{d}x
\end{aligned}$$

$$\stackrel{(a)}{=}\pi\lambda_k \sum_{n=0}^{\Delta_k-1} \frac{1}{n!}(TP_k^{-1})^n \sum_{\bar{m}\in M} \frac{C(\bar{m})F(\bar{m})\Gamma(\sum m_l+1)}{\left[\sum_{j=1}^{K}\lambda_j(T\widehat{P}_j)^{\frac{2}{\alpha}}\mathcal{C}_j+\pi\sum_{j=1}^{K}\lambda_j(\widehat{P}_j\widehat{\Delta}_j\widehat{B}_j)^{2/\alpha}\right]^{\sum m_l+1}}$$

where (a) follows from $\int_0^\infty e^{-ax^2}x^{2n+1} = 1/(a)^{n+1}$. □

From (2.37), we can observe that probability of coverage is no longer scale invariant in a multi-antenna HetNet even for the interference limited case. Coverage probability for a user associated with the tier k is given as

$$\mathrm{P}_{ck} = \mathbb{P}\left[\gamma_k > T | k = \text{associated tier}\right] = \frac{\mathbb{P}\left[\gamma_k > T, k = \text{associated tier}\right]}{A_k},$$

which is a decreasing function of BS intensities λ_j's $j \neq k$ of other tiers. We also observe that P_{ck} is a decreasing function of Ψ_j's of all the tiers.

2.6 Rate Coverage

In this section, we focus on the downlink rate achievable by a typical user and compute the rate coverage of a typical user. This section generalizes the main ideas developed in [58] for single-antenna HetNets to multi-antenna HetNets. Following the same setup as [58], we assume that each k^{th} tier BS has same time-frequency resources W_k, which are equally distributed among all the users served by a given BS. Further assume that the k^{th} tier BS that serves the typical user located at the origin, termed *tagged BS*, allocates $\mathcal{O}_k \leq W_k$ to each user, including the typical user. Therefore, the instantaneous rate R_k achievable by a typical user when it connects to

a k^{th} tier BS is

$$R_k = \mathcal{O}_k \log_2 (1 + \gamma_k(x_k)). \tag{2.38}$$

As discussed in detail in [58], the effective time-frequency resources $\mathcal{O}_k$ allocated to a typical user depend upon the number of users, equivalently load, served by the tagged BS, which is a random variable due to the random locations and hence the coverage areas of each BS. However, as argued in [58] and verified further in [21], approximating this load for each tier with its respective mean does not compromise the accuracy of results. Using results from [58], the mean load served by the tagged BS from k^{th} tier can be approximated as $N_k = 1 + \frac{1.28\lambda_u A_k}{\lambda_k}$, where λ_u is the density of the users and A_k is the association probability given by Lemma 4. Note that the effect of multi-antenna transmission is captured in A_k. Now since each k^{th} tier BS can schedule Ψ_k users in a single resource block, total available (time-frequency) resource allocated to each user is

$$\mathcal{O}_k = \frac{W_k}{N_k/\Psi_k}. \tag{2.39}$$

Combining the SINR distribution derived in the previous section and the average load result discussed above, the rate CCDF, equivalently rate coverage, can be derived on the same lines as [58]. For easier exposition, we first derive the rate CCDF conditional on the serving BS being in the k^{th} tier. The result is given by the following Theorem.

Theorem 4. *The rate coverage for random selected user associated with k^{th} tier is*

given by $\mathcal{R}_k =$

$$\mathbb{P}[R_k > \rho] = \frac{2\pi\lambda_k}{A_k} \int_0^{\infty} \sum_{n=0}^{\Delta_k - 1} \frac{1}{n!} (tP_k^{-1} x^{\alpha_k})^n e^{-tP_k^{-1} x^{\alpha_k} N - \sum_{j=1}^{K} \lambda_j (t\widehat{P}_j)^{\frac{2}{\alpha_j}} x^{\frac{2}{\widehat{\alpha}_j}} \mathcal{C}_j} \sum_{\bar{m} \in M} C(\bar{m}) \cdot$$

$$\prod_{l=1}^{n} \left(N \mathbb{1}_{l=1} + 2\pi \sum_{j=1}^{K} (-1)^l D_j(l) P_j^l (t\widehat{P}_j)^{\frac{2}{\alpha_j} - l} \frac{x^{\frac{2}{\widehat{\alpha}_j}}}{x^{l\alpha_k}} \right)^{m_l} x e^{-\pi \sum_{j=1}^{K} \lambda_j (\widehat{P}_j \widehat{\Delta}_j \widehat{B}_j)^{\frac{2}{\alpha_j}} x^{\frac{2}{\widehat{\alpha}_j}}} \, \mathrm{d}x,$$

with $u_j = \frac{1}{1 + \frac{t}{\widehat{\Delta}_j \widehat{B}_j}}$ *and* $t = 2^{\frac{\rho N_k}{(W_k \Psi_k)}} - 1$ *and* $N_k = 1 + \frac{1.28 \lambda_u A_k}{\lambda_k}$ *is the mean number of users served by the tagged BS.*

Proof. The proof is similar to [58], hence omitted. Note that the only difference is the presence of Ψ_k, which depends upon the multi-antenna transmission. Putting $\Psi_k = 1$ specializes this result to SISO HetNets, discussed in detail in [58]. □

It is worth highlighting that although the conditional rate coverage computed above uses the mean load approximation for the tagged BS, we can easily incorporate the distribution of user load (see [58]), which is skipped to avoid repetition. The rate coverage $\mathrm{R_c} = \mathbb{P}[R > \rho]$ can now be computed as weighted sum of rate coverage of i^{th} tier weighted by association probability of the respective tier

$$\mathrm{R_c} = \mathbb{P}[R > \rho] = \sum_{i=1}^{K} A_k \mathbb{P}[R_k > \rho]. \tag{2.40}$$

Before concluding this section, it is important to note that a higher value of Ψ_k means more users share the same time-frequency resources, which in turn means that each user gets higher chunk of W_k. This is also evident from (2.39), where $\mathcal{O}_k \propto \Psi_k$. But since coverage probability is a decreasing function of Ψ_j's , the overall rate coverage expression represents a trade-off between available resources and SINR.

2.7 Numerical Results

In this section, we validate our analysis and provide key design insights for multi-antenna HetNets. Before discussing the results, we briefly describe the simulation procedure. We choose a large spatial window and generate K independent PPPs with the given densities. For every realization, a typical user is assumed at the origin and we select a serving BS according to the selection criteria (2.24). Let this BS belongs to tier i. After this, fading random variable h_{xi} is generated for the selected BS according to $\Gamma(\Delta_i, 1)$ distribution and fading random variables g_{xj} are generated for remaining BSs according to $\Gamma(\Psi_j, 1)$. A user is said to be in coverage if the SINR (or SIR in no-noise case) from the selected BS is greater than the target. The coverage probability is finally computed by averaging the indicator of coverage over sufficient realizations of the point process.

For concreteness, we restrict our simulation results to a two-tier HetNet with no noise, with the first tier denoting macrocells and the second denoting small cells, e.g., femtocells. With slight overloading of notation, the parameters are denoted by arrays, e.g., $\lambda = [150, 300]$ means $\lambda_1 = 150, \lambda_2 = 300$. Following three antenna configurations are considered:

4-2 antenna configuration: Macrocells have 4 antennas per BS, while femocells have 2 antennas per BS.

2-1 antenna configuration: Macrocells have 2 antennas per BS, while femocells have 1 antenna per BS.

SISO configuration: All the BSs have single antenna.

In terms of multi-antenna transmission techniques, we restrict our attention to the following two techniques:

Single-user beamforming (SUBF): where each BS serves single user per resource block, i.e., $\Delta_i = M_i, \Psi_i = 1$.

Full spatial division multiplexing (SDMA): where each i^{th} tier BS serves M_i users per resource block, i.e., $\Delta_i = 1, \Psi_i = M_i$.

Note that when we combine these two multi-antenna transmission schemes with the three different antenna configurations discussed above, we already have *7 simulation cases* to consider. We list these cases below for ease of exposition:

4-2 antenna configuration

- *Case 1.* Both tiers use SUBF.
- *Case 2.* Both tiers use SDMA.
- *Case 3.* First tier uses SDMA and other SUBF.
- *Case 4.* First tier uses SUBF and other SDMA.

2-1 antenna configuration

- *Case 5.* First tier uses SUBF.
- *Case 6.* First tier uses SDMA.

SISO configuration

- *Case 7.* Both tiers use SISO.

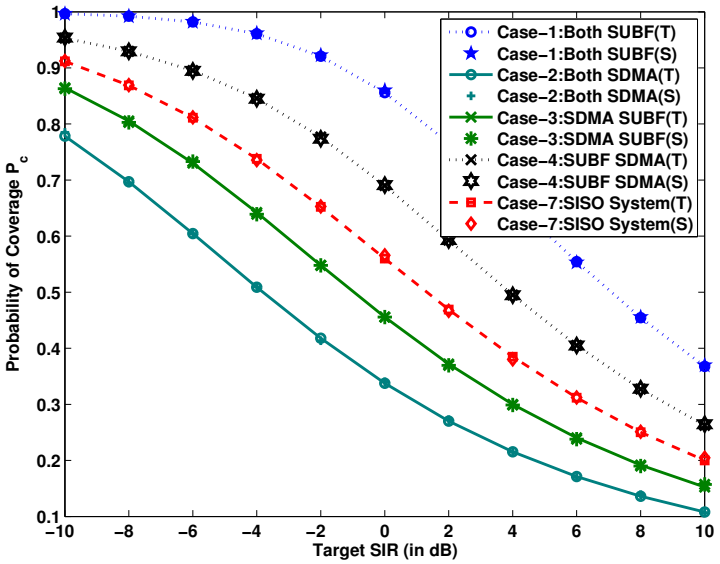

Figure 2.4: Coverage probability of a two-tier HetNet with $\alpha = 4, \lambda = [150, 300], P_1 = 5P_2$ for 4-2 antenna configuration with SUBF, SDMA techniques and SISO system. T and S respectively denote theoretical and simulation results. Selection bias is $\sqrt{\Psi_j \Delta_j}$.

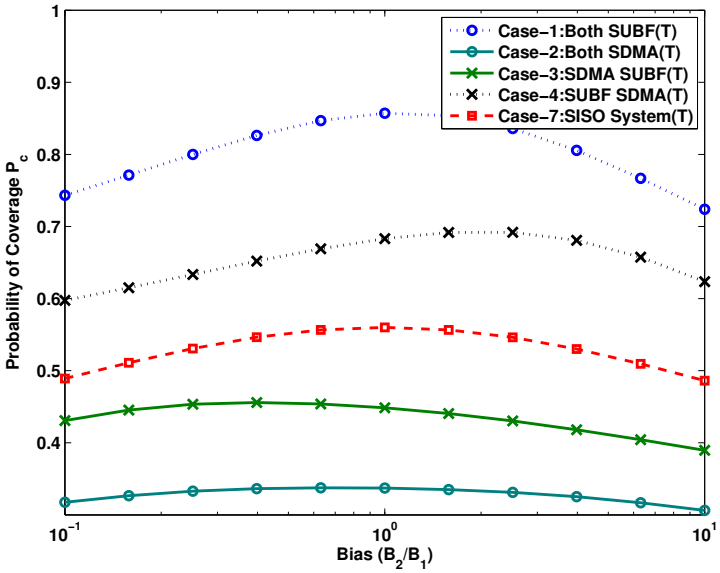

Figure 2.5: Coverage probability versus relative bias B_2/B_1 in a two-tier HetNet with $\alpha = 4, \lambda = [150, 300], P_1 = 5P_2$ for SIR target 0 dB for *4-2 antenna configuration.*

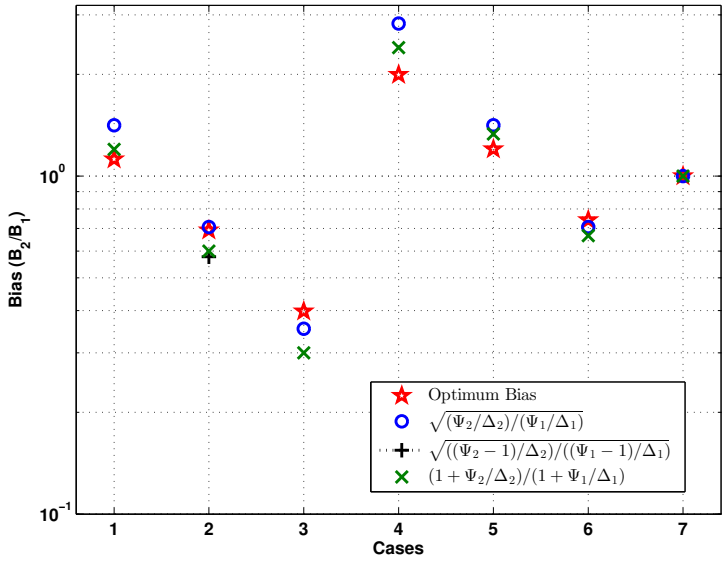

Figure 2.6: Comparison of different candidates functions with numerically optimized bias for all 7 simulation cases ($\alpha = 4$, target SIR = 0 dB, $\lambda = [150, 300]$, $P_1 = 5P_2$).

2.7.1 Coverage Probability

Fig. 2.4 shows the probability of coverage for cases 1-4 corresponding to *4-2 antenna configuration* and case 7 corresponding to the *SISO configuration*. It can be seen that case 1, where both the tiers perform SUBF, results in the highest coverage. This result is consistent with [22], where SUBF was shown to provide highest coverage under a slightly different cell selection model. On the other hand, SDMA performs worse than SISO because the effective fading gain from interfering BSs increases in mean and thus causes stronger interference whereas the effective fading gain of the serving link remains the same as the SISO case. The other intermediate cases, where one tier performs SUBF and the other performs SDMA, fall in between these two extremes.

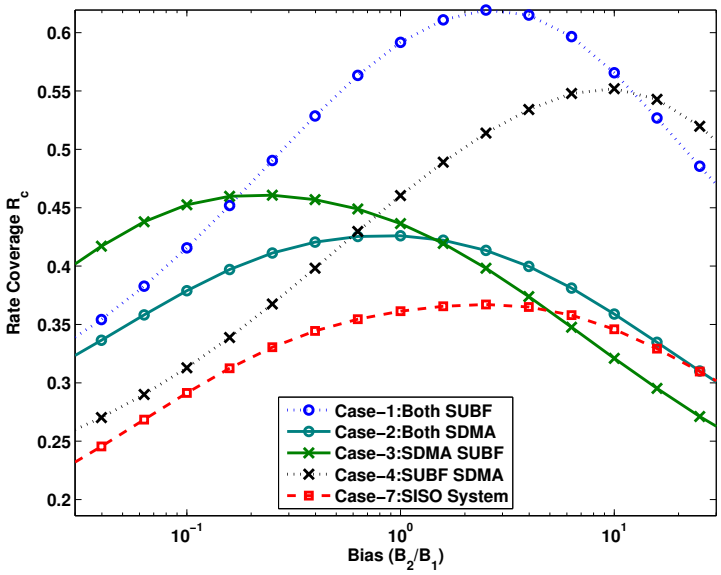

Figure 2.7: Rate coverage probability versus relative bias B_2/B_1 in a two-tier HetNet with $\alpha = 4, \lambda = [150, 300], P_1 = 5P_2 = 50$ for rate threshold 1 bps/Hz.

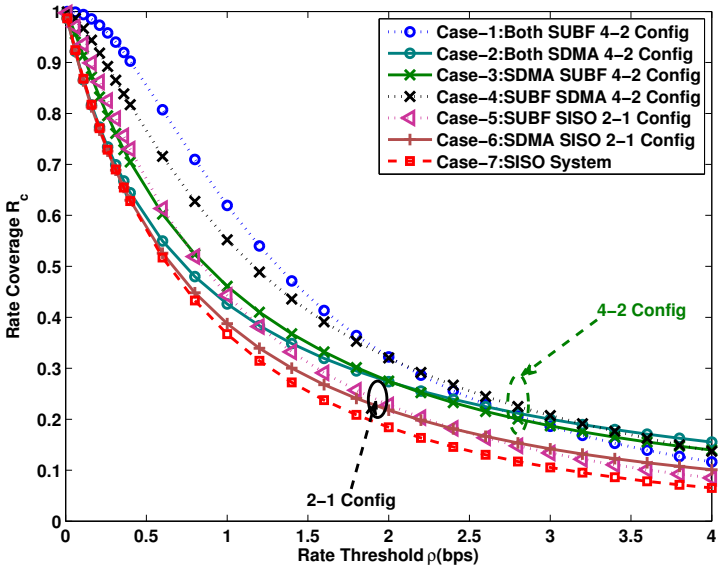

Figure 2.8: Rate coverage with optimum bias $b = B_2/B_1$ in a two-tier HetNet with $\alpha = 4, \lambda = [150, 300], P_1 = 5P_2$ for all 7 simulation cases.

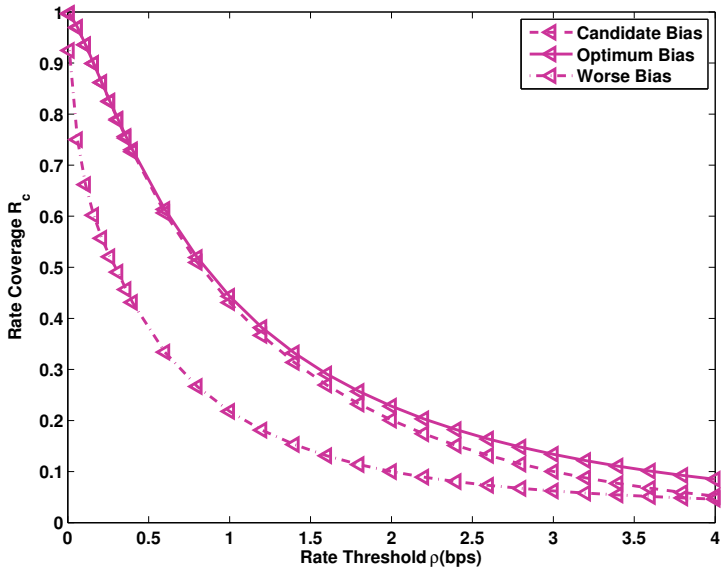

Figure 2.9: Comparison of rate coverage with optimum bias $b = B_2/B_1$, candidate bias $B_i = \sqrt{\Psi_i \Delta_i}$ and worst bias in the range $[0.01, 100]$ in a two-tier HetNet with $\alpha = 4, \lambda = [150, 300], P_1 = 5P_2 = 50$ for simulation case 5.

2.7.2 Optimal Bias

We now compute the optimal selection bias needed to maximize coverage probability. Recall that the BS selection based on the highest mean SINR may not always maximize coverage. We will also validate the selection bias approximations discussed in Section 2.4 using these numerical results. Fig. 2.5 presents the probability of coverage for target SIR 0 dB as a function of B_2/B_1 for cases 1-4 corresponding to *4-2 antenna configuration* and case 7 corresponding to *SISO configuration*. Fig. 2.6 compares different selection (bias) candidate functions for all 7 simulation cases. To compute the optimal bias, we simulate the system with each bias value between .01 to 100 and choose the bias which maximizes the probability of coverage. This optimal bias is then compared to the bias found from various candidate functions for different

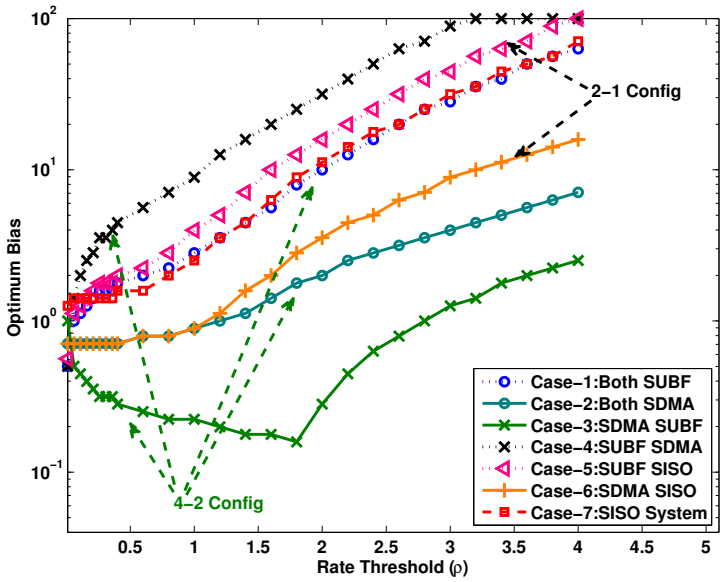

Figure 2.10: Optimum bias $b = B_2/B_1$ for maximizing rate coverage probability versus target rate threshold in a two-tier HetNet with $\alpha = 4, \lambda = [150, 300], P_1 = 5P_2 = 50$ for different simulation cases.

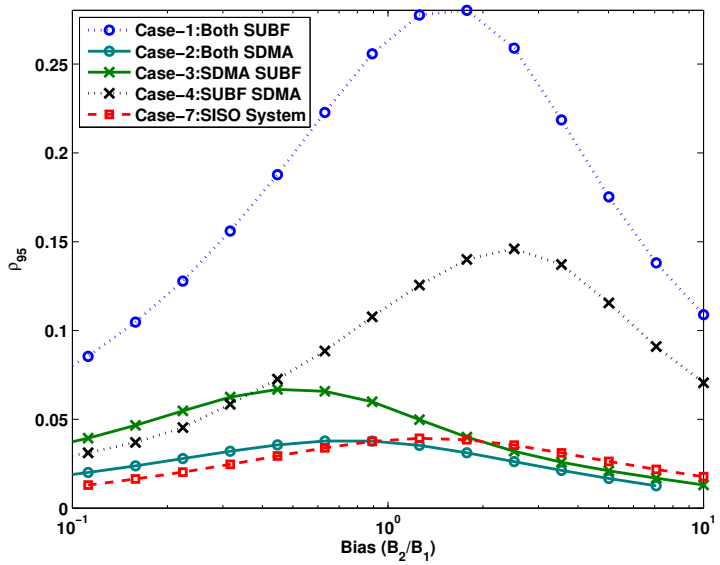

Figure 2.11: The 5^{th} percentile rate ρ_{95} versus bias $b = B_2/B_1$ for a two-tier HetNet with $\alpha = 4, \lambda = [150, 300], P_1 = 5P_2$.

values of system parameters. It is evident that the candidate function (2.19) is a close match.

2.7.3 Rate Coverage and Optimal Bias

We show the variation of rate coverage with bias in Fig. 2.7 for rate target 1 bps/Hz for *4-2 antenna configuration*. It can be seen that rate coverage heavily depends on selection bias. Also, the rate coverage is maximized at a particular value of selection bias in multi-antenna HetNets, which is consistent with the intuition gained about SISO HetNets in [58]. It is worth noting that the optimal bias in this case is not necessarily the same as the one that maximizes coverage probability. We numerically compute these optimum biases for all 7 simulation cases and plot the resulting rate coverages in Fig. 2.8. The SISO case results in the worst rate coverage. At the lower thresholds, case 1 (both tiers using SUBF) performs the best, while at higher thresholds, case 2 (both tiers using SDMA) is superior. Other two cases corresponding to the *4-2 antenna configuration* perform in between these two extremes. For *2-1 antenna configuration*, we observe a similar behavior where case 5 (first tier with SUBF) performs better for smaller rate thresholds while case 6 (first tier using SDMA) performs better for higher thresholds.

In Fig. 2.9, we compare rate coverage with optimum bias, the candidate bias function (2.19) and the worst bias (the bias which gives the lowest rate coverage among the values between $[0.01, 100]$) for simulation case 5. Recall that the case 5 corresponds to *2-1 antenna configuration*, where first tier performs SUBF and the second performs SISO. Comparing the optimal rate coverage with the one achieved

under worst bias again highlights the fact that choosing a poorly designed bias value can significantly degrade rate coverage. More interestingly, we observe that the candidate bias function that we derived for coverage maximization works reasonably well for this case as well. This can at least be used as a starting point for numerical search algorithms to find optimal bias. That being said, the difference in the two cases is higher at higher rate thresholds. This is explained in Fig.2.10, where we present the variation of optimal bias with rate threshold for all 7 simulation cases. Clearly, the optimal system design in this case depends upon the target rate, which in turn depends upon the target application, e.g., video.

In Fig.2.10, we can also observe the effect of transmission schemes on optimal bias. Required selection bias values for moderate rate thresholds follow the following order: case $4 > 5 > 7 > 1 > 6 > 2 > 3$. This ordering is consistent with intuition. For instance, when the macrocell uses SUBF and femtocell uses SDMA or SISO, the coverage regions of macrocells are further expanded due to beamforming gain, which results in the need for higher selection bias for the second tier to balance load across the tiers compared to the case when the first tier performs SISO transmission. On the other hand, if we now assume that the first tier performs SDMA and the second tier performs SUBF, the coverage regions of the second tier are naturally expanded due to the beamforming gain, i.e., the load across the tiers is more balanced, which reduces the need for a high external bias for the second tier. In general, whenever small cells can use multi-antenna transmission for range expansion, e.g., by SUBF, the external bias required to balance load would be smaller compared to the SISO case. The other cases can also be explained similarly.

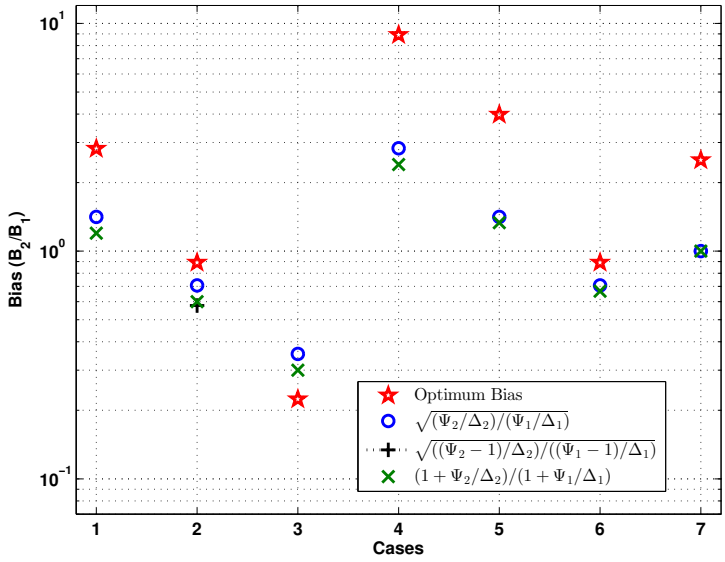

Figure 2.12: Comparison of different candidates functions with numerically optimized bias for target rate = 1bps/Hz,$\lambda = [150; 300]$; $P_1 = 5P_2$ for all 7 simulation cases.

In Fig. 2.11, we present the 5^{th} percentile rate, i.e., the target rate such that the 95% users achieve rate higher than the target. The trends for the optimum bias are consistent with those discussed above. The rate coverage results are also consistent with those discussed for Fig. 2.7. Finally, Fig. 2.12 compares the optimal bias for rate coverage and bias from the candidate functions for different cases. Recall that even though these candidate functions were derived for coverage maximization, they still provide good starting points for numerical search algorithms to find rate maximizing bias, as stated earlier in this section.

2.8 Conclusion

In this paper, we have investigated downlink multi-antenna HetNets with flexible cell selection and shown that simple selection bias-based cell selection criterion closely approximates more complex selection rules to maximize mean SINR. Under this simpler cell selection rule, we derived exact expressions for coverage probability and rate achievable by a typical user. An approximation of the coverage optimal cell selection bias for each tier is also derived in closed form. Due to this connection with biasing, there is a natural expansion of coverage regions of small cells whenever small cells can use multi-antenna transmission for range expansion, e.g., by using beamforming. This leads to a natural balancing of load across tiers, which reduces the additional artificial cell selection bias needed to offload sufficient traffic to small cells.

Chapter 3

Macro-diversity in Cellular Networks with Random Blockages

In this chapter, we consider association issues in cellular systems when blockages are present. Various blockages present in the environment in the form of buildings and foliage severely impact the performance of cellular networks. These blockages may result in significant drop in signal strengths or even outages for some users. This effect is more severe at high frequencies including mmWave frequencies due to high penetration loss present at these frequencies [7, 8]. As described in the first chapter, large bandwidth available at mmWave spectrum makes it a prime candidate for 5G cellular networks [5, 6, 65]. Despite its promising benefits including high data rates, communication at mmWave frequencies suffers from high penetration losses and is severely impacted by the blockages present in the environment in the form of buildings or foliage [8]. These blockages may result in significant drop in signal strengths or even outages for some users. Therefore, users will prefer to connect to line-of-sight (LOS) base-stations (BSs) to ensure better signal strength and high data rates. In addition, a user can block the desired signals from its serving BS due to its own body [23, 24], hurting the overall reliability of the communication links. To overcome this issue, macro diversity can be leveraged where a user is connected to multiple BSs simultaneously so that when one link is blocked, there can be other BSs

available to the user immediately [13, 26]. From an operator's perspective, utilizing macro diversity can also decrease the required BS deployment density necessary to maintain a certain level of reliability. However, presence of large blockages will result in correlation among different links which need to be investigated to understand the gain obtained by macro-diversity which is the main focus of this chapter.

3.1 Related Work

In the past, the impact of blockages is generally included in the shadowing model as an additional loss. This approach, however, is simplistic and is not suitable to study mmWave communication where blockages play a significant role in determining its performance. Another approach to model blockages by using ray tracing in a deterministic environment is numerically complex and not tractable. In [66], a tractable approach using random Boolean scheme with linear segments [67–69] was proposed to model the random blockages in a cellular system. This analysis was extended in [9] to include rectangular blockages and in [24] to include circular blockages. In [8], the above blockage model was incorporated in mmWave systems to study the impact of blockages on the system performance. It was shown in [8] that the system performance is dependent on the blockages as a function of the product of blockage density and average blockage length.

There are some approaches to handle blockage problems and increase link reliability, in particular for mmWave frequencies, for example, to use reflections from walls and other surfaces to steer around obstacles [70] or by switching the beam from a LOS link to a NLOS link [71]. As discussed above, NLOS links, however, may not

support high data rate for mmWave communication. Another approach is to maintain link connectivity by use of relays and routing algorithms [72, 73]. However, this leads to non-tractability due to its complex algorithms and scheduling schemes. The third approach is to use macro diversity with multiple BSs [25, 26]. Macro-diversity over shadowing fading was studied in [74, 75]. In [76], the performance of coordinated beamforming with dynamic BS clusters was studied. The work [77] discussed about the fundamental limits of cooperation for multicell cooperative networks with multiple receive antennas. In [26], the authors proposed a multi-BS architecture for 60GHz WLAN in which a MAC layer access controller device is employed to enable each station to associate and cooperate with multiple BSs. In the proposed architecture, when one of wireless links is blocked, another BS can be selected to complete remaining transmissions.

Recent analytical work [9, 24] to study the impact of blockages in mmWave systems assumes a single active link per user and does not include macro-diversity. In [27], a stochastic geometry framework is presented to study the macro-diversity for mmWave system in presence of random blockages, however, it assumes independence among blocking events of the different links. When simultaneous multiple links are considered, the larger blockages may decrease the diversity gains due to induced correlation in blocking of these links and the system performance may no longer remain just a function of the product of the blockage density and average blockage length.

3.2 Contributions

In this chapter, we evaluate the benefits of macro-diversity for a cellular system in the presence of random blockages. The contributions of the chapter can be summarized as below:

Analytical framework for dependent blocking: We present a framework to analyze the correlation present among blocking of multiple communication links in a cellular system with random blockages. Given the lengths of the links and their orientations, we compute the joint probability of these links being non-blocked. We show that unlike the independent case, this probability depends on both the blockage density and maximum blockage length, not just the product of the two. We show that increasing maximum blockage length while keeping the product constant increases the correlation among blocking of multiple links.

Gains from macro-diversity: We then use the proposed framework to evaluate gains obtained by macro-diversity. We consider a system where each user is connected to multiple BSs simultaneously. For this system, we compute the average probability of having at least one LOS BS out of all connected links (termed as probability of reliability). We show that the required BS density to achieve a certain level of reliability can be decreased significantly by maintaining multiple BS links simultaneously. The dependency in blocking decreases the diversity gain in comparison to the case where blocking is independent among links. We also show that to maintain same level of probability of reliability, the BS density must scale as square of the blockage density.

Analyzing diversity gains in the presence of self-blocking: We also consider self-blocking. If the person using a mobile phone comes in-between the serving BS and the mobile, its body can block signals from its own serving BSs. This is known as self-blocking. We consider a scheme where the multiple BSs are selected in a way to avoid self-blocking of all BSs at any time and derive the probability of reliability for this case.

3.3 System Model

We consider a cellular network consisting of BSs whose locations are modeled as a homogeneous Poisson point process (PPP) with density λ and users modeled as a stationary Point process (PP). We consider a typical user at the origin $\mathbf{O}$. Let $\Xi = \{\mathbf{x}_i, i \in \mathbf{N}\}$ denote the BS PPP where locations $\mathbf{x}_i$ are ordered according to their distances R_i from the typical user.

3.3.1 Modeling Random Blockages

To model the blockages present in the channel, we consider the line Boolean scheme Ψ similar to [9]. In this model, we assume that all the blockage elements are in form of lines. In real scenario, the blockages are polygon shaped. However, since we are interested in their intersections with the links, assuming their shapes as lines is a reasonable approximation. The centers of these lines are modeled as a homogeneous PPP ψ of density μ. The lengths ℓ_k of blockage lines are iid random variables with distribution $F_L(\cdot)$. The orientations θ_k of the blockage lines are assumed to be iid random variables with distribution $F_\Theta(\cdot)$. Let us define average LOS radius of a

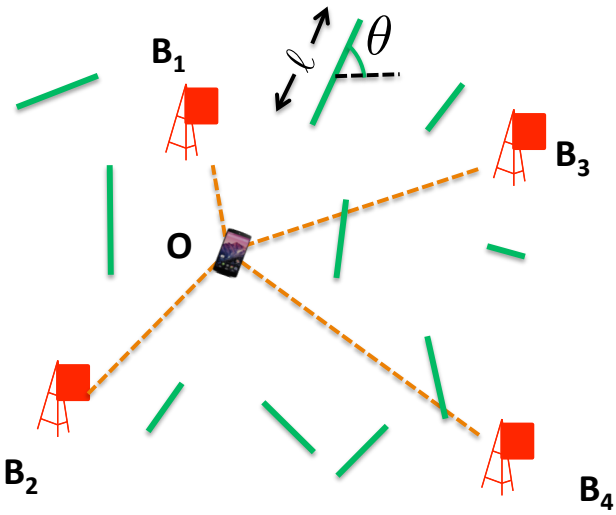

Figure 3.1: An illustration showing a user at the origin in presence of blockages. Each blockage is modeled as linear segment of length ℓ_k and orientation θ_k. A link to any BS is said to be blocked or unreachable if a blockage falls on the link.

blockage process as $\beta = \mu\frac{2}{\pi}\mathbb{E}[\ell]$ [9]. The analysis performed in this paper can be extended to Boolean schemes with other shapes such as rectangles or circles [9, 78]. In this paper, we will also consider a special case of the above blockage process where ℓ and θ are uniformly distributed *i.e.* $\ell \sim U(0, L_m), \theta \sim U(0, \pi)$ which is termed a *uniform blockage process*.

3.3.2 Connectivity Model

We assume that all the users are simultaneously connected to n closest BSs (See Fig. 5.1) where n is termed the *macro-diversity order*. We assume that a user will be able to quickly establish communication links with any of the n BSs connected to it. Recall that the link to a BS can be LOS if there are no blockages intersecting

the link between the BS and the user, otherwise the link is said to be in NLOS. Let $\mathcal{A}_i$ denote the event that the ith BS is LOS. At any point of time, the user will establish a communication link with the closest LOS BS, termed *the associated BS* out of these n connected BSs. If all n of the closest BSs are blocked, we say that the user is not reachable.

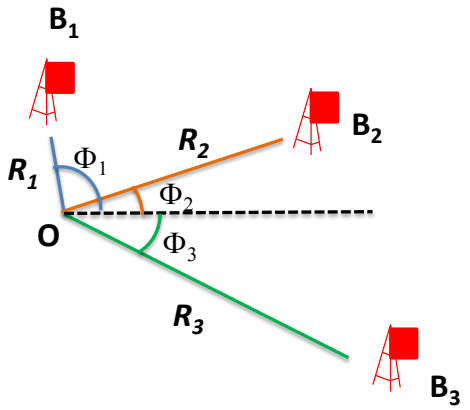

Figure 3.2: A cellular system with third order diversity ($n = 3$). The typical user at **O** has three active BSs it can associate to.

The probability of reliability p_{R} of a cellular system is defined as the probability that at least one connected BS out of the n connected BSs is LOS to a typical user and is given as

$$p_{\mathrm{R}} = \mathbb{P}\left[\bigcup_{i=1}^{n} \mathcal{A}_i\right]. \tag{3.1}$$

The probability of reliability is also useful from the system point of view. For example, a cellular operator may be interested in the question that if each user can use nth order macro-diversity, what the required BS density should be to achieve certain level of reliability probability.

Table 3.1: Summary of Notation

Notation	Description
Ξ, λ	The PPP modeling the BS locations, its density.
Ψ, ψ, μ	The Boolean scheme modeling the blockage locations, the PPP modeling the centers of blockages and its density.
ℓ_k, θ_k	The length and orientation of the kth blockage.
$F_L(), F_\Theta()$	The distribution of blockage lengths ℓ and orientations θ. $F_L(\mathcal{L})$ denotes the probability that $\ell \in \mathcal{L}$.
$\Psi(\ell, \theta)$	The derived blockage process from Ψ. Blockages have length between ℓ and $\ell + \mathrm{d}\ell$ and orientation between θ and $\theta + \mathrm{d}\theta$.
β, L_m	A parameter for the blockage process defined as $\mu\mathbb{E}[\ell]\frac{2}{\pi}$, the maximum blockage length.
$\mathbf{B}_j, R_i, \mathbf{Z}_j$	The jth closest BS from the user at the origin, the distance of this BS from the user, the link between this BS and the origin.
n	The order of macro diversity i.e. the number of simultaneous connected BSs.
Φ_i	The angle between $\mathbf{Z}_j$ and $\mathbf{Z}_n$.
Φ	The angle between $\mathbf{Z}_1$ and $\mathbf{Z}_2$ for special case of second order diversity.
$\mathcal{A}_j$	The event that the jth link is LOS.
p_{R}	The probability of reliability.
$\mathcal{P}_i$	The parallelogram constructed on the ith link as shown in Fig. 3.3.
γ	A parameter defined to be equal to $\frac{\beta}{2\sqrt{\lambda\pi}}$.
ω	The blocking cone created by the body of the user.

3.4 Reliability Analysis for Second Order Macro-Diversity

In this section, we will consider a system of second order diversity ($n = 2$). In this case, the typical user is connected with two BSs, $\mathbf{B}_1$ and $\mathbf{B}_2$ with link lengths equal to R_1 and R_2. Let us denote the angle between the two links $\mathbf{Z_1}$ and $\mathbf{Z_2}$ as Φ. Without loss of generality, we assume that $\mathbf{x}_2$ is at x axis and $\Phi \geq 0$. The joint

distribution of R_1 and R_2 is given as

$$f(r_1, r_2) = (2\pi\lambda)^2 r_1 r_2 \exp(-\lambda\pi r_2^2), \text{ if } r_1 \leq r_2 \tag{3.2}$$

and $\Phi \sim \text{Uniform}(0, \pi)$.

Now, let us consider a derived Boolean scheme $\Psi(\ell, \theta)$ of blockages with lengths between ℓ and $\ell + \mathrm{d}\ell$ and orientations between θ and $\theta + \mathrm{d}\theta$. Note that this can be obtained by thinning the original PP ψ. Therefore, centers of $\Psi(\ell, \theta)$ form a PPP with intensity $\mu F_L(\mathrm{d}\ell) F_\Theta(\mathrm{d}\theta)$. Given the two links $\mathbf{Z_1}$ and $\mathbf{Z_2}$, let $\mathcal{A}_1$ and $\mathcal{A}_2$ respectively denote the events that these links are unblocked. Therefore, the probability that at least one of the links is not blocked is given as

$$\mathbb{P}\left[\mathcal{A}_1 \cup \mathcal{A}_2\right] = \mathbb{P}\left[\mathcal{A}_1\right] + \mathbb{P}\left[\mathcal{A}_2\right] - \mathbb{P}\left[\mathcal{A}_1 \cap \mathcal{A}_2\right]. \tag{3.3}$$

The event that the link $\mathbf{Z}_1$ is not blocked by a blockage in $\Psi(\ell, \theta)$ is equivalent to the event that centers of all blockages in this collection $\Psi(\ell, \theta)$ lie outside the parallelogram $\mathcal{P}_1$ shown in Fig. 3.3. The area of $\mathcal{P}_1$ is given as

$$A_1(R_1, \ell, \theta, \Phi) = \ell R_1 \sin(|\theta - \Phi|).$$

Hence, the probability of the event that the link $\mathbf{Z}_1$ is not blocked by an blockage in $\Psi(\ell, \theta)$ is given by void probability of a PPP and is equal to $\exp\left(-\mu F_L(\mathrm{d}\ell) F_\Theta(\mathrm{d}\theta)\right.$ $\left. A_1(R_1, \phi, \ell, \theta)\right)$. Therefore, the probability of the event $\mathcal{A}_1$ that the link $\mathbf{Z}_1$ is not blocked is

$$\mathbb{P}\left[\mathcal{A}_1\right] = \prod_{\ell,\theta} \exp(-\mu F_L(\mathrm{d}\ell) F_\Theta(\mathrm{d}\theta) A_1(R_1, \phi, \ell, \theta))$$

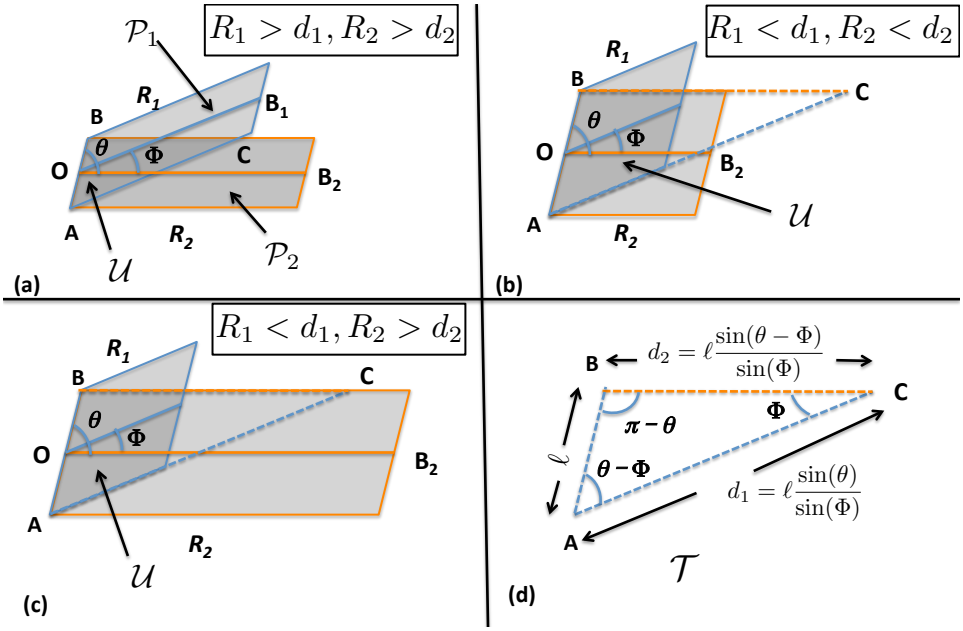

Figure 3.3: Illustration showing the joint area of the two parallelograms $\mathcal{P}_1$ and $\mathcal{P}_2$. Subfigures (a), (b) and (c) show shapes for the region $\mathcal{U}$ common in both parallelograms dependent on the values of ℓ, θ, R_1, R_2 and Φ. The conditions are mentioned in the subfigures where d_1 and d_2 are lengths of AC and BC. Fig. (d) The triangle $\mathcal{T}$ circumscribes the common region $\mathcal{U}$.

$$
\begin{aligned}
&= \exp\left(-\int_0^\infty \int_0^\pi \mu A_1(R_1, \phi, \ell, \theta) F_L(\mathrm{d}\ell) F_\Theta(\mathrm{d}\theta)\right) \\
&= \exp\left(-\int_0^\infty \int_0^\pi \mu \ell R_1 \sin(|\theta - \Phi|) F_L(\mathrm{d}\ell) F_\Theta(\mathrm{d}\theta)\right) \\
&= \exp\left(-\mu \mathbb{E}\left[\ell\right] R_1 \frac{2}{\pi}\right) = \exp(-\beta R_1). \qquad (3.4)
\end{aligned}
$$

Similarly the probability of the event $\mathcal{A}_2$ that the link $\mathbf{Z}_2$ is not blocked is

$$
\mathbb{P}\left[\mathcal{A}_2\right] = \exp\left(-\int_0^\infty \int_0^\pi \mu A_2(R_2, \phi, \ell, \theta) F_L(\mathrm{d}\ell) F_\Theta(\mathrm{d}\theta)\right) = \exp(-\beta R_2). \qquad (3.5)
$$

Now we will compute the joint probability $\mathbb{P}\left[\mathcal{A}_1 \cap \mathcal{A}_2\right]$. Similar to the previous

case, the event that both links are not blocked by any blockage in $\Psi(\ell,\theta)$ is equivalent to the event that centers of all blockages in the collection $\Psi(\ell,\theta)$ lie outside the shaded region (which is the union of two parallelograms $\mathcal{P}_1$ and $\mathcal{P}_2$) shown in Fig. 3.3. Let $A(R_1,R_2,\phi,\ell,\theta)$ be the area of shaded region. The shape of the intersection (denoted by $\mathcal{U}$) of the two parallelograms can be triangular or trapezoidal, dependent on the values of R_1,R_2,Φ,θ,ℓ (See Fig. 3.3(a-c)). Let triangle $\mathcal{T}:\Delta$ABC denote the triangle circumscribing $\mathcal{U}$. The area of this triangle is given as

$$T=\frac{\ell^2\sin(\theta)\sin(|\theta-\Phi|)}{2\sin(\Phi)}.$$

The trapezoidal shape occurs only when $R_1<\ell_1$ or $R_2<\ell_2$. The area of $\mathcal{T}\setminus\mathcal{U}$ is given by $\left(1-\min\left(\frac{R_2}{\ell_1},\frac{R_1}{\ell_2}\right)\right)^2 T$. Therefore, the area of $\mathcal{P}_1\cup\mathcal{P}_2$ is given as

$$\begin{aligned}A(R_1,R_2,\Phi,\ell,\theta)&=\ell R_1\sin(|\theta-\Phi|)+\ell R_2\sin(\theta)\\&-1(\theta>\phi)\frac{\ell^2\sin(\theta)\sin(\theta-\Phi)}{2\sin(\Phi)}\left[1-\left(1-\min\left(1,\frac{R_1\sin(\Phi)}{\ell\sin(\theta)}\frac{R_2\sin(\Phi)}{\ell\sin(\theta-\Phi)}\right)\right)^2\right].\end{aligned}\tag{3.6}$$

Hence, the probability that both of the links are not blocked $\Psi(\ell,\theta)$ is $\exp\left(-\mu F_L(\mathrm{d}\ell)\right.$ $\left.F_\Theta(\mathrm{d}\theta)A(R_1,R_2,\phi,\ell,\theta)\right)$ and the probability that both links are not blocked is

$$\begin{aligned}\mathbb{P}\left[\mathcal{A}_1\cap\mathcal{A}_2\right]&=\prod_{\ell,\theta}\exp(-\mu F_L(\mathrm{d}\ell)F_\Theta(\mathrm{d}\theta)A(R_1,R_2,\phi,\ell,\theta))\\&=\exp\left(-\int_0^\infty\int_0^\pi\mu A(R_1,R_2,\phi,\ell,\theta)F_L(\mathrm{d}\ell)F_\Theta(\mathrm{d}\theta)\right)\end{aligned}\tag{3.7}$$

Let us define $\mathcal{N}(R_1,R_2,\Phi)$ as the mean shaded area averaged over blockage size and orientation distribution which is given as

$$\mathcal{N}(R_1,R_2,\Phi)=\int_0^\infty\int_0^\pi A(R_1,R_2,\phi,\ell,\theta)F_L(\mathrm{d}\ell)F_\Theta(\mathrm{d}\theta).\tag{3.8}$$

Then, $\mathbb{P}\left[\mathcal{A}_1 \cap \mathcal{A}_2\right]$ is given by

$$\mathbb{P}\left[\mathcal{A} \cap \mathcal{A}_2\right] = p(R_1, R_2, \Phi) = \exp\left(-\mu\mathcal{N}(R_1, R_2, \Phi)\right). \tag{3.9}$$

Therefore, using (3.3), the probability that at least one of the link is not blocked is given as

$$\mathbb{P}\left[\mathcal{A}_1 \cup \mathcal{A}_2\right] = \exp(-\beta R_1) + \exp(-\beta R_2) - \exp\left(-\mu\mathcal{N}(R_1, R_2, \Phi)\right). \tag{3.10}$$

Now, the probability of reliability is given as

$$\begin{aligned}
p_{\mathrm{R}} &= \mathbb{E}_{R_1,R_2}\left[\mathbb{P}\left[\mathcal{A}_1 \cup \mathcal{A}_2\right]\right] \\
&= \frac{1}{\pi}\int_0^\infty\int_0^\infty\int_0^\pi \left(\exp(-\beta r_1) + \exp(-\beta r_2) - \exp\left(-\mu\mathcal{N}(r_1, r_2, \phi)\right)\right) f_{R_1,R_2}(r_1, r_2)\mathrm{d}\phi\mathrm{d}r_1\mathrm{d}r_2 \\
&= \frac{(2\pi\lambda)^2}{\pi}\int_0^\infty\int_0^{r_2}\int_0^\pi \left(\exp(-\beta r_1) + \exp(-\beta r_2)\right. \\
&\qquad\qquad \left. - \exp\left(-\mu\mathcal{N}(r_1, r_2, \phi)\right)\right) r_1 r_2 \exp(-\lambda\pi r_2^2)\mathrm{d}\phi\mathrm{d}r_1\mathrm{d}r_2.
\end{aligned} \tag{3.11}$$

Using the transformations $x_1 = \beta r_1, x_2 = \beta r_2$, we get

$$p_{\mathrm{R}} = \frac{1}{4\gamma^4\pi}\int_0^\infty\int_0^{x_2}\int_0^\pi \left(e^{-x_1} + e^{-x_2} - e^{-\mu s\left(\frac{x_1}{\beta}, \frac{x_2}{\beta}, \phi\right)}\right) x_1 x_2 e^{-\frac{x_2^2}{4\gamma^2}}\mathrm{d}\phi\mathrm{d}x_1\mathrm{d}x_2 \tag{3.12}$$

where

$$\gamma = \frac{\beta}{2\sqrt{\pi\lambda}}. \tag{3.13}$$

Solving the first two integrals in (3.12), we get the final expression for probability of reliability which is given in the following Theorem.

Theorem 5. *The reliability probability in a cellular network with second order diversity is given as*

$$p_{\mathrm{R}} = 2 + \gamma^2 - \gamma(5 + 2\gamma^2)W(\gamma) - \frac{1}{4\gamma^4\pi}\int_0^{\pi}\int_0^{\infty} x_2 \exp\left(-\frac{x_2^2}{4\gamma^2}\right)\int_0^{x_2}\exp\left(-\mu s\left(\frac{x_1}{\beta},\frac{x_2}{\beta},\phi\right)\right)x_1\mathrm{d}x_1\mathrm{d}x_2\mathrm{d}\phi \quad (3.14)$$

where $\mathcal{N}(r_1, r_2, \phi)$ *is given in* (3.8)*, and*

$$W(x) = \frac{\sqrt{\pi}}{2}\mathrm{erfcx}(x) = \frac{\sqrt{\pi}}{2}\exp\left(x^2\right)\mathrm{erfc}(x). \quad (3.15)$$

Before going further, we will give the following Lemma regarding the monotonicity of probability of reliability with respect to blockage length's distribution.

Lemma 6. *For all the blockage processes with the same* β *and scaled length distribution* $F_c'(\mathrm{d}\ell) = F_L(\mathrm{d}\ell/c)$*, the quantity* $\mu\mathcal{N}(R_1, R_2, \Phi)$ *monotonically decreases with increasing* c *and so does the probability of reliability.*

Proof. To prove the Lemma, we show that $\mu\mathcal{N}(R_1, R_2, \Phi)$ for the blockage with distribution $F_c'(\mathrm{d}\ell)$ is less than $\mu\mathcal{N}(R_1, R_2, \Phi)$ for the blockage with distribution $F_L(\mathrm{d}\ell)$ for $c > 1$. For the rest of the proof, we assume $c > 1$. It can been shown easily that given ℓ and θ,

$$\frac{1}{c}A(R_1, R_2, \phi, c\ell, \theta) \leq A(R_1, R_2, \phi, \ell, \theta).$$

Now, for the blockage process with distribution $F_c'(\mathrm{d}\ell)$, $\mu\mathcal{N}(R_1, R_2, \Phi)$ is given as

$$\mu\mathcal{N}_c(R_1, R_2, \Phi) = \beta\pi\frac{\int_0^{\infty}\int_0^{\pi} A(R_1, R_2, \phi, \ell, \theta)F_c'(\mathrm{d}\ell)F_{\Theta}(\mathrm{d}\theta)}{\int_0^{\infty}\ell F_c'(\mathrm{d}\ell)}$$

$$= \beta\pi \frac{\int_0^\infty \int_0^\pi A(R_1, R_2, \phi, \ell, \theta) F_L(\mathrm{d}\ell/c) F_\Theta(\mathrm{d}\theta)}{\int_0^\infty \ell F_L(\mathrm{d}\ell/c)}$$
$$= \beta\pi \frac{\int_0^\infty \int_0^\pi A(R_1, R_2, \phi, c\ell', \theta) F_L(\mathrm{d}\ell/c) F_\Theta(\mathrm{d}\theta)}{c\int_0^\infty \ell' F_L(\mathrm{d}\ell')}$$
$$\leq \beta\pi \frac{\int_0^\infty \int_0^\pi A(R_1, R_2, \phi, \ell', \theta) F_L(\mathrm{d}\ell/c) F_\Theta(\mathrm{d}\theta)}{\int_0^\infty \ell' F_L(\mathrm{d}\ell')} = \mu\mathcal{N}(R_1, R_2, \Phi)$$

which completes the proof.

□

One direct result of the above Lemma is for uniform distribution of blockage length $\ell \sim U(0, Lm)$, the probability of reliability decreases with increasing L_m. This result is intuitive as less but bulky blockages make the blocking probability of two links more correlated while small but more blockages result in independence between blocking of any two links.

The function $\mathcal{N}(\cdot, \cdot, \cdot)$ in Lemma 6 is dependent on on the distribution of ℓ and θ, and in general, is difficult to compute. In next subsections, we will consider a few special cases to simplify the function $\mathcal{N}(\cdot, \cdot, \cdot)$ to get closed form expressions for the probability of reliability.

3.4.1 Probability of Reliability for Independent Blocking

In this subsection, we consider the independent blocking scenario where both links are blocked or not independently. Then, $\mathbb{P}[\mathcal{A}_1 \cap \mathcal{A}_2]$ is equal to

$$\mathbb{P}_{\mathrm{IND}}[\mathcal{A}_1 \cap \mathcal{A}_2] = \mathbb{P}[\mathcal{A}_1]\,\mathbb{P}[\mathcal{A}_2] = \exp(-\beta R_1 - \beta R_2). \tag{3.16}$$

Note that the area of $\mathcal{P}_1 \cup \mathcal{P}_2$ is greater than the sum of the areas of the two parallelograms *i.e.*

$$A(R_1, R_2, \Phi, \ell, \theta) \leq \ell R_1 \sin(|\theta - \Phi|) + \ell R_2 \sin(\theta).$$

Averaging with respect to ℓ and θ, we get

$$\begin{aligned} \mathcal{N}(R_1, R_2, \Phi) &\leq \mu \mathbb{E}\left[\ell\right] \frac{2}{\pi}(R_1 + R_2) \\ \mathbb{P}\left[\mathcal{A}_1 \cap \mathcal{A}_2\right] &= \exp(-\mu \mathcal{N}(R_1, R_2, \Phi)) \geq \exp(-\beta R_1 - \beta R_2) = \mathbb{P}_{\text{IND}}\left[\mathcal{A}_1 \cap \mathcal{A}_2\right]. \end{aligned} \tag{3.17}$$

Therefore, the independent blocking case upper bounds the probability of reliability in the dependent blocking scenario. We now provide the probability of reliability for the independent blocking case in the following Theorem.

Theorem 6. *The reliability probability in a cellular network with second order diversity and independent blocking is given as*

$$\overline{p_{\text{R}}} = \frac{1}{\gamma}\left[\gamma^3 - W(\gamma)(2\gamma^4 + 5\gamma^2 - 1) + W(2\gamma)(8\gamma^2 - 1)\right].$$

Proof. For the independent blocking case, the probability of reliability is given as

$$\begin{aligned} \overline{p_{\text{R}}} &= \mathbb{E}_{R_1, R_2, \Phi}\left[\mathbb{P}\left[\mathcal{A}_1 \cup \mathcal{A}_2\right]\right] = \mathbb{E}_{R_1, R_2, \Phi}\left[1 - \mathbb{P}\left[\mathcal{A}_1^{\complement} \cap \mathcal{A}_2^{\complement}\right]\right] \\ &= 1 - \mathbb{E}_{R_1, R_2, \Phi}\left[\mathbb{P}\left[\mathcal{A}_1^{\complement}\right] \mathbb{P}\left[\mathcal{A}_2^{\complement}\right]\right] \end{aligned}$$

where the last step is due to independence of events $\mathcal{A}_1^{\complement}$ and $\mathcal{A}_2^{\complement}$. Now, using (3.4) and (3.5), we get

$$\overline{p_{\text{R}}} = 1 - \int_0^\infty \int_0^\infty (1 - e^{-\beta r_1})(1 - e^{-\beta r_2}) f(r_1, r_2) \mathrm{d}r_1 \mathrm{d}r_2 \tag{3.18}$$

$$= 1 - (2\pi\lambda)^2 \int_0^{\infty} (1 - e^{-\beta r_2}) r_2 e^{-\lambda\pi r_2^2} \int_0^{r_1} (1 - e^{-\beta r_1}) r_1 \mathrm{d}r_1 \mathrm{d}r_2. \tag{3.19}$$

Now using the transformations $x_1 = \beta r_1$ and $x_2 = \beta r_2$, we get

$$\begin{aligned}
\overline{p_{\mathrm{R}}} &= 1 - \frac{1}{4\gamma^4} \int_0^{\infty} (1 - e^{-x_2}) x_2 e^{-x_2^2/(4\gamma^2)} \int_0^{x_1} (1 - e^{-x_1}) x_1 \mathrm{d}x_1 \mathrm{d}x_2 \\
&= 1 - \frac{1}{8\gamma^4} \int_0^{\infty} e^{-x_2^2/(4\gamma^2)} x_2 (1 - e^{-x_2}) [x_2^2 - 2 + 2e^{-x_2}(x_2 + 1)] \mathrm{d}x_2 \\
&= \frac{1}{\gamma} \left[\gamma^3 - W(\gamma)(2\gamma^4 + 5\gamma^2 - 1) + W(2\gamma)(8\gamma^2 - 1) \right].
\end{aligned}$$

□

The above Theorem directly gives the following Corollary.

Corollary 5. *Given a certain value of* $\overline{p_{\mathrm{R}}}$*, the required BS density is given by* $\lambda = \frac{\beta^2}{4\pi\gamma_s^2}$ *where* γ_s *is the solution of the following equation*

$$\gamma^3 - W(\gamma)(2\gamma^4 + 5\gamma^2 - 1) + W(2\gamma)(8\gamma^2 - 1) - \gamma\overline{p_{\mathrm{R}}} = 0. \tag{3.20}$$

Given $\overline{p_{\mathrm{R}}}$, the above expression can be easily solved for γ using a numerical method.

3.4.2 Probability of Reliability for Dependent Uniform Blocking

In this subsection, we will consider a special case of uniform blockage process and provide a few bounds for the probability of reliability. Note that for this case, the average LOS radius is given as $\beta = \mu L_m/\pi$.

3.4.2.1 Lower Bound I

Note that the area A is the sum of A_1 (the area of $\mathcal{P}_1$) and A_2 (the area of $\mathcal{P}_2$) minus the area of the common region $\mathcal{U}$ (in shape of either a trapezoid or a triangle). We can lower bound this area A by replacing the area of $\mathcal{U}$ by the area of its circumscribing triangle $\mathcal{T}$. Note that for certain values of θ and ℓ, the area of $\mathcal{T}$ may become greater than the area of parallelogram $\mathcal{P}_1$. In this case, we can lower bound the area A by just the area of parallelogram $\mathcal{P}_2$. Hence, we get the following lower bound for area A:

$$A(R_1, R_2, \phi, \ell, \theta) \geq \begin{cases} A_1 + A_2 & \text{for } \theta \leq \phi \\ A_1 + A_2 - T & \text{for } \pi > \theta > \phi, \sin(\theta) < 2R_1 \sin(\phi)/\ell \\ A_2 & \text{for } \pi > \theta > \phi, 1 \geq \sin(\theta) > 2R_1 \sin(\phi)/\ell. \end{cases} \tag{3.21}$$

Now, integrating (3.21) with respect to distribution of θ and ℓ gives the lower bound for $\mathcal{N}(R_1, R_2, \Phi)$ which is denoted by $\underline{\underline{\mathcal{N}}}(R_1, R_2, \Phi)$ and given as

$$\mathcal{N}(R_1, R_2, \Phi) \geq \underline{\underline{\mathcal{N}}}(R_1, R_2, \Phi) = \frac{L_m}{\pi}\left(R_1 + R_2 - R_1 F\left(\frac{R_1}{L_m}, \Phi\right)\right)$$

where $F(a, \Phi) =$

$$\begin{cases} 0 < \Phi \leq \frac{\pi}{2} & \begin{cases} 2a \leq 1 & \frac{1}{2} + \frac{a}{3}(2a-3)\sin^2(\Phi) + \frac{1}{3}T_1 - \frac{2}{3}T_2 + \\ & \frac{4}{3}T_3 - \frac{2}{3}T_4 + \frac{1}{12}T_6 \\ 2a > 1, 2a\sin(\Phi) \leq 1 & \frac{1}{2} - a(2a+1)\sin^2(\Phi) + \frac{1}{3}T_1 - \frac{2}{3}T_2 + \frac{2}{3}T_3 + \\ & \frac{1}{12}T_6 + T_7 \\ 2a\sin(\Phi) \geq 1 & \frac{1}{12a}(1 + (\pi - \Phi)\cot(\Phi)) \end{cases} \\ \frac{\pi}{2} < \Phi < \pi & \begin{cases} 2a \leq 1 & \frac{1}{2} + \frac{a}{3}(2a-3)\sin^2(\Phi) + \frac{1}{3}T_1 - \frac{2}{3}T_2 + \frac{2}{3}T_5 \\ & + \frac{1}{12}T_6 \\ 2a > 1 & \frac{1}{12a}(1 + (\pi - \Phi)\cot(\Phi)) \end{cases} \end{cases}$$

with

$$
\begin{aligned}
T_1 &= \cos(\Phi)\sqrt{1-4a^2\sin^2(\Phi)} \\
T_2 &= a^2\sin^2(\Phi)\cos(\Phi)\log\left(1+\sqrt{1-4a^2\sin^2(\Phi)}\right) \\
T_3 &= a^2\sin^2(\Phi)\cos(\Phi)\log(2a\sin(\Phi)) \\
T_4 &= a^2\sin^2(\Phi)\cos(\Phi)\log(2a(1+\cos(\Phi))) \\
T_5 &= a^2\sin^2(\Phi)\cos(\Phi)\log(2a(1-\cos(\Phi))) \\
T_6 &= \frac{1}{a}\cot(\Phi)\sin^{-1}(2a\sin(\Phi)) \\
T_7 &= \frac{(\pi-2\Phi)}{3}a^2\sin^2(\Phi)\cos(\Phi).
\end{aligned}
$$

Note that $F(a,0)=1$ and $F(a,\pi)=0$.

It can be seen that the lower bound on the mean area $\underline{\underline{\mathcal{N}}}(R_1,R_2,\Phi)$ is dependent on both the blocking parameter β and the maximum blockage length L_m. The monotonicity of A with respect to L_m (as shown in Lemma 6) implies that for a constant β, as L_m increases (which means less but big blockages), $F(a,\Phi)$ increases towards $\frac{1}{2}(1+\cos(\Phi))$. For small L_m, (which means more but small blockages), $F(a,\Phi)$ decreases to 0 which corresponds to the independent case. For intermediate values of L_m, $F(a,\Phi)$ will range between 0 and $\frac{1}{2}(1+\cos(\Phi))$.

Now, the lower bound on reliability probability can be obtained by using Theorem 5 and is given as:

$$
\begin{aligned}
p_{\mathrm{R}} \geq \underline{\underline{p_{\mathrm{R}}}} &= 2+\gamma^2-\gamma(5+2\gamma^2)W(\gamma) \\
&\quad -\frac{1}{2\gamma^2\pi}\int_0^{\pi}\int_0^{\infty}\exp(-x_1(1-F(x_1/(\beta L_m),\phi)))x_1 S(x_1)dx_1\mathrm{d}\phi
\end{aligned}
$$

where $S(x) = \exp\left(\gamma^2 - \left(\frac{1}{2\gamma}x + \gamma\right)^2\right)\left[1 - 2\gamma W\left(\frac{1}{2\gamma}x + \gamma\right)\right]$.

3.4.2.2 Asymptotic Lower Bound

We can also bound the Area A as follows:

$$A(R_1, R_2, \phi, \ell, \theta) \geq \begin{cases} A_1 + A_2 & \text{for } \theta \leq \phi \\ A_2 & \text{for } \pi > \theta > \phi \end{cases}. \tag{3.22}$$

Now, integrating (3.22) with respect to θ and ℓ gives the following lower bound (denoted by $\underline{\mathcal{N}}$) for mean area $\mathcal{N}(R_1, R_2, \Phi)$:

$$\mathcal{N}(R_1, R_2, \Phi) \geq \underline{\mathcal{N}}(R_1, R_2, \Phi) = \frac{L_m}{\pi}\left(R_1 + R_2 - R_1\frac{1}{2}\left(1 + \cos(\Phi)\right)\right). \tag{3.23}$$

As discussed above, for a given β, the lower bound becomes asymptotically tight as $L_m \to \infty$. Now, using the lower bound in (3.23) and Theorem 5, a lower bound (denoted by $\underline{p_{\mathrm{R}}}$) on reliability probability can be obtained as follows:

$$\begin{aligned} p_{\mathrm{R}} \geq \underline{p_{\mathrm{R}}} = 1 + \gamma^2 - \gamma(5 + 2\gamma^2)W(\gamma) + \frac{4\gamma}{\pi}\int_0^{\pi/2}(2 + \sin^2(\phi))W((1 + \sin^2(\phi))\gamma))\mathrm{d}\phi \\ + \frac{2}{\pi}\frac{1}{\gamma}\int_0^{\pi/2}\big[W(\gamma) - W((1 + \sin^2(\phi))\gamma)) \\ + 2\gamma^2\sin^2(\phi)W((1 + \sin^2(\phi))\gamma)) - \sin^2(\phi)\gamma\big]\operatorname{cosec}^4(\phi)\mathrm{d}\phi. \end{aligned} \tag{3.24}$$

Proof. Using Theorem 5 and the lower bound of $\mathcal{N}(R_1, R_2, \Phi)$ derived in (3.23), the lower bound on the reliability probability can be given as:

$$\begin{aligned} \underline{p_{\mathrm{R}}} =& 2 + \gamma^2 - \gamma(5 + 2\gamma^2)W(\gamma) - \\ & \frac{1}{4\gamma^4\pi}\int_0^{\pi}\int_0^{\infty} x_2 \exp\left(-\frac{x_2^2}{4\gamma^2}\right)\int_0^{x_2}\exp\left(-x_1\sin^2(\phi/2) - x_2\right)x_1\mathrm{d}x_1\mathrm{d}x_2\mathrm{d}\phi \\ =& 2 + \gamma^2 - \gamma(5 + 2\gamma^2)W(\gamma) - \end{aligned}$$

$$\frac{1}{4\gamma^4\pi}\int_0^{\pi}\int_0^{\infty} x_2 \exp\left(-x_2-\frac{x_2^2}{4\gamma^2}\right)\int_0^{x_2}\exp\left(-x_1\sin^2(\phi/2)\right)x_1\mathrm{d}x_1\mathrm{d}x_2\mathrm{d}\phi$$
$$=2+\gamma^2-\gamma(5+2\gamma^2)W(\gamma)-$$
$$\frac{1}{4\gamma^4\pi}\int_0^{\pi}\int_0^{\infty} x_2 \exp\left(-x_2-\frac{x_2^2}{4\gamma^2}\right)\frac{1-\exp\left(-x_2\sin^2(\phi/2)\right)\left(1+x_2\sin^2(\phi/2)\right)}{\sin^2(\phi/2)}\mathrm{d}x_2\mathrm{d}\phi.$$

Now, using a $\phi/2\rightarrow\phi$ substitution and some manipulations, we get

$$=2+\gamma^2-\gamma(5+2\gamma^2)W(\gamma)-\frac{2}{\pi}\frac{1}{4\gamma^4}\int_0^{\pi/2}\frac{1}{\sin^4(\phi)}\left[\int_0^{\infty} x\exp(-x-x^2/(4\gamma^2))\mathrm{d}x\right.$$
$$-\sin^2(\phi)\int_0^{\infty} x^2\exp(-x(1+\sin^2(\phi))-x^2/(4\gamma^2))\mathrm{d}x$$
$$\left.-\int_0^{\infty} x\exp(-x(1+\sin^2(\phi))-x^2/(4\gamma^2)))\mathrm{d}x\right].$$

Now, by evaluating the inner integral, we get

$$\underline{p_{\mathrm{R}}}=2+\gamma^2-\gamma(5+2\gamma^2)W(\gamma)-\frac{2}{\pi}\frac{1}{4\gamma^4}\int_0^{\pi/2}\frac{1}{\sin^4(\phi)}\left[2\gamma^2(1-2\gamma W(\gamma))\right.$$
$$-\sin^2(\phi)4\gamma^3\left(W((1+\sin^2(\phi))\gamma)(2(1+\sin^2(\phi))^2\gamma^2+1)-(1+\sin^2(\phi))\gamma\right)$$
$$\left.-2\gamma^2(1-2\gamma(1+\sin^2(\phi))W((1+\sin^2(\phi))\gamma))\mathrm{d}x\right].$$

Now, after some further manipulations, we get

$$\underline{p_{\mathrm{R}}}=1+\gamma^2-\gamma(5+2\gamma^2)W(\gamma)+\frac{4\gamma}{\pi}\int_0^{\pi/2}(2+\sin^2(\phi))W((1+\sin^2(\phi))\gamma))\mathrm{d}\phi$$
$$+\frac{2}{\pi}\frac{1}{\gamma}\int_0^{\pi/2}\left[W(\gamma)-W((1+\sin^2(\phi))\gamma))\right.$$
$$\left.+2\gamma^2\sin^2(\phi)W((1+\sin^2(\phi))\gamma))-\sin^2(\phi)\gamma\right]\mathrm{cosec}^4(\phi)\mathrm{d}\phi.$$

□

The lower bound given in (3.24) can also be approximated using a linear approximation as follows

$$\underline{p_{\mathrm{R}}}\approx\frac{1}{\gamma}\left[3\gamma+\gamma^3-W(\gamma)(2\gamma^4+7\gamma^2+2)+2W(2\gamma)\right].$$

Proof. We start the proof by noting that $\underline{\mathcal{N}}$ in (3.23) can be approximated as

$$\underline{\mathcal{N}}(R_1, R_2, \Phi) \approx \frac{L_m}{\pi}\left(R_2 + R_1\frac{\Phi}{\pi}\right). \tag{3.25}$$

Now, using Theorem 5 and (3.25), the lower bound on the reliability probability is given as:

$$\begin{aligned}\underline{p_{\mathrm{R}}} \approx & 2+\gamma^2-\gamma(5+2\gamma^2)W(\gamma)- \\ & \frac{1}{4\gamma^4\pi}\int_0^{\pi}\int_0^{\infty} x_2 \exp\left(-\frac{x_2^2}{4\gamma^2}\right)\int_0^{x_2}\exp\left(-x_1\phi/\pi - x_2\right) x_1 \mathrm{d}x_1\mathrm{d}x_2\mathrm{d}\phi.\end{aligned}$$

Now, by interchanging the limits for x_1 and ϕ, we get

$$\begin{aligned}\underline{p_{\mathrm{R}}} \approx & 2+\gamma^2-\gamma(5+2\gamma^2)W(\gamma)- \\ & \frac{1}{4\gamma^4\pi}\int_0^{\infty} x_2 \exp\left(-x_2-\frac{x_2^2}{4\gamma^2}\right)\int_0^{x_2} x_1 \int_0^{\pi}\exp\left(-x_1\phi/\pi\right)\mathrm{d}\phi\mathrm{d}x_1\mathrm{d}x_2 \\ = & 2+\gamma^2-\gamma(5+2\gamma^2)W(\gamma) \\ & -\frac{1}{4\gamma^4\pi}\int_0^{\infty}\exp(-x_2-x_2^2/(4\gamma^2))x_2\int_0^{x_2} x_1\frac{1-\exp(-x_1)}{x_1/\pi}\mathrm{d}x_1\mathrm{d}x_2 \\ = & 2+\gamma^2-\gamma(5+2\gamma^2)W(\gamma)-\frac{1}{4\gamma^4}\int_0^{\infty}\exp(-x_2-x_2^2/(4\gamma^2))x_2(x_2-1+e^{-x_2})\mathrm{d}x_2 \\ = & \frac{1}{\gamma}\left[3\gamma+\gamma^3-(7\gamma^2+2\gamma^4+2)W(\gamma)+2W(2\gamma)\right].\end{aligned}$$

□

Now using the bounds computed above along with Theorem 6 and Lemma 6, we give the following Theorem.

Theorem 7. *The probability of reliability of a cellular system with second order macro-diversity in the presence of a uniform blockage process of parameter L_m with*

fixed β, is bounded as

$$\underline{p_{\mathrm{R}}}(\beta/\sqrt{\lambda}) \leq p_{\mathrm{R}}(\lambda, \mu, L_m) \leq \overline{p_{\mathrm{R}}}(\beta/\sqrt{\lambda}) \tag{3.26}$$

where the lower bound is tight for $L_m \to \infty$ and the upper bound for $L_m \to 0$.

It can be seen from Theorem 7 that probability of reliability is bounded above and lower by expressions which are functions of only $\beta/\sqrt{\lambda}$. It implies that BS density needs to scale as β^2 (and hence as square of blockage density (μ^2)) to maintain the same order of reliability. This trend is consistent with a system with no diversity [9].

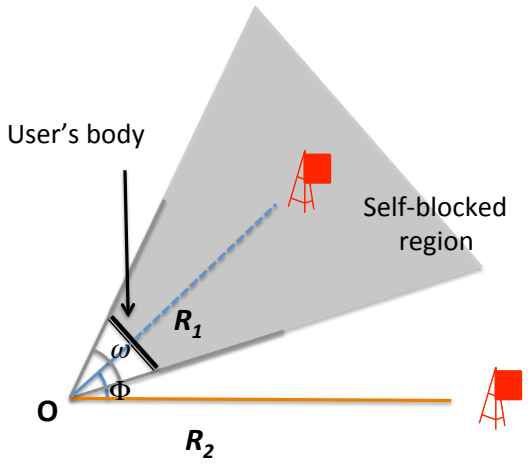

Figure 3.4: Blocking cone created by the user's own body which can block its own serving BS.

3.4.3 Reliability Analysis under Self-blocking

In this subsection, we include the self-blocking in our analysis where a user can self-block its own serving BS. Self-blocking in a cellular network can be modeled

using a blocking cone with angle ω in the body's direction which blocks all the BSs behind the body (see Fig. 3.4) [23, 24]. In this case, we assume that the two control link BSs for a user will be chosen in a way such that always, at least one of the two BSs is not blocked by its own body. This means that the angle between the two BSs must be more than ω. In other words, given the closest BS at distance R_1, the second BS should be chosen such that the angle Φ between the two BSs satisfies $\pi \geq \Phi > \omega$ or $\pi \leq \Phi < -\omega$. Let us denote the distance to the second BS is D_2. We assume that the users orientation are uniformly distributed between 0 and 2π. Therefore, given the two selected control links, the marginal probability that each link is not self-blocked is given by $c = 1 - \frac{\omega}{\pi}$ and the joint probability that both links are not self-blocked is given by $c_2 = 1 - \frac{2\omega}{\pi}$.

The joint distribution of R_1, D_2 and Φ can be computed as

$$f_{R_1,D_2,\Phi}(r_1, r_2, \phi) =$$
$$2\pi\lambda^2 r_1 r_2 \exp(-\lambda\pi c r_2^2 - \lambda\pi(1-c)r_1^2)\mathbb{1}\left(r_1 \leq r_2\right)\mathbb{1}\left((\pi \geq \phi > \omega) \cup (-\pi \leq \phi < -\omega)\right).$$

Integrating the above with respect to Φ and R_1, we can get the marginal distribution of D_2 which is given as

$$f_{D_2}(r_2) = \frac{2c\pi\lambda r_2}{1-c}\left[\exp\left(-\lambda\pi c r_2^2\right) - \exp\left(-\lambda\pi r_2^2\right)\right]. \tag{3.27}$$

Now, let $\mathcal{A}_1$ be the event that the link $\mathbf{Z}_1$ is not blocked (neither blocked by a blockage or self-blocked). Similarly let $\mathcal{A}_2$ be the event that the link $\mathbf{Z}_2$ is not blocked. Then, $\mathbb{P}\left[\mathcal{A}_1\right]$ and $\mathbb{P}\left[\mathcal{A}_2\right]$ is given as

$$\mathbb{P}\left[\mathcal{A}_1\right] = c\exp(-\beta R_1), \qquad \mathbb{P}\left[\mathcal{A}_2\right] = c\exp(-\beta R_2) \tag{3.28}$$

and the joint probability of both linked unblocked is given as

$$\mathbb{P}\left[\mathcal{A}_1 \cap \mathcal{A}_2\right] = c_2 \exp(-\mu \mathcal{N}(R_1, D_2, \Phi)) \tag{3.29}$$

Now, the probability of reliability is given as

$$\begin{aligned} p_{\mathrm{R}} &= \mathbb{E}_{R_1,R_2}\left[\mathbb{P}\left[\mathcal{A}_1 \cup \mathcal{A}_2\right]\right] \\ &= 2\pi\lambda^2 \int_0^{\infty}\int_0^{r_2}\int_0^{2\pi} \left(c\exp(-\beta r_1) + c\exp(-\beta r_2) - c_2 \exp\left(-\mu\mathcal{N}(r_1, r_2, \phi)\right)\right) \\ &\quad \exp(-\lambda\pi c r_2^2 - \lambda\pi(1-c) r_1^2)\mathbb{1}\left((\pi \geq \phi > \omega) \cup (-\pi \leq \phi < -\omega)\right) \mathrm{d}\phi \mathrm{d}r_1 \mathrm{d}r_2. \end{aligned} \tag{3.30}$$

Now using the transformations $x_1 = \beta r_1$ and $x_2 = \beta r_2$, and noting the symmetry of inner term with respect to ϕ around x axis, we get

$$\begin{aligned} p_{\mathrm{R}} =& \frac{1}{4\gamma^2\pi}\int_0^{\infty}\int_0^{x_2}\int_{\omega}^{\pi} \left(c\exp(-x_1) + c\exp(-x_2) - c_2\exp\left(-\mu\mathcal{N}(x_1/\beta, x_2/\beta, \phi)\right)\right) \\ & \exp(-cx_2^2/(4\gamma^2) - (1-c)x_1^2/(4\gamma^2))\mathrm{d}\phi\mathrm{d}x_1\mathrm{d}x_2 \\ =& c\left(2 - \frac{2\gamma}{1-c}\left(W(\gamma) - \frac{W(\gamma/\sqrt{c})}{\sqrt{c}}\right)\right) \\ & - \frac{c_2}{4\gamma^2\pi}\int_0^{\infty}\int_0^{x_2}\int_{\omega}^{\pi} \exp\left(-\mu\mathcal{N}(x_1/\beta, x_2/\beta, \phi)\right) \\ & \qquad \times \exp(-cx_2^2/(4\gamma^2) - (1-c)x_1^2/(4\gamma^2))\mathrm{d}\phi\mathrm{d}x_1\mathrm{d}x_2. \end{aligned} \tag{3.31}$$

For the independent case, the probability of reliability can be obtained by replacing function $\mathcal{N}(r_1, r_1, \phi)$ in (3.31) by $\beta r_1 + \beta r_2$ to get:

$$\begin{aligned} \overline{p_{\mathrm{R}}} =& c\left(2 - \frac{2\gamma}{1-c}\left(W(\gamma) - \frac{W(\gamma/\sqrt{c})}{\sqrt{c}}\right)\right) - \frac{c_2 c}{4\gamma^2}\int_0^{\infty}\int_0^{x_2} \exp\left(-x_1 - x_2\right) \\ & \qquad \times \exp(-cx_2^2/(4\gamma^2) - (1-c)x_1^2/(4\gamma^2))\mathrm{d}x_1\mathrm{d}x_2 \\ =& c\left[2 - \frac{2\gamma}{1-c}\left(W(\gamma) - \frac{W(\gamma/\sqrt{c})}{\sqrt{c}}\right) - \frac{c_2}{4\gamma^2}\int_0^{\infty}\int_0^{x_2} \exp\left(-x_1 - x_2\right)\right. \end{aligned}$$

$$\times \exp(-cx_2^2/(4\gamma^2) - (1-c)x_1^2/(4\gamma^2))\mathrm{d}x_1\mathrm{d}x_2\Big]. \tag{3.32}$$

Consider the special case $\omega = \pi/2$. Here $c = 1/2$ and the last term can be further solved owing to the symmetry of the inner terms with respect to x_1 and x_2:

$$\overline{p_{\mathrm{R}}} = c\left[2 - \frac{2\gamma}{1-c}\left(W(\gamma) - \frac{W(\gamma/\sqrt{c})}{\sqrt{c}}\right) - \frac{c_2\gamma}{2(1-c)^2}\left(1 - \frac{2}{\sqrt{1-c}}W\left(\frac{\gamma}{\sqrt{1-c}}\right)\right)^2\right]. \tag{3.33}$$

The lower bounds computed in the previous subsections can similarly be obtained for the self-blocking case by replacing the joint distribution of R_1, R_2 with the joint distribution of R_1, D_2 and Φ and adding the probability of self-blocking in terms $\mathbb{P}\left[\mathcal{A}_1\right], \mathbb{P}\left[\mathcal{A}_2\right]$ and $\mathbb{P}\left[\mathcal{A}_1 \cup \mathcal{A}_2\right]$. The asymptotic lower bound is given as

$$\begin{aligned}\underline{p_{\mathrm{R}}} = {} & c\left(2 - \frac{2\gamma}{1-c}\left(W(\gamma) - \frac{W(\gamma/\sqrt{c})}{\sqrt{c}}\right)\right) \\ & - \frac{c_2}{2\gamma^2\pi}\int_0^{\infty}\int_{\omega}^{\pi} S(x)\exp(-x\sin^2(\Phi/2) - (1-c)x^2/4\gamma^2)x\mathrm{d}x\end{aligned} \tag{3.34}$$

where

$$S(x) = \frac{1}{c}\exp\left(\gamma_c^2 - \left(\frac{1}{2\gamma_c}x + \gamma_c\right)^2\right)\left(1 - 2\gamma_c W\left(\frac{1}{2\gamma_c}x + \gamma_c\right)\right). \tag{3.35}$$

3.5 Reliability Analysis for nth Order Diversity

We now consider the general case with nth order diversity. In this case, the typical user at the origin $\mathbf{O}$ is connected with n BSs $\mathbf{B}_1 \cdots \mathbf{B}_n$ with link lengths equal to $R_1 \cdots R_n$. Let us denote the angle between the link $\mathbf{Z}_n$ and other links $\mathbf{Z}_1, \mathbf{Z}_2 \cdots \mathbf{Z}_{n-1}$ respectively as $\Phi_1 \cdots \Phi_{n-1}$. Without loss of generality, we assume

that $\mathbf{x}_n$ is at x axis. The joint distribution of R_n's is given as (see proof below):

$$f(r_1, r_2, \cdots, r_n) = (2\pi\lambda)^n r_1 r_2 \cdots r_n \exp(-\lambda\pi r_n^2), \text{ if } r_1 \leq r_2 \leq \cdots \leq r_n \tag{3.36}$$

and $\Phi_i \sim \text{Uniform}(0, 2\pi)$.

Proof. For any $i \leq n$, conditioned on the event $R_j = r_j (j \leq i)$, the distribution of R_{i+1} is given as

$$\begin{aligned}
&\mathbb{P}\left[R_{i+1} \leq r_{i+1} | R_j = r_j, j \leq i\right] \\
&= \mathbb{P}\left[\text{There exists at least one point in the ring } r_i \leq r \leq r_{i+1}\right] \\
&= 1 - \exp\left(-\lambda\pi(r_{i+1}^2 - r_i^2)\right).
\end{aligned} \tag{3.37}$$

Hence, the conditional PDF of R_{i+1} is given as

$$f_{R_{i+1}}(r_{i+1} | R_j = r_j, j \leq i) = 2\lambda\pi r_{i+1} \exp\left(-\lambda\pi(r_{i+1}^2 - r_i^2)\right) \tag{3.38}$$

$$\implies f_{\{R_j\}, R_{i+1}}(\{r_j\}, r_{i+1}) = 2\lambda\pi r_{i+1} \exp\left(-\lambda\pi(r_{i+1}^2 - r_i^2)\right) f_{\{R_j\}}(\{r_j\}). \tag{3.39}$$

Now iterating (3.39) for $n-1$ times from $i = n-1$ up to $i = 1$, we get the joint distribution as follows

$$\begin{aligned}
f_{\{R_j\}, j \leq n}(\{r_j\}) &= (2\lambda\pi)^n r_n r_{n-1} \cdots r_1 \prod_{i=1}^{n-1} \exp\left(-\lambda\pi(r_{i+1}^2 - r_i^2)\right) \\
&= (2\lambda\pi)^n r_n r_{n-1} \cdots r_1 \exp\left(-\lambda\pi r_n^2\right).
\end{aligned} \tag{3.40}$$

□

Following the similar arguments as taken in the second order case, the probability of reliability can be computed which is given in the following Theorem.

Theorem 8. *Let $\mathcal{P}_i$ denote a parallelogram with sides $\mathbf{Z}_i$ (with length r_i and orientation ϕ_i) and* **AB** *(with length ℓ and orientation θ) as shown in Fig. 3.5. Let $A(S, \{r_i\}, \{\phi_i\}, \ell, \theta)$ is the area of union of parallelograms $\mathcal{P}_i$'s ($i \in S$) where S is a subset of $\{1, 2, \cdots, n\}$. Let $\mathcal{N}(\{r_i\}, \{\phi_i\})$ denote the average of the area A over (L, Θ) which is given as*

$$\mathcal{N}(S, \{r_i\}, \{\phi_i\}) = \int_0^\infty \int_0^\pi A(S, \{r_i\}, \{\phi_i\}, \ell, \theta) F_L(\mathrm{d}\ell) F_\Theta(\mathrm{d}\theta). \tag{3.41}$$

Now, the reliability probability in a cellular network with nth order of macro-diversity is given as

$$p_{\mathrm{R}} = \frac{1}{(2\pi)^{n-1}} \int_{[0,2\pi]^{n-1}} \int_{(\mathbb{R}^+)^n} K(\{r_i\}, \{\phi_i\}) f_{\{R_i\}}(\{r_i\}) \mathrm{d}r_1 \mathrm{d}r_2 \cdots \mathrm{d}r_n \mathrm{d}\phi_1 \cdots \mathrm{d}\phi_{n-1}$$

where $f_{\{R_i\}}(\{r_i\})$ is the joint distribution of R_i's given in (3.36) *and*

$$K(\{r_i\}, \{\phi_i\}) = \sum_{S: S \subset [1,n]}^{n} (-1)^{|S|-1} \exp(-\mu \mathcal{N}(S, \{r_i\}, \{\phi_i\})).$$

Due to large numbers of variables in Theorem 8, it is not possible to analytically solve the expression. Hence, we consider the two special cases to bound the probability of reliability.

3.5.1 Independent Blocking

We first consider the independent blocking case. As argued in the $n = 2$ case, the probability of reliability in the independent blocking scenario provides an upper bound to the probability of reliability in the dependent blocking scenario.

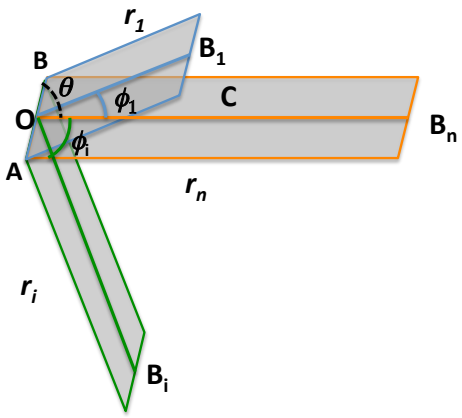

Figure 3.5: The union of n parallelograms $\mathcal{P}_n$ described in Theorem 8.

Let $\mathcal{A}_j$ denote the probability that jth link ($\mathbf{Z}_j$) is not blocked. Hence, the probability that at least one link is unblocked is given as

$$\mathbb{P}\left[\cup\mathcal{A}_j\right] = 1 - \mathbb{P}\left[\cap\mathcal{A}_j^{\complement}\right] = 1 - \prod_{j=1} n\mathbb{P}\left[\mathcal{A}_j\right] = 1 - \prod_{j=1}^{n}(1-\exp(-\beta R_j)).$$

Therefore the probability of reliability is given as

$$\begin{aligned}
\overline{p_{\mathrm{R}}} &= 1 - \int_0^\infty \int_0^\infty \cdots \int_0^\infty (1-e^{-\beta r_1})(1-e^{-\beta r_2})\cdots(1-e^{-\beta r_n}) f(r_1, r_2, \cdots, r_n) \\
&\qquad \mathrm{d}r_1 \mathrm{d}r_2 \cdots r_n \\
&= 1 - (2\pi\lambda)^n \int_0^\infty \int_0^{r_n} \cdots \int_0^{r_2} (1-e^{-\beta r_1})(1-e^{-\beta r_2})\cdots(1-e^{-\beta r_n}) r_1 r_2 r_n \\
&\qquad \exp(-\lambda\pi r_n^2)\mathrm{d}r_1 \mathrm{d}r_2 \cdots \mathrm{d}r_n \\
&= 1 - \frac{2\cdot(2\gamma)^{-2n-2}}{\Gamma(n+1)} \int_0^\infty e^{-t^2/(4\gamma^2)} \left[t^2 - 2 + 2e^{-t}(t+1)\right]^n dt \qquad (3.42)
\end{aligned}$$

where the last step is due to mathematical induction.

Proof. The probability of reliability for the independence blocking case is given as

$$\overline{p_{\mathrm{R}}} = 1 - \int_0^\infty \int_0^\infty \cdots \int_0^\infty (1-e^{-\beta r_1})(1-e^{-\beta r_2})\cdots(1-e^{-\beta r_n}) f(r_1, r_2, \cdots, r_n) \mathrm{d}r_1 \mathrm{d}r_2 \cdots \mathrm{d}r_n$$

$$= 1 - (2\pi\lambda)^n \int_0^\infty \int_0^{r_n} \cdots \int_0^{r_2} \prod_{i=1}^{n} r_i (1 - e^{-\beta r_i}) \exp(-\lambda\pi r_n^2) \mathrm{d}r_1 \mathrm{d}r_2 \cdots \mathrm{d}r_n.$$

Using the substitutions $x_i = \beta r_i$, we get

$$\overline{p_{\mathrm{R}}} = 1 - \frac{(2\pi\lambda)^n}{\beta^{2n}} \int_0^\infty \int_0^{x_n} \cdots \int_0^{x_2} \prod_{i=1}^{n} x_i (1 - e^{-x_i}) \exp\left(-\frac{\lambda\pi}{\beta^2} x_n^2\right) \mathrm{d}x_1 \mathrm{d}x_2 \cdots \mathrm{d}x_n. \tag{3.43}$$

Let us define the function $J(n-i, y)$ by the following recursion

$$\begin{aligned} J(i, y) &= \int_0^y t(1 - e^{-t}) J(i-1, t) \mathrm{d}t \\ J(0, y) &= 1. \end{aligned}$$

Then, (3.43) can be written as

$$\overline{p_{\mathrm{R}}} = 1 - \frac{(2\pi\lambda)^n}{\beta^{2n}} \int_0^\infty \exp\left(-t^2/(4\gamma^2)\right) t(1 - e^{-t}) J(n-1, t) \mathrm{d}t. \tag{3.44}$$

Now, we will prove the following using mathematical induction.

$$J(i, y) = \frac{1}{2^i} \frac{1}{i!} \left[y^2 - 2 + 2(y+1)e^{-y}\right]^i. \tag{3.45}$$

Step 1: For $i = 0$,

$$J(0, y) = \frac{1}{2^0} \frac{1}{0!} \left[y^2 - 2 + 2(y+1)e^{-y}\right]^0 = 1.$$

Step 2: Let us assume

$$J(i, y) = \frac{1}{2^i} \frac{1}{i!} \left[y^2 - 2 + 2(y+1)e^{-y}\right]^i.$$

Then

$$J(i+1, y) = \int_0^y t(1 - e^{-t}) J(i, t) \mathrm{d}t = \frac{1}{2^i} \frac{1}{i!} \int_0^y t(1 - e^{-t}) \left[t^2 - 2 + 2(t+1)e^{-t}\right]^i \mathrm{d}t$$

$$
\begin{aligned}
&\overset{(a)}{=} \frac{1}{2^{i+1}} \frac{1}{i!} \int_0^{y^2-2+2(y+1)e^{-y}} u^i \mathrm{d}u \\
&= \frac{1}{2^{i+1}} \frac{1}{(i+1)!} \left[y^2 - 2 + 2(y+1)e^{-y}\right]^{i+1}
\end{aligned}
$$

which proves the identity (3.45). Using this identity in (3.44), we get

$$
\begin{aligned}
\overline{p_{\mathrm{R}}} &= 1 - \frac{2^{-2n+1}\gamma^{-2n}}{(n-1)!} \int_0^{\infty} \exp\left(-t^2/(4\gamma^2)\right) t(1-e^{-t}) \left[t^2 - 2 + 2(t+1)e^{-t}\right]^{(n-1)} \mathrm{d}t \\
&= 1 - \frac{2 \cdot (2\gamma)^{-2n-2}}{\Gamma(n+1)} \int_0^{\infty} e^{-t^2/(4\gamma^2)} \left[t^2 - 2 + 2e^{-t}(t+1)\right]^n dt
\end{aligned}
$$

where the last step is due to integration by part. □

3.5.2 Dependent Blocking in Presence of Uniform Blockages

We now consider a cellular system with blockage process where blockage lengths and orientations are uniformly distributed. Due to number of variables, the area of the union of parallelograms $\mathcal{P}_j$ is complex to be evaluated. Hence, we provide a tractable lower bound for the dependent blockage case.

Let A_j denote the area of the parallelogram $\mathcal{P}_j$. Now consider a set $S = \{i_1, i_2, \cdots, i_k\} \subset \{1, 2, \cdots, n\}$ with increasing order of indexes. Without loss of generality assume that $\Phi_{i_k} = 0$. Given θ, let $\mathcal{E}_j$ denote event that $(\theta \leq \Phi_{i_j} \leq \pi + \theta)$. This event is equivalent to the condition that the parallelogram $\mathcal{P}_{i_j}$ does not overlap with parallelogram $\mathcal{P}_{i_k}$. It can be seen that there can not be two or more mutually disjoint parallelograms which does not overlap with $\mathcal{P}_{i_k}$ also.

Now, we can bound the Area $A(S, \ell, \theta)$ from below as follows:

$$
A(S, \ell, \theta) \geq A_{i_k} + A_{i_{k-1}} \mathbb{1}\left(\mathcal{E}_{i_{k-1}}\right) + A_{i_{k-2}} \mathbb{1}\left(\mathcal{E}^{\complement}_{i_{k-1}} \cap \mathcal{E}_{i_{k-2}}\right) + A_{i_{k-3}} \mathbb{1}\left(\cap_{j=1}^{2} \mathcal{E}^{\complement}_{i_{k-j}} \cap \mathcal{E}_{i_{k-3}}\right)
$$

$$+\cdots+A_{i_{k-l}}\mathbb{1}\left(\cap_{j=1}^{l-1}\mathcal{E}_{i_{k-j}}^{\complement}\cap\mathcal{E}_{i_{k-l}}\right)+\cdots+0\cdot\mathbb{1}\left(\cap_{j=1}^{k-1}\mathcal{E}_{i_{k-j}}^{\complement}\right). \tag{3.46}$$

In the above lower bound, we always include the area of the largest parallelogram $\mathcal{P}_{i_k}$. Now, if next largest parallelogram $\mathcal{P}_{i_{k-1}}$ is not overlapping with $\mathcal{P}_{i_k}$ (which is equivalent to $\mathcal{E}_{i_{k-1}}$), then we will include $\mathcal{P}_{i_k}$ in the lower bound. Now, as discussed above, there cannot be any other parallelogram $\mathcal{P}_{i_j}$ $(j \leq k-1)$ which does not overlap with either of the two parallelograms $\mathcal{P}_{i_k}$ and $\mathcal{P}_{i_{k-1}}$. But, if $\mathcal{P}_{i_{k-1}}$ overlaps with $\mathcal{P}_{i_k}$, then we will consider the next largest parallelogram $\mathcal{P}_{i_{k-2}}$. We continue the search until we get the one parallelogram disjoint to $\mathcal{P}_{i_k}$. If there are no such disjoint parallelogram, then we will keep only the area of $\mathcal{P}_{i_k}$ in the lower bound.

Now, integrating (3.46) with respect to θ and ℓ gives the following lower bound (denoted by $\underline{\mathcal{N}}$) of function $\mathcal{N}(S,\{R_i\},\{\Phi_i\})$:

$$\mathcal{N}(S,\{R_i\},\{\Phi_i\}) \geq \underline{\mathcal{N}}(S,\{R_i\},\{\Phi_i\}) = \frac{L_m}{\pi}\left(r_{i_k}+\sum_{j=1}^{k-1} r_{i_j}\frac{1}{2^{j-1}}\sin^2(\Phi_{i_j}/2)\right).$$

Proof. Recall that given θ, let $\mathcal{E}_j$ denote event that $(\theta \leq \Phi_{i_j} \leq \pi+\theta)$. Hence,

$$\mathbb{P}\left[\mathcal{E}_j\right] = \mathbb{E}_\theta\left[\theta \leq \Phi_{i_j} \leq \pi+\theta\right] = \frac{1}{2}.$$

Also, the area of $\mathcal{P}_{i_j}$ is given as

$$A_{i_j} = R_{i_j}\ell\sin(|\theta-\Phi_{i_j}|).$$

Now, taking expectation of the both sides of (3.46) with respect to ℓ and θ, we get

$$\mathbb{E}\left[A(S,\ell,\theta)\right] \geq \mathbb{E}\left[A_{i_k}\right] + \sum_{m=1}^{k}\mathbb{E}\left[A_{i_{k-m}}\mathbb{1}\left(\cap_{j=1}^{m-1}\mathcal{E}_{i_{k-j}}^{\complement}\cap\mathcal{E}_{i_{k-m}}\right)\right]$$

$$= R_{i_k}\mathbb{E}\left[\ell\right]\ \mathbb{E}\left[\sin(|\theta-\Phi_{i_k}|)\right] + \sum_{m=1}^{k} R_{i_{k-m}}\mathbb{E}\left[\ell\right]\ \mathbb{E}\left[\sin(|\theta-\Phi_{i_{k-m}}|)\mathbb{1}\left(\cap_{j=1}^{m-1}\mathcal{E}_{i_{k-j}}^{\complement}\cap\mathcal{E}_{i_{k-m}}\right)\right].$$

Now $\mathcal{E}_j$'s are mutually independent and also independent to $\Phi_m, j \neq m$. Therefore, we get

$$\mathbb{E}\left[A(S,\ell,\theta)\right] \geq R_{i_k}\frac{L_m}{\pi} + \frac{L_m}{2}\sum_{m=1}^{k} R_{i_{k-m}}\mathbb{E}\left[\sin(|\theta-\Phi_{i_{k-m}}|)\mathbb{1}\left(\mathcal{E}_{i_{k-m}}\right)\right]\prod_{j=1}^{m-1}\mathbb{P}\left[\mathcal{E}_{i_{k-j}}^{\complement}\right]$$
$$= \frac{L_m}{\pi}\left(R_{i_k} + \sum_{j=1}^{k-1} R_{i_j}\frac{1}{2^{j-1}}\sin^2(\Phi_{i_j}/2)\right).$$

Here, the last step is due to the following:

$$\mathbb{E}\left[\sin(|\theta-\Phi_{i_j}|)\mathbb{1}\left(\mathcal{E}_{i_j}\right)\right] = \frac{1}{\pi}\int_0^{\Phi_{i_j}}\sin(\Phi_{i_j}-\theta)\mathrm{d}\theta = \frac{1}{\pi}\cos(\Phi_{i_j}-\theta)\Big|_0^{\Phi_{i_j}} = \frac{2}{\pi}\sin^2(\Phi_{i_j}/2).$$

□

Now using the Theorem 8, the lower bound on the probability of reliability can be computed which is given as follows:

$$p_{\mathrm{R}} \geq \underline{p_{\mathrm{R}}} = \frac{1}{(2\pi)^{n-1}}\frac{1}{2^n\gamma^{2n}}\int_{[0,2\pi]^{n-1}}\int_{x_1\leq x_2\cdots\leq x_n} K(\{x_i\},\{\phi_i\})\exp\left(-x_n^2/(4\gamma^2)\right)$$
$$\times x_1x_2\cdots x_n\mathrm{d}x_1\mathrm{d}x_2\cdots\mathrm{d}x_n\mathrm{d}\phi_1\cdots\mathrm{d}\phi_{n-1} \tag{3.47}$$

where

$$K(\{x_i\},\{\phi_i\}) = \sum_{k=1}^{n}\sum_{S:S\subset[1,n],|S|=k}^{n}(-1)^{k-1}\exp\left(-x_{i_k} - \sum_{j=1}^{k-1}x_{i_j}\frac{1}{2^{j-1}}\sin^2(\phi_{i_j}/2)\right).$$

Similar to the $n = 2$ case, it can be shown that $\mu A(S,\ell,\theta)$ and hence probability of reliability decreases with increasing L_m for a given β, and the lower bound becomes asymptotic tight for large L_m as $L_m \to \infty$. Now by combining the upper

bound computed from the independent blocking, lower bound computed above and monotonicity of probability of reliability, we get the following Theorem.

Theorem 9 (General n case)**.** *The probability of reliability of a cellular system with nth order macro-diversity in presence of a blockage process (with* $\ell \sim U(0, L_m)$ *and* $\theta \sim U(0, \pi)$*) with fixed* β*, is bounded as*

$$\overline{p_{\mathrm{R}}}(\beta/\sqrt{\lambda}) \geq p_{\mathrm{R}}(\lambda, \mu, L_m) \geq \underline{p_{\mathrm{R}}}(\beta/\sqrt{\lambda}) \tag{3.48}$$

where $\overline{p_{\mathrm{R}}}$ *and* $\underline{p_{\mathrm{R}}}$ *is given in* (3.42) *and* (3.47)*. The two bounds are achieved when the maximum blockage size* L_m *is 0 and* ∞ *respectively.*

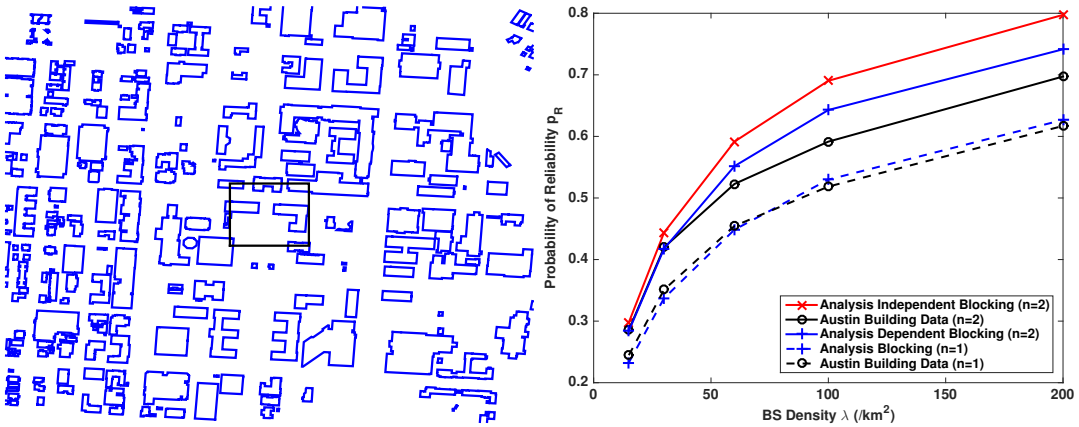

Figure 3.6: Validation of analysis with real building data (a) The used building map near the University of Texas at Austin. The rectangular area in the center denotes the locations of generated users. BSs are uniformly generated over the whole space. (b) The probability of reliability for a cellular system with first and second order diversity.

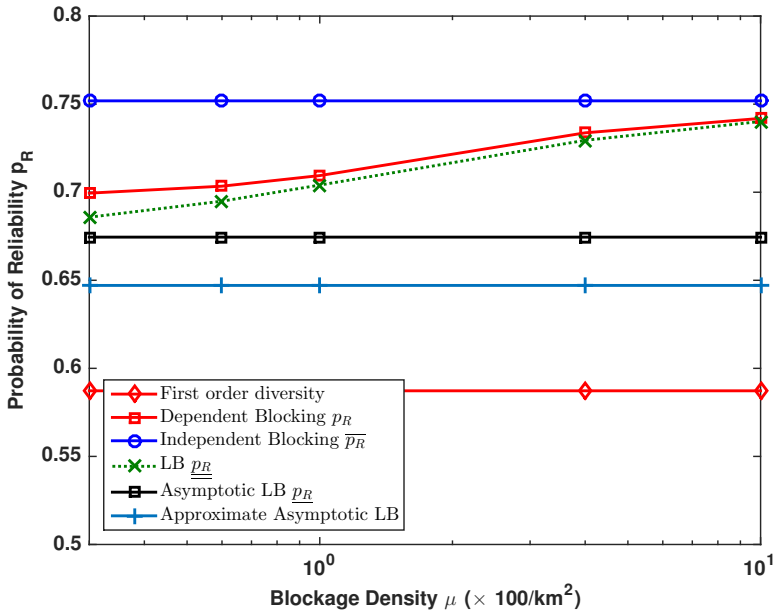

Figure 3.7: Probability of reliability in presence of blockages with fixed β and varying density (μ) in a cellular system with second order diversity. The p_{R} for independent blockage case and computed lower bounds are also shown.

3.6 Numerical Results

In this section, we present few numerical results to provide further insights. The numerical results are obtained by numerically evaluating the analytical expressions from the previous sections and validated by simulation. We consider blockage process with uniform distribution of blockages lengths and orientation and with parameter β. The BS density is assumed to be $\lambda = 30$ BS/km^2.

Validation with Real Building Data. To validate our analysis, we consider a region near the University of Texas at Austin [14] as shown in Fig. 3.6(a) with BSs location modeled as PPP and users uniformly located in the smaller rect-

angle uniformly. For a system with second order macro-diversity, we plot the actual reliability probability with the one computed from the analysis in Fig. 3.6(b). The parameters are obtained by fitting the LOS probability for single BS link and are given as $\beta = 0.012/\text{m}$ and $\mu = 2.25 \times 10^{-4}\text{m}^2$. It can be observed that analysis approximates the performance in the real scenario well.

Impact of Blockage Correlation: We now show the impact of blockage correlation by decreasing the blockage size with fixed β. Fig. 3.7 shows the variation of probability of reliability with respect to blockage density μ while keeping β fixed at 6.4km^{-1}. As shown in analysis, the probability of reliability decreases when L_m increases or μ decreases. Fig. 3.7 also shows p_{R} for the independent blocking case and asymptotic lower bound for $L_m \to \infty$ case. It can be seen that p_{R} reaches the independent blocking case for high blockage density and low blockage size. This result shows that correlation in blockages can decrease the reliability probability by 15%.

Impact of Self-Blocking: We now consider a cellular system with second order macro-diversity and self-blocking with blocking angle of 60^{o}. Fig. 3.8 shows the variation of probability of reliability with respect to blockage density μ while keeping β fixed at 6.4km^{-1}. Due to self-blocking the probability of reliability has further decreased than the case with no self-blocking. Fig. 3.8 also shows p_{R} for the independent blocking case and asymptotic lower bound for $L_m \to \infty$ case. It can be seen that p_{R} decreases when L_m increases or μ decreases and reaches $\overline{p_{\text{R}}}$ for high blockage density.

Impact of Blockage Density and Scaling: Fig. 3.9 shows the variation of probability of reliability with respect to blockage density μ while keeping L_m fixed at

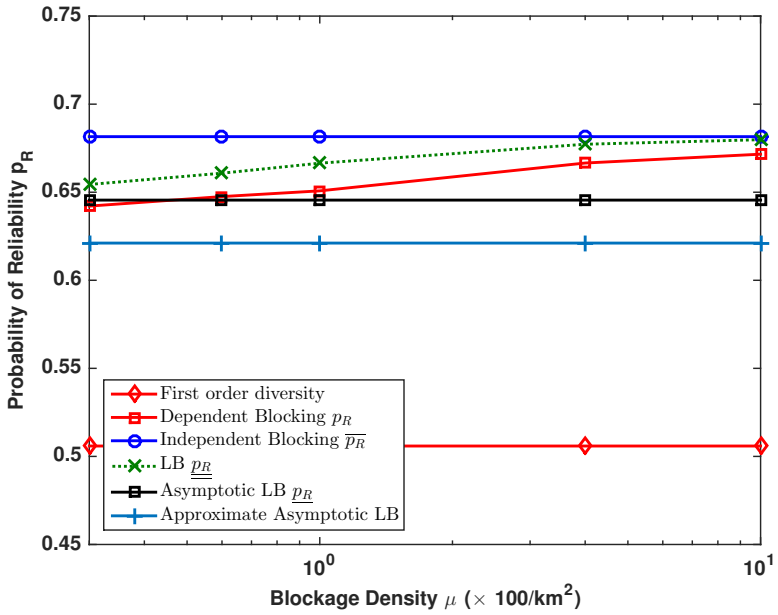

Figure 3.8: The probability of reliability in presence of self-locking and blockages with fixed β and varying density (μ) in a second order cellular system. The p_{R} for independent blockage case and computed lower bounds are also shown.

100m and with fixed BS density, along with p_{R} for the independent blocking case and asymptotic lower bound for $L_m \to \infty$ case. It can be obeserved that the bounds for p_{R} become tighter for higher blockage density. Since the BS density is kept fixed, the probability of reliability decreases significantly with μ. To show the required scaling requirements, we show in Fig. 3.10, variation of probability of reliability with respect to blockage density μ while keeping L_m fixed at 100m and scaling BS density as μ^2. It can be seen that the probability of reliability decreases slightly with μ but remains quite flat with constant upper and lower bounds. This implies that BS density should scale as μ^2 to keep the same level of LOS connectivity in the system.

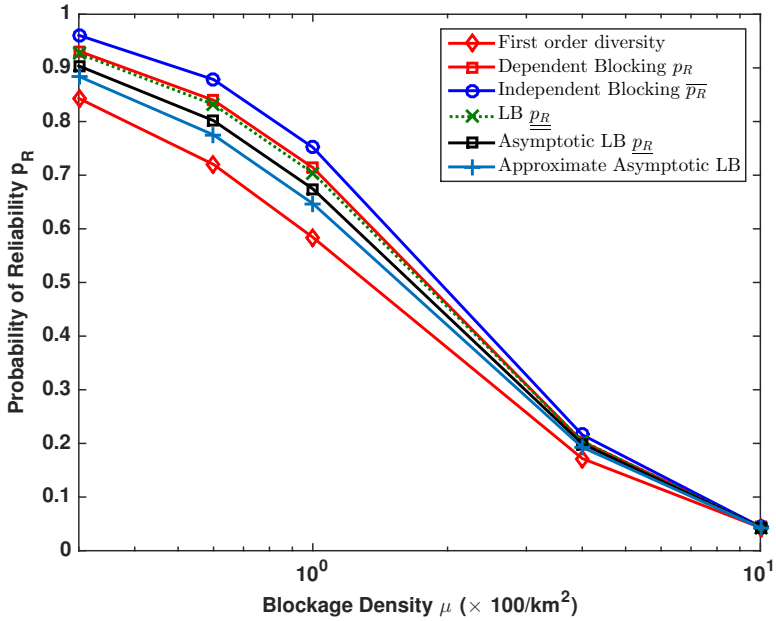

Figure 3.9: Probability of reliability in presence of blockages with fixed $L_m = 100m$ and varying density (μ) in a cellular system with second order diversity. The p_{R} for independent blockage case and computed lower bounds are also shown. The bounds become more tight for larger blockage density.

Impact of Macro-Diversity: We now show the gain of macro-diversity. We assume uniform blockage with density $\mu = 100/\mathrm{km}^2$ and maximum blockage length $L_m = 100\mathrm{m}$ which is equivalent to $\beta = 6.4\mathrm{km}^{-1}$. Fig. 3.11 shows required density (obtained from solving the reverse problem) as a function of p_{R} for various diversity order for the independent blocking case. It can be seen that if each user can be connected to four BSs at any time, the required BS density to achieve a certain probability of reliability is decreased by order of tens. In particular, for $p_{\mathrm{R}} = 0.9$, the required BS density for $n = 4$ is $90\mathrm{BS}/\mathrm{km}^2$ which is 10 times less than the required BS density for $n = 1$.

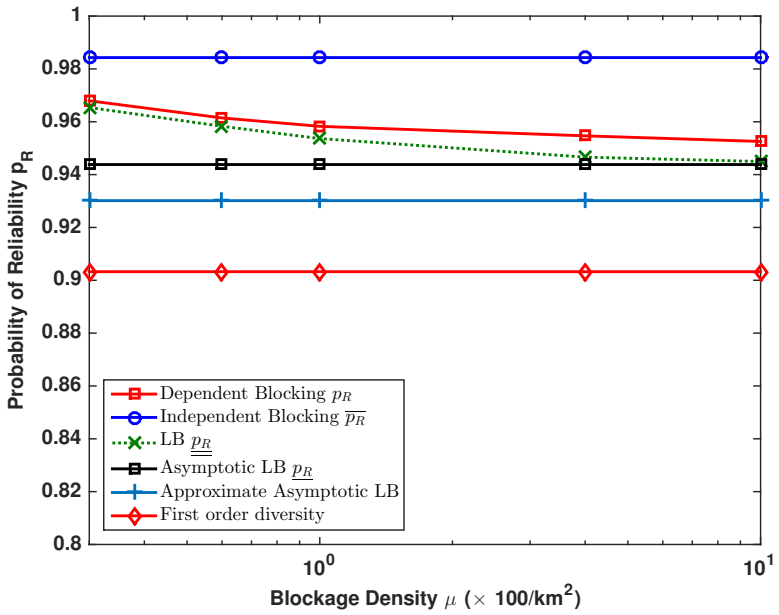

Figure 3.10: Probability of reliability in presence of blockages with fixed $L_m = 100m$ and varying blockage density (μ) and scaling BS density (λ) as μ^2 in a cellular system with second order diversity. p_{R} for independent blockage case and computed lower bounds are also plotted.

3.7 Conclusions

In this paper, we evaluated the gains of macro-diversity for a mmWave cellular system in presence of random blockages. We proposed a framework to analyze the correlation among blocking of multiple links in a cellular system and computed the system's reliability. We also study the impact of blockage sizes and show that diversity gains are higher when blockages are small. We also show that BS density should scale as square of blockage density to maintain a certain level of system reliability. The work has numerous extension. First, the proposed framework can be extended to analyze the coverage probability and rate coverage in the system with multi-BS diversity.

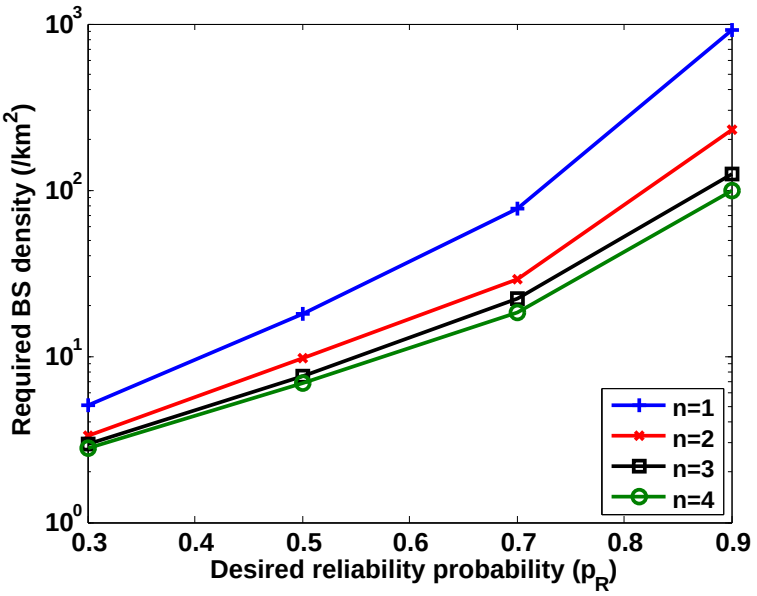

Figure 3.11: Required BS density versus desired probability of reliability for various diversity order (n) in independent blockage case. Higher diversity order can reduce the required BS density by order of magnitudes.

Second, the framework can used to develop a correlated shadowing model to study the impact of correlated shadowing on cellular systems' performance. Third, the framework can be extended to include multi-cell cooperation where a user is served simultaneously by multiple BSs possibly, with possible load optimization.

Chapter 4

Uncoordinated Sharing of Spectrum Licenses in mmWave Cellular Systems

As described in the first chapter, communication at mmWave frequencies has non-trivial differences when compared to communication at conventional cellular frequencies (below 6GHz). For example, the typical use of many antennas in mmWave systems results in highly directional communication [7, 79], and under some circumstances, it is noise limited [13, 80–82]. In general, mmWave communication causes less interference to neighboring BSs operating in the same frequency bands compared to communication at conventional cellular frequencies (CCF) [6, 8] which requires us to rethink how mmWave spectrum should be licensed. In conventional cellular licensing, commercial operators buy exclusive licenses which give each of them exclusive and complete control over a band of spectrum. This conventional exclusive licensing is not efficient for mmWave for the aforementioned reasons. In this chapter,[1] we will explore the possibility of a new kind of sharing which we call as *uncoordinated spectrum license sharing*: independent cellular operators who own licenses for separate frequency bands agree to share the complete rights of operation in each other's bands without any explicit coordination. Sharing licenses (if possible), will allow all

[1]This work has appeared in [83] and [84] in parts. I am the first author of both of these articles.

networks to use the full spectrum simultaneously without impacting the individual achieved rates and help networks to reduce their expenses by sharing the license costs. Such uncoordinated sharing of licenses was not possible in CCF due to high interference caused by serving BSs which renders the channel unusable to any nearby BS of other networks operating in the same frequency band. In the rest of the chapter, we will use spectrum license sharing to denote uncoordinated spectrum license sharing unless explicitly stated.

4.1 Related Work

For mmWave bands, there are no regulatory rules for cellular services yet, although there are many incumbent services including fixed services, satellite to earth communications, military, and research activities and unlicensed operations. It has been reported that the spectrum remains underutilized [85] due to this exclusive licensing at CCF which is expected to be even worse for mmWave bands. There has been significant work related to cognitive radios to help fill the gaps in the underutilized spectrum by letting secondary users make use of the spectrum band via sensing based access control [86–90] for CCF. In [33, 91–93], various aspects and performance of spectrum sharing were studied in a cellular setting. Most related to this paper, in [33], dynamic spectrum sharing between different operators was shown to achieve reasonable sensing performance in 3GPP LTE-A systems with carrier aggregation. Various cognitive license sharing schemes such as licensed shared access (LSA) and authorized shared access (ASA) were proposed [94, 95] which allow more than one entity to use the spectrum. In the presence of incumbent services, the above mentioned

techniques [94, 95] would authorize a cellular system to transmit, only when the incumbent services are idle [96–98]. Implementation would require some kind of sensing or central coordination, which may waste important resources resulting in underutilization of spectrum. Further, it was shown in [99,100] that spectrum gaps will be rare for ultra-dense deployment of small cells in a multi-tier network and spectrum sensing based cognitive approaches may not give the desired gain. Another way to resolve the transmission conflicts between multiple licensees (or entities in case of unlicensed spectrum) is by the use of a central database which keeps track of transmission of each licensee [101]. This reduces the requirement of continuous listening/sensing of the spectrum by each licensee/entity but creates significant feedback/transmission overhead and possibly delay due to the central database.

In recent work, stochastic geometry has emerged as a tractable approach to model and analyze various wireless systems. For example, the performance of a single operator mmWave system had been investigated in prior work using tools from stochastic geometry [8, 14, 102, 103]. In [102], a stochastic geometry framework for analysis of mmWave network was proposed. In [8,103], a blocking model for mmWave communication was proposed to distinguish between line-of-sight (LOS) and non-LOS (NLOS) transmission links and performance metrics such as coverage probability and per-user rate were derived using stochastic geometry. In [14], a stochastic geometry framework was presented for mmWave network with backhaul and co-existent microwave network. In [104], it was shown that even a very dense mmWave network tends to be noise limited for certain choices of parameters. A major limitation of the prior work on mmWave systems [8,14,102–104] is the assumption of a single operator.

To study the impact of an operator's active BS on closely located BSs of other operators, a more general framework containing multiple operators is needed. For CCF, a heterogeneous system (HetNet) consisting of multiple tiers of the same operator was studied in [17] where all the tiers were operating in the same frequency band. Similarly for mmWave, a numerical framework was presented for a mmWave HetNet with generalized fading in [105]. In [105], only single operator was considered and BSs were assumed to have open access to all the users, while as envisioned in this paper, commercial providers are expected to have closed access to its customers or users. Cognitive networks have also been studied using tools from stochastic geometry for CCF. For example, in [106], a stochastic geometry model was presented for spectrum sharing to characterize the system performance in terms of transmit capacity. In [107], a cognitive carrier sensing protocol was proposed and analyzed for a network consisting of multiple primary and secondary users and spectrum access probabilities and transmission capacity were computed. There is limited work to analyze the impact of spectrum sharing among operators at CCF using stochastic geometry. For example, in [108], the impact of infrastructure and CCF spectrum sharing was studied using stochastic geometry. As discussed above, communication at mmWave frequencies has different characteristics and modeling considerations when compared to CCF. Therefore, these results need to be reevaluated for mmWave systems and a new mathematical model is required for possible license sharing in mmWave systems. In the above mentioned prior work [8, 14, 17, 102–108], the impact of inter-operator interference in mmWave systems and the feasibility of license sharing are not studied, which is the main focus here.

4.2 Contributions

We establish the feasibility of uncoordinated sharing of spectrum licenses in a multi-operator mmWave system. A main conclusion of our work is that sharing of spectrum licenses among multiple mmWave operators can improve their overall performance, even without any explicit coordination among them, if the main beam is sufficiently narrow. The main contributions of this chapter can be categorized broadly as follows.

Modeling a multi-operator cellular system: We model a multi-operator mmWave system using a two-level architecture, where the system consists of multiple heterogeneous networks, each owned by an independent mmWave cellular operator. Each operator owns a license for a frequency band and its network consists of its own BSs and users which are independent of other networks. This model provides a general framework for access and license sharing by introducing the notion of access and sharing groups. The operators can form multiple access groups where users of each member of an access group can connect to BSs of any member of the same access group. Similarly, the operators can form sharing groups where each member of a sharing group can use the spectrum of all members of the same sharing group.

Establishing the feasibility of uncoordinated sharing of spectrum licenses: We derive the combined mean user-load on BSs of each network. We derive expressions for SINR and rate coverage of a typical user of an operator using the tools from stochastic geometry. Then, we compare systems with shared licenses and exclusive licenses and show that spectrum license sharing achieves higher performance in terms of per user rate. We investigate the effect of antenna beamwidth on the

feasibility of license sharing and show that spectrum license sharing is more favorable as communication becomes more directional. Finally, we quantify the benefit of license sharing in term of license cost reduction and show that networks can possibly reduce their costs significantly if they share their licenses.

Modeling co-located operators: To include the impact of correlation among deployments of operators, we also consider a co-located deployment where site locations are defined by a single PPP and each operator has one BS at each site. We show that spectrum sharing is feasible even in this case. This important result indicates that multiple operators can also share site infrastructure (such as macrocell towers, as is common practice today) while also sharing their spectrum licenses. A practical deployment with some co-location and some unique sites will lie between these two extremes of independent and totally co-located BS locations.

4.3 System Model

We consider a system consisting of M different cellular operators which coexist in a particular mmWave band. Each operator owns a network Φ_m consisting of its own BSs and users. The locations of BSs are modeled using a Poisson Point Process (PPP) with intensity λ_m and the locations of users are modeled as independent PPP with intensity λ_m^{u}. The PPP assumption can be justified by the fact that nearly any BS distribution in 2D results in a small fixed SINR shift relative to the PPP [109, 110]. The locations of BSs of multiple operators have been modeled by superposition of independent PPPs in the past work [108]. Different point processes such as the Log-Gaussian Cox process can also be used to model the locations of a multi-operator

system as discussed in [111]. For tractability we have assumed independence among operators; but, to address the impact of correlation of locations among the operators, we also consider another case with full spatial correlation among operators where all operators are co-located with their locations defined by a single PPP. One can think of real multi-operator deployments as lying between these two corner cases of complete independence and co-location. The BSs of each network can transmit with power P_m. We denote the total spectrum by B and suppose that the m^{th} operator owns a license for an orthogonal spectrum of B_m bandwidth which it can share with others. We consider a typical user UE_0 at the origin without loss of generality. Let us assume this is a user of the n^{th} operator.

4.3.1 Channel Model

Let us consider a link between this typical user and a BS of network m located at x distance from the origin. This link can be LOS or NLOS which we denote by the variable link type s, which can take values $s = \mathrm{L}$ (for LOS) or $s = \mathrm{N}$ (for NLOS). We assume that the probability of a link being LOS is dependent on x and independent of types of other links and is given by $p(x) = \exp(-\beta x)$ [8, 9]. The analysis can be extended to other blocking models. The path loss from the BS to the user is modeled as $\ell_s(x) = C_s\,(x)^{-\alpha_s}$ where α_s is the pathloss exponent and C_s is the gain for s type links. Conditioned on this typical user, the BSs of the each network m can be categorized into LOS or NLOS based on the type of their link to this typical user. Therefore, the BS PPP of network m can be seen as superposition of the following two independent (non-homogeneous) BS PPPs because of the independent thinning

Table 4.1: Summary of Notation

Notation	**Description**
Φ_m, λ_m	PPP consisting of the locations of BSs of operator m, BS density of operator m
P_m, B_m, W_m	Transmit power of BSs of operator m, licensed bandwidth of operator m, bandwidth available to operator m via sharing of licenses
Φ_m^{u}, λ_m^{u}	PPP modeling locations of users of operator m, the density of this PPP
L, N	Possible values of link type: L denotes LOS, N denotes NLOS
$\{m, p\}$	Notation representing the tier having all BSs of link type p of operator m
Φ_{mp}, λ_{mp}	The PPP modeling the locations of BSs of the tier $\{m, p\}$, the density of this PPP
$G_1, G_2, \theta_{\mathrm{b}}$	BS antenna parameters: maximum gain, minimum gain and beamwidth
C_p, α_p	Path-loss model parameters: path-loss gain and path-loss exponent of any link of type $p \in \{\mathrm{L}, \mathrm{N}\}$
$p(r), \beta$	$p(r)$ is the probability of being LOS for a link of distance r, β is the blocking parameter.
UE_0	A typical user at origin for which analysis is performed.
n	The operator which UE_0 belongs to
S_n	The set consisting of all operators which a user of operator n has access to
$\mathrm{BS}_{mj}, \mathbf{x}_{mj}, x_{mj}$	j^{th} BS of the network m, its location (here $\mathbf{x}_{mj} \in \Phi_m$), its distance from the origin
s_{mj}	Fading faced by the link between BS_{mj} and the user, the type of this link
k, i	The operator associated with UE_0, the index of the serving BS of this operator
s, x	Type of the link between the serving BS and the user, its distance from the origin
Q_k	The sharing group of operator k which is also the set of all operators interfering to the operator k.
m	Indices representing an operator or a network, in particular a member of set Q_k
$D_{mp}^{ks}(x)$	Exclusion radius for BSs of tier $\{m, p\}$ when UE_0 is associated with BS of tier $\{k, s\}$ located at x

Table 4.1: Cont.

A_k^n	Association probability of a user of network n to be associated with BS of operator k
$\mathrm{P}_{ks}^{\mathrm{c}}$	Probability of SINR coverage of UE_0 when associated with tier $\{k, s\}$
N_m^u	The mean number of users associated to a BS of network m
$\kappa_m(z)$	Probability of a BS of network m having z number of associated users
$R_{ki}, \mathrm{R}_k^{\mathrm{c}}$	Instantaneous rate and rate coverage of UE_0 when associated with network k
$\mathrm{R}^{\mathrm{c}}(\rho)$	Rate coverage of UE_0, *i.e.* $\mathbb{P}[R_k \geq \rho]$

theorem [63],

1. $\Phi_{m,\mathrm{L}}$ with density $\lambda_{m,\mathrm{L}}(x) = \lambda_m p(x)$ containing all the BSs with LOS link to UE_0, and

2. $\Phi_{m,\mathrm{N}}$ with density $\lambda_{m,\mathrm{N}}(x) = \lambda_m(1 - p(x))$ containing all the BSs with NLOS link to UE_0.

Note that this results in total $2M$ classes (known as tiers) of BSs where each tier is denoted by $\{m, s\}$. Here m and s represent the index of the network and the link type, respectively. The average number of BSs of tier $\{m, s\}$ in area A is given by $\Lambda_{m,s}(A) = \int_A \lambda_{m,s}(\|\mathbf{x}\|)\mathrm{d}\mathbf{x}$. Therefore, the average number of LOS and NLOS BSs in a ball $\mathcal{B}(r)$ with radius r for network m are given by

$$\Lambda_{m,\mathrm{L}}(\mathcal{B}(r)) = 2\pi \int_0^r \lambda_m p(x) x \mathrm{d}x = 2\pi \int_0^r \lambda_m e^{-\beta x} x \mathrm{d}x = \pi\lambda_m \frac{2}{\beta^2}\gamma(2, \beta r)$$
$$\Lambda_{m,\mathrm{N}}(\mathcal{B}(r)) = 2\pi \int_0^r \lambda_m (1 - p(x)) x \mathrm{d}x = \pi\lambda_m \left(r^2 - \frac{2}{\beta^2}\gamma(2, \beta r)\right).$$

Let us denote the j^{th} BS of network m as BS_{mj}. Hence, the effective channel between BS_{mj} and the user UE_0 is given as $h_{mj} P_m \ell_{s_{mj}}(x_{mj})$ where s_{mj} denotes the link type

between the user and BS_{mj} and h_{mj} is an exponential random variable denoting Rayleigh fading. We observe and show in the numerical section that considering a more general fading model such as Nakagami does not provide any additional design insights, but it does complicate the analysis significantly. Therefore we will consider only Rayleigh fading for our analysis. We do not consider shadowing separately as it is mostly covered by the blocking model. We show in the numerical section that including shadowing does not change any of the observed trends.

We assume that BSs of every network are equipped with a steerable antenna having radiation pattern given as [8]

$$G(\theta) = \begin{cases} G_1 & |\theta| < \theta_{\text{b}}/2 \\ G_2 & \text{otherwise} \end{cases}.$$

Here $G_1 \gg G_2$ and θ_{b} denotes beamwidth. The angle between the BS BS_{mj} antenna and direction pointing to the user UE_0 is denoted by θ_{mj}. We have assumed the same antenna pattern for all networks to avoid complicating the expressions unnecessarily. The analysis can be extended to a system where each network has a different transmit antenna pattern. We assume that the user is equipped with a single omni-directional antenna. Although users will also have directional antennas, it will be analytically equivalent to aggregating the transmitter and receiver gains at BS antennas. Hence, considering the UE antenna gain and the BS antenna gain separately does not change the observed trends. Note that we consider single stream operation in this work. More advanced mmWave cellular systems may employ massive MIMO [112, 113] or multi-stream MIMO using hybrid beamforming [65]. Generalizing to these other architectures is a topic of future work.

4.3.2 Access and License Sharing Model

We assume that a user of operator n can be associated with any BS from a particular set of operators denoted by access set S_n. Two special cases of access are open and closed. In an open access system, a user can connect to any operator and therefore $S_n = \{1, 2, \cdots M\}$. In a closed access system, a user can connect only to the operator it belongs to, and therefore $S_n = \{n\}$.

We assume that license sharing is performed by forming mutually exclusive groups, known as *sharing groups*. All the operators in each group share the whole spectrum license such that each operator within a group has equal bandwidth available to it. The effective bandwidth available to each operator after sharing is denoted by W_m. For example, in a system of 5 operators, suppose that operators 1, 2 and 3 form a group and operators 4 and 5 are in second group. Hence, after license sharing, 1, 2 and 3 will have access to the the aggregate band of total $B_1 + B_2 + B_3$ bandwidth, *i.e.* $W_1 = W_2 = W_3 = B_1 + B_2 + B_3$. Similarly operators 4 and 5 will have access to the aggregate band of bandwidth $W_4 = W_5 = B_4 + B_5$. We denote the sharing group containing the k^{th} operator by Q_k. The user UE_0 experiences interference from all networks operating in the spectrum of associated operator k. The set of the interfering networks is equal to the sharing group containing the k^{th} operator which is Q_k. Note that the aggregate spectrum of a sharing group can be fully used by all members. Hence, for a particular network, the set of interfering networks remains the same for its complete available spectrum band. One example of license sharing is a system with fully shared licenses, in which there is only one sharing group containing all the operators and all of them can use the whole frequency band. Here,

the available bandwidth W_k to each operator is B and the set of interfering networks is $Q_k = \{1, 2, \cdots M\}$. For the case when all operators have exclusive licenses, there are M sharing groups each containing only one operator which indicates that no operator shares its license. Hence, the bandwidth available to the operator k is $W_k = B_k$ and Q_k is equal to $\{k\}$.

Now, the effective received power from a BS BS_{mj} at user UE_0 is given as

$$P_{mj} = P_j h_{mj} \ell_{s_{mj}}(x_{mj}) G(\theta_{mj}). \tag{4.1}$$

Hence, the average received power from BS_{mj} at UE_0 without the antenna gain is given by

$$P_{mj}^{\text{avg}} = P_m \ell_{s_{mj}}(x_{mj}). \tag{4.2}$$

We assume the maximum average received power based association in which any user associates with the BS providing highest P_{mj}^{avg} among all the networks it has access to (*i.e.* access set). Let us denote the operator the user UE_0 associates with by k and the index of the serving BS by i. Since the serving BS aligns its antenna with the user, the angle θ_{ki} between the serving BS antenna and user direction is 0^{o} and the effective received power of this BS is given as $P_{ki} = P_k h_{ki} \ell_{s_{ki}}(x_{ki}) G(0) = P_k h_{ki} \ell_{s_{ki}}(x_{ki}) G_1$. For each interfering BS BS_{mj} where $m \in Q_k$ and $(m, j) \neq (k, i)$, the angle θ_{mj} is assumed to be uniformly distributed between $-\pi$ and π.

Now, the SINR at the typical user UE_0 that is associated with the i^{th} BS of the operator k is given as

$$\text{SINR}_{ki} = \frac{P_k h_{ki} \ell_{s_{ki}}(x_{ki}) G_1}{\sigma_k^2 + I} \tag{4.3}$$

where I is the interference from all BSs of networks in set Q_k and is given by $I =$

$$\sum_{m\in Q_k}\sum_{\mathbf{x}_{mj}\in\Phi_m} P_m h_{mj}\ell_{s_{mj}}(x_{mj})G(\theta_{mj}) = \sum_{m\in Q_k}\sum_{p\in\{\mathrm{L},\mathrm{N}\}}\sum_{\mathbf{x}_{mj}\in\Phi_{m,p}\setminus\{\mathbf{x}_{ki}\}} P_m h_{mj}\ell_p(x_{mj})G(\theta_{mj}). \tag{4.4}$$

Note that the operator $\setminus$ denotes the set difference operation which is defined as $A\setminus B = \{z : z \in A, z \notin B\}$ for any sets A and B. Since the PPP process $\Phi = \bigcup_{m=1}^{M}\Phi_m$ is a simple PP, the probability that there are two BSs at the same location is 0. If $(m \neq k)$ or $(m = k, p \neq s)$, then $\Phi_{m,p}\setminus\{\mathbf{x}_{ki}\}$ is equal to $\{\mathbf{x}_{mj} \in \Phi_{m,p}\}$ as there cannot be a BS in $\Phi_{m,p}$ at $\mathbf{x}_{ki}$. If $(m = k, p = s)$, then $\Phi_{k,s} \setminus \{\mathbf{x}_{ki}\} = \{\mathbf{x}_{kj} \in \Phi_{k,s}, j \neq i\}$. The noise power for operator k is given by $\sigma_k^2 = N_0 W_k$ where N_0 is the noise power density. Since σ_k^2 is dependent on the allocated bandwidth, it varies accordingly with association.

4.4 SINR and Rate Coverage Probability

In this section, we will first investigate the association of a typical user of n^{th} network to a BS and then compute the coverage probability for this user. Recall that the coverage probability is defined as the probability that the SINR at the user from its associated BS is above a threshold T

$$\mathrm{P}^{\mathrm{c}}(T) = \mathbb{P}\left[\mathrm{SINR} > T\right]. \tag{4.5}$$

4.4.1 Association Criterion and Probability

Recall that a user of the n^{th} operator can be associated with a BS of any operator from the set S_n. Let E_{ki} denote the event that the typical user is associated

with the BS BS_{ki} (*i.e.* the i^{th} BS of operator k). Let us denote the distance of this BS by $x = x_{ki}$ and type by $s = s_{ki}$ for compactness. The event E_{ki} is equivalent to the event that no other BS has higher P^{avg} at the user. This event can be further written as combination of following two events: (i) the event that no other BS of operator k has higher P^{avg} at the user, and (ii) that no BS of any other accessible operator m has higher P^{avg} at the user:

$$E_{ki} = \{P_{ki}^{\text{avg}} > P_{kj}^{\text{avg}} \ \forall i \neq j\} \cap \{P_{ki}^{\text{avg}} > P_{mj}^{\text{avg}} \ \forall m \in S_n \setminus \{k\}\}. \tag{4.6}$$

Substituting (4.2) in (4.6),

$$E_{ki} = \left\{ \frac{C_{s_{ki}}}{(x_{ki})^{\alpha_{s_{ki}}}} > \frac{C_{s_{kj}}}{(x_{kj})^{\alpha_{s_{kj}}}} \ \forall i \neq j \right\} \bigcap \left\{ \frac{C_{s_{ki}} P_k}{(x_{ki})^{\alpha_{s_{ki}}}} > \frac{C_{s_{mj}} P_m}{(x_{mj})^{\alpha_{s_{mj}}}} \ \forall m \in S_n \setminus \{k\} \right\}.$$

The above condition can also be further split over LOS and NLOS tiers of each network, then it can be expressed as an equivalent condition over locations of all BSs as follows:

$$\begin{aligned} E_{ki} = {} & \{x_{kj} > x \ \forall \ s_{kj} = s, i \neq j\} \bigcap \left\{ x_{kj} > \left(\frac{C_{s'}}{C_s} \right)^{\frac{1}{\alpha_{s'}}} x^{\frac{\alpha_s}{\alpha_{s'}}} \ \forall s_{kj} \neq s, i \neq j \right\} \\ & \bigcap \left\{ x_{mj} > \left(\frac{P_m}{P_k} \right)^{\frac{1}{\alpha_s}} x \ \forall s_{mj} = s, m \in S_n \setminus \{k\} \right\} \\ & \bigcap \left\{ x_{mj} > \left(\frac{P_m C_{s'}}{P_k C_s} \right)^{\frac{1}{\alpha_{s'}}} x^{\frac{\alpha_s}{\alpha_{s'}}} \ \forall s_{mj} \neq s, m \in S_n \setminus \{k\} \right\} \end{aligned}$$

where s' denotes the complement of the link type s. In other words, if $s = \text{L}$, then $s' = \text{N}$ and if $s = \text{N}$, then $s' = \text{L}$. The first condition restricts all BSs of operator k with link type s (same as type of serving BS) to be located outside a 2D ball. The second term is for all BSs of operator k and link type s'. Similarly the third and

fourth terms are for BSs of all other accessible operators with link type s and s', respectively.

As seen from these conditions, the average received power based association rule effectively creates exclusion regions around the user for BSs of each network in S_n. Let us denote the exclusion radius for the tier $\{m,p\}$ by $D_{mp}^{ks}(x)$. For example, the exclusion region for all LOS BSs of operator m when the user is associated with a NLOS BS of operator k is given by

$$D_{m\mathrm{L}}^{k\mathrm{N}}(x) = \left(\frac{P_m}{P_k}\frac{C_\mathrm{L}}{C_\mathrm{N}}\right)^{\frac{1}{\alpha_\mathrm{L}}} x^{\frac{\alpha_\mathrm{N}}{\alpha_\mathrm{L}}}. \tag{4.7}$$

Note that for BSs of the networks that are not in set S_n, there are no exclusion regions, *i.e.* $D_{mp}^{ks}(x) = 0\ \forall m \notin S_n$. This exclusion region denotes the region where interfering BSs cannot be located and hence, affects the sum interference.

The probability that all BSs of the tier $\{m,p\}$ are outside the exclusion radius d is given by the void probability of the PPP Φ_{mp} which is $\mu_{m,p}(d) = \exp(-\Lambda_{m,p}(\mathcal{B}(d)))$. Since the PPPs of the tiers are mutually independent, the probability that BSs of the tiers other than $\{k,i\}$ are located outside the exclusion region, can be calculated by multiplying the individual void probabilities of each tier:

$$f_{k,s}^{o}(x) = \mu_{k,s'}\big(D_{ks'}^{ks}(x)\big) \prod_{m\in S_n\setminus\{k\}} \mu_{m,s}\big(D_{ms}^{ks}(x)\big)\mu_{m,s'}\big(D_{ms'}^{ks}(x)\big). \tag{4.8}$$

Therefore, the probability density function of the distance x to this associated BS is given as

$$f_{k,s}(x) = 2\pi\lambda_{k,s}x\ \mu_{k,s}(x)\ \mu_{k,s'}\big(D_{ks'}^{ks}(x)\big) \prod_{m\in S_n\setminus\{k\}} \mu_{m,s}\big(D_{ms}^{ks}(x)\big)\mu_{m,s'}\big(D_{ms'}^{ks}(x)\big). \tag{4.9}$$

The probability that a user of operator n is associated with a BS of operator k can be computed by summation over both LOS and NLOS tiers:

$$A_k^n = \int_0^\infty \left(f_{k,\mathrm{L}}(x) + f_{k,\mathrm{N}}(x)\right) \mathrm{d}x. \tag{4.10}$$

Let $\mathrm{P}_{k\mathrm{L}}^{\mathrm{c}}$ and $\mathrm{P}_{k\mathrm{N}}^{\mathrm{c}}$ denote the coverage probabilities for the typical user which is associated with a LOS and NLOS BS of operator k, respectively. They can be computed by integrating the CCDF of SINR from serving BS over pdf of distance x from serving BS as follows:

$$\begin{aligned}
\mathrm{P}_{ks}^{\mathrm{c}}(T) &= \int_0^\infty \mathbb{P}\left[\mathrm{SINR}_{ks}(x) > T\right] f_{k,\mathrm{L}}(x)\mathrm{d}x \\
&= \int_0^\infty \mathbb{P}\left[P_k h_{ks} C_s G(0) > T(I + \sigma_k^2) x^{\alpha_s}\right] f_{k,s}(x)\mathrm{d}x.
\end{aligned} \tag{4.11}$$

Since $h_{ks} \sim \exp(1)$, the probability in (4.11) can be replaced as

$$\begin{aligned}
\mathrm{P}_{ks}^{\mathrm{c}}(T) &= \int_0^\infty \mathbb{E}\left[\exp\left(-\frac{T\sigma_k^2 x^{\alpha_s}}{C_s G_1 P_k} - \frac{T I x^{\alpha_s}}{C_s G_1 P_k}\right)\right] f_{k,s}(x)\mathrm{d}x \\
&= \int_0^\infty \exp\left(-\frac{T N_0 W_k x^{\alpha_s}}{C_s G_1 P_k}\right) \mathcal{L}_I\left(\frac{T x^{\alpha_s}}{C_s G_1 P_k}\right) f_{k,\mathrm{L}}(x)\mathrm{d}x
\end{aligned} \tag{4.12}$$

where $\mathcal{L}_I(t)$ denotes the Laplace transform of the interference I caused by BSs of all networks in set Q_k and is defined as $\mathcal{L}_I(t) = \mathbb{E}\left[e^{-tI}\right]$.

Since the association with different tiers are disjoint events, the SINR coverage probability of the typical user can be computed by summing these individual tier coverage probabilities over all accessible tiers:

$$\mathrm{P}^{\mathrm{c}}(T) = \sum_{k \in S_n} \mathrm{P}_k^{\mathrm{c}}(T) = \sum_{k \in S_n} \left[\mathrm{P}_{k\mathrm{L}}^{\mathrm{c}}(T) + \mathrm{P}_{k\mathrm{N}}^{\mathrm{c}}(T)\right] \tag{4.13}$$

where $\mathrm{P}_k^{\mathrm{c}}(T)$ is the sum of coverage probabilities of both tiers of the operator k. To proceed further, we need to first characterize the interference I for which we will compute its Laplace transform defined as $\mathcal{L}_I(t) = \mathbb{E}\left[e^{-tI}\right]$.

4.4.2 Interference Characterization

If the user of operator n is associated with operator k, it experiences interference from all networks operating in spectrum W_k. Recall that all these interfering networks form set Q_k. Hence, the total interference is given by (4.4). Due to mutual independence of the tiers, its Laplace transform can written as product of the following terms:

$$\mathcal{L}_I(t) = \mathbb{E}\left[e^{-tI}\right] = \prod_{m \in Q_k} \mathcal{L}_{I_m}(t) = \prod_{m \in Q_k} \left(\mathcal{L}_{I_{m\mathrm{L}}}(t)\mathcal{L}_{I_{m\mathrm{N}}}(t)\right) \tag{4.14}$$

where $\mathcal{L}_{I_m}(t)$ refers to the interference caused by network m and $\mathcal{L}_{I_{m\mathrm{L}}}(t)$ and $\mathcal{L}_{I_{m\mathrm{N}}}(t)$ denote the Laplace transforms of LOS and NLOS interference from network m which are given in the following Lemma.

Lemma 7. *The Laplace transforms of the interference from LOS and NLOS BSs of network m to a user of operator n which is associated with a type s BS of operator k in a multi-operator system are given as*

$$\begin{aligned}
\mathcal{L}_{I_{m\mathrm{L}}}(t) = \exp\ \big(&-\lambda_m[\theta_{\mathrm{b}} F_{\mathrm{L}}(\beta, \alpha_{\mathrm{L}}, tG_1 P_m C_{\mathrm{L}}, D_{m\mathrm{L}}^{ks}(x)) \\
&+(2\pi - \theta_{\mathrm{b}}) F_{\mathrm{L}}(\beta, \alpha_{\mathrm{L}}, tG_2 P_m C_{\mathrm{L}}, D_{m\mathrm{L}}^{ks}(x))]\big) \\
\mathcal{L}_{I_{m\mathrm{N}}}(t) = \exp\ \big(&-\lambda_m[\theta_{\mathrm{b}} F_{\mathrm{N}}(\beta, \alpha_{\mathrm{N}}, tG_1 P_m C_{\mathrm{N}}, D_{m\mathrm{N}}^{ks}(x)) \\
&+(2\pi - \theta_{\mathrm{b}}) F_{\mathrm{N}}(\beta, \alpha_{\mathrm{N}}, tG_2 P_m C_{\mathrm{N}}, D_{m\mathrm{N}}^{ks}(x))]\big)
\end{aligned}$$

$$\textit{where } F_{\mathrm{L}}(b,a,A,x)=\int_x^{\infty}\frac{e^{-by}Ay^{-a}}{1+Ay^{-a}}y\mathrm{d}y,\ \textit{and}$$
$$F_{\mathrm{N}}(b,a,A,x)=\int_x^{\infty}(1-e^{-by})\frac{Ay^{-a}}{1+Ay^{-a}}y\mathrm{d}y.$$

Proof. The interference from all LOS BSs of network m at UE_0 is given as

$$I_{m\mathrm{L}}=\sum_{\mathbf{x}_{mj}\in\Phi'_{m,\mathrm{L}}}h_{mj}\|x_{mj}\|^{-\alpha_{\mathrm{L}}}P_mC_{\mathrm{L}}G(\theta_{mj})$$

where $\Phi'_{m,\mathrm{L}}=\Phi_{m,\mathrm{L}}\cap\bar{\mathcal{B}}\left(0,D^{ks}_{m\mathrm{L}}(x)\right)$ and $\bar{\mathcal{B}}\left(0,r\right)$ denotes the compliment of a ball of radius r located at origin. This is due to the fact that all interfering BSs are located outside the radius $D^{ks}_{m\mathrm{L}}(x)$. The Laplace transform of $I_{m\mathrm{L}}$ is given as

$$\mathcal{L}_{I_{m\mathrm{L}}}(t)=\mathbb{E}\left[\exp\left(-t\sum_{\mathbf{x}_{mj}\in\Phi'_{m\mathrm{L}}}h_{mj}\|x_{mj}\|^{-\alpha_{\mathrm{L}}}P_mC_{\mathrm{L}}G(\theta_{mj})\right)\right].$$

Now, using the PGFL of PPP [63], the Laplace transform can be written as

$$\mathcal{L}_{I_{m\mathrm{L}}}(t)=\exp\left(-2\pi\lambda_m\int_{D^{ks}_{m\mathrm{L}}(x)}^{\infty}p(y)\left(1-\mathbb{E}\left[e^{-thG(\theta)P_mC_{\mathrm{L}}y^{-\alpha_{\mathrm{L}}}}\right]\right)y\mathrm{d}y\right).$$

Now, using the moment generating function (MGF) of exponentially distributed h and pdf of uniformly distributed θ, we get

$$\mathcal{L}_{I_{m\mathrm{L}}}(t)=\exp\left(-\lambda_m\int_{D^{ks}_{m\mathrm{L}}}^{\infty}p(y)\left(2\pi-\int_0^{2\pi}\frac{d\theta}{1+tG(\theta)P_mC_{\mathrm{L}}y^{-\alpha_{\mathrm{L}}}}\right)y\mathrm{d}y\right).$$

Now, integrating with θ and then using the definition of function $F_{\mathrm{L}}(\cdot)$, we get

$$\mathcal{L}_{I_{m\mathrm{L}}}(t)=\exp\left(-\lambda_m\int_{D^{ks}_{m\mathrm{L}}}^{\infty}\int_0^{2\pi}\frac{tG(\theta)P_mC_{\mathrm{L}}y^{-\alpha_{\mathrm{L}}}}{1+tG(\theta)P_mC_{\mathrm{L}}y^{-\alpha_{\mathrm{L}}}}\mathrm{d}\theta e^{-\beta y}y\mathrm{d}y\right)$$
$$=\exp\left(-\lambda_m\int_{D^{ks}_{m\mathrm{L}}}^{\infty}\left(\theta_{\mathrm{b}}\frac{tG_1P_mC_{\mathrm{L}}y^{-\alpha_{\mathrm{L}}}}{1+tG_1P_mC_{\mathrm{L}}y^{-\alpha_{\mathrm{L}}}}+(2\pi-\theta_{\mathrm{b}})\frac{tG_2P_mC_{\mathrm{L}}y^{-\alpha_{\mathrm{L}}}}{1+tG_2P_mC_{\mathrm{L}}y^{-\alpha_{\mathrm{L}}}}\right)e^{-\beta y}y\mathrm{d}y\right)$$

$$= \exp\left(-\lambda_m \left[\theta_{\mathrm{b}} F_{\mathrm{L}}\left(\beta, \alpha_{\mathrm{L}}, tG_1 P_m C_{\mathrm{L}}, D_{m\mathrm{L}}^{ks}(x)\right)\right.\right.$$
$$\left.\left.+(2\pi - \theta_{\mathrm{b}}) F_{\mathrm{L}}\left(\beta, \alpha_{\mathrm{L}}, tG_2 P_m C_{\mathrm{L}}, D_{m\mathrm{L}}^{ks}(x)\right)\right]\right).$$

The Laplace transform of the interference from the NLOS BSs can be computed similarly. □

Note that the term containing G_1 and θ_{b} denotes the interference from the aligned BSs whose antennas are directed towards the considered user while the term containing G_2 and $(2\pi - \theta_{\mathrm{b}})$ represents the interference from the unaligned BSs. Since $G_1 \gg G_2$, the interference from the aligned BS is significantly larger than the interference from the unaligned BS and hence, dominates the Laplace transform expression. Therefore, the value of θ_{b} plays a significant role in characterizing the interference and determining the benefits of spectrum license sharing.

Now, we provide the final expression for SINR coverage probability.

Theorem 10. *The SINR coverage probability of a typical user of operator n in a multi-operator mmWave cellular system is given as*

$$\mathrm{P}^{\mathrm{c}}(T) = \sum_{k \in S_n} \sum_{s \in \{\mathrm{L},\mathrm{N}\}} \int_0^\infty \prod_{m \in Q_k} \mathcal{L}_{I_{m\mathrm{L}}}\left(\frac{Tx^{\alpha_s}}{C_s G_1 P_k}\right) \mathcal{L}_{I_{m\mathrm{N}}}\left(\frac{Tx^{\alpha_s}}{C_s G_1 P_k}\right)$$
$$\exp\left(-\frac{N_0 W_k T x^{\alpha_s}}{C_s G_1 P_k}\right) f_{k,s}(x)\mathrm{d}x \tag{4.15}$$

where $\mathcal{L}_{I_{mp}}(t)$ is computed in Lemma 7 and $f_{k,s}(x)$ is given in (4.9).

Proof. Substituting the value of $\mathcal{L}_I(t)$ from Lemma 7 in (4.13), we get the result. □

In (4.15), the first summation is over all networks which the user of operator n can connect to, weighted by the association probability. This weighting is included inside the term $f_{k,s}(x)$.

Since due to complexity of the above expressions, it is difficult to derive direct insights, we also consider a simple case to get closed form expressions.

Corollary 6. *Consider a mmWave system with n identical operators with closed access and fully shared licenses. Assuming that the LOS and NLOS channel have same pathloss parameters with* $\alpha_{\mathrm{L}} = \alpha_{\mathrm{N}} = 4$ *and the side lobe gain* $G_2 = 0$*, the probability of coverage for the interference limited scenario is given as*

$$\mathrm{P_c}(T) = \frac{1}{1 + \frac{\theta_{\mathrm{b}}}{2\pi} T^{\frac{1}{2}} \left((n-1)\frac{\pi}{2} + \arctan(T^{\frac{1}{2}}) \right)}. \tag{4.16}$$

It can be observed from the (4.16) that the probability of coverage decreases monotonically with the number of operators n.

4.4.3 Rate Coverage

In this section, we derive the downlink rate coverage. Recall that the rate coverage is defined as the probability of the rate of a typical user being greater than the threshold ρ,

$$\mathrm{R}(\rho) = \mathbb{P}\left[\mathrm{Rate} > \rho\right]. \tag{4.17}$$

Let us assume that O_k denotes the frequency resources allocated to each user associated with the 'tagged' BS of operator k. Therefore, the instantaneous rate of

the considered typical user is given as $R_{ki} = O_k \log(1 + \text{SINR}_{ki})$. The value of O_k depends upon the number of users (N_k^{u}), equivalently the load, served by the tagged BS. The load N_k^{u} is a random variable due to the randomly sized coverage areas of each BS and random number of users in the coverage areas. As shown in [14, 58] approximating this load with its respective mean does not compromise the accuracy of results. Since user distribution of each network is assumed to be PPP, the average number of users associated with the tagged BS of network k associated with the typical user can be modeled similarly to [14, 58]:

$$N_k^{\text{u}} = 1 + 1.28 \frac{1}{\lambda_k} \sum_{m:k \in S_m} \lambda_m^{\text{u}} A_k^m. \tag{4.18}$$

Note that the summation is over all the networks whose users can connect to the network k and the sum denotes the combined density of associated users from each network.

Now, we assume that the scheduler at the tagged BS gives $1/N_k^{\text{u}}$ fraction of resources to each of the N_k^{u} users. This assumption can be justified as most schedulers such as round robin or proportional fair give approximately $1/N_k^{\text{u}}$ fraction of resources to each user on average. Using the mean load approximation, the instantaneous rate of a typical user of operator n which is associated with i^{th} BS of operator k is given as

$$R_{ki} = \frac{W_k}{N_k^{\text{u}}} \log(1 + \text{SINR}_{ki}). \tag{4.19}$$

Let $\text{R}_k^{\text{c}}(\rho)$ denote the rate coverage probability when user is associated with operator k. Then the total rate coverage will be equal to the sum of $\text{R}_k^{\text{c}}(\rho)$'s over all

accessible networks:

$$\mathrm{R}^{\mathrm{c}}(\rho) = \sum_{k \in S_n} \mathrm{R}^{\mathrm{c}}_k(\rho). \tag{4.20}$$

$\mathrm{R}^{\mathrm{c}}_k(\rho)$ can be derived in terms of SINR coverage probability as follows:

$$\begin{aligned}\mathrm{R}^{\mathrm{c}}_k(\rho) &= \mathbb{P}\left[R_{ki} > \rho\right] = \mathbb{P}\left[W_k/N^{\mathrm{u}}_k \log\left(1 + \mathrm{SINR}_{ki}\right) > \rho\right] \\ &= \mathbb{P}\left[\mathrm{SINR}_{ki} > 2^{\rho \frac{N^{\mathrm{u}}_k}{W_k}} - 1\right] = \mathrm{P}^{\mathrm{c}}_k\left(2^{\rho N^{\mathrm{u}}_k/W_k} - 1\right).\end{aligned}$$

Now, the rate coverage is given as

$$\mathrm{R}^{\mathrm{c}}(\rho) = \sum_{k \in S_n} \mathrm{P}^{\mathrm{c}}_k\left(2^{\rho N^{\mathrm{u}}_k/W_k} - 1\right). \tag{4.21}$$

We, now, turn back to the simple case considered in Corollary 6 to simplify the expressions and provide further insights.

Corollary 7. *Consider a mmWave system with n identical operators with closed access and fully shared licenses of bandwidth $\bar{B}$ each as considered in Corollary 6. The rate coverage for the interference limited scenario is given as*

$$\mathrm{R}_{\mathrm{c}}(\rho) = \frac{1}{1 + \frac{\theta_{\mathrm{b}}}{2\pi}\left(2^{\rho'/n} - 1\right)^{\frac{1}{2}}\left((n-1)\frac{\pi}{2} + \arctan\left(\left(2^{\rho'/n} - 1\right)^{\frac{1}{2}}\right)\right)} \tag{4.22}$$

where $\rho' = \rho N^{\mathrm{u}}/\bar{B}$.

The denominator in (4.22) behaves differently with respect to n for different regimes of ρ'. For small ρ, rate coverage decreases with respect to n making exclusive licenses more beneficial. For large ρ, the rate coverage increases with respect to n which favors sharing spectrum licenses. Let us compare the case of $n = 1$ and

$n = 2$. For $\theta_{\mathrm{b}} = 2\pi$, the license sharing becomes more beneficial than exclusive licenses when $\rho' > 3.3$ which is equivalent to $\mathrm{R_c} = 0.20$ indicating that at maximum, only 20% users would be benefiting if the licenses are shared. This effectively means that spectrum sharing is not beneficial from the operator's perspective. Whereas for $\theta_{\mathrm{b}}/2 = 10^{\mathrm{o}}$, the switch occurs at $\mathrm{R_c} = 0.83$ indicating that 83% users are benefiting from spectrum sharing and making sharing of licenses favorable from the operator's perspective. Therefore, the directionality of antennas (θ_{b}) plays a crucial role in determining the least value of $\mathrm{R_c}$ where license sharing starts becoming more beneficial than exclusive licenses. We later show similar trends with target rate and beamwidth using simulations.

4.5 Performance Comparison

We use the preceding mathematical framework to compare the benefits of spectrum license sharing. We enumerate three specific cases (or systems) considering different combinations of accesses and license sharing schemes. Also see Fig. 4.1 for a visual explanation.

System 1: Closed Access and Exclusive Licenses: In System 1, each user must associate with only its own network and each operator can use its own spectrum only. This case is equivalent to a set of M single operator systems which has been studied in prior work [8]. This system serves as a baseline case to evaluate benefits of sharing. The SINR coverage probability of UE_0 is given by (4.15) with $k = n$, $S_n = \{n\}$. Recall that in this system, the spectrum accessible to each operator is its own licensed spectrum only, *i.e.* $W_n = B_n$, $Q_n = \{n\}$.

System 2: Open Access and Full Spectrum License Sharing: In System 2, each user can be associated with any network and the spectrum license is shared between all operators. In this case, the probability of association of a user with any BS of the operator k is independent of which operator this user belongs to and is given as

$$A_k^n = A_k = A_{k,\mathrm{L}} + A_{k,\mathrm{N}} = \int_0^\infty \left(f_{k,\mathrm{L}}(x) + f_{k,\mathrm{N}}(x)\right) \mathrm{d}x.$$

The SINR coverage probability of UE_0 is given by (4.15) with $S_n = \{1, 2, \cdots M\}$. The average load to the tagged BS of operator k is given as $N_k^{\mathrm{u}} = 1 + 1.28 \sum_m \lambda_m^{\mathrm{u}} \frac{A_k}{\lambda_k}$. The spectrum accessible to each operator W_k is the complete band B and $Q_n = \{1, 2 \cdots M\}$. Since users can be served by BS of any operator, it requires full coordination, sharing of control channels and technology sharing among operators. The quality of service to a user will be the same regardless of the operator it belongs to. This will limit the technological advantage of an operator over other operators and hence, operators may not want to open up their networks to each other. Therefore, System 2 is likely not a practical system but instead serves as an upper bound to the two other more practical systems. Note that if all M networks are identical with respect to every parameter, then this system is equivalent to a single operator system with the aggregate BS and UE density. In this case, from a user association perspective, there is no discrimination based on the network which a particular BS belongs to. Also all networks transmit in the same band. So the users effectively see a single network with aggregate BS density of all the networks. Similarly from the operator's perspective, users of all the networks look the same due to open access.

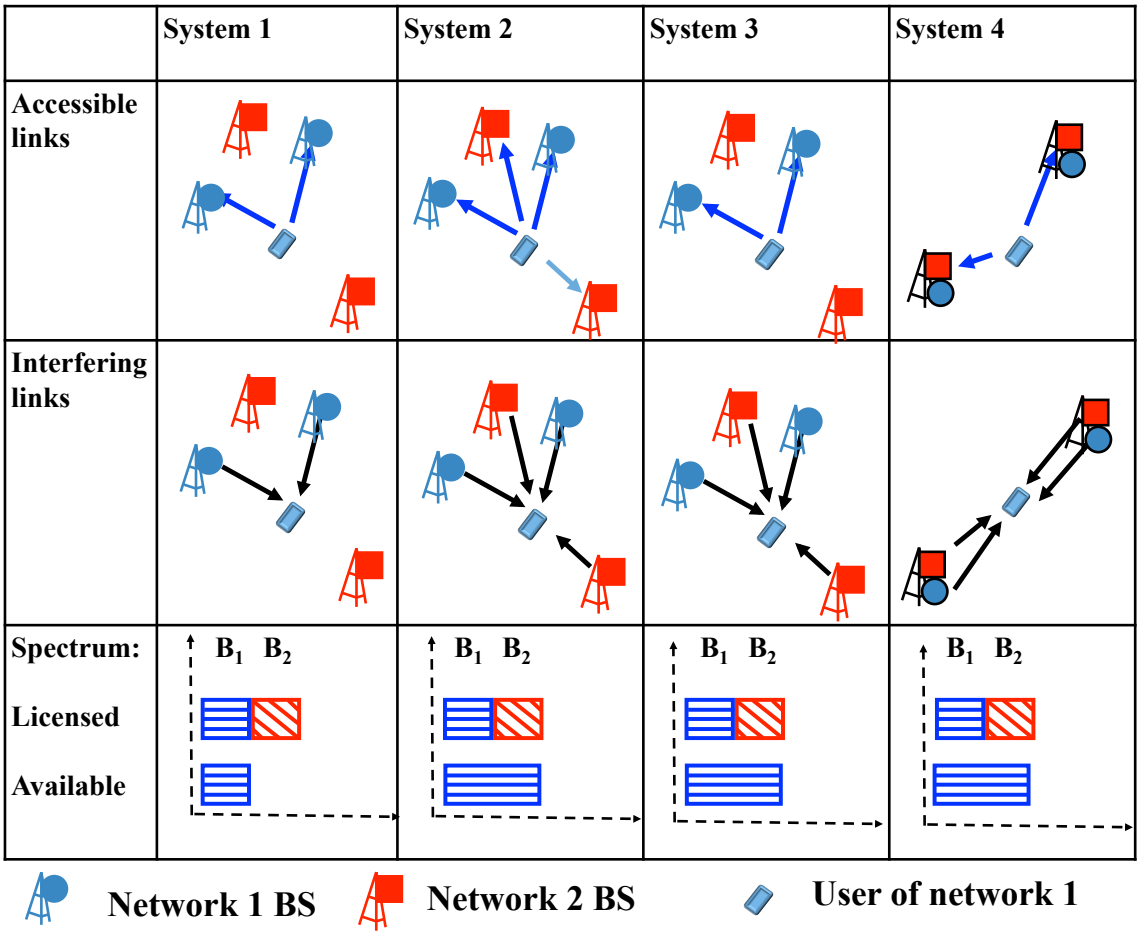

Figure 4.1: Illustration describing the differences between the four systems. For a typical user of operator 1, the figure shows all accessible networks this user can connect to, all interfering networks, and the available spectrum after license sharing.

Hence, the users of different operators can be replaced by users of a single operator with the aggregate UE density.

System 3: Closed Access and Full Spectrum License Sharing: In System 3, each user must associate with its own network but the whole spectrum is shared between all the operators. This case does not require any transmission co-

ordination among networks or common control channels, nor does it require sharing of infrastructure or back-haul resources. This system is close to the practical implementation where subscribers must connect to their respective service providers only. The SINR coverage probability of the considered typical user of operator n is given by (4.15) with $k = n$, $S_n = \{n\}$. For this system, the spectrum accessible to each operator is B and $Q_n = \{1, 2 \cdots M\}$.

Along with the above three systems, we consider one additional system System 4 as defined below. This system will help us understand if independent operators can still share BS tower infrastructure while sharing the spectrum licenses. As mentioned before, there may be correlation among BSs locations of different operators with possible co-location of BSs, therefore it is important to understand how gain from license sharing will be affected when the correlation is present.

System 4: Co-located BSs with Closed Access and Full Spectrum License Sharing: System 4 has closed access and fully shared licenses where the respective BSs of all the operators are all co-located. The system model for this case remains the same as the previous three systems except for the following two differences: 1) The BS locations are modeled by a single PPP $\Phi = \{\mathbf{x}_j\}$ with intensity λ and 2) for a typical user, the BSs of all the operators located at the same location are either all LOS or all NLOS. We first briefly show the computation the probability of SINR coverage of this system. Consider a typical user of operator n. The BS PPP Φ can be divided into two independent PPPs, Φ_{L} and Φ_{N} with intensity $\lambda_{\mathrm{L}}(x) = \lambda p(x)$ and $\lambda_{\mathrm{N}}(x) = \lambda(1 - p(x))$. The probability density function of the distance x to the

associated BS of operator n is given as

$$f_s(x) = 2\lambda_s \pi x \exp\left(-\Lambda_s(\mathcal{B}(x))\right) \exp\left(-\Lambda_{s'}\left(\mathcal{B}\left(D^s_{s'}(x)\right)\right)\right) \tag{4.23}$$

where the exclusion radius $D^s_p(x)$ is the same for BSs of all the operators and given as $D^s_p(x) = \left(\frac{C_p}{C_s}\right)^{\frac{1}{\alpha_p}} x^{\frac{\alpha_s}{\alpha_p}}$. The interference I at the user from BSs of all the operators is given as

$$I = x_i^{-\alpha_s} C_s \sum_{m \in Q_n \setminus \{n\}} P_m h_{mi} G(\theta_{mi}) + \sum_{p=\mathrm{L,N}} \sum_{\mathbf{x}_j \in \Phi_p \setminus \{\mathbf{x}_i\}} x_j^{-\alpha_p} C_p \sum_{m \in Q_n} P_m h_{mj} G(\theta_{mj}). \tag{4.24}$$

The following Lemma characterizes the Laplace transform of the interference in (4.24) in the co-located BSs case.

Lemma 8. *The Laplace transform of interference to a typical user of operator n with closed access which is associated to a BS of type s in a multi-operator system with co-located BSs is given as*

$$\begin{aligned}\mathcal{L}_I(t) = & \prod_{m \in Q_n \setminus \{k\}} \left(\frac{\theta_\mathrm{b}/(2\pi)}{1 + t x^{-\alpha_s} C_s P_m G_1} + \frac{(2\pi - \theta_\mathrm{b})/(2\pi)}{1 + t x^{-\alpha_s} C_s P_m G_2} \right) \\ & \times \prod_{p=\mathrm{L,N}} \exp\left(-2\pi\lambda \int_{D^s_p(x)}^{\infty} p(y) \left(1 - \prod_{m \in Q_n} \left(\frac{\theta_\mathrm{b}/(2\pi)}{1 + t y^{-\alpha_p} C_p P_m G_1} + \right. \right. \right. \\ & \left. \left. \left. \frac{(2\pi - \theta_\mathrm{b})/(2\pi)}{1 + t y^{-\alpha_p} C_p P_m G_2} \right) \right) y \mathrm{d}y \right)\end{aligned}$$

Proof. The Laplace transform of interference in (4.24) can be computed as $\mathcal{L}_I(t) = \mathbb{E}_{h,\theta}\left[e^{-t x^{-\alpha_s} C_s \sum_{m \in Q_k \setminus \{k\}} P_m h_{mi} G(\theta_{mi})} \right] \prod_{p=\mathrm{L,N}} \mathbb{E}_{\Phi_p,h,\theta}\left[e^{-t \sum_{\mathbf{x}_j \in \Phi_p \setminus \{\mathbf{x}_i\}} x_j^{-\alpha_p} C_p \sum_{m \in Q_k} P_m h_{mj} G(\theta_{mj})} \right]$.

Now, using the PGFL of PPP and independence of h_{mi}'s and θ_{mi}'s, $\mathcal{L}_I(t)$ can be written as

$$\mathcal{L}_I(t) = \prod_{m\in Q_k\setminus\{k\}} \mathbb{E}_{h,\theta}\left[e^{-tx^{-\alpha_s}C_sP_mh_{mi}G(\theta_{mi})}\right] \prod_{p=\mathrm{L,N}} \exp\left(-2\pi\lambda\int_{D_p^s(x)}^{\infty} p(y)\mathbb{E}_{h,\theta}\left[1-e^{-ty^{-\alpha_p}C_p\sum\limits_{m\in Q_k}P_mh_mG(\theta_m)}\right] y\mathrm{d}y\right).$$

Now, using the MGF of exponentially distributed h_{mi}'s in the first product term and the independence of h_m's in the second product term, we get

$$\mathcal{L}_I(t) = \prod_{m\in Q_k\setminus\{k\}} \mathbb{E}_{\theta}\left[\frac{1}{1+tx^{-\alpha_s}C_sP_mG(\theta_{mi})}\right] \prod_{p=\mathrm{L,N}} \exp\left(-2\pi\lambda\int_{D_p^s(x)}^{\infty} p(y)\mathbb{E}_{\theta}\left[1-\prod_{m\in Q_k}\mathbb{E}_h\left[e^{-ty^{-\alpha_p}C_pP_mh_mG(\theta_m)}\right]\right] y\mathrm{d}y\right).$$

Now, using the MGF of exponentially distributed h_m's, we can write

$$\mathbb{E}_h\left[e^{-ty^{\alpha_p}C_pP_mh_mG(\theta_m)}\right] = 1/\left(1+ty^{-\alpha_p}C_pP_mG(\theta_m)\right).$$

Since $G(\theta_m)$'s are discrete random variables with $\mathbb{P}\left[G(\theta_m)=G_1\right]=\theta_{\mathrm{b}}/(2\pi)$ and $\mathbb{P}\left[G(\theta_m)=G_2\right]=1-\theta_{\mathrm{b}}/(2\pi)$, we get the Lemma. □

Similar to previous subsections, the coverage probability of the considered typical user is given as

$$\mathrm{P^c}(T) = \sum_{s=\mathrm{L,N}}\int_0^{\infty}\exp\left(-\frac{TN_0W_nx^{\alpha_s}}{C_sG(0)P_n}\right)\mathcal{L}_I\left(\frac{Tx^{\alpha_s}}{C_sG(0)P_n}\right)f_s(x)\mathrm{d}x \tag{4.25}$$

where $\mathcal{L}_I(t)$ is given in Lemma 8 and $f_s(x)$ is given in (4.23). Since full sharing of spectrum licenses is assumed for this system, the spectrum accessible to each operator is B and and $Q_n=\{1,2\cdots M\}$. Hence, similar to System 3, the average load is given as $N_n^{\mathrm{u}}=1+1.28\lambda_n^{\mathrm{u}}\frac{1}{\lambda_n}$.

4.6 Partial Loading of the Network

In the previous section, we assumed that all the BSs have at least one user associated and they are all transmitting. Such an assumption is justified when the user density is very high in comparison to the BS density resulting in many associated users per BS and negligible probability of any BS being inactive. For very dense networks, however, this assumption will break down and many BSs will not be occupied at all times. An interesting case to consider is where the system is not fully loaded and there are some BSs having no (active) users to associate with. In such a case, interference will reduce which should favor license sharing. From [58], the number of users associated with a BS of network m for a closed access system can be approximated as the following distribution:

$$\kappa_m(N_m^{\mathrm{u}}) = \frac{3.5^{3.5}}{\Gamma(n+1)} \frac{\Gamma(n+3.5)}{\Gamma(3.5)} (\eta_m)^n (3.5+\eta_m)^{-n-3.5} \tag{4.26}$$

where η_m denotes the ratio between density of associated users and BS density for network m. The $\kappa_m(N_m^{\mathrm{u}})$ approximation has been shown to closely match the load distribution in simulations [14, 58]. For the multi-network system, η_m is computed as

$$\eta_m = \sum_{q:m\in S_q} \lambda_q^{\mathrm{u}} \frac{A_m^q}{\lambda_m}, \tag{4.27}$$

where the sum is over all the networks whose users can connect to BSs of network m. The multiplication of association probability of a user of network q and user density of network q gives the density of the network q's associated users for network m.

The probability that a BS is off is equal to the probability that a BS has no user associated to it which is equal to $\kappa_m(0)$. Therefore for Systems 1, 2 and 3, the

interfering BSs can be obtained by independent thinning of original BS PPP with probability $1-\kappa_m(0)$. The coverage probability of the Systems 1, 2 and 3 are given by Theorem 10 with λ_m substituted by $\lambda'_m = \lambda_m(1-\kappa_m(0))$.

For System 4, the sum interference I at the user from BSs of all the networks in partial loading case is given as

$$I = x^{-\alpha_s} C_s \sum_{m \in Q_n \setminus \{n\}} P_m h_{im} G(\theta_{im}) \delta_{mi} + \sum_{p=\mathrm{L,N}} \sum_{\mathbf{x}_j \in \Phi_p \setminus \{\mathbf{x}_i\}} x_j^{-\alpha_p} C_p \sum_{m \in Q_n} P_m h_{mj} G(\theta_{mj}) \delta_{mj} \tag{4.28}$$

where δ_{mj} is an indicator which is 1 when BS BS_{mj} is on. Hence, the Laplace transform of interference in partial loading can be computed as =

$$\begin{aligned}\mathcal{L}_I(t) = & \prod_{m \in Q_k \setminus \{k\}} \left(\kappa(0) + (1-\kappa(0)) \sum_{j=1,2} \frac{a_j/\pi}{1 + t x^{-\alpha_s} C_s P_m G_j} \right) \\ & \times \prod_{p=\mathrm{L,N}} \exp\left(-2\lambda \int_{D_p^s(x)}^{\infty} p(y) \left(1 - \prod_{m \in Q_k} (\kappa(0) \right.\right. \\ & \left.\left. + (1-\kappa(0)) \sum_{j=1,2} \frac{a_j}{1 + y^{-\alpha_p} t C_p P_m G_j} \right) \right) y \mathrm{d}y \Bigg) \end{aligned} \tag{4.29}$$

where $a_1 = \theta_\mathrm{b}/2, a_2 = \pi - \theta_\mathrm{b}/2$. The coverage probability of this system is given by (4.25) with $\mathcal{L}_I(t)$ given in (4.29) and $f_s(x)$ given in (4.23).

Proof. The Laplace transform of interference in partial loading case (4.28) is given as $\mathcal{L}_I(t) =$

$$\mathbb{E}_{h,\theta}\left[e^{-t x^{-\alpha_s} C_s \sum_{m \in Q_k \setminus \{k\}} P_m h_{mi} G(\theta_{mi}) \delta_{mi}} \right] \prod_{p=\mathrm{L,N}} \mathbb{E}_{\Phi_p,h,\theta}\left[e^{-t \sum_{\mathbf{x}_j \in \Phi_p \setminus \{\mathbf{x}_i\}} x_j^{-\alpha_p} C_p \sum_{m \in Q_k} P_m h_{mj} G(\theta_{mj}) \delta_{mi}} \right].$$

Since δ_{mi}'s are Bernoulli random variables with $\mathbb{P}[\delta_{mi}=0] = \kappa(0)$, $\mathcal{L}_I(t)$ can be written as

$$\begin{aligned}
\mathcal{L}_I(t) = & \prod_{m\in Q_k\setminus\{k\}} \mathbb{E}_{h,\theta}\left[\kappa(0)+(1-\kappa(0))e^{-tx^{-\alpha_s}C_sP_mh_{mi}G(\theta_{mi})}\right] \\
& \prod_{p=\mathrm{L,N}} \exp\left(-2\pi\lambda\int_{D_p^s(x)} p(y)\mathbb{E}_{h,\theta,\delta}\left[1-e^{-ty^{-\alpha_p}C_p\sum_{m\in Q_k}P_mh_mG(\theta_m)\delta_m}\right] y\mathrm{d}y\right) \\
= & \prod_{m\in Q_k\setminus\{k\}} \mathbb{E}_{\theta}\left[\kappa(0)+(1-\kappa(0))\frac{1}{1+tx^{-\alpha_s}C_sP_mG(\theta_{mi})}\right] \\
& \prod_{p=\mathrm{L,N}} \exp\left(-2\pi\lambda\int_{D_p^s(x)} p(y)\mathbb{E}_{\theta}\left[1-\prod_{m\in Q_k}(\kappa(0)\right.\right. \\
& \qquad \left.\left.+(1-\kappa(0))\mathbb{E}_h\left[e^{-ty^{\alpha_p}C_pP_mh_mG(\theta_m)}\right]\right)\right] y\mathrm{d}y\Bigg)
\end{aligned}$$

which can be simplified further following the same steps as in the proof of Lemma 8 to get (4.29). □

4.7 Numerical Results

In this section, we provide results numerically computed from the analytic expressions derived in previous sections. We compare the four aforementioned systems to provide insights and discuss the impact of license sharing. For these numerical results, we consider a system consisting of two cellular operators with identical parameters, both operating in mmWave band. Each operator owns a network of BSs with density of $30/\mathrm{km}^2$ which is equivalent to average cell radius of 103 m and have users with density of $200/\mathrm{km}^2$. We consider the exponential blockage model *i.e.* $p(x) = \exp(-\beta x)$ with $\beta = 0.007$ which has an average LOS region of 144 m. The

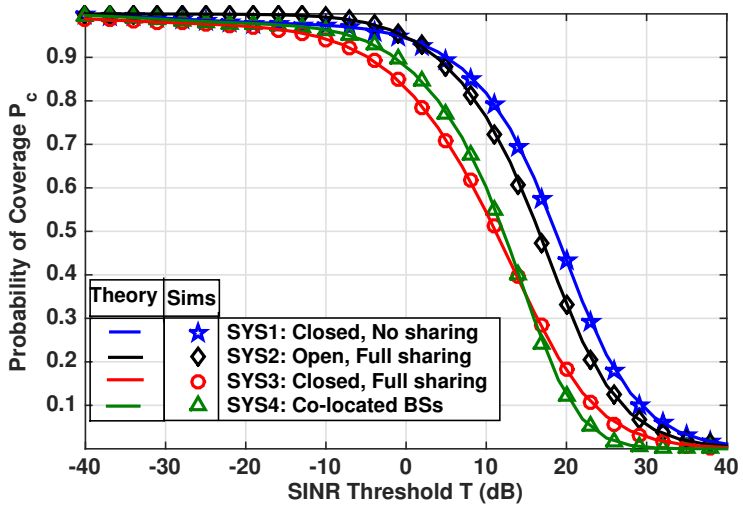

Figure 4.2: Probability of SINR coverage in a two-network mmWave system with BS antenna beamwidth $\theta_{\mathrm{b}} = 20^{\mathrm{o}}$ for different cases. Line-curves denote values from the analysis and markers denote respective values from simulation.

transmit power is assumed to be 26dBm. For most of the results, the operating frequency is 28GHz for which pathloss exponents for LOS and NLOS are $\alpha_{\mathrm{L}} = 2, \alpha_{\mathrm{N}} = 4$ and the corresponding gains are $C_{\mathrm{L}} = -60\mathrm{dB}, C_{\mathrm{N}} = -70\mathrm{dB}$. The total system bandwidth is 200 MHz. We assume that each operator owns a license to 100 MHz. Recall that for System 1, each operator can use only its own spectrum. In Systems 2, 3 and 4, both operators share each other's spectrum licenses and therefore, get 200MHz of spectrum.

Validation of analysis and SINR coverage trends: Fig. 4.2 compares the probability of coverage for these systems and validates our analysis with simulation. The typical user in System 2 has high SINR coverage due to its open access. The closed access in System 3 allows BSs of another networks to be located closer than the serving BS and may lead to large interference. Therefore the user in System 3 has low

SINR coverage. System 1 has the same closed access as System 3, but the spectrum is not shared. Therefore the user faces no interference from other networks and hence, the SINR coverage is greater than System 3. In comparing System 1 and System 2, we observe different behaviors for different SINR ranges. Recall that System 2 is similar to System 1, but with double BS and MS density and double bandwidth. Hence, a serving BS is relatively closer in System 2 from System 1 by a factor of $\sqrt{2}$. Now, for the high SINR region (which is mainly due to LOS serving links), this increases the received power of a serving BS by a factor of $\sqrt{2}^{\alpha_{\mathrm{L}}} = 2$. Since the noise power also increases by a factor of 2 due to increase in bandwidth, it effectively cancels the increase in the power caused by increased proximity of serving BS. As far as interference is considered, since doubling density increases the probability of interferers to be LOS, interference increases significantly in System 2. Therefore SINR coverage is higher in System 1 than System 2. For the low SINR region (which is mostly due to NLOS serving links), the received power of a serving BS increases by a factor of $\sqrt{2}^{\alpha_{\mathrm{N}}} = 4$ and the probability of serving link turning to LOS is also increased due to increased proximity of serving BS. Therefore System 2 has higher SINR coverage than System 1 in the low SINR region. System 4 has similar values and trends as System 3 when compared to other systems. System 4 has similar values and trends as System 3 when compared to other systems. While comparing Systems 3 and 4, we see a trade-off similar to [108] . In System 4, there cannot be any BS of other operators closer to the user than the serving BS which is not the case for System 3. This causes System 4 to perform better than System 3 for cell edge users with low serving signal power. The same co-location argument also guarantees that

System 4 will always have $M-1$ interfering BSs of the other operators at the same location as the serving BS. Therefore, System 3 performs better for users with high serving power.

Sharing licenses achieves higher rate coverage: Fig. 4.3 compares the probability of rate coverage for four systems which incorporates the effect of load and bandwidth. Since each network has a large bandwidth and large SINR coverage in System 2, its rate coverage is the highest among all systems. Such a system, however, as mentioned earlier, may not be practical and mainly serves as a benchmark for practical systems. A more interesting comparison is between System 1 and 3 (or 4). Here we can see that even though System 1 has higher SINR coverage than System 3 (and 4), the latter achieves higher median rate, due to the extra bandwidth gained from spectrum license sharing. In particular, System 3 and 4 have respectively 25% and 32% higher median rates than System 1.

Validation of the model with realistic scenario: To validate our PPP assumption and to show that it is reasonable, we also present a simulation result where the BSs are deployed in a square grid and the BS antenna pattern is parabolic, as specified by the 3GPP standard [1]. In System 2 and 3, both operators have their own square grid deployments which is shifted from each other by a random amount in each realization of the simulation. We also consider log-normal shadowing ($\sigma_{\text{LOS}} = 5.2$dB and $\sigma_{\text{NLOS}} = 7.6$dB). Fig. 4.4 compares the probability of rate coverage for four systems with these modifications. We observe similar trends for spectrum license sharing which justifies our assumptions regarding deployment and shadowing. Fig. 4.5 shows the probability of rate coverage for four systems with Nakagami fading

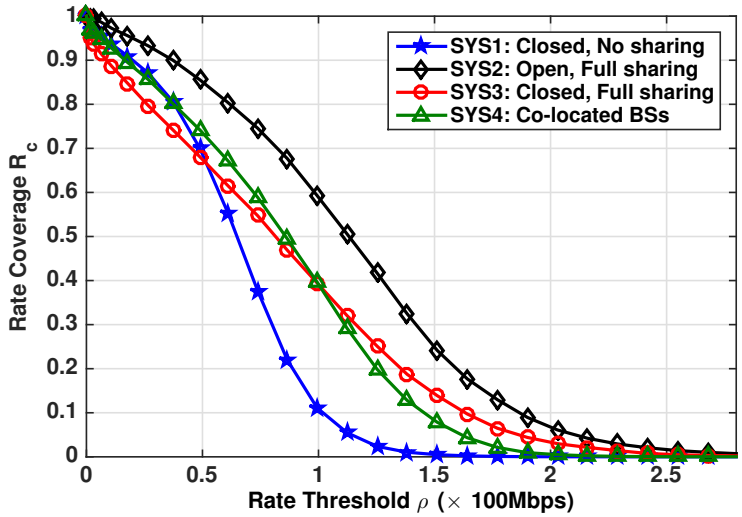

Figure 4.3: Rate coverage in a two-network mmWave system with Rayleigh fading and BS antenna beamwidth $\theta_b = 20^o$ for different cases. Systems 3 and 4 with shared license perform better than System 1 with exclusive licenses.

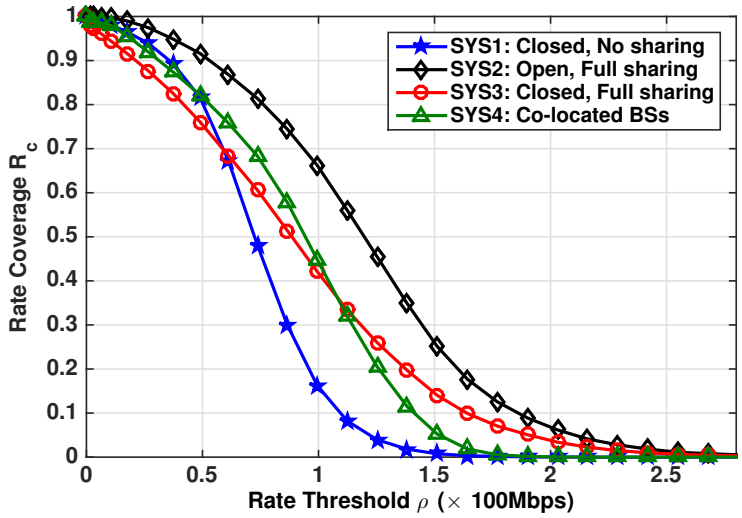

Figure 4.4: Rate coverage in a two-network mmWave system with grid BS deployment and 3GPP antenna pattern [1] for different cases. The trends for this case are similar to Fig. 4.3 which validates our assumptions regarding the system model.

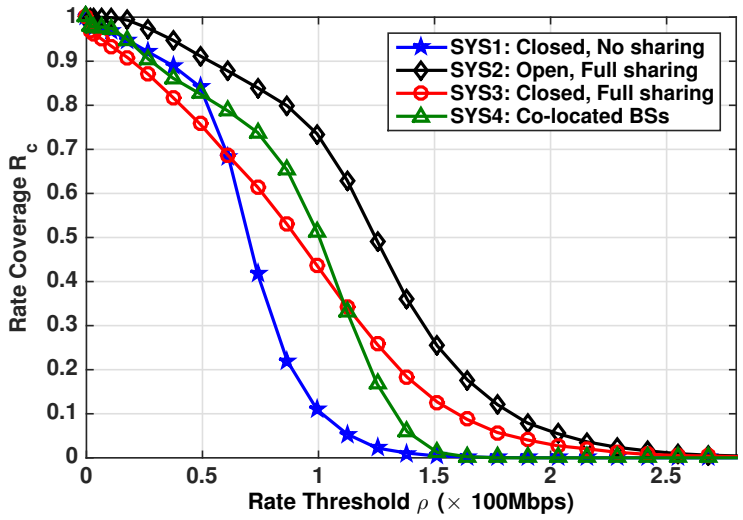

Figure 4.5: Rate coverage in a two-network mmWave system with Nakagami fading (with parameter 10) and BS antenna beamwidth $\theta_b = 20^o$ for different cases. When compared to Rayleigh fading (Fig. 4.3), the insights are similar which justifies the Rayleigh fading assumption for analysis

(with parameter 10) instead of Rayleigh. It can be seen that the trends are similar to those of Rayleigh distribution as we claimed in Section IIA.

Impact of beamwidth on median rate: Fig. 4.6 compares the median rate of the four systems for various values of beamwidth. It can be seen that above a certain threshold for the beamwidth, it becomes more beneficial to have exclusive license, due to high interference. As the beamwidth decreases, license sharing becomes more beneficial. For the given parameters, the threshold is at about 25^o. Since mmWave has typical beamwidth less than 15^o, sharing should increase the achievable rate.

Partial loading favors sharing: Fig. 4.7 compares the probability of rate coverage for four systems under partial loading with user density of $30/\text{km}^2$. It can be observed that due to reduced interference, System 3 (and 4) has even higher gain

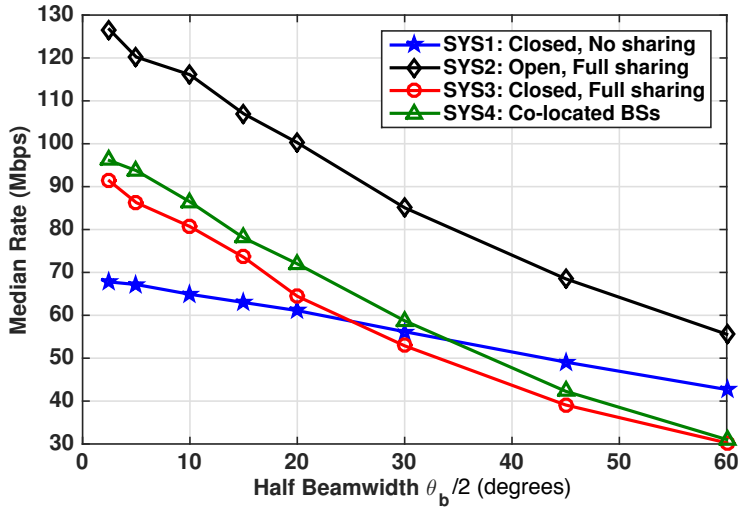

Figure 4.6: Median rate versus BS antenna beamwidth in two-network mmWave system under different cases for Rayleigh fading. Systems with sharing of license outperforms System 1 with no shared license for moderate and low values of antenna beamwidth.

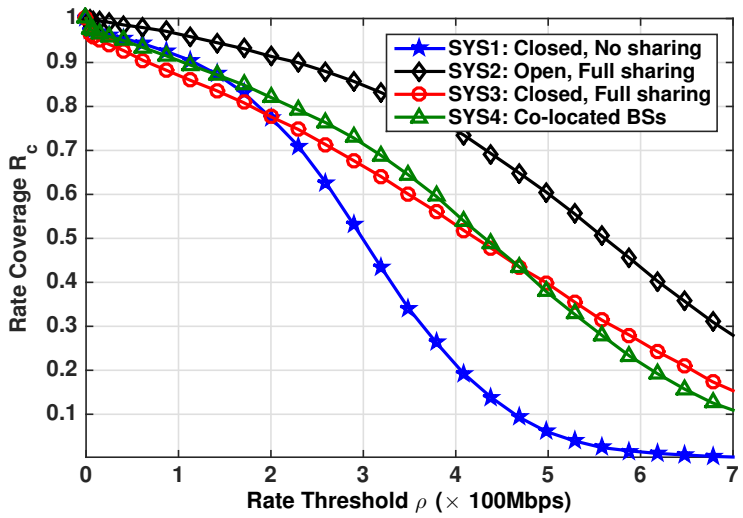

Figure 4.7: Rate coverage in a two-network mmWave system under partial loading with Rayleigh fading for different cases. Partial loading favors spectrum license sharing.

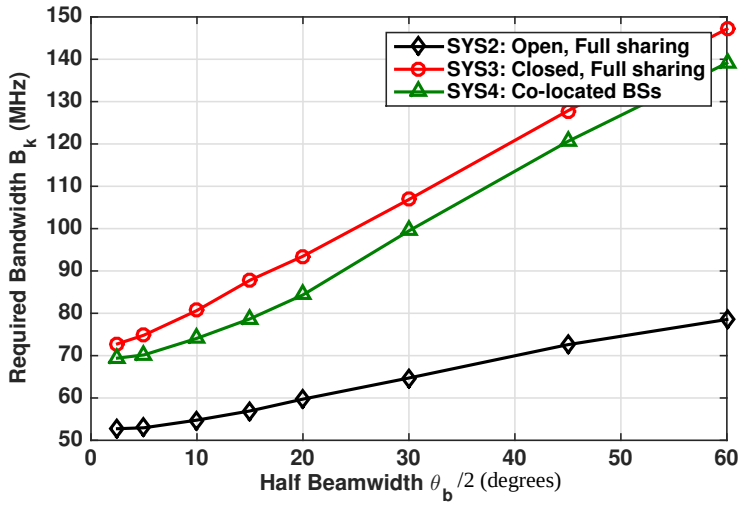

Figure 4.8: Required bandwidth for each network (with sharing of licenses) to achieve the same median rate achieved by the network with no sharing of spectrum with each network having 100MHz spectrum license. Sharing can reduce the license cost by more than 25%.

than System 1. In particular, System 3 has 40% higher median rate than System 1 in partial loading case compared to only 25% gain in the previous case when user density was 200/km^2.

Sharing reduces spectrum cost significantly: Now, we compare the following two cases. In the first case, each network owns a 100 MHz bandwidth exclusive license. This case is the same as System 1. In the second case, the networks share licenses completely and choose to buy just enough spectrum to achieve the same median rate as in the first case. Fig. 4.8 shows this required spectral bandwidth for each network. With a 10^o beamwidth antenna, each network only needs to buy 75 MHz of bandwidth which would save 25% of the license cost assuming linear pricing of the spectrum.

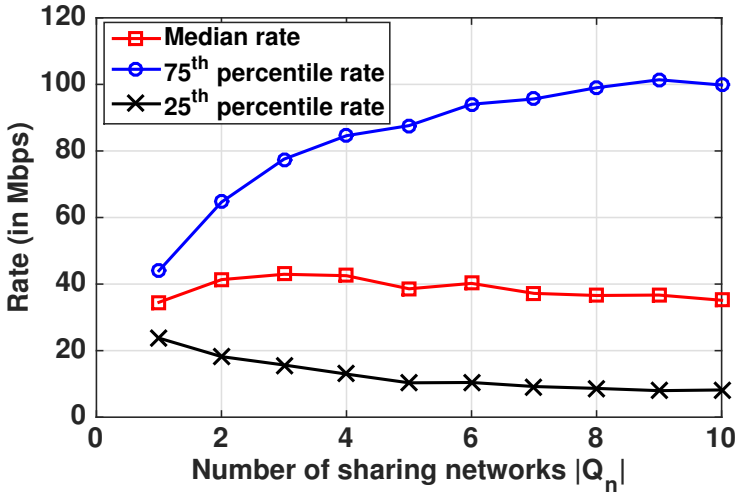

Figure 4.9: Rate versus number of sharing networks in a mmWave cellular system with 10 networks. A trade-off between increasing the available bandwidth and increasing interference is observed.

Optimal cardinality of sharing groups depends on the target rate: Now, we consider a system with 10 operators with 50MHz bandwidth each and closed access. Fig. 4.9 shows variation of the per-user rate for different percentiles with respect to cardinality $|Q_n|$ of sharing group which is equal to the number of operators sharing licenses with network n. We can see that the 75^{th} percentile rate increases with $|Q_n|$ while the 25^{th} percentile rate decreases. For the median rate, we see an increase up to $|Q_n| = 3$ and then the median rate decreases. This trade-off is due to the fact that as more operators share their licenses, the total available bandwidth and the sum interference both increase. It can be observed that depending on the target performance, the optimal number of networks that should share their licenses varies.

Impact of asymmetry among operators: We now consider the case when

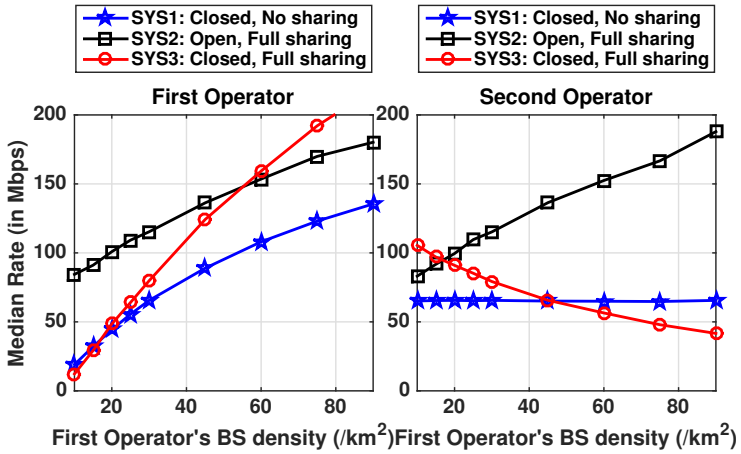

Figure 4.10: Variation of median rate with BS density of first operator in a two operator system. The BS density of second operator is fixed at 30/km^2. The user densities of both operators are same and fixed. Both operators gain from license sharing only when first operator density between 15 to 45/km^2. Spectrum license sharing is more beneficial for the operator with higher density.

both operators are not identical. Fig. 4.10 shows the variation of median rate of the first and the second operators with respect to BS density of the first operator in a two-operator system with fixed user density of 200/km^2. The BS density of first operator is fixed at 30/km^2. The gain from license sharing increases as the BS density increases for the operator with higher density and decreases for the other operator. We can observe that both operators can simultaneously gain from license sharing only when both operators have similar BS densities which is between 15 to 45/km^2 here.

We now consider one more asymmetric case when the first operator size changes instead of just BS density. Fig. 4.11 shows the variation of median rate of the first and the second operators with respect to BS density of the first operator in a two-operator system. Here BS density of the first operator acts as a proxy for its network size.

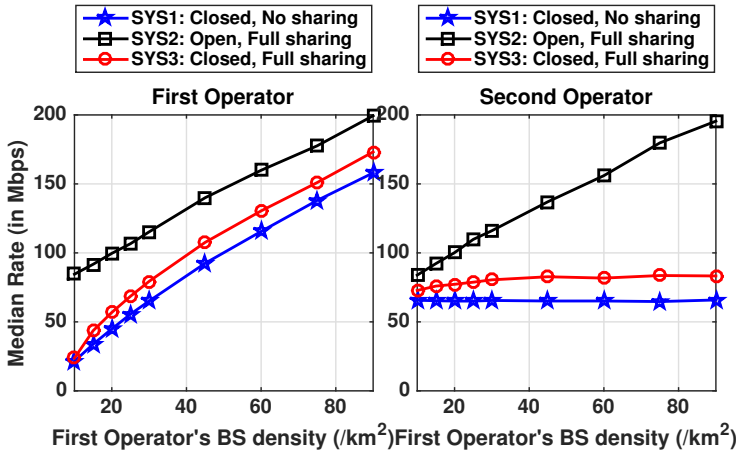

Figure 4.11: Variation of median rate with network size of the first operator in a two operator system. The BS density of second operator is fixed at 30/km^2, licensed bandwidth at 100MHz and user density at 200/km^2. Here, BS density, user density and licensed bandwidth of the first operator vary linearly with network size and all parameters are the same as second operator when BS density of the first operator matches with the second operator. Both operators gain from license sharing but the gain of the operator with lower size is more.

BS density, user density and licensed bandwidth of the first operator vary linearly with network size. The BS density of second operator is fixed at 30/km^2, licensed bandwidth at 100MHz and user density at 200/km^2. For normalization, both operators are assumed to be identical when BS density of the first operator is 30BSs/km^2. When the first operator's size is three times more than the second operator, the gain from license sharing is 26% for the second operator (with lower size) in comparison to the 9% gain for the first operator. In this case, the spectrum sharing seems more beneficial to the operator with smaller infrastructure.

Results for 73GHz band: We also consider mmWave communication at 73GHz with 1 GHz bandwidth. The near-field path-loss gains are decreased by a

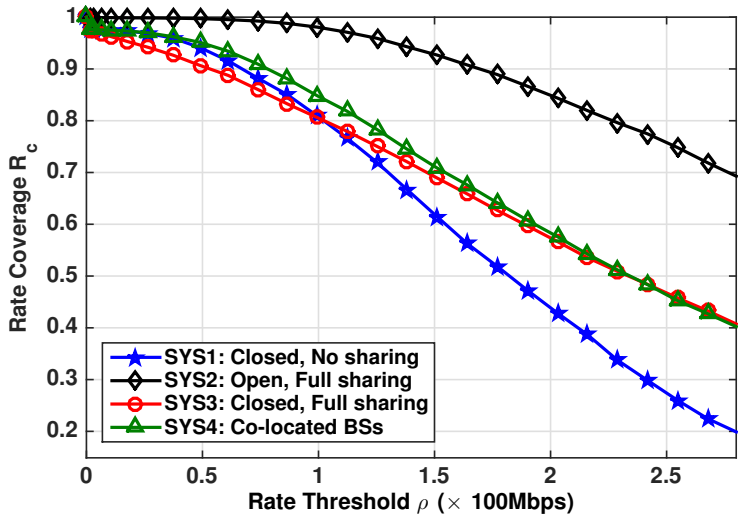

Figure 4.12: Rate coverage in a two-network mmWave system at 73 GHz frequency with Rayleigh fading for different cases. Similar trends for spectrum sharing are observed for the 28 GHz and 73 GHz bands.

factor of $10\log 10(73/28)^2 = 8.32$dB when compared with 28GHz for both LOS and NLOS. Fig. 4.12 compares the rate coverage for four systems for 73GHz and shows similar trends as 28 GHz. Due to reduced interference, license sharing achieves slightly higher gain (28%) compared to 28 GHz case (*i.e.* 25%).

4.8 Conclusions

We have modeled a two-level architecture of a mmWave multi-operator system and derived the SINR and per-user rate distribution. We show that license sharing among operators improves system performance by increasing per-user rate. We conclude that it is economical for operators to share their spectrum licenses without increasing any overhead. We show that narrow beams play a key role in making spectrum license sharing feasible. Since an increase in the number of networks increases

both the sum interference and bandwidth, the optimal cardinality of the sharing group will depend on the target rate.

Chapter 5

Restricted Secondary Licensing in mmWave Cellular Systems

In the last chapter, we showed that mmWave systems experience relatively low interference due to directionality and sensitivity to blockage which leads to possibility of sharing the mmWave spectrum among different operators without any coordination. However, due to increased interference from other operators, the cell edge users suffer and uncoordinated sharing of spectrum licenses results in lower edge rates. Also, an operator may be ready to share its spectrum, but it may still want to distinguish itself as the primary owner of a spectrum to achieve certain level of quality of service or to get a competitive edge in the market. Therefore, it is intuitive to have a licensing scheme where the owner of the spectrum has higher control of the spectrum and it can impose some restrictions on the other operators it lends the spectrum to. One important things while imposing such restrictions on the secondary operators is that too high coordination requirements can eat away the gains from spectrum sharing. Therefore, there must be a certain limit on how much coordination is required from the secondary operators. One practical solution is to have some static coordination based on large channel statistics which does not require continuous sensing of the

[1]This work has appeared in [114] and [115] in parts. I am the first author of both of these articles.

spectrum. While spectrum sharing can be beneficial for mmWave systems even without any coordination [83], its gain over exclusive licensing can probably be magnified with some static coordination. In this chapter, we study such static coordination based licensing scheme which we term as restricted secondary licensing and explore the potential gains of such spectrum sharing.

5.1 Related Work

At conventional cellular frequencies, operators own exclusive licenses that give them the absolute right of using a particular frequency band. One drawback of exclusive licensing is that some portions of the spectrum remain highly underutilized [85]. To overcome that, secondary network operation–also known as cognitive radio networks [86–90]–can be used [34,35]. The key operational concept of secondary networks is to serve their users without exceeding a certain interference threshold at the primary network, that owns the spectrum. One main approach to guarantee that is continuous spectrum sensing [34, 35]. This, however, consumes a lot of power and time-frequency resources, which diminishes the practicality of spectrum-sensing based cognitive radio systems. In the previous chapter, we showed that spectrum sharing is feasible for mmWave systems even without any coordination. It represents, therefore, the opposite extreme versus instantaneous spectrum-sensing based cognitive radios. An intermediate solution, between these two extremes, is to allow some static coordination based on large channel statistics instead of the continuous sensing.

Using stochastic geometry tools, some research has been done on analyzing the performance of cognitive radio networks at conventional cellular frequen-

cies [35, 116, 117]. In [116], a network of a primary transmitter-receiver pairs and secondary PPP users was considered, and the outage probability of the primary links were evaluated. In [35], a cognitive cellular network with multiple primary and secondary base stations was modeled, and the gain in the outage probability due to cognition was quantified. In [117], a cognitive carrier sensing protocol was proposed for a network consisting of multiple primary and secondary users, and the spectrum access probabilities were characterized. The work in [35, 116, 117], though, did not consider mmWave systems and their differentiating features. In [83], stochastic geometry was employed to analyze spectrum-sharing in mmWave systems but with no coordination between the different operators. When some coordination exists between these operators, evaluating the network performance becomes more challenging and requires new analysis, which is one of the contributions in our work.

5.2 Contributions

In this chapter, we consider a downlink mmWave cellular system with a primary and a secondary operator to evaluate the benefits of secondary licensing in mmWave systems. The main contributions of this chapter are summarized as follows.

- **A tractable model for secondary licensing in mmWave networks:** We propose a model for mmWave cellular systems where an operator owns an exclusive-use license to a certain band with a provision to give a restricted license to another operator for the same band. Note that there are different ideas in the spectrum market for how this restricted license works [118]. We call the operator that originally owns the spectrum the *primary operator*, and

the operator with restricted license the *secondary operator*. In our model, this restricted secondary license requires the licensee to adjust the transmit power of its BSs such that the average interference at any user of the primary operator is less than a certain threshold. Due to this restriction, the transmit power of the secondary BSs depends on the primary users in its neighborhood, and hence, it is a random variable. This required developing new analytical tools to characterize the system performance, which is one of the chapter's contributions over prior work.

- **Characterizing the performance of the restricted spectrum sharing networks:** Using stochastic geometry tools, we derive expressions for the coverage probability and area spectral efficiency of the primary and restrcited secondary networks as functions of the interference threshold. Results show that restricted secondary licensing can achieve coverage and rate gains for the secondary networks with a negligible impact on the primary network performance. Compared to the case when the secondary operator is allowed to share the spectrum without any coordination [83], our results show that restricted secondary licensing can increase the sum-rate of the sharing operators. This is in addition to the practical advantage of providing a way to differentiate the spectrum access of the different operators.

- **Optimal licensing and pricing:** We present a revenue-pricing model for both the primary and secondary operators in the presence of a central licensing entity such as the FCC. We show that with the appropriate adjustment of

the interference threshold, both the original operator and the central entity can benefit from the secondary network license. Therefore, they have a clear incentive to allow restricted secondary licensing. Further, the results show that the secondary interference threshold needs to be carefully adjusted to maximize the utility gains for the primary operator and the central licensing authority. As the optimal interference thresholds that maximize the central authority can be different than that of the primary operator, the central authority may have an incentive to push the primary operator to share even if it experiences more degradation than otherwise allowable.

5.3 Network and System Model

In this chapter, we consider a mmWave cellular system where an operator owns an exclusive-use license to a frequency band of bandwidth W. There is a provision that this licensee can also give a restricted secondary license to another operator for the same band. To distinguish the two networks, we call the first operator the primary operator and the second operator as secondary operator.

The primary operator has a network of BSs and users. We model the locations of the primary BSs as a Poisson point process (PPP) $\Phi_{\mathrm{P}} = \{\mathbf{x}_i\}$ with intensity λ_{P} and the location of users as another PPP Ψ_{P} with intensity μ_{P}. We denote the distance of ith primary BS from the origin by $x_i = \|\mathbf{x}_i\|$. Each BS of the primary operator transmits with a power P_{P}. We assume that the secondary license allows the owning entity to use the licensed band with a restriction on the transmit power: each BS of the secondary operator adjusts its transmit power so that its average interference on

any primary user does not exceed a fixed threshold ξ. We model the BS locations of the secondary operator as a PPP $\Phi_{\mathrm{S}} = \{\mathbf{y}_i\}$ with intensity λ_{S} and locations of its users as another PPP Ψ_{S} with intensity μ_{S}. Further, we let $y_i = \|\mathbf{y}_i\|$ denote the distance of the ith secondary BS from the origin. The transmit power of the ith secondary BS is denoted by $P_{\mathrm{S}i}$. We assume that all the four PPPs are independent. The PPP assumption can be justified by the fact that nearly any BS distribution in 2D results in a small fixed SINR shift relative to the PPP [109, 110] and has been used in the past to model single and multi-operator mmWave systems [8, 14, 83, 108].

5.3.1 Channel and SINR Model

We consider the performance of the downlink of the primary and secondary networks separately. In each case, we consider a typical user to be located at the origin. We assume an independent blocking model where a link between a user and a BS located at distance r from this user can be either NLOS (denoted by N) with a probability $p_{\mathrm{N}}(r)$ or a LOS (denoted by L) with a probability $p_{\mathrm{L}}(r) = 1 - p_{\mathrm{N}}(r)$ independent to other links. One particular example of this model is the exponential blocking model [8], where $p_{\mathrm{L}}(r) = \exp(-\beta r)$. The pathloss from a BS to a user is given as $\ell_t(r) = C_t r^{-\alpha_t}$ where $t \in \{\mathrm{L}, \mathrm{N}\}$ denotes the type of the BS-user link, α_t is the pathloss exponent, and C_t is near-field gain for the t type links.

For the typical primary user UE_{P}, let $s_{\mathbf{x}}$ denote the type of the link between the BS at $\mathbf{x}$ and this user, and let $g_{\mathbf{x}}$ represent the channel fading. Similarly, for the typical secondary user UE_{S}, let $t_{\mathbf{x}_i}$ and $h_{\mathbf{x}_i}$ denote the type of its link to the BS at $\mathbf{x}$ and its channel fading. For analytical tractability, we assume all the channels have

normalized Rayleigh fading, which means that all the fading variables are exponential random variables with mean 1.

We assume that each BS is equipped with a steerable directional antenna. The BS antennas at the primary BSs has the following radiation pattern [8, 102, 119]

$$G_{\mathrm{P}}(\theta) = \begin{cases} G_{\mathrm{P1}} & \text{if } |\theta| \leq \theta_{\mathrm{Pb}}/2 \\ G_{\mathrm{P2}} & \text{if } |\theta| > \theta_{\mathrm{Pb}}/2 \end{cases}, \tag{5.1}$$

where $\theta \in [-\pi, \pi]$ is the angle between the beam and the user, G_{P1} is the main lobe gain, G_{P2} is the side lobe gain, and θ_{Pb} is half-power beamwidth. To satisfy the power conservation constraint, which requires the total transmitted power to be constant and not a function of the beamwidth, we normalize the gains such that $G_{\mathrm{P1}}\frac{\theta_{\mathrm{Pb}}}{2\pi} + G_{\mathrm{P2}}\frac{(2\pi-\theta_{\mathrm{Pb}})}{2\pi} = 1$. Similarly, the radiation pattern of the antennas at a secondary BS is given by $G_{\mathrm{S}}(\theta)$ with parameters G_{S1},G_{S1} and θ_{Sb}.

Both operators follow maximum average received power based association where a user connects to a BS providing the maximum received power averaged over fading. We call this BS the *tagged* BS. The tagged BS steers its antenna beam towards the user to guarantee the maximum antenna gain (G_{P1} or G_{S1}). We take this steering direction as a reference for the other directions. We denote the angle between the antenna of a BS at $\mathbf{x}$ and the primary user by $\theta_{\mathbf{x}}$ and the secondary user by $\omega_{\mathbf{x}}$. We assume that a user can connect only to a BS in their own network. Now, we provide the SINR expression for the typical user of each operator (See Fig. 5.1).

1. Primary user $\mathrm{UE_P}$ at the origin: Let us denote the tagged BS by $\mathbf{x}_0 \in \Phi_{\mathrm{P}}$. The

Table 5.1: Summary of Notation

Notation	**Description**
$\Phi_{\mathrm{P}}, \lambda_{\mathrm{P}}, \mathbf{x}_i$	For the primary operator: PPP modeling locations of BSs, BS density, location of ith BS.
$\Psi_{\mathrm{P}}, \mu_{\mathrm{P}}$,$\mathrm{UE}_{\mathrm{P}}$	For the primary : PPP modeling locations of users, user density, the typical user at the origin.
$P_{\mathrm{P}}, G_{\mathrm{P}}(\cdot), N_{\mathrm{P}}$	For the primary : transmit power of BSs, BS antenna pattern, and number of BS antennas.
W, ξ	Licensed bandwidth, maximum interference limit for secondary operator.
$\Phi_{\mathrm{S}}, \lambda_{\mathrm{S}}, \mathbf{y}_i$	For the secondary operator: PPP modeling locations of BSs, BS density, location of ith BS.
$\Psi_{\mathrm{S}}, \mu_{\mathrm{S}}$,$\mathrm{UE}_{\mathrm{S}}$	For the secondary: PPP modeling locations of users, user density, the typical user at the origin.
$P_{\mathrm{S}i}, \overline{\zeta_i}, G_{\mathrm{P}}(\cdot), N_{\mathrm{S}}$	For the secondary: transmit power of the ith BS, Normalized transmit power of the the ith BS defined as $P_{\mathrm{S}i}/\xi$, BS antenna pattern, and number of BS antennas.
L, N	Possible values of link type: L denotes LOS, N denotes NLOS.
$s_{\mathbf{x}}, g_{\mathbf{x}}$	For the link between UE_{P} and BS at $\mathbf{x}$: $s_{\mathbf{x}} \in \{\mathrm{L}, \mathrm{N}\}$ denotes the link type and $g_{\mathbf{x}}$ is the fading.
$t_{\mathbf{x}}, h_{\mathbf{x}}$	For the link between UE_{S} and BS at $\mathbf{x}$: $t_{\mathbf{x}} \in \{\mathrm{L}, \mathrm{N}\}$ denotes the link type and $h_{\mathbf{x}}$ is the fading.
$\mathcal{H}_i, T_i, F_i$	$\mathcal{H}_i$ is the closet (radio distance wise) primary user for the ith secondary BS, T_i is the type of the link between this BS and $\mathcal{H}_i$, F_i is the fading.
C_t and α_t	Path-loss model parameters: path-loss gain and path-loss exponent of any link of type $t \in \{\mathrm{L}, \mathrm{N}\}$.
$p_{\mathrm{L}}(r), p_{\mathrm{N}}(r)$	The probability of being LOS or NLOS for a link of distance r.
$E_{st}(x)$	Exclusion radius for primary users of type t from the secondary BS when it is associated with a s type primary user located at distance x.
$\sigma^2_{\mathrm{P}}, \sigma^2_{\mathrm{S}}$	Noise power at the UE_{P} and UE_{S}.
$P^{\mathrm{c}}_{\mathrm{P}}(\cdot), P^{\mathrm{c}}_{\mathrm{S}}(\cdot)$	Coverage probability of UE_{P} and UE_{S}.
$\mathrm{R}^{\mathrm{c}}_{\mathrm{P}}(\cdot), \mathrm{R}^{\mathrm{c}}_{\mathrm{P}}(\cdot)$	Rate coverage of UE_{P} and UE_{S}.
$\mathcal{M}_{\mathrm{P}}(\cdot), \mathcal{M}_{\mathrm{S}}(\cdot)$	Revenue functions for the primary and secondary operator.
$\mathcal{P}_{\mathrm{P}}(\cdot), \mathcal{P}_{\mathrm{SC}}(\cdot)$	License cost functions for the primary and secondary operators to the central entity.

Table 5.1: Cont.

$\mathcal{P}_{\mathrm{SP}}(\cdot)$	License cost functions given by the secondary operator to the primary operator.
$\mathcal{U}_{\mathrm{P}}(\cdot), \mathcal{U}_{\mathrm{S}}(\cdot), \mathcal{U}_{\mathrm{C}}(\cdot)$	The total revenue functions of the primary operator, the secondary operator and the central entity.

SINR for this typical user is then given as

$$\mathrm{SINR}_{\mathrm{P0}} = \frac{P_{\mathrm{P}} G_{\mathrm{P1}} g_{\mathbf{x}_0} C_{s_{\mathbf{x}_0}} x_0^{-\alpha_{s_{\mathbf{x}_0}}}}{\sigma_{\mathrm{P}}^2 + \sum\limits_{\mathbf{x}_i \in \Phi_{\mathrm{P}} \setminus \mathbf{x}_0} P_{\mathrm{P}} G_{\mathrm{P}}(\theta_i) g_{\mathbf{x}_i} C_{s_{\mathbf{x}_i}} x_i^{-\alpha_{s_{\mathbf{x}_i}}} + \sum\limits_{\mathbf{y}_i \in \Phi_{\mathrm{S}}} P_{\mathrm{S}i} G_{\mathrm{S}}(\omega_i) g_{\mathbf{y}_i} C_{s_{\mathbf{y}_i}} y_i^{-\alpha_{s_{\mathbf{y}_i}}}}. \tag{5.2}$$

2. Secondary user UE_{S} at the origin: Let us denote the tagged BS by $\mathbf{y}_0 \in \Phi_{\mathrm{S}}$. The SINR for this typical user is then given as

$$\mathrm{SINR}_{\mathrm{S0}} = \frac{P_{\mathrm{S0}} G_{\mathrm{S1}} h_{\mathbf{y}_0} C_{t_{\mathbf{y}_0}} y_0^{-\alpha_{t_{\mathbf{y}_0}}}}{\sigma_{\mathrm{S}}^2 + \sum\limits_{\mathbf{x}_i \in \Phi_{\mathrm{P}}} P_{\mathrm{P}} G_{\mathrm{P}}(\theta_i) h_{\mathbf{x}_i} C_{t_{\mathbf{x}_i}} x_i^{-\alpha_{t_{\mathbf{x}_i}}} + \sum\limits_{\mathbf{y}_i \in \Phi_{\mathrm{S}} \setminus \mathbf{y}_0} P_{\mathrm{S}i} G_{\mathrm{S}}(\omega_i) h_{\mathbf{y}_i} C_{t_{\mathbf{y}_i}} y_i^{-\alpha_{t_{\mathbf{y}_i}}}}. \tag{5.3}$$

5.3.2 Restricted Secondary Licensing

We now describe the restrictions on the secondary licenses and the sensing mechanism used by the secondary licensee. We assume that all secondary BSs scan for primary users in their neighborhood. Each secondary BS associates itself with the closest (radio-distance wise *i.e.* the one providing it the highest average received power) primary user. We call this associated primary user as the home primary user of the ith secondary BS and denote it by $\mathcal{H}_i$. Also, we call the secondary BSs attached to the ith primary user as its native BSs (see Fig. 5.2) and denote the set of these BSs by $\mathcal{N}_i$.

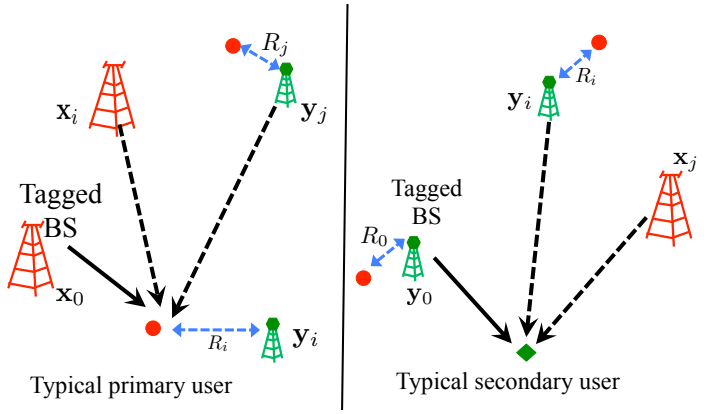

Figure 5.1: System model illustrating the SINR model for the typical primary and the secondary user. ith secondary BS is attached to the closest primary user where distance between the two is denoted by R_i.

Let us denote the distance between ith secondary BS and its home primary user $\mathcal{H}_i$ by R_i, and the type of the link between them by T_i. Note that R_i for a secondary BS is not independent to the R_i's of its adjacent secondary BSs. This is due to the fact that the transmit power of each secondary BS is determined by the same primary user process.

For a given $R_i = r$ and $T_i = T$, all the other primary users will be outside certain exclusion regions, which is different for the LOS and NLOS users. For a primary user of link type t, the radius of its exclusion region, denoted by $E_{Tt}(r)$, is given as

$$E_{Tt}(r) = (C_t/C_T)^{\frac{1}{\alpha_t}} \, r^{\frac{\alpha_T}{\alpha_t}}. \tag{5.4}$$

Now, the joint distribution of R_i and T_i is given as follows:

$$f_{R_i}(r, T_i = T) = 2\pi\mu_{\mathrm{P}} p_T(r) r \exp\left(-\mu_{\mathrm{P}} \left(V_{\mathrm{L}}(E_{T\mathrm{L}}(r)) + V_{\mathrm{N}}(E_{T\mathrm{N}}(r))\right)\right), \tag{5.5}$$

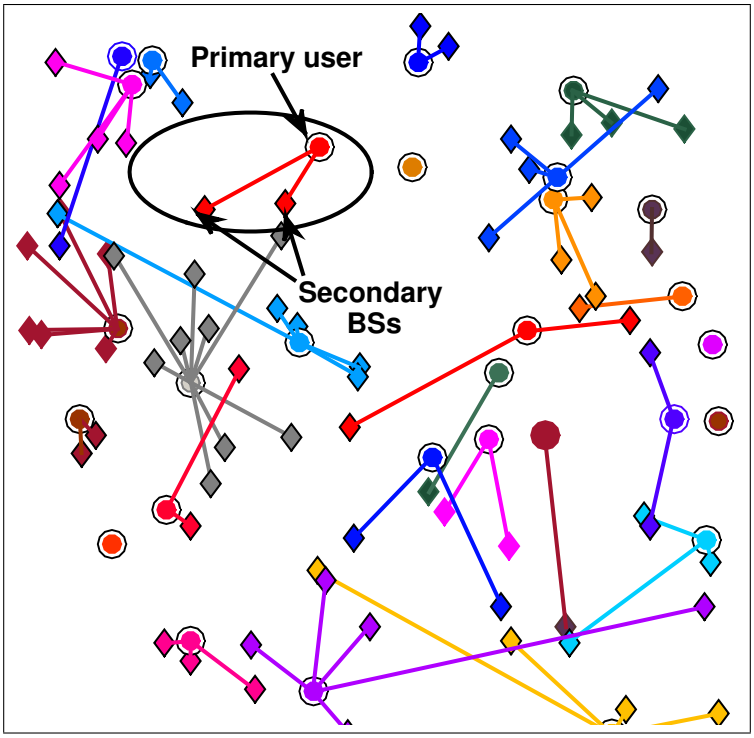

Figure 5.2: The association of secondary BSs (diamonds) to their home primary user (circles) in a particular realization of the adopted mmWave system. Each secondary BS adjusts its transmit power to keep the interference on its home primary user less than a given limit ξ.

where $V_T(r)$ denotes the volume for LOS or NLOS and is defined as $V_T(r) = 2\pi \int_0^r p_T(r) r dr$. Note that $E_{Tt}(r) = r$ when $T = t$.

Proof. Here, we compute the joint distribution of R_i and $T_i = \mathrm{L}$. The proof for $T_i = \mathrm{N}$ is similar. Consider the i^{th} secondary BS. Now, the primary user PPP can be divided into two independent PPPs: Ψ_{PL} consisting of all primary user having LOS link to the i^{th} secondary BS and Ψ_{PN} with all primary user having NLOS link to the i^{th} secondary BS. Now, let $R_{\mathrm{L}i}$ denote the distance of the closest primary user in Ψ_{PL}

whose distribution can computed as follows:

$$\mathbb{P}\left[R_{\mathrm{L}i} > r\right] = \exp\left(-\int_0^{\infty} \mu_{\mathrm{P}} p_{\mathrm{L}}(r) 2\pi r dr\right) = e^{-\mu_{\mathrm{P}} V_{\mathrm{L}}(r)}$$
$$f_{R_{\mathrm{L}i}}(r) = \frac{\mathrm{d}}{\mathrm{d}r}\mathbb{P}\left[R_{\mathrm{L}i} > r\right] = 2\pi\mu_{\mathrm{P}} p_{\mathrm{L}}(r) r \exp(-\mu_{\mathrm{P}} V_{\mathrm{L}}(r))$$

where the first step is from the void probability of the non-homogenous PPP Ψ_{PL}. Similarly the distance distribution of the closest primary user in Ψ_{PN} can also be computed. Now, the joint probability of the event $R_i > r$ and the event that $\mathcal{H}_i$ is a LOS BS (*i.e.* $T_i = \mathrm{L}$) is computed as

$$\mathbb{P}\left[R_i > r, T_i = \mathrm{L}\right] = \int_r^{\infty} f_{R_{\mathrm{L}i}}(u)\mathbb{P}\left[C_{\mathrm{N}} R_{\mathrm{N}i}^{-\alpha_{\mathrm{N}}} < C_{\mathrm{L}} u^{-\alpha_{\mathrm{L}}}\right] \mathrm{d}u$$
$$= \int_r^{\infty} f_{R_{\mathrm{L}i}}(u)\mathbb{P}\left[R_{\mathrm{N}i} > \left(\frac{C_{\mathrm{N}}}{C_{\mathrm{L}}}\right)^{\frac{1}{\alpha_{\mathrm{N}}}} u^{\frac{\alpha_{\mathrm{L}}}{\alpha_N}}\right] \mathrm{d}u$$
$$= \int_r^{\infty} f_{R_{\mathrm{L}i}}(u)\mathbb{P}\left[R_{\mathrm{N}i} > E_{\mathrm{LN}}(u)\right] \mathrm{d}u = \int_r^{\infty} 2\pi\mu_{\mathrm{P}} p_{\mathrm{L}}(u) r \exp(-\mu_{\mathrm{P}} V_{\mathrm{L}}(u) - \mu_{\mathrm{P}} V_{\mathrm{N}}(E_{\mathrm{LN}}(u))) \mathrm{d}u$$

where the last step is from the void probability of Ψ_{PN}. Therefore, the joint distribution can be computed as follows:

$$f_{R_i}(r, T_i = \mathrm{L}) = \frac{\mathrm{d}}{\mathrm{d}r}\mathbb{P}\left[R_i > r, T_i = \mathrm{L}\right] = 2\pi\mu_{\mathrm{P}} p_{\mathrm{L}}(r) r \exp(-\mu_{\mathrm{P}} V_{\mathrm{L}}(r) - \mu_{\mathrm{P}} V_{\mathrm{N}}(E_{\mathrm{LN}}(r))).$$

□

Recall that the ith secondary BS is restricted to transmit at a certain power such that the average interference at the home user, which is equal to $P_{\mathrm{S}i} C_{T_i} / R_i^{\alpha_{T_i}} \mathrm{m}$ is below a threshold ξ. Therefore, its transmit power is given by

$$P_{\mathrm{S}i} = \xi R_i^{\alpha_{T_i}} / C_{T_i}. \tag{5.6}$$

The joint distribution of $P_{\mathrm{S}i}$ and T_i can be computed using transformation of variables as

$$f_{P_{\mathrm{S}i}}(p, T_i = T) = \\ \frac{2\pi\mu_{\mathrm{P}}a^2}{\alpha_T} p^{\frac{2}{\alpha_T}-1} p_T\left(ap^{\frac{1}{\alpha_T}}\right) \exp\left(-\mu_{\mathrm{P}}V_T\left(ap^{\frac{1}{\alpha_T}}\right) - \mu_{\mathrm{P}}V_{T^{\complement}}\left(E_{TT^{\complement}}\left(ap^{\frac{1}{\alpha_T}}\right)\right)\right),$$

where $a = (C_T/\xi)^{1/\alpha_T}$ and $T^{\complement}$ denotes the complement of T *i.e.* $T^{\complement} = \mathrm{L}$ if $T = \mathrm{N}$ and vice-versa.

Independent transmit power approximation (ITPA): As discussed earlier in this section, R_i for a secondary BS is not independent to the R_i's of its adjacent secondary BSs and the R_i's and T_i's of any two nearby secondary BSs are highly correlated and hence, their transmit powers $P_{\mathrm{S}i}$'s are also correlated. It is very difficult to analyze this correlation and compute the joint distribution of $\{P_{\mathrm{S}k}, k \in I \subset \mathbb{N}\}$. For tractability, we will further approximate the analysis by assuming that R_i and T_i are independent over i, which is a standard assumption in modeling similar association of the interfering mobile transmitters to their respective BSs in uplink analysis [120]. In Section 5.6, we will validate this approximation and show that this approximation provides very close results in comparison with the exact analysis. With this approximation, we can replace $P_{\mathrm{S}i}$ with another random variable ζ_i with the same distribution as $P_{\mathrm{S}i}$ but independent with other ζ_k's ($i \neq k$). The derived PPP such formed from Φ_{S} is denoted by Φ_{IS}. When exact expressions are not possible, we will solve the expressions assuming ITPA. Finally, if $\overline{\zeta_i} = P_{\mathrm{S}i}/\xi$ denotes the independent random variable version of normalized transmit power of ith BS, then $\overline{\zeta_i} = R_i^{\alpha_{T_i}}/C_{T_i}$, which is a random variable independent of ξ.

5.4 Performance Analysis

In this section, we compute the coverage probability of the typical users $\mathrm{UE_S}$ and $\mathrm{UE_P}$. Recall that it is defined as the probability that the SINR at a typical user from its associated BS is above a threshold τ,

$$\mathrm{P^c}(\tau) = \mathbb{P}\left[\mathrm{SINR} > \tau\right]. \tag{5.7}$$

5.4.1 Coverage Probability of the Secondary Operator

From the perspective of $\mathrm{UE_S}$, the secondary BSs can be divided into two independent PPPs: LOS BSs Φ_{SL} and NLOS BSs Φ_{SN} based on the link type $t_{\mathbf{y}_i}$ of each BS. Similarly, the primary BSs are divided into LOS BSs Φ_{PL} and NLOS BSs Φ_{PN}. Recall that we adopt a maximum average received power based association, in which any secondary user will associate with the BS providing highest average received power. Since each BS has a different transmit power $P_{\mathrm{S}i}$, the BS association to the typical user will be affected by this transmit power. Let $\mathcal{L}_I(s)$ denote the Laplace transform of interference I. Now, we give the approximate coverage probability of $\mathrm{UE_S}$ in the following Lemma.

Lemma 9. *The coverage probability of a typical secondary user can be approximated as*

$$\mathrm{P_S^c}(\tau) \approx \mathrm{P_S^{c,app}}(\tau) \tag{5.8}$$

where $\mathrm{P_S^{c,app}}(\tau)$ *is the coverage probability of a typical secondary user under ITPA and is given as*

$$\mathrm{P}_{\mathrm{S}}^{\mathrm{c,app}}(\tau)=\sum_{t_0\in\{\mathrm{L,N}\}}\int_0^{\infty}2\pi\lambda_{\mathrm{S}}K_{t_0}\left(u\right)\exp\left(-\frac{\tau u^{\alpha_{t_0}}}{\xi G_{\mathrm{S1}}}\sigma_{\mathrm{S}}^2\right)\mathcal{L}_{I_{\mathrm{P}}}\left(\frac{\tau u^{\alpha_{t_0}}}{\xi G_{\mathrm{S1}}}\right)\mathcal{L}_{I'_{\mathrm{S}}}\left(\frac{\tau u^{\alpha_{t_0}}}{\xi G_{\mathrm{S1}}}\right)$$
$$\exp\left(-2\pi\lambda_{\mathrm{S}}\int_0^{u^{\alpha_{t_0}/\alpha_{\mathrm{L}}}}K_{\mathrm{L}}\left(z\right)z\mathrm{d}z-2\pi\lambda_{\mathrm{S}}\int_0^{u^{\alpha_{t_0}/\alpha_{\mathrm{N}}}}K_{\mathrm{N}}\left(z\right)z\mathrm{d}z\right)u\mathrm{d}u \quad (5.9)$$

where I_{P} is the interference from the primary BSs, I'_{S} is the interference from the secondary BSs satisfying $u^{-\alpha_{t_{\mathbf{y}0}}}>\overline{\zeta}C_{t_{\mathbf{y}_j}}\mathbf{y}_j^{-\alpha_{t_{\mathbf{y}_j}}}$ with ITPA assumption and $K_t\left(u\right)$ is defined as

$$K_t\left(u\right)=\mathbb{E}_{\overline{\zeta}}\left[p_t\left(u\overline{\zeta}^{\frac{1}{\alpha_t}}C_t^{\frac{1}{\alpha_t}}\right)\overline{\zeta}^{\frac{2}{\alpha_t}}\right]C_t^{\frac{2}{\alpha_t}}. \quad (5.10)$$

Proof. Let Φ be an arbitrary PPP. Now let us assign to each i^{th} secondary BS, a mark $e(\mathbf{y}_i,\Phi)$ as indicator of $\mathbf{y}_i$ being selected as serving BS from Φ and another mark $S(\mathbf{y}_i,\Phi)$ as SINR at SU_0 if BS at $\mathbf{y}_i$ is selected for serving and interferers are from Φ,

$$e(\mathbf{y}_i,\Phi)=\mathbb{1}\left(\frac{P_{\mathrm{S}i}C_{t_{\mathbf{y}_i}}}{\|\mathbf{y}_i\|^{\alpha_{t_{\mathbf{y}_i}}}}>\frac{P_{\mathrm{S}j}C_{t_{\mathbf{y}_j}}}{\|\mathbf{y}_j\|^{\alpha_{t_{\mathbf{y}_j}}}}\forall j,\in\Phi\right),\quad S(\mathbf{y}_i,\Phi)=\frac{G_{\mathrm{S1}}h_{\mathbf{y}_i}P_{\mathrm{S}i}C_{t_{\mathbf{y}_i}}\|\mathbf{y}\|^{-\alpha_{t_{\mathbf{y}_i}}}}{I_{\mathrm{P}}+I_{\mathrm{S}}(\Phi)+\sigma_{\mathrm{S}}^2} \quad (5.11)$$

where $I_{\mathrm{P}}=\sum_{\mathbf{x}_j\in\Phi_{\mathrm{P}}}P_{\mathrm{P}}G_{\mathrm{P}}(\theta_j)h_{\mathbf{x}_j}C_{t_{\mathbf{x}_j}}x_j^{-\alpha_{t_{\mathbf{x}_j}}}$, and $I_{\mathrm{S}}(\Phi)=\sum_{\mathbf{y}_j\in\Phi}P_{\mathrm{S}j}G_{\mathrm{P}}(\omega_j)h_{\mathbf{y}_j}C_{t_{\mathbf{y}_j}}y_j^{-\alpha_{t_{\mathbf{y}_j}}}$.

Using the above two indicators, the coverage probability of UE_{S} can be written as

$$\mathrm{P}_{\mathrm{S}}^{\mathrm{c}}(\tau)=\sum\nolimits_{t_0\in\{\mathrm{L,N}\}}\mathbb{E}\left[\sum\nolimits_{\mathbf{y}_i\in\Phi_{2t_0}}\mathbb{1}(S(\mathbf{y}_i,\Phi_{\mathrm{S}}\setminus\mathbf{y}_i)>\tau,e(\mathbf{y}_i,\Phi_{\mathrm{S}}\setminus\mathbf{y}_i)=1)\right]. \quad (5.12)$$

This is due to the fact that $e(\mathbf{y}_i,\Phi_{\mathrm{S}}\setminus\mathbf{y}_i)$ can be 1 only for one BS that is at $\mathbf{y}_0$, therefore (5.12) will give the coverage probability provided by BS at $\mathbf{y}_0$. (5.12) can

be further written as

$$\begin{aligned}\mathrm{P}_{\mathrm{S}}^{\mathrm{c}}(\tau) &\overset{(a)}{=} \sum\nolimits_{t_0\in\{\mathrm{L,N}\}} \int_0^{\infty} \lambda_{\mathrm{S}} p_{t_0}(\|\mathbf{y}\|)\mathbb{P}^{\mathbf{y}!}\left[S(\mathbf{y},\Phi_{\mathrm{S}})>\tau, e(\mathbf{y},\Phi_{\mathrm{S}})=1\right]\mathrm{d}\mathbf{y} \\ &\overset{(b)}{=} \sum\nolimits_{t_0\in\{\mathrm{L,N}\}} \int_0^{\infty} \lambda_{\mathrm{S}} p_{t_0}(\|\mathbf{y}\|)\mathbb{P}\left[S(\mathbf{y},\Phi'_{\mathrm{S}})>\tau \,\middle|\, e(\mathbf{y},\Phi'_{\mathrm{S}})=1\right]\mathbb{P}\left[e(\mathbf{y},\Phi'_{\mathrm{S}})=1\right]\mathrm{d}\mathbf{y}\end{aligned} \tag{5.13}$$

where (a) is due to the Campbell Mecke theorem and (b) is due to the Slivnyak theorem. Note that Φ'_{S} is the process Φ_{S} conditioned on the value of $P_{\mathrm{S}0}$. This is due to the fact that the secondary BSs transmit powers are not independent to each other and the fact that serving BS power is $P_{\mathrm{S}0}$, will change the distribution of all $P_{\mathrm{S}i}$'s. To clarify this dependence explicitly, we have used the notion Φ'_{S} to denote the process Φ_{S} with modified P_{S} distribution. Due to the dependency, it is difficult to solve (5.13) further. Therefore, we will approximate the $\mathrm{P}_{\mathrm{S}}^{\mathrm{c}}(\tau)$ using ITPA. We will replace $P_{\mathrm{S}i}$'s of each BSs in Φ_{S} with ζ_i's which are independent across secondary BSs, but have the same distribution as $P_{\mathrm{S}i}$'s. Let us denote this new derived PPP as Φ_{IS}. This derived PPP Φ_{IS} is not dependent on the value of $P_{\mathrm{S}0}$ and we can now replace Φ'_{S} with Φ_{IS} in (5.13). This approximation has been used in past for uplink analysis and shown to provide good approximations [120]. The secondary SINR coverage $\mathrm{P}_{\mathrm{S}}^{\mathrm{c,app}}(\tau)$ under the independent transmit power approximation is given as

$$\begin{aligned}&\mathrm{P}_{\mathrm{S}}^{\mathrm{c,app}}(\tau) \\ &= \sum\nolimits_{t_0\in\{\mathrm{L,N}\}} \int_0^{\infty} \lambda_{\mathrm{S}} p_{t_0}(\|\mathbf{y}\|)\mathbb{P}\left[S(\mathbf{y},\Phi_{\mathrm{IS}})>\tau \,\middle|\, e(\mathbf{y},\Phi_{\mathrm{IS}})=1\right]\mathbb{P}\left[e(\mathbf{y},\Phi_{\mathrm{IS}})=1\right]\mathrm{d}\mathbf{y}\end{aligned} \tag{5.14}$$

Now $\mathbb{P}\left[e(\mathbf{y},\Phi_{\mathrm{IS}})=1\right]$ can be computed as

$$\mathbb{P}\left[e(\mathbf{y},\Phi_{\mathrm{IS}})=1\right]$$

$$= \mathbb{P}\left[\mathbb{1}\left(\frac{\zeta_0 C_{t_0}}{y^{\alpha_{t_0}}} > \frac{\zeta_j C_{t_j}}{y_j^{\alpha_{t_j}}}\ \forall \mathbf{y}_j \in \Phi_{\mathrm{IS}}\right)\right] = \mathbb{P}\left[\prod_{\mathbf{y}_j \in \Phi_{\mathrm{IS}}} \mathbb{1}\left(\frac{\zeta_0 C_{t_0}}{y^{\alpha_{t_0}}} > \frac{\zeta_j C_{t_j}}{y_j^{\alpha_{t_j}}}\right)\right]$$

$$\overset{(a)}{=} \prod\nolimits_{t\in\{\mathrm{L},\mathrm{N}\}} \mathbb{P}\left[\prod\nolimits_{\mathbf{y}_j \in \Phi_{\mathrm{IS}t}} \mathbb{1}\left(\zeta_0 C_{t_0}/y^{\alpha_{t_0}} > \zeta_j C_t / y_j^{\alpha_t}\right)\right]$$

$$\overset{(b)}{=} \prod\nolimits_{t\in\{\mathrm{L},\mathrm{N}\}} \exp\left(-2\pi\lambda_{\mathrm{S}} \int_0^\infty \mathbb{E}_\zeta\left[\mathbb{1}\left(\zeta C_t/u^{\alpha_t} > \zeta_0 C_{t_0}/y^{\alpha_{t_0}}\right)\right] p_t(u) u \mathrm{d}u\right)$$

$$\overset{(c)}{=} \prod\nolimits_{t\in\{\mathrm{L},\mathrm{N}\}} \exp\left(-2\pi\lambda_{\mathrm{S}} \int_0^\infty \mathbb{E}_{\overline{\zeta}}\left[\mathbb{1}\left(\overline{\zeta} C_t/u^{\alpha_t} > \overline{\zeta}_0 C_{t_0}/y^{\alpha_{t_0}}\right)\right] p_t(u) u \mathrm{d}u\right)$$

where (a) is due to independence of LOS and NLOS tiers, (b) is from PGFL of PPP and (c) is due to the fact that $\zeta = \overline{\zeta}\xi$. Now using the transformation $u = (\overline{\zeta} C_t)^{\frac{1}{\alpha_t}} z$, we get

$$\begin{aligned}
&\mathbb{P}\left[e(\mathbf{y}, \Phi_{\mathrm{IS}}) = 1\right] \\
&= \prod_{t\in\{\mathrm{L},\mathrm{N}\}} \exp\left(-2\pi\lambda_{\mathrm{S}} \int_0^\infty \mathbb{E}_{\overline{\zeta}}\left[\mathbb{1}\left(\frac{1}{z^{\alpha_t}} > \frac{\overline{\zeta}_0 C_{t_0}}{y^{\alpha_{t_0}}}\right) p_t((\overline{\zeta} C_t)^{\frac{1}{\alpha_t}} z)(\overline{\zeta} C_t)^{\frac{2}{\alpha_t}} z \mathrm{d}z\right]\right) \\
&= \prod_{t\in\{\mathrm{L},\mathrm{N}\}} \exp\left(-2\pi\lambda_{\mathrm{S}} \int_0^{\left(\overline{\zeta}_0 C_{t_0}/y^{\alpha_{t_0}}\right)^{-\frac{1}{\alpha_t}}} K_t(z)\, z \mathrm{d}z\right). \qquad (5.15)
\end{aligned}$$

Using the value from (5.15), (5.13) can be written as

$$\begin{aligned}
\mathrm{P}_{\mathrm{S}}^{\mathrm{c,app}}(\tau) = \sum_{t_0\in\{\mathrm{L},\mathrm{N}\}} \mathbb{E}_{\overline{\zeta}_0}\Bigg[&\int_0^\infty \lambda p_{t_0}(y) \\
&\mathbb{P}\left[\frac{G_{\mathrm{S}1} h_{\mathbf{y}} \overline{\zeta}_0 \xi C_{t_0} y^{-\alpha_{t_0}}}{I_{\mathrm{P}} + I_{\mathrm{S}} + \sigma_{\mathrm{S}}^2} > \tau \middle| \left(\frac{\overline{\zeta}_0 \xi C_{t_0}}{y^{\alpha_{t_0}}} > \frac{\overline{\zeta}_j \xi C_{t_j}}{y^{\alpha_{t_j}}} \forall j \in \Phi_{\mathrm{IS}}\right)\right] \\
&\exp\left(-2\pi\lambda_{\mathrm{S}} \int_0^{\left(\overline{\zeta}_0 C_{t_0}/y^{\alpha_{t_0}}\right)^{-\frac{1}{\alpha_{\mathrm{L}}}}} K_{\mathrm{L}}(z)\, z \mathrm{d}z\right) \\
&\exp\left(-2\pi\lambda_{\mathrm{S}} \int_0^{\left(\overline{\zeta}_0 C_{t_0}/y^{\alpha_{t_0}}\right)^{-\frac{1}{\alpha_{\mathrm{N}}}}} K_{\mathrm{N}}(z)\, z \mathrm{d}z\right) 2\pi y \mathrm{d}y\Bigg].
\end{aligned}$$

Now, substituting $y = u\overline{\zeta_0}^{1/\alpha_{t_0}} C_{t_0}^{1/\alpha_{t_0}}$, we get

$$\begin{aligned}
\mathrm{P}_{\mathrm{S}}^{\mathrm{c,app}}(\tau) = \sum_{t_0 \in \{\mathrm{L},\mathrm{N}\}} \mathbb{E}_{\overline{\zeta_0}} \Bigg[\int_0^{\infty} \lambda p_{t_0}(u\overline{\zeta_0}^{1/\alpha_{t_0}} C_{t_0}^{1/\alpha_{t_0}}) \\
\mathbb{P}\left[\frac{G_{\mathrm{S1}} \xi h_{\mathbf{y}} u^{-\alpha_{t_0}}}{I_{\mathrm{P}} + I_{\mathrm{S}} + \sigma_{\mathrm{S}}^2} > \tau \;\middle|\; \left(u^{\alpha_{t_0}} < \frac{y^{\alpha_{t_j}}}{\overline{\zeta_j} C_{t_j}} \forall j \in \Phi_{\mathrm{IS}} \right) \right] \\
\exp\left(-2\pi\lambda_{\mathrm{S}} \int_0^{u^{\alpha_{t_0}/\alpha_{\mathrm{L}}}} K_{\mathrm{L}}(z)\, z \mathrm{d}z \right) \\
\exp\left(-2\pi\lambda_{\mathrm{S}} \int_0^{u^{\alpha_{t_0}/\alpha_{\mathrm{N}}}} K_{\mathrm{N}}(z)\, z \mathrm{d}z \right) \overline{\zeta_0}^{2/\alpha_{t_0}} {C_{\mathrm{L}}}^{2/\alpha_{t_0}} 2\pi u \mathrm{d}u \Bigg]
\end{aligned}$$

which can be further simplified by moving the expectation inside as

$$\begin{aligned}
\mathrm{P}_{\mathrm{S}}^{\mathrm{c,app}}(\tau) = \sum_{t_0 \in \{\mathrm{L},\mathrm{N}\}} \int_0^{\infty} 2\pi\lambda_{\mathrm{S}} \mathbb{E}_{\overline{\zeta_0}} \left[p_{t_0}(u\overline{\zeta_0}^{1/\alpha_{t_0}} C_{t_0}^{1/\alpha_{t_0}}) \overline{\zeta_0}^{2/\alpha_{t_0}} \right] \mathbb{P}\left[\frac{G_{\mathrm{S1}} \xi h_{\mathbf{y}} u^{-\alpha_{t_0}}}{I_{\mathrm{P}} + I'_{\mathrm{S}} + \sigma_{\mathrm{S}}^2} > \tau \right] \\
\exp\left(-2\pi\lambda_{\mathrm{S}} \int_0^{u^{\alpha_{t_0}/\alpha_{\mathrm{L}}}} K_{\mathrm{L}}(z)\, z \mathrm{d}z \right) \exp\left(-2\pi\lambda_{\mathrm{S}} \int_0^{u^{\alpha_{t_0}/\alpha_{\mathrm{N}}}} K_{\mathrm{N}}(z)\, z \mathrm{d}z \right) {C_{\mathrm{L}}}^{2/\alpha_{t_0}} u \mathrm{d}u
\end{aligned} \tag{5.16}$$

where I'_{S} is interference from the conditioned secondary PPP. Using the MGF of $h_{\mathbf{y}}$, the inner SINR probability term can be written as

$$\mathbb{P}\left[\frac{G_{\mathrm{S1}} h_{\mathbf{y}} \xi u^{-\alpha_{t_0}}}{I_{\mathrm{P}} + I'_{\mathrm{S}} + \sigma_{\mathrm{S}}^2} > \tau \right] = \exp\left(-\frac{\tau u^{\alpha_{t_0}}}{\xi G_{\mathrm{S1}}} \sigma_{\mathrm{S}}^2 \right) \mathcal{L}_{I_{\mathrm{P}}}\left(\frac{\tau u^{\alpha_{t_0}}}{\xi G_{\mathrm{S1}}} \right) \mathcal{L}_{I'_{\mathrm{S}}}\left(\frac{\tau u^{\alpha_{t_0}}}{\xi G_{\mathrm{S1}}} \right) \tag{5.17}$$

Using the definition of $K_t(z)$ and substituting (5.17) in (5.16), we get the Lemma. □

This result is interesting because the distribution of the secondary transmit power P_{S} is decoupled from most of the terms, which noticeably simplifies the final expressions. As seen from (5.3), the term P_{S} is present in the association rule, serving power, and the interference. In Lemma 9, this dependency of the coverage probability

on P_{S} is reduced to only one function $K_t(\cdot)$ (see the above proof for the techniques used), making the whole integral easily computable, which is a key analytical contribution of the chapter. Now, we derive the Laplace transforms of I_{P} and I'_{S} which are given in the following Lemmas.

Lemma 10. *The Laplace transform of the interference I'_{S} from the derived secondary network Φ_{IS} is given as*

$$\mathcal{L}_{I'_{\mathrm{S}}}(s) = \exp\left(-\lambda_{\mathrm{S}} \sum_{k=1}^{2} a_k F_{\mathrm{S}}(s\xi G_{\mathrm{S}k}, u^{\alpha_{t_0}})\right) \tag{5.18}$$

where $a_1 = \theta_{\mathrm{Sb}}/(2\pi),\ a_2 = 1 - a_1$ *and* $F_{\mathrm{S}}(B, e) = 2\pi \sum_{t\in\{\mathrm{L},\mathrm{N}\}} \int_{e^{\frac{1}{\alpha_t}}}^{\infty} \frac{K_t(v)}{1 + B^{-1} v^{\alpha_t}} v \mathrm{d}v.$

Proof. The interference from the derived conditional secondary PPP is given as

$$I'_{\mathrm{S}} = \sum_{\mathbf{y}_i \in \Phi_{\mathrm{IS}}} h_{\mathbf{y}_i} \mathbb{1}\left(\frac{y_i^{\alpha_{t_{\mathbf{y}_i}}}}{\overline{\zeta_i} C_{t_{\mathbf{y}_i}}} > u^{\alpha_{t_0}}\right) \xi \overline{\zeta_i} C_{t_{\mathbf{y}_i}} y_i^{-\alpha_{t_{\mathbf{y}_i}}} G_{\mathrm{S}}(\theta_i).$$

Therefore, the Laplace transform of I'_{S} can be expressed as

$$\mathcal{L}_{I'_{\mathrm{S}}}(s) = \mathbb{E}\left[\exp\left(-s \sum_{\mathbf{y}_i \in \Phi_{\mathrm{IS}}} h_{\mathbf{y}_i} \mathbb{1}\left(\frac{y_i^{\alpha_{t_{\mathbf{y}_i}}}}{\overline{\zeta_i} C_{t_{\mathbf{y}_i}}} > u^{\alpha_{t_0}}\right) \xi \overline{\zeta_i} C_{t_{\mathbf{y}_i}} y_i^{-\alpha_{t_{\mathbf{y}_i}}} G_{\mathrm{S}}(\theta_i)\right)\right] \tag{5.19}$$

Note that ζ_i terms in (5.19) are independent marks.

I'_{S} can be split into interference from LOS and NLOS BSs in Φ_{S} as $I'_{\mathrm{S}} = I'_{\mathrm{SL}} + I'_{\mathrm{SN}}$. Hence, the Laplace transform of I'_{S} can be expressed as product of Laplace transforms of I'_{SL} and I'_{SN}. Now, the Laplace transform of I'_{SL} is given as

$$\mathcal{L}_{I'_{\mathrm{SL}}}(s) = \mathbb{E}\left[\exp\left(-s \sum_{\mathbf{y}_i \in \Phi_{\mathrm{SL}}} h_{\mathbf{y}_i} \mathbb{1}\left(\frac{y_i^{\alpha_{\mathrm{L}}}}{\overline{\zeta_i} C_{\mathrm{L}}} > u^{\alpha_{t_0}}\right) \xi \overline{\zeta_i} C_{\mathrm{L}} y_i^{-\alpha_{\mathrm{L}}} G_{\mathrm{S}}(\theta_i)\right)\right] \tag{5.20}$$

$$\overset{(a)}{=} \exp\left(-\lambda_{\mathrm{S}} 2\pi \mathbb{E}_{P_{\mathrm{S}},\theta}\left[\int_0^{\infty}\left(1-e^{-sh_{\mathbf{y}}\xi\bar{\zeta}C_{\mathrm{L}}y^{-\alpha_{\mathrm{L}}}G_{\mathrm{S}}(\theta)}\right)\mathbb{1}\left(\frac{y^{\alpha_{\mathrm{L}}}}{\bar{\zeta}C_{\mathrm{L}}}>u^{\alpha_{t_0}}\right)p_{\mathrm{L}}(y)y\mathrm{d}y\right]\right) \tag{5.21}$$

where (a) is due to PGFL of the PPP. Now using the transformation $y = v(\bar{\zeta}C_{\mathrm{L}})^{1/\alpha_{\mathrm{L}}}$, we get

$$\mathcal{L}_{I'_{\mathrm{SL}}}(s) = \exp\left(-\lambda_{\mathrm{S}} 2\pi \mathbb{E}_{P_{\mathrm{S}},\theta}\left[\int_0^{\infty}\left(1-e^{-sh_{\mathbf{y}}\xi v^{-\alpha_{\mathrm{L}}}G_{\mathrm{S}}(\theta)}\right)\right.\right.$$
$$\left.\left.\mathbb{1}\left(v^{\alpha_{\mathrm{L}}}>u^{\alpha_{t_0}}\right)p_{\mathrm{L}}(v(\bar{\zeta}C_{\mathrm{L}})^{\frac{1}{\alpha_{\mathrm{L}}}})(\bar{\zeta}C_{\mathrm{L}})^{\frac{2}{\alpha_{\mathrm{L}}}}v\mathrm{d}v\right]\right).$$

Now moving the expectation with respect to θ and $\bar{\zeta}$ inside the integration, we get

$$\mathcal{L}_{I'_{\mathrm{SL}}}(s) = \exp\left(-\lambda_{\mathrm{S}} 2\pi \int_{u^{\frac{\alpha_{t_0}}{\alpha_{\mathrm{L}}}}}^{\infty} \mathbb{E}_{\theta}\left[1-e^{-sh_{\mathbf{y}}\xi v^{-\alpha_{\mathrm{L}}}G_{\mathrm{S}}(\theta)}\right]K_{\mathrm{L}}(v)\,v\mathrm{d}v\right). \tag{5.22}$$

Now, using definition of a_k's, the inner term can be written as

$$1-\mathbb{E}\left[\exp\left(-sh_{\mathbf{y}}\xi v^{-\alpha_{\mathrm{L}}}G_{\mathrm{S}}(\theta)\right)\right] = \mathbb{E}\left[\frac{s\xi v^{-\alpha_{\mathrm{L}}}G_{\mathrm{S}}(\theta)}{1+s\xi v^{-\alpha_{\mathrm{L}}}G_{\mathrm{S}}(\theta)}\right] = \sum_{k=1}^{2}\frac{a_k}{1+\xi^{-1}s^{-1}G_{\mathrm{S}k}^{-1}v^{\alpha_{\mathrm{L}}}}. \tag{5.23}$$

Using (5.23) in (5.22), we get

$$\mathcal{L}_{I_{\mathrm{SL}}}(s) = \exp\left(-\lambda_{\mathrm{S}} 2\pi \int_{u^{\frac{\alpha_{t_0}}{\alpha_{\mathrm{L}}}}}^{\infty} \sum_{k=1}^{2}\frac{a_k}{1+\xi^{-1}s^{-1}G_{\mathrm{S}k}^{-1}v^{\alpha_{\mathrm{L}}}}K_{\mathrm{L}}(v)\,v\mathrm{d}v\right).$$

Similarly $\mathcal{L}_{I'_{\mathrm{SN}}}(s)$ can be computed. Multiplying the values of $\mathcal{L}_{I'_{\mathrm{SL}}}(s)$ and $\mathcal{L}_{I'_{\mathrm{SN}}}(s)$ and using the definition of $F_{\mathrm{S}}(B,e)$, we get the Lemma. □

Lemma 11. *The Laplace transform of the interference I_{P} from the primary network is given as*

$$\mathcal{L}_{I_{\mathrm{P}}}(s) = \exp\left(-\lambda_{\mathrm{P}}\sum_{k=1}^{2} b_k F_{\mathrm{P}}(sG_{\mathrm{P}k})\right) \tag{5.24}$$

where $b_1 = \theta_{\mathrm{Pb}}/(2\pi), b_2 = 1 - b_1$,

$$F_{\mathrm{P}}(B) = 2\pi \sum_{t\in\{\mathrm{L},\mathrm{N}\}} \int_0^\infty \frac{M_t\left(u\right)}{1 + B^{-1}v^{\alpha_t}} v\mathrm{d}v, \text{ and } \quad M_t\left(u\right) = p_t\left(uP_{\mathrm{P}}^{\frac{1}{\alpha_t}} C_t^{\frac{1}{\alpha_t}}\right) P_{\mathrm{P}}^{\frac{2}{\alpha_t}} C_{\mathrm{L}}^{\frac{2}{\alpha_t}}.$$

Proof. The primary interference is given as $I_{\mathrm{P}} = \sum_{\mathbf{x}_i\in\Phi_{\mathrm{P}}} h_{\mathbf{x}_i} P_{\mathrm{P}} C_{t_{\mathbf{x}_i}} x_i^{-\alpha_{t_{\mathbf{x}_i}}} G_{\mathrm{P}}(\theta_i)$. Similar to the proof of Lemma 10, $\mathcal{L}_{I_{\mathrm{P}}}(s) = \mathcal{L}_{I_{\mathrm{PL}}}(s)\mathcal{L}_{I_{\mathrm{PN}}}(s)$. Using the PPP's PGFL, $\mathcal{L}_{I_{\mathrm{PL}}}(s)$ can be computed as

$$\mathcal{L}_{I_{\mathrm{PL}}}(s) = \exp\left(-\lambda_{\mathrm{P}} 2\pi \mathbb{E}_\theta\left[\int_0^\infty \left(1 - e^{-sh_{\mathbf{x}_i} P_{\mathrm{P}} C_{\mathrm{L}} x^{-\alpha_{\mathrm{L}}} G_{\mathrm{P}}(\theta)}\right) p_{\mathrm{L}}(x) x\mathrm{d}x\right]\right).$$

Now using the transformation $x = v(P_{\mathrm{P}}C_{\mathrm{L}})^{1/\alpha_{\mathrm{L}}}$, we get $\mathcal{L}_{I_{\mathrm{PL}}}(s)$

$$= \exp\left(-\lambda_{\mathrm{P}} 2\pi \mathbb{E}_{P_{\mathrm{S}},\theta}\left[\int_0^\infty \left(1 - e^{-sh_{\mathbf{x}_i} v^{-\alpha_{\mathrm{L}}} G_{\mathrm{P}}(\theta)}\right) p_{\mathrm{L}}(v(P_{\mathrm{P}i}C_{\mathrm{L}})^{\frac{1}{\alpha_{\mathrm{L}}}})(P_{\mathrm{P}}C_{\mathrm{L}})^{\frac{2}{\alpha_{\mathrm{L}}}} v\mathrm{d}v\right]\right).$$

Now, interchanging the order of expectation and integration and using $M_t\left(\cdot\right)$'s definition, we get

$$\mathcal{L}_{I_{\mathrm{PL}}}(s) = \exp\left(-\lambda_{\mathrm{P}} 2\pi \int_0^\infty \mathbb{E}_\theta\left[1 - e^{-sh_{\mathbf{x}} v^{-\alpha_{\mathrm{L}}} G_{\mathrm{P}}(\theta)}\right] M_{\mathrm{L}}\left(v\right) v\mathrm{d}v\right). \tag{5.25}$$

Now, using definition of b_k's, the inner term can be written as

$$1 - \mathbb{E}\left[\exp\left(-sh_{\mathbf{x}} v^{-\alpha_{\mathrm{L}}} G_{\mathrm{P}}(\theta)\right)\right] = \mathbb{E}\left[\frac{sv^{-\alpha_{\mathrm{L}}} G_{\mathrm{P}}(\theta)}{1 + sv^{-\alpha_{\mathrm{L}}} G_{\mathrm{P}}(\theta)}\right] = \sum_{k=1}^{2} \frac{b_k}{1 + s^{-1} G_{\mathrm{P}k}^{-1} v^{\alpha_{\mathrm{L}}}}. \tag{5.26}$$

Using (5.26) in (5.25), we get

$$\mathcal{L}_{I_{\mathrm{PL}}}(s) = \exp\left(-\lambda_{\mathrm{S}} 2\pi \int_0^\infty \sum_{k=1}^{2} \frac{b_k}{1 + s^{-1} G_{\mathrm{P}k}^{-1} v^{\alpha_{\mathrm{L}}}} M_{\mathrm{L}}\left(v\right) v\mathrm{d}v\right).$$

Similarly $\mathcal{L}_{I_{\mathrm{PN}}}(s)$ can be computed. Using the values of $\mathcal{L}_{I_{\mathrm{PL}}}(s)$ and $\mathcal{L}_{I_{\mathrm{PN}}}(s)$ and the definition of $F_{\mathrm{P}}(B)$, we get the Lemma. □

Now, substituting the Laplace transform of the primary and secondary interference at the $\mathrm{UE_S}$ in Lemma 9, we can compute the final expression of the coverage probability, which we give in the following theorem. [1]

Theorem 11. *The coverage probability of a typical user of the secondary operator in a mmWave system with restricted secondary licensing can be approximated using ITPA assumption as*

$$\begin{aligned}
&\mathrm{P}_{\mathrm{S}}^{\mathrm{c}}(\tau) \approx \mathrm{P}_{\mathrm{S}}^{\mathrm{c,app}}(\tau) \\
&= \sum_{t_0 \in \{\mathrm{L,N}\}} \int_0^{\infty} 2\pi\lambda_{\mathrm{S}} \exp\left[-\lambda_{\mathrm{P}} \sum_{k=1}^{2} b_k F_{\mathrm{P}}\left(\frac{\tau u^{\alpha_{t_0}} G_{\mathrm{P}k}}{\xi G_{\mathrm{S1}}} \right) - \lambda_{\mathrm{S}} \sum_{k=1}^{2} a_k F_{\mathrm{S}}\left(\frac{\tau u^{\alpha_{t_0}} G_{\mathrm{S}k}}{G_{\mathrm{S1}}}, u^{\alpha_{t_0}} \right) \right. \\
&\left. - \frac{\tau u^{\alpha_{t_0}}}{\xi G_{\mathrm{S1}}} \sigma_{\mathrm{S}}^2 - 2\pi\lambda_{\mathrm{S}} \int_0^{u^{\alpha_{t_0}/\alpha_{\mathrm{L}}}} K_{\mathrm{L}}(z)\, z \mathrm{d}z - 2\pi\lambda_{\mathrm{S}} \int_0^{u^{\alpha_{t_0}/\alpha_{\mathrm{N}}}} K_{\mathrm{N}}(z)\, z \mathrm{d}z \right] K_{t_0}(u) u \mathrm{d}u.
\end{aligned} \tag{5.27}$$

Since the expression in Theorem 11 is complicated, we consider the following three special cases to give simple and closed form expressions.

Special Cases:

(i) Consider a mmWave network with identical parameters for LOS and NLOS channels (which is also the typical assumption for a UHF system). For this case, we can combine the LOS and NLOS PPPs in to a single PPP of type t for which $K_t(u)$ is given as

$$K_t(u) = \mathbb{E}_{\bar{\zeta}}\left[\bar{\zeta}^{\frac{2}{\alpha}} \right] C^{\frac{2}{\alpha}} = \mathbb{E}\left[R^2 \right] = (\mu_{\mathrm{P}}\pi)^{-1}, \tag{5.28}$$

[1] Note that Theorem 11 as well as Theorem 12 is an approximate expression due to the fact that the transmit powers of secondary BSs are assumed to be independent to each other in the derivation. We have commented on the accuracy of this approximation in Section 5.6.

which is no longer a function of u. Let us denote this constant by K. Similarly, $M_t(u)$ can be simplified as $M_t(u) = P_{\mathrm{P}}^{\frac{2}{\alpha}} C^{\frac{2}{\alpha}}$, which is no longer a function of u and hence can be denoted by M. Therefore, $F_{\mathrm{S}}(B,e)$ and $F_{\mathrm{P}}(B/\xi)$ can be simplified as follows:

$$F_{\mathrm{S}}(B,e) = K\int_{(e)^{\frac{1}{\alpha}}}^{\infty} \frac{1}{1+(B)^{-1}v^{\alpha}} 2\pi v \mathrm{d}v = KB^{\frac{2}{\alpha}} \int_{(e/B)^{\frac{1}{\alpha}}}^{\infty} \frac{1}{1+v^{\alpha}} 2\pi v \mathrm{d}v,$$
$$F_{\mathrm{P}}(B/\xi) = \int_0^{\infty} \frac{2\pi P_{\mathrm{P}}^{\frac{2}{\alpha}} C_t^{\frac{2}{\alpha}}}{1+\xi B^{-1} v^{\alpha}} v \mathrm{d}v = (\xi B^{-1})^{-\frac{2}{\alpha}} \int_0^{\infty} \frac{2\pi P_{\mathrm{P}}^{\frac{2}{\alpha}} C^{\frac{2}{\alpha}}}{1+v^{\alpha}} v \mathrm{d}v.$$

Now, Let us define $\rho(\alpha,\tau) = \int_{\tau^{-1/\alpha}}^{\infty} \frac{1}{1+v^{\alpha}} 2v\mathrm{d}v$ and $\rho(\alpha) = \rho(\alpha,\infty)$, then
$F_{\mathrm{S}}(B,e) = \pi K B^{\frac{2}{\alpha}} \rho(\alpha, B/e) \Rightarrow$
$$F_{\mathrm{S}}\left(\frac{\tau u^{\alpha}}{G_{\mathrm{S1}}} G_{\mathrm{S}k}, u^{\alpha}\right) = \pi K \tau^{\frac{2}{\alpha}} u^2 \left(\frac{G_{\mathrm{S}k}}{G_{\mathrm{S1}}}\right)^{\frac{2}{\alpha}} \rho\left(\alpha, \frac{\tau G_{\mathrm{S}k}}{G_{\mathrm{S1}}}\right),$$
$$F_{\mathrm{P}}\left(\frac{B}{\xi}\right) = \pi \left(\frac{B P_{\mathrm{P}} C}{\xi}\right)^{\frac{2}{\alpha}} \rho(\alpha) \Rightarrow F_{\mathrm{P}}\left(\frac{\tau u^{\alpha} G_{\mathrm{P}k}}{\xi G_{\mathrm{S1}}}\right) = \pi \left(\frac{P_{\mathrm{P}} \tau C}{\xi} \frac{G_{\mathrm{P}k}}{G_{\mathrm{S1}}}\right)^{\frac{2}{\alpha}} u^2 \rho(\alpha).$$

Let us define

$$F_{\mathrm{P}}'' = \sum_{k=1}^{2} b_k \left(\frac{G_{\mathrm{P}k}}{G_{\mathrm{S1}}}\right)^{\frac{2}{\alpha}} \rho(\alpha)$$

and

$$F_{\mathrm{S}}''(\tau) = \sum_{k=1}^{2} a_k \left(\frac{G_{\mathrm{S}k}}{G_{\mathrm{S1}}}\right)^{\frac{2}{\alpha}} \rho\left(\alpha, \frac{\tau G_{\mathrm{S}k}}{G_{\mathrm{S1}}}\right)$$

. Then, the approximate coverage probability is given as

$$\mathrm{P}_{\mathrm{S}}^{\mathrm{c,app}}(\tau) = 2\pi\lambda_{\mathrm{S}} K \int_0^{\infty} e^{-\frac{\tau\sigma_{\mathrm{S}}^2}{\xi G_{\mathrm{S1}}} u^{\alpha} - u^2 \left(\pi\lambda_{\mathrm{P}} \xi^{-\frac{2}{\alpha}} \tau^{\frac{2}{\alpha}} (P_{\mathrm{P}} C)^{\frac{2}{\alpha}} F_{\mathrm{P}}'' + \pi\lambda_{\mathrm{S}} K \tau^{\frac{2}{\alpha}} F_{\mathrm{S}}''(\tau) + \pi\lambda_{\mathrm{S}} K\right)} u \mathrm{d}u.$$

(ii) Consider a mmWave system with identical LOS and NLOS channels in the interference limited scenario. In this case, the coverage probability is given as

$$\mathrm{P}_{\mathrm{S}}^{\mathrm{c}}(\tau) \approx$$

$$\left[1+\tau^{\frac{2}{\alpha}}\left(\frac{\lambda_{\mathrm{P}}}{\xi^{\frac{2}{\alpha}}\lambda_{\mathrm{S}}}\frac{(P_{\mathrm{P}}C)^{\frac{2}{\alpha}}}{(\mu_{\mathrm{P}}\pi)^{-1}}\sum_{k=1}^{2}b_k\left(\frac{G_{\mathrm{P}k}}{G_{\mathrm{S1}}}\right)^{\frac{2}{\alpha}}\rho(\alpha)+\sum_{k=1}^{2}a_k\left(\frac{G_{\mathrm{S}k}}{G_{\mathrm{S1}}}\right)^{\frac{2}{\alpha}}\rho\left(\alpha,\frac{\tau G_{\mathrm{S}k}}{G_{\mathrm{S1}}}\right)\right)\right]^{-1} \tag{5.29}$$

Impact of secondary densification and ξ: We can see from the result in (5.29) that $\mathrm{P}_{\mathrm{S}}^{\mathrm{c}}(\tau)$ is invariant if the term $\xi\lambda_{\mathrm{S}}^{\alpha/2}$ is kept constant. This is due to the following observation: if we increase the secondary BS density λ_{S} by a factor of a, the distance of the secondary BSs decreases by a factor of $\sqrt{a}$ and therefore, the secondary interference increases by the factor of $a^{\alpha/2}$, and if we increase the interference limit ξ by a, the secondary interference also increases by a. Therefore, densifying the secondary network while reducing its interference threshold by the appropriate ratio keeps the coverage probability constant.

Impact of narrowing secondary antenna: If we assume that the secondary antennas are uniform linear arrays of N_{S} antennas, then a_k's and $G_{\mathrm{S}k}$'s can be approximated as [121]

$$a_1=\frac{\kappa}{N_{\mathrm{S}}}, G_{\mathrm{S1}}=N_{\mathrm{S}}, a_2=1-\frac{\kappa}{N_{\mathrm{S}}}, \text{ and } G_{\mathrm{S2}}=\frac{(1-\kappa)N_{\mathrm{S}}}{N_{\mathrm{S}}-\kappa}(\approx 1-\kappa \text{ for large } N_{\mathrm{S}})$$

where κ is some constant. Now, the term denoting primary interference decreases as $\frac{\kappa}{N_{\mathrm{S}}^{2/\alpha}}$ and the term denoting the secondary interference decreases as $\frac{\kappa}{N}\rho(\alpha,\tau)+\left(\frac{1-\kappa}{N_{\mathrm{S}}}\right)^{2/\alpha}\rho\left(\alpha,\tau\frac{1-\kappa}{N_{\mathrm{S}}}\right)$. Therefore, narrowing the secondary antennas beamwidth noticeably improves the secondary performance.

Impact of narrowing primary antenna: With a similar assumption for the primary BSs to have uniform linear arrays of N_{P} antennas, b_k's and $G_{\mathrm{P}k}$'s can

be approximated as $b_1 = \frac{\kappa}{N_{\mathrm{P}}}, G_{\mathrm{P1}} = N_{\mathrm{P}}, b_2 = 1 - \frac{\kappa}{N_{\mathrm{P}}}$, and $G_{\mathrm{P2}} = \frac{(1-\kappa)N_{\mathrm{P}}}{N_{\mathrm{P}}-\kappa} (\approx 1-\kappa$ for large N). Now, the term denoting the primary interference decreases as $\frac{\kappa}{N_{\mathrm{P}}^{1-2/\alpha}} + (1-\kappa)^{2/\alpha}$ while the term denoting the secondary interference remains constant. Therefore, narrowing the primary beamwidth slightly improves the secondary performance. For high value of ξ where the secondary interference dominates, the secondary performance does not improve by narrowing the primary antennas.

(iii) Suppose that both operators have the same beam patterns with zero side-lobe gain. In this case, the coverage probability can be simplified to a closed form expression:

$$\mathrm{P}_{\mathrm{S}}^{\mathrm{c}}(\tau) = \left[1 + \frac{\theta_b}{2\pi}\tau^{2/\alpha}\left(\frac{\lambda_{\mathrm{P}}}{\lambda_{\mathrm{S}}}\xi^{-\frac{2}{\alpha}}\frac{P_{\mathrm{P}}^{\frac{2}{\alpha}}\rho(\alpha)}{(\mu_{\mathrm{P}}\pi C^{\frac{2}{\alpha}})^{-1}} + \rho(\alpha,\tau)\right)\right]^{-1}$$

which, for $\alpha = 4$, becomes

$$\mathrm{P}_{\mathrm{S}}^{\mathrm{c}}(\tau) = \left[1 + \frac{\theta_b\sqrt{\tau}}{2\pi}\left(\frac{1}{\sqrt{\xi}}\frac{\lambda_{\mathrm{P}}}{\lambda_{\mathrm{S}}}\frac{\sqrt{CP_{\mathrm{P}}}}{(\mu_{\mathrm{P}})^{-1}}\frac{\pi^2}{2} + \tan^{-1}(\sqrt{\tau})\right)\right]^{-1}.$$

5.4.2 Coverage Probability of the Primary Operator

Similar to the secondary case, for $\mathrm{UE_P}$ also, all the primary and secondary BSs can be divided into two independent LOS and NLOS PPPs based on the link type between each BS and $\mathrm{UE_P}$. Recall that we have assumed maximum average received power based association, in which any primary user will associate with the BS $\mathbf{x}_0$ providing highest average received power. We, now compute the coverage probability of the typical primary user which is given in Lemma 12.

Lemma 12. *The coverage probability of the primary operator is given as*

$$P_{\mathrm{P}}^{\mathrm{c}}(\tau) = \sum_{t_0 \in \{\mathrm{L},\mathrm{N}\}} \int_0^{\infty} 2\pi\lambda_{\mathrm{P}} M_{t_0}(u) \exp\left(-\frac{\tau u^{\alpha_{t_0}}}{G_{\mathrm{P1}}}\sigma_{\mathrm{P}}^2\right) \mathcal{L}_{I'_{\mathrm{P}}}\left(\frac{\tau u^{\alpha_{t_0}}}{G_{\mathrm{P1}}}\right) \mathcal{L}_{I_{\mathrm{S}}}\left(\frac{\tau u^{\alpha_{t_0}}}{G_{\mathrm{P1}}}\right)$$
$$\exp\left(-2\pi\lambda_{\mathrm{P}} \int_0^{u^{\alpha_{t_0}/\alpha_{\mathrm{L}}}} M_{\mathrm{L}}(z)\, z\mathrm{d}z - 2\pi\lambda_{\mathrm{P}} \int_0^{u^{\alpha_{t_0}/\alpha_{\mathrm{N}}}} M_{\mathrm{N}}(z)\, z\mathrm{d}z\right) u\mathrm{d}u \quad (5.30)$$

where I'_{P} is the interference from the primary operator conditioned on the fact that the serving BS is at $\mathbf{x}_0$ and I'_{S} is the interference from the secondary operator.

Proof. The proof is similar to the proof of Lemma 9. The only difference is that the computations for the primary and secondary operators are interchanged and there will not be any expectation with respect to the transmit power of the primary BSs as the primary transmit power is deterministic. We also do not need to approximate Φ_{S} with Φ_{IS} to get this Lemma. □

We now compute the Laplace transforms of the primary and secondary interference which is given in the following two Lemmas.

Lemma 13. *The Laplace transform of the interference I'_{P} from the conditioned primary network is given as*

$$\mathcal{L}_{I'_{\mathrm{P}}}(s) = \exp\left(-\lambda_{\mathrm{P}} \sum_{k=1}^{2} b_k E_{\mathrm{P}}(sG_{\mathrm{P}k}, u^{\alpha_{t_0}})\right) \quad (5.31)$$

where $E_{\mathrm{P}}(B,e)$ is given as: $E_{\mathrm{P}}(B,e) = B^{\frac{2}{\alpha_t}} \sum_{t\in\{\mathrm{L},\mathrm{N}\}} \int_{(e/B)^{\frac{1}{\alpha_t}}}^{\infty} \frac{1}{1+v^{\alpha_t}} M_t\left(vB^{\frac{2}{\alpha_t}}\right) 2\pi v\mathrm{d}v.$

Proof. The proof is similar to the proof of Lemma 10 with only difference being lack of any expectation with respect to the primary BSs' transmit powers. □

The following Lemma gives the approximate Laplace transform of the interference from the secondary operator where functions $E_{\mathcal{F}\mathrm{S}}$ and $E_{\mathcal{N}\mathrm{S}}$ are due to $I_{\mathcal{F}\mathrm{S}}$ and $I_{\mathcal{N}\mathrm{S}}$ respectively.

Lemma 14. *The Laplace transform of the interference from the secondary network can be approximated as*

$$\mathcal{L}_{I_{\mathrm{S}}}(s) \approx \mathcal{L}_{I_{\mathrm{app,S}}}(s). \tag{5.32}$$

Here, $\mathcal{L}_{I_{\mathrm{app,S}}}(s)$ is the Laplace transform of the interference under the ITPA assumption and is given as

$$\mathcal{L}_{I_{\mathrm{app,S}}}(s) = \exp\left(-\lambda_{\mathrm{S}} \sum_{k=1}^{2} a_k \left(E_{\mathcal{F}\mathrm{S}}\left(sG_{\mathrm{S}k}, \xi\right) + E_{\mathcal{N}\mathrm{S}}(sG_{\mathrm{S}k})\right)\right), \tag{5.33}$$

where $E_{\mathcal{F}\mathrm{S}}(B,\xi)$ and $E_{\mathcal{N}\mathrm{S}}(B)$ are given as

$$E_{\mathcal{F}\mathrm{S}}(B,\xi) = (B\xi)^{\frac{2}{\alpha_t}} \sum_{t\in\{\mathrm{L,N}\}} \int_{(\xi B)^{-\frac{1}{\alpha_t}}}^{\infty} \frac{K_t\left(v(B\xi)^{\frac{1}{\alpha_t}}\right)}{1+v^{\alpha_t}} 2\pi v \mathrm{d}v \tag{5.34}$$

$$E_{\mathcal{N}\mathrm{S}}(B) = \frac{1}{1+(B\xi)^{-1}} \int_0^1 \left(K_{\mathrm{L}}(v) + K_{\mathrm{N}}(v)\right) 2\pi v \mathrm{d}v. \tag{5.35}$$

Proof. The secondary interference is given as

$$I_{\mathrm{S}}(s) = \sum_{t\in\{\mathrm{L,N}\}} \sum_{\mathbf{y}_i\in\Phi_{\mathrm{S}t}} g_{\mathbf{y}_i} P_{\mathrm{S}i} C_t y_i^{-\alpha_t} G_{\mathrm{S}}(\theta_i) \tag{5.36}$$

We first note that the transmit powers of secondary BS are correlated which makes the expression intractable. Therefore, we will replace Φ_{S} with Φ_{IS} to approximate the above expression as

$$I_{\mathrm{S}}(s) \approx I_{\mathrm{app,S}}(s) = \sum_{t\in\{\mathrm{L,N}\}} \sum_{\mathbf{y}_i\in\Phi_{\mathrm{IS}t}} g_{\mathbf{y}_i} \zeta_i C_t y_i^{-\alpha_t} G_{\mathrm{S}}(\theta_i) \tag{5.37}$$

Now, note that the transmit power of each secondary BS is correlated with the location of the typical primary user. Since we have conditioned on the location of this typical user, the distribution of ζ may change. Including the exact correlation among these is difficult and it may make analysis intractable. Therefore, in this analysis, we model this correlation by truncating the distribution of ζ for the BSs in native $\mathcal{N}_0$ and for those who are not in this set. In Section 5.6, we will validate this approximation with other approximations.

The approximate secondary interference $I_{\text{app,S}}$ can be written as sum of following two interferences: the interference $I_{\mathcal{F}\text{S}}$ from the BSs that are not in native set $\mathcal{N}_0$ and interference $I_{\mathcal{N}\text{S}}$ from the BSs that are in $\mathcal{N}_0$. Let us first consider $I_{\mathcal{F}\text{S}}$ which is given as

$$I_{\mathcal{F}\text{S}}(s) = \sum_{t\in\{\text{L,N}\}} \sum_{\mathbf{y}_i\in\Phi_{\text{S}t}} g_{\mathbf{y}_i} \mathbb{1}\left(C_{T_i} R_i^{-\alpha_{T_i}} > C_t y_i^{-\alpha_t}\right) \xi\overline{\zeta_i} C_t y_i^{-\alpha_t} G_{\text{S}}(\theta_i) \tag{5.38}$$

where the indicator term denotes that only those secondary BSs are considered whose receiver power at the their home primary user is greater than their received power at UE_P which means that UE_P is not the home primary user for these BSs. Now its Laplace transform is equal to

$$\begin{aligned}\mathcal{L}_{I_{\mathcal{F}\text{S}}}(s) &\overset{(a)}{=} \prod_{t\in\{\text{L,N}\}} \mathbb{E}\left[\exp\left(-s \sum_{\mathbf{y}_i\in\Phi_{\text{S}t}} g_{\mathbf{y}_i} \mathbb{1}\left(1/\overline{\zeta} > C_t y_i^{-\alpha_t}\right) \xi\overline{\zeta_i} C_t y_i^{-\alpha_t} G_{\text{S}}(\theta_i)\right)\right] \\ &\overset{(b)}{=} \prod_t \exp\left(-\lambda_{\text{S}} 2\pi \mathbb{E}_{\overline{\zeta},\theta}\left[\int_0^\infty \left(1 - e^{-s g_{\mathbf{y}} \xi\overline{\zeta} C_t y^{-\alpha_t} G_{\text{S}}(\theta)}\right) \mathbb{1}\left(\overline{\zeta} < C_t^{-1} y_i^{\alpha_t}\right) p_t(y) y \text{d}y\right]\right)\end{aligned}$$

where (a) is from independence of LOS and NLOS tiers and (b) is due to the PGFL

of PPP. Now, using the transformation $y = v(\overline{\zeta}C_t)^{1/\alpha_t}$, we get

$$\begin{aligned}\mathcal{L}_{I_{\mathcal{F}\mathrm{S}}}(s) &= \prod_t \exp\left(-\lambda_{\mathrm{S}} 2\pi \mathbb{E}_{\overline{\zeta},\theta}\left[\int_0^\infty \left(1-\exp\left(-s g_{\mathbf{y}} \xi v^{-\alpha_t} G_{\mathrm{S}}(\theta)\right)\right.\right.\right. \\ &\quad \left.\left.\left. \times \mathbb{1}\left(v>1\right)\right) p_t(v(\overline{\zeta}C_t)^{\frac{1}{\alpha_t}}) v(\overline{\zeta}C_t)^{\frac{2}{\alpha_t}} \mathrm{d}v\right]\right) \\ &\overset{(a)}{=} \prod_t \exp\left(-\lambda_{\mathrm{S}} 2\pi \mathbb{E}_{\theta}\left[\int_1^\infty \left(1-\exp\left(-s g_{\mathbf{y}} \xi v^{-\alpha_t} G_{\mathrm{S}}(\theta)\right)\right) K_t\left(v\right) v \mathrm{d}v\right]\right)\end{aligned} \tag{5.39}$$

where (a) is due to interchanging the integration and the expectation with respect to $\overline{\zeta}$ and applying K_t's definition.

Now, using the MGF of $g_{\mathbf{y}}$ and the distribution of $G_{\mathrm{S}}(\theta)$, we get

$$\mathcal{L}_{I_{\mathcal{F}\mathrm{S}}}(s) = \prod_t \exp\left(-\lambda_{\mathrm{S}} 2\pi \int_1^\infty \sum_{k=1}^{2} \frac{a_k}{1+s^{-1}\xi^{-1}G_{\mathrm{S}k}^{-1} v^{\alpha_t}} K_t\left(v\right) v \mathrm{d}v\right).$$

Now substituting $u = (s\xi G_{\mathrm{S}k})^{-1/\alpha_t} v$, we get $\mathcal{L}_{I_{\mathcal{F}\mathrm{S}}}(s)$

$$= \prod_t \exp\left(-\lambda_{\mathrm{S}} 2\pi (s\xi G_{\mathrm{S}k})^{2/\alpha_t} \int_{(s\xi G_{\mathrm{S}k})^{-1/\alpha_t}}^\infty \sum_{k=1}^{2} \frac{a_k}{1+u^{\alpha_{s_{\mathbf{y}}}}} K_t\left((s\xi G_{\mathrm{S}k})^{1/\alpha_t} u\right) u \mathrm{d}u\right).$$

Using the definition of $E_{\mathcal{F}\mathrm{S}}(B,\xi)$, we get

$$\mathcal{L}_{I_{\mathcal{F}\mathrm{S}}}(s) = \exp\left(-\lambda_{\mathrm{S}} \sum_{k=1}^{2} a_k E_{\mathcal{F}\mathrm{S}}\left(s G_{\mathrm{S}k}, \xi\right)\right). \tag{5.40}$$

Now, let us consider $I_{\mathcal{N}\mathrm{S}}$ which is given as

$$I_{\mathcal{N}\mathrm{S}}(s) = \sum_{t\in\{\mathrm{L},\mathrm{N}\}} \sum_{i\in\Phi_{\mathrm{S}\mathrm{L}}} g_{\mathbf{y}_i}\left(1-\mathbb{1}\left(C_{T_i} R_i^{-\alpha_{T_i}} > C_{\mathrm{L}} y_i^{-\alpha_L}\right)\right) \xi G_{\mathrm{S}}(\theta_i)$$

where the indicator term are exact opposite of the previous case and denotes that only those secondary BSs are considered whose receiver power at the their home primary

user is not greater than their received power at $\mathrm{UE_P}$. Note that the interference from each of these secondary BSs is equal to ξ. Hence, its Laplace transform is given as

$$\mathcal{L}_{I_{\mathcal{N}\mathrm{S}}}(s) = \prod_{t\in\{\mathrm{L},\mathrm{N}\}} \mathbb{E}\left[\exp\left(-s\sum_{i\in\Phi_{\mathrm{SL}}} g_{\mathbf{y}_i}\mathbb{1}\left(C_{T_i}R_i^{-\alpha_{T_i}} < C_t y_i^{-\alpha_t}\right)\xi G_{\mathrm{S}}(\theta_i)\right)\right]$$
$$\overset{(a)}{=} \prod_{t\in\{\mathrm{L},\mathrm{N}\}} \exp\left(-\lambda_{\mathrm{S}}2\pi\mathbb{E}_{\bar{\zeta},\theta}\left[\int_0^\infty (1-\exp\left(-sg_{\mathbf{y}}\xi G_{\mathrm{S}}(\theta)\right.\right.\right.$$
$$\left.\left.\left.\times\mathbb{1}\left(\frac{y^{\alpha_t}}{\bar{\zeta}C_t}<1\right)\right)\right)p_t(y)y\mathrm{d}y\right]\right)$$

where (a) is due to PGFL of a PPP. Substituting $y = (\bar{\zeta}C_t)^{1/\alpha_t}v$, we get

$$\mathcal{L}_{I_{\mathcal{N}\mathrm{S}}}(s) = \prod_{t\in\{\mathrm{L},\mathrm{N}\}} \exp\left(-\lambda_{\mathrm{S}}2\pi\mathbb{E}_{\bar{\zeta},\theta}\left[\int_0^\infty \left(1-e^{-sg_{\mathbf{y}}\xi G_{\mathrm{S}}(\theta)}\right)\right.\right.$$
$$\left.\left.\mathbb{1}\left(v^{\alpha_t}<1\right)p_t((\bar{\zeta}C_t)^{\frac{1}{\alpha_t}}v)(\bar{\zeta}C_t)^{\frac{2}{\alpha_t}}v\mathrm{d}v\right]\right). \tag{5.41}$$

Now using the MGF of exponential $g_{\mathbf{y}}$ and the PMF of $G_{\mathrm{S}}(\theta)$, we get

$$\mathcal{L}_{I_{\mathcal{N}\mathrm{S}}}(s) = \exp\left(-\lambda_{\mathrm{S}}2\pi\left[\sum_{k=1}^{2}\frac{a_k}{1+(s\xi G_{\mathrm{S}k})^{-1}}\right]\left(\int_0^1 K_{\mathrm{L}}(v)\,v\mathrm{d}v + \int_0^1 K_{\mathrm{N}}(v)\,v\mathrm{d}v\right)\right). \tag{5.42}$$

Using (5.40) and (5.42), we get the Lemma. □

Now, substituting the Laplace transforms of I'_{P} and I_{S} in Lemma 12, we can compute the final expression of the coverage probability, which is given in the following theorem.

Theorem 12. *The coverage probability of a typical user of the primary operator in a mmWave system with secondary licensing can be approximated as*

$$\mathrm{P}_{\mathrm{P}}^{\mathrm{c}}(\tau) \approx \mathrm{P}_{\mathrm{P}}^{\mathrm{c,app}}(\tau). \tag{5.43}$$

Here, $\mathrm{P}_{\mathrm{P}}^{\mathrm{c,app}}(\tau)$ *is the coverage probability of a typical user of the primary opertor under ITPA assumption and is given as*

$$\mathrm{P}_{\mathrm{P}}^{\mathrm{c,app}}(\tau) = \sum_{t_0\in\{\mathrm{L},\mathrm{N}\}} \int_0^{\infty} 2\pi\lambda_{\mathrm{P}} M_{t_0}(u)\, e^{-\frac{\tau u^{\alpha_{t_0}}}{G_{\mathrm{P1}}}\sigma_{\mathrm{S}}^2}$$
$$e^{-\lambda_{\mathrm{P}}\sum_{k=1}^{2} b_k E_{\mathrm{P}}\left(\frac{\tau u^{\alpha_{t_0}}}{G_{\mathrm{P1}}} G_{\mathrm{P}k}, u^{\alpha_{t_0}}\right) - \lambda_{\mathrm{S}}\sum_{k=1}^{2} a_k E_{\mathcal{F}\mathrm{S}}\left(\frac{\tau u^{\alpha_{t_0}}}{G_{\mathrm{P1}}} G_{\mathrm{S}k}, \xi\right)} \times \quad e^{-\lambda_{\mathrm{S}}\sum_{k=1}^{2} a_k E_{\mathcal{N}\mathrm{S}}\left(\frac{\tau u^{\alpha_{t_0}}}{G_{\mathrm{P1}}} G_{\mathrm{S}k}\right)}$$
$$e^{\left(-2\pi\lambda_{\mathrm{P}}\int_0^{u^{\alpha_{t_0}/\alpha_{\mathrm{L}}}} M_{\mathrm{L}}(z)z\mathrm{d}z - 2\pi\lambda_{\mathrm{P}}\int_0^{u^{\alpha_{t_0}/\alpha_{\mathrm{N}}}} M_{\mathrm{N}}(z)z\mathrm{d}z\right)} u\mathrm{d}u. \tag{5.44}$$

Special Cases: Similar to the secondary case, consider a mmWave network with identical parameters for LOS and NLOS channels. For this case, $M_t(u)$ and $K_t(u)$ are replaced by constant M and K. Now, $E_{\mathrm{P}}(B,e)$, $E_{\mathcal{F}\mathrm{S}}(B)$ and $E_{\mathcal{F}\mathrm{S}}(B,\xi)$ can be simplified as follows:

$$E_{\mathrm{P}}(B,e) = \pi M B^{\frac{2}{\alpha}}\rho(\alpha, B/e),$$
$$E_{\mathcal{F}\mathrm{S}}(B,\xi) = (\xi B)^{\frac{2}{\alpha}}\pi K\rho(\alpha,\xi B),$$
$$E_{\mathcal{N}\mathrm{S}}(B) = \frac{\pi K}{1+(B\xi)^{-1}}$$

Now,

$$E_{\mathrm{P}}\left(\frac{\tau u^{\alpha}}{G_{\mathrm{P1}}} G_{\mathrm{P}k}, u^{\alpha_{t_0}}\right) = \pi M u^2 \tau^{\frac{2}{\alpha}} \left(\frac{G_{\mathrm{P}k}}{G_{\mathrm{P1}}}\right)^{\frac{2}{\alpha}} \rho\left(\alpha, \frac{\tau G_{\mathrm{P}k}}{G_{\mathrm{P1}}}\right),$$
$$E_{\mathcal{F}\mathrm{S}}\left(\frac{\tau u^{\alpha} G_{\mathrm{S}k}}{G_{\mathrm{P1}}}, \xi\right) = \pi K u^2 \left(\tau\xi\frac{G_{\mathrm{S}k}}{G_{\mathrm{P1}}}\right)^{\frac{2}{\alpha}} \rho\left(\alpha, \xi\frac{\tau u^{\alpha} G_{\mathrm{S}k}}{G_{\mathrm{P1}}}\right),$$
$$E_{\mathcal{N}\mathrm{S}}\left(\frac{\tau u^{\alpha} G_{\mathrm{S}k}}{G_{\mathrm{P1}}}\right) = \frac{\pi K}{1+(\frac{\tau G_{\mathrm{S}k}}{G_{\mathrm{P1}}}\xi)^{-1} u^{-\alpha}}$$

Then, the primary coverage probability under ITPA assumption is given as

$$\mathrm{P}_{\mathrm{P}}^{\mathrm{c,app}}(\tau) = 2\pi\lambda_{\mathrm{P}} M \int_0^{\infty} e^{-\frac{\tau u^{\alpha}}{\xi G_{\mathrm{S1}}}\sigma_{\mathrm{S}}^2 - u^2\pi\tau^{\frac{2}{\alpha}}\left(\lambda_{\mathrm{P}}\sum_{k=1}^{2} b_k M\left(\frac{G_{\mathrm{P}k}}{G_{\mathrm{P1}}}\right)^{\frac{2}{\alpha}}\rho\left(\alpha,\frac{\tau G_{\mathrm{P}k}}{G_{\mathrm{P1}}}\right)\right)}$$

$$e^{-u^2\pi\tau^{\frac{2}{\alpha}}\left(\lambda_{\mathrm{S}}\sum_{k=1}^{2}a_k K\xi^{\frac{2}{\alpha}}\left(\frac{G_{\mathrm{S}k}}{G_{\mathrm{P}1}}\right)^{\frac{2}{\alpha}}\rho\left(\alpha,\xi\frac{\tau u^{\alpha}G_{\mathrm{S}k}}{G_{\mathrm{P}1}}\right)\right)-\pi\lambda_{\mathrm{S}}\sum_{k=1}^{2}a_k K/\left(1+\left(\frac{\tau G_{\mathrm{S}k}}{G_{\mathrm{P}1}}\xi\right)^{-1}u^{-\alpha}\right)-\pi\lambda_{\mathrm{P}}Mu^2}u\mathrm{d}u.$$

Assuming similar assumptions for the primary and secondary antennas as taken in the secondary case, we can get insights about how antenna beamwidth affects the primary performance.

Impact of narrowing primary antenna beamwidth: The term denoting secondary interference decreases with N_{P} as

$$u^2 c^{\frac{2}{\alpha}}\rho\left(\alpha,u^{\alpha}\frac{c}{N_{\mathrm{P}}}\right)\frac{\kappa}{N_{\mathrm{P}}^{2/\alpha}}+\frac{1}{1+N_{\mathrm{P}}u^{-\alpha}/c}\left(\approx\frac{1}{N_{\mathrm{P}}}\frac{c}{u^{\alpha}}\text{ as }N_{\mathrm{P}}\to\infty\right).$$

Here, c is some variable independent of N_{P}. Similarly, the term denoting the primary interference decreases with N_{P} as

$$\frac{\kappa}{N_{\mathrm{P}}}\rho(\alpha,\tau)+\left(\frac{1-\kappa}{N_{\mathrm{P}}}\right)^{2/\alpha}\rho\left(\alpha,\tau\frac{1-\kappa}{N_{\mathrm{P}}}\right).$$

Therefore, narrowing the primary antennas beamwidth improves the primary performance significantly.

Impact of narrowing secondary antenna beamwidth: Here, the term denoting the secondary interference changes with N_{S} as

$$\begin{aligned}&u^2 d^{\frac{2}{\alpha}}\rho\left(\alpha,u^{\alpha}N_{\mathrm{S}}d\right)\frac{\kappa}{N_{\mathrm{S}}^{1-2/\alpha}}+\frac{\kappa}{N_{\mathrm{S}}}\frac{1}{1+u^{-\alpha}/(N_{\mathrm{S}}d)}\\&+u^2((1-\kappa)d)^{\frac{2}{\alpha}}\rho\left(\alpha,u^{\alpha}(1-\kappa)d\right)+\frac{1}{(1+u^{-\alpha}/((1-\kappa)d))},\end{aligned}$$

where d is some variable independent of N_{S}. The term denoting the primary interference remains unchanged with with N_{S}. Therefore, narrowing the secondary beamwidth has very little affect on the primary performance.

5.4.3 Rate Coverage for the Primary and Secondary Operators

In this section, we derive the downlink rate coverage which is defined as the probability that the rate of a typical user is greater than the threshold ρ, $\mathrm{R}^{\mathrm{c}}(\rho) = \mathbb{P}\left[\mathrm{Rate} > \rho\right]$.

Let O_{S} (or O_{P}) denote the time-frequency resources allocated to each user associated with the 'tagged' BS of a secondary user (or a primary user). The instantaneous rate of the considered typical secondary user can then be written as $R_{\mathrm{S}} = O_{\mathrm{S}} \log\left(1 + \mathrm{SINR}_{\mathrm{S}}\right)$. The value of O_{S} depends upon the number of users (n_{S}), equivalently the load, served by the tagged BS. The load n_{S} is a random variable due to the randomly sized coverage areas of each BS and random number of users in the coverage areas. As shown in [14, 58], approximating this load with its respective mean does not compromise the accuracy of results. Since the user distribution of each network is assumed to be PPP, the average number of users associated with the tagged BS of each networks associated with the typical user can be modeled similarly to [14, 58]: $n_{\mathrm{S}} = 1 + 1.28\frac{\mu_{\mathrm{S}}}{\lambda_{\mathrm{S}}}$ and $n_{\mathrm{P}} = 1 + 1.28\frac{\mu_{\mathrm{P}}}{\lambda_{\mathrm{P}}}$. Now, we assume that the scheduler at the tagged BS gives $1/n$ fraction of resources to each user. This assumption can be justified as most schedulers such as round robin or proportional fair give approximately $1/n_{\mathrm{S}}$ (or $1/n_{\mathrm{P}}$) fraction of resources to each user on average. Using the mean load approximation, the instantaneous rate of a typical secondary user which is associated with BS at $\mathbf{y}_0$ is given as

$$R_{\mathrm{S}} = \frac{W}{n_{\mathrm{S}}} \log\left(1 + \mathrm{SINR}_{\mathrm{S}}\right). \tag{5.45}$$

Now, $\mathrm{R}_{\mathrm{S}}^{\mathrm{c}}(\rho)$ and $\mathrm{R}_{\mathrm{P}}^{\mathrm{c}}(\rho)$ can be derived in terms of coverage probability as follows:

$$\begin{aligned}\mathrm{R}_{\mathrm{S}}^{\mathrm{c}}(\rho) &= \mathbb{P}\left[R_{\mathrm{S}} > \rho\right] = \mathbb{P}\left[\frac{W}{n_{\mathrm{S}}}\log\left(1+\mathrm{SINR}_{\mathrm{S}}\right) > \rho\right] \\ &= \mathbb{P}\left[\mathrm{SINR}_{\mathrm{S}} > 2^{\rho\frac{n_{\mathrm{S}}}{W}} - 1\right] = \mathrm{P}_{\mathrm{S}}^{\mathrm{c}}\left(2^{\rho n_{\mathrm{S}}/W} - 1\right), \\ \mathrm{R}_{\mathrm{P}}^{\mathrm{c}}(\rho) &= \mathrm{P}_{\mathrm{P}}^{\mathrm{c}}\left(2^{\rho n_{\mathrm{P}}/W} - 1\right). \end{aligned} \tag{5.46}$$

We now define the median rate which works as a proxy to the network performance.

Definition 1. *Let $\mathcal{B}$ denote a region with unit area. The median rate $\mathcal{R}$ of an operator is define as the sum of the median rates of all the users served in $\mathcal{B}$, which is*

$$\mathcal{R} = \mathbb{E}\left[\sum_{u\in\Psi\cap\mathcal{B}} \mathbb{M}_u\left[R\right]\right] \tag{5.47}$$

where $\mathbb{M}_u\left[R\right]$ is the median rate of the user at u.

From the stationarity of the user PPP,

$$\mathcal{R} = \mathbb{E}\left[\sum_{u\in\Psi\cap\mathcal{B}} \mathbb{M}_u\left[R\right]\right] = \mu\int_{\mathcal{B}} \mathbb{M}^0\left[R\right]\mathrm{d}u = \mu\mathbb{M}^0\left[R\right] \tag{5.48}$$

where $\mathbb{M}^0$ denotes the median rate at the origin under Palm (*i.e.* conditioned on the fact that there is a user at 0). Note that this is equal to the rate threshold where rate coverage of the typical user at the origin is 0.5. Let $(\mathrm{P}^{\mathrm{c}})^{-1}(\cdot)$ denote the inverse of $\mathrm{P}^{\mathrm{c}}(\cdot)$. Now using (5.46), we can compute the median rate of the primary and secondary operators as follows:

$$\mathcal{R}_{\mathrm{P}} = W\frac{\mu_{\mathrm{P}}}{1+1.28\mu_{\mathrm{P}}/\lambda_{\mathrm{P}}}\log\left(1+\left(\mathrm{P}_{\mathrm{P}}^{\mathrm{c}}\right)^{-1}(0.5)\right) \tag{5.49}$$

$$\mathcal{R}_{\mathrm{S}} = W\frac{\mu_{\mathrm{S}}}{1+1.28\mu_{\mathrm{S}}/\lambda_{\mathrm{S}}}\log\left(1+\left(\mathrm{P}_{\mathrm{S}}^{\mathrm{c}}\right)^{-1}(0.5)\right). \tag{5.50}$$

5.5 License Pricing and Revenue Model

In this section, we present the utility model, and describe the general license pricing and revenue functions. We assume a centralized licensing model in which a central entity, such as FCC, has a control over the licensing for the primary and secondary operators. Therefore, even though the primary operator has an "exclusive-use" license, the decision to sell a restricted license to a secondary operator is taken by both the primary operator and the central licensing authority. These two entities will also share the revenue of the restricted secondary license.

Let $\mathcal{M}_{\mathrm{P}}(\mathcal{R}_{\mathrm{P}})$ define the per-unit-area revenue function of the primary operator from its own users when it provides a sum rate of $\mathcal{R}_{\mathrm{P}}$. Similarly, we define the secondary revenue function $\mathcal{M}_{\mathrm{S}}(\cdot)$ that models the revenue of the secondary network from its users. One special case is the linear mean revenue function, which is given as follows

$$\mathcal{M}_{\mathrm{P}}(\mathcal{R}_{\mathrm{P}}) = M_{\mathrm{P}}\mathcal{R}_{\mathrm{P}}, \qquad \mathcal{M}_{\mathrm{S}}(\mathcal{R}_{\mathrm{S}}) = M_{\mathrm{S}}\mathcal{R}_{\mathrm{S}}, \tag{5.51}$$

with M_{P} and M_{S} representing the linear primary and secondary revenue constants.

To characterize the licensing cost, we assume the licenses are given on a unit area region basis. Let the primary licensing function $\mathcal{P}_{\mathrm{P}}(\mathcal{R}_{\mathrm{P}})$ denote the license price paid by the primary to central entity when it provides the median rate of $\mathcal{R}_{\mathrm{P}}$ to its users. Similarly, we define secondary licensing function $\mathcal{P}_{\mathrm{SC}}(\cdot)$ which denotes the price paid by the secondary operator to the central entity. We also assume that secondary operator has to pay some license price to the primary operator as an incentive to let it use the primary license band which is given as $\mathcal{P}_{\mathrm{SP}}(\mathcal{R}_{\mathrm{S}})$. We also define a special

case as linear licensing function where the licensing cost paid by the primary and the secondary operators to the central entity and by the secondary operator to the primary operator are given as

$$\mathcal{P}_{\mathrm{P}}(\mathcal{R}_{\mathrm{P}}) = \Pi_{\mathrm{P}}\mathcal{R}_{\mathrm{P}}, \qquad \mathcal{P}_{\mathrm{SC}}(\mathcal{R}_{\mathrm{S}}) = \Pi_{\mathrm{SC}}\mathcal{R}_{\mathrm{S}}, \qquad \mathcal{P}_{\mathrm{SP}}(\mathcal{R}_{\mathrm{S}}) = \Pi_{\mathrm{SP}}\mathcal{R}_{\mathrm{S}}.$$

The utility function of an entity is defined by its total revenue which for the three entities is given as follows:

$$\mathcal{U}_{\mathrm{P}}(\mathcal{R}_{\mathrm{P}}) = \mathcal{M}_{\mathrm{P}}(\mathcal{R}_{\mathrm{P}}) - \mathcal{P}_{\mathrm{P}}(\mathcal{R}_{\mathrm{P}}) + \mathcal{P}_{\mathrm{SP}}(\mathcal{R}_{\mathrm{S}}), \tag{5.52}$$

$$\mathcal{U}_{\mathrm{S}}(\mathcal{R}_{\mathrm{S}}) = \mathcal{M}_{\mathrm{S}}(\mathcal{R}_{\mathrm{S}}) - \mathcal{P}_{\mathrm{SC}}(\mathcal{R}_{\mathrm{S}}) - \mathcal{P}_{\mathrm{SP}}(\mathcal{R}_{\mathrm{S}}), \tag{5.53}$$

$$\mathcal{U}_{\mathrm{C}}(\mathcal{R}_{\mathrm{S}}) = \mathcal{P}_{\mathrm{P}}(\mathcal{R}_{\mathrm{P}}) + \mathcal{P}_{\mathrm{SC}}(\mathcal{R}_{\mathrm{S}}). \tag{5.54}$$

Note that the secondary median rate depends on the maximum interference limit ξ. By increasing this limit, secondary network can increase its median rate for which it has to pay more to central entity and the primary operator. Increasing this limit, however, decreases the primary median rate which impacts the primary network revenue from its own users. Therefore, there exists a trade-off when varying the interference limit ξ.

5.6 Simulation Results and Discussion

In this section, we provide numerical results computed from the analytical expressions derived in previous sections, and draw insights into the performance of restricted secondary licensing in mmWave systems. For these numerical results, we adopt an exponential blockage model, i.e., the LOS link probability is determined by

$p_{\mathrm{L}}(x) = \exp(-x/\beta)$, with a LOS region $\beta = 150$m. The LOS and NLOS pathloss exponents are $\alpha_{\mathrm{L}} = 2.5$ and $\alpha_{\mathrm{N}} = 3.5$, and the corresponding gains are $C_{\mathrm{L}} = C_{\mathrm{N}} = -60$dB. Unless otherwise mentioned, the primary network has an average cell radius of 100m, which is equivalent to a BS density of $\approx 30/\mathrm{km}^2$. The transmit power of the primary BSs is 40dBm, while the transmit power of each secondary BS is determined according to (5.6) to ensure that its average interference on its home primary user in less than the threshold ξ. Both networks operate at 28GHz carrier frequency over a shared bandwidth of 500MHz. Note that the noise power at the BS is -110dB. Therefore, if ξ is between -110dB and -120dB, the secondary interference will be in the order of the noise. For the antenna patterns, the primary and secondary BSs employ a sectored beam pattern models as described in Section 5.3.1. First, we verify the derived analytical results for the primary and secondary coverage probabilities, before delving into the spectrum sharing rate and utility characterization.

5.6.1 Coverage and Rate Results

Since the secondary operator shares the same time-frequency resources with the primary, it is important to characterize the impact of sharing on the primary performance. In this subsection, we evaluate the coverage and rate for both operators, and study the impact of secondary network's densification and narrowing the beamforming beams on the performance of the two networks.

Validation of analysis: Recall that in the secondary performance analysis, we assumed for tractability that the transmit powers of secondary BSs are independent to each other. Additionally, for the primary performance analysis, we assumed

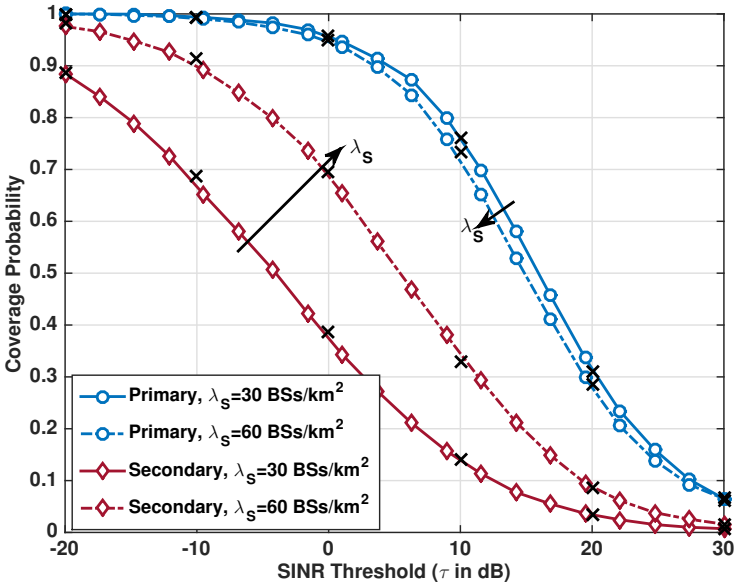

Figure 5.3: Coverage probabilities of the two licensees for two different values of λ_S with $\xi = -120$dB. The secondary can improve its coverage by choosing an appropriate density without impacting the primary coverage.

that the correlation between the location of the typical primary user and the transmit power of any secondary BS can be modeled by a simple truncation of the distribution of P_S. In the simulation, we relax this approximation. Instead, in each iteration, we first generate all four processes (Φ_P, Ψ_P, Φ_S and Ψ_S). We, then, compute and assign the home primary user to each secondary BS based on the pathloss and compute each secondary BS's transmit power. Finally, we compute the SINR for each typical user. Fig. 5.3 shows the coverage probabilities of both operators for two different values of the secondary density, $\lambda_S = 30$ BSs/km^2 and $\lambda_S = 60$ BSs/km^2 along with results from the analysis. The density of the primary BSs is fixed at $\lambda_P = 30$ BSs/km^2 and the maximum secondary interference threshold is set to -120 dB. We can see that despite the various assumptions taken in the analysis, the analysis matches the

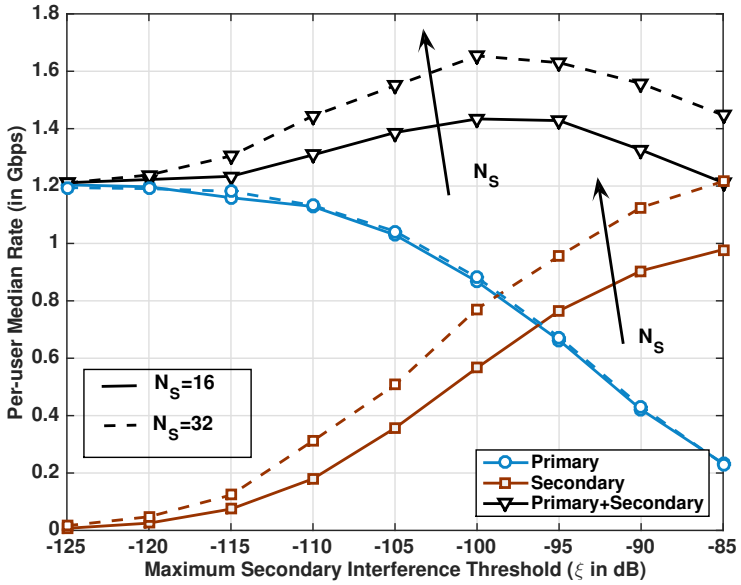

Figure 5.4: Sum median rate of the primary and secondary networks as well as the total sum median rate versus ξ. The networks have equal density of 56 BS/km^2, which corresponds to an average cell radius of 75m.

simulations closely. Rest of the results in this section are obtained using simulations without the ITPA assumption.

Impact of the secondary densification: An interesting note from Fig. 5.3 is that increasing the secondary network density significantly improves the secondary network coverage while causing a negligible impact on the primary network performance. In particular, when λ_S increases from 30 to 60 BSs/km^2, the median SINR of the secondary network increases from -4dB to 6dB while the median SINR of primary network decreases only by 2 dB. This indicates that in mmWave, both primary and secondary can achieve significant coverage probability by selecting appropriate values of ξ and BS densities.

Impact of the secondary antenna beamwidth: One important feature of mmWave systems is their ability to use large antennas arrays and narrow directional beams. To examine the impact of antenna beamwidth, we plot the median per-user rate of both the primary and secondary networks along with their sum-rate for two different values of number of secondary antennas in Fig. 5.4. These rates are plotted versus the secondary interference threshold ξ. First, Fig. 5.4 shows that the secondary network performance improves as the number of its BS antennas increase (or equivalently as narrower beams are employed). Another interesting note is that the primary performance is almost invariant of the secondary antennas beamwidth. This means that the secondary network can always improve its performance by employing narrower beamforming beams without impacting the primary performance. This will also lead to an improvement in the overall system performance. Finally, we note that for every secondary BS beamwidth, there exists a finite value for the interference threshold ξ at which the sum-rate is maximized. Therefore, this threshold need to be wisely adjusted for the spectrum sharing network based on the different network parameters to guarantee achieving the best performance.

To verify the insights drawn from the analytical expressions about narrowing the primary and secondary beamforming beamwidth in Sections 5.4.1 - 5.4.2, we plot the primary and secondary median rates versus the BS antenna beamwidth in Fig. 5.5. This figure shows the narrowing the beams of the BSs in one network (primary or secondary) improves the performance of this network with almost no impact on the other network performance. This trend happens even with higher secondary interference threshold as depicted in Fig. 5.5.

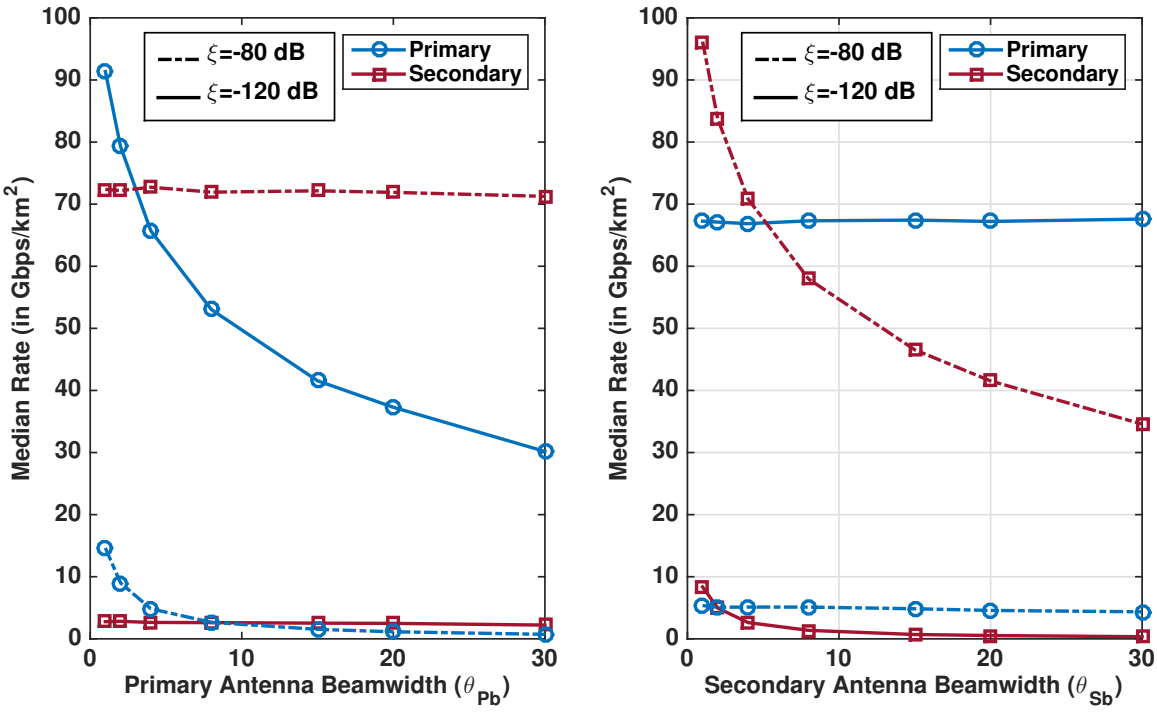

Figure 5.5: Effect of primary and secondary antenna beamwidth over primary and secondary operators for two values of interference threshold ξ. Both operators have equal density of 60 BSs/km^2. Secondary antenna beamwidth significantly improves its own performance but does not impact primary performance. Therefore, secondary antennas can be made narrow to get high rates without causing additional interference on primary. Similar trends can also be observed for primary antennas.

Comparison with uncoordinated spectrum sharing: Now, we compare the gain from restricted secondary licensing proposed in this chapter over the uncoordinated spectrum sharing considered in [83]. We consider a scenario where two operators buy exclusive licenses to two different mmWave bands with equal bandwidth. The two operators decide to share their licenses in the following way: each operator is known as a primary in its own band and a secondary in the other operator's band. In the restricted secondary licensing, each operator can transmit in

other operator bands with the restriction on its transmit power. In the uncoordinated sharing, the two operators are allowed to transmit in each other bands with no restriction. For simplicity, we assume that the two operators, in the uncoordinated sharing case, have the same transmit power. To have a fair comparison, we choose the transmit power in uncoordinated case such that the total power (sum of the transmit power of the two operators) is equal to the total power of the restricted secondary sharing case. Fig. 5.6(a) compares the median rates of an operator achieved in its primary and secondary bands as well as its aggregate median rate for the two sharing cases. First, this figure shows that restricted secondary licensing can achieve higher sum rates compared to uncoordinated sharing if the interference threshold is appropriately adjusted. The figure also indicates that the restricted licensing approach provides a mean for differentiating the access to guarantee that the primary user gets better performance in its band. This is captured by the higher rate of the primary operator in the restricted secondary licensing case compared to the primary rate in the uncoordinated sharing for wide range of ξ values.

In Fig. 5.6(b), we show the impact of secondary network density (λ_{S}) on the gain of restricted secondary licensing over uncoordinated sharing. Fig. 5.6(b) illustrates that increasing λ_{S} decreases the rate of the primary operator in two sharing approaches, which is expected. Interestingly, the degradation in the primary performance is smaller in the restricted licensing case which leads to higher overall gain compared to the uncoordinated sharing. This also means that the gain of restricted licensing over uncoordinated sharing increases in dense networks, which is particularly important for mmWave systems. In conclusion, the results in Fig. 5.6(a) - Fig. 5.6(b)

indicate that static coordination is in fact beneficial for mmWave dense networks as it leads to higher rates and provides a way of differentiating the access between the spectrum sharing operators.

5.6.2 Primary and Secondary Utilities: The Benefits of Spectrum Sharing

In this subsection, we explore the potential gains of secondary licensing in mmWave cellular systems. We adopt the pricing model from Section 5.5, with revenue constants $M_{\mathrm{P}} = 1, M_{\mathrm{S}} = 1$, and licensing cost constants $\Pi_{\mathrm{P}} = 0.25, \Pi_{\mathrm{SC}} = 0.125$.

Gain of the primary network from restricted secondary licensing: In Fig. 5.7, we plot the utility functions of the primary operator, the secondary operator, and the central licensing authority, defined in (5.52)-(5.54), versus the secondary interference threshold ξ for three different values of the secondary-to-primary licensing constant Π_{SP}. In this result, we consider a primary network of density $30/\mathrm{km}^2$, and a secondary network of density of $60/\mathrm{km}^2$. First, the figure shows that increasing ξ improves the secondary operator utility which is expected. Interestingly, the utility of the primary network does not always decrease with increase in ξ. The figure indicates that ξ that maximizes the primary network utility is finite, which means that the primary network can actually benefit from the restricted secondary licensing. The intuition is that the secondary network needs to pay for its interference to the primary network. As this interference increases, the money that the primary network gets from the restricted secondary licensing is more that its revenue from its own network. This underling trade-off normally yields an optimal value for the secondary interference threshold that maximizes the primary network utility. This means that the primary

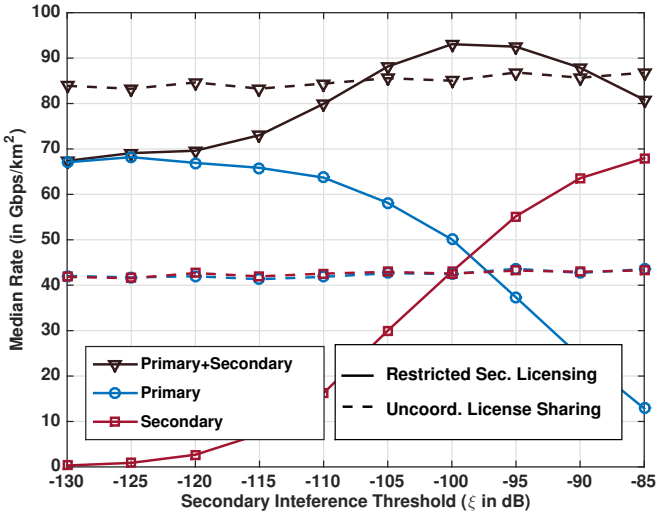

(a)

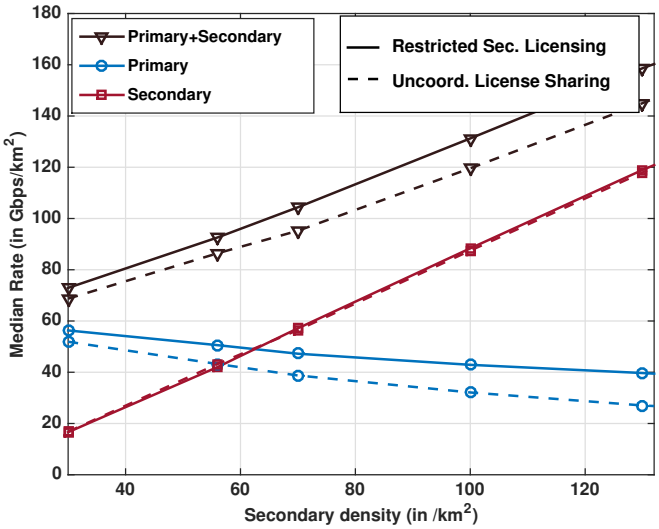

(b)

Figure 5.6: Comparison of restricted secondary licensing over uncoordinated sharing. (a) Variation of median rates of an operator in the primary and secondary bands and its sum median rate with ξ. Both operators have equal density of 60 BSs/km^2. Secondary licensing can achieve higher sum rates compared to uncoordinated sharing if ξ is appropriately adjusted. (b) Variation of median rates of an operator in the primary and secondary bands and its sum median rate with secondary density λ_S. Primary BS density is kept constant at 60 BSs/km^2. The gain of restricted secondary licensing over uncoordinated sharing increases with λ_S.

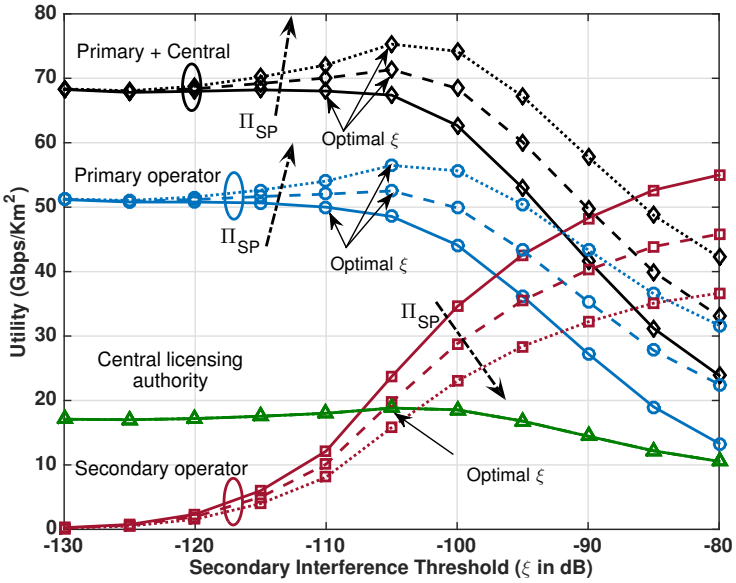

Figure 5.7: Utility of primary network, the central licensing authority and the sum of the former two utilities as function of the maximum secondary interference threshold ξ. The optimal threshold for the total utilities falls in between the optimal thresholds of utilities of the primary and the central entity $\Pi_{SP} = .125, .25, .375$.

network has clear incentive to share its spectrum using restricted secondary licensing.

Joint optimization of the primary and the central entity: The utility of the central licensing authority remains constant for different values of Π_{SP}, which can be noted from (5.52)-(5.54). As the value of ξ that maximizes the utility of the central authority can be larger than that maximizing the primary utility as shown in Fig. 5.7, the central licensing authority has the incentive to push the primary to share with more degradation than the primary would otherwise share. Fig. 5.7, also plots the total utility function which defined as the sum of the primary and central licensing authority's utilities. Intuitively, the optimal threshold for the total utility falls in between the optimal thresholds of the primary and central entity utilities.

5.7 Conclusion

In this chapter, we modeled a mmWave cellular system with a primary operator that has an "exclusive-use" license with a provision to sell a restricted secondary license to another operator that has a maximum allowable interference threshold. This licensing approach provides a way of differentiating the spectrum access for the different operators, and hence is more practical. Due to this restriction on the secondary interference, though, the transmit power of a secondary BSs is a random variable. This required developing new analytical tools to analyze the network coverage and rate. Results showed that secondary can achieve good rate coverage with a small impact on the primary performance. Results also indicated that narrow beams and dense networks can further improve secondary network performance. Compared to uncoordinated sharing, we showed that a reasonable gain can be achieved with the proposed static coordinated sharing approach. Further, restricted secondary licensing can guarantee a certain spectrum access quality for the primary user, which is not the case in uncoordinated sharing. We also considered a revenue model for both operators in the presence of a central licensing authority. Using this model, we showed that the primary operator can achieve good benefits from restricted secondary licensing, and hence has a good incentive to share its spectrum. Results also illustrated that the central licensing authority can get more gain with restricted secondary licensing. As the optimal interference thresholds for the central licensing and primary operators can be different, the central authority may push the primary operator to share with more degradation than the primary would otherwise share. Overall, the primary and secondary operators as well as the central licensing authority can benefit from

restricted secondary licensing.

Chapter 6

Conclusions

6.1 Summary

In this dissertation, various cell selection rules to optimize coverage probability and rate coverage were discussed for a downlink multi-antenna HetNet. Due to use of multiple antennas, there is a natural expansion of coverage regions of small cells whenever small cells can use multi-antenna transmission for range expansion, e.g., by using beamforming. This leads to a natural balancing of load across tiers, which reduces the additional artificial cell selection bias needed to offload sufficient traffic to small cells. The approximate selection biases were computed to maximize coverage which also provide good starting points for numerical search algorithms to find rate maximizing biases. Then, this dissertation evaluated the gains of macro-diversity for a cellular system in presence of random blockages and showed that the use of multiple BSs can reduce the required network infrastructure to achieve the same level of reliability. In the last two contributions, the gains of spectrum sharing for mmWave cellular systems were studied. The third contribution studied the feasibility of uncoordinated spectrum sharing in mmWave bands and showed that license sharing among operators improves system performance by increasing per-user median rate. However, the sharing of spectrum can degrade the performance of cell edge users due to additional inter-operator interference. Therefore, the dissertation also studied

the impact of static coordination in a mmWave cellular system with primary and secondary operators in presence of a central entity. It was shown that the secondary can achieve good rate coverage with a small impact on the primary performance. This implied that it may be important to have some level of coordination among operators to guarantee some level of quality of service.

6.2 Future Work

The research performed in this dissertation has numerous extensions. Some of the extensions have already been implemented by others, for example, in [122–127]. In this section, we discuss some of the future extensions of this dissertation.

6.2.1 Incorporating UEs with Multiple Antennas

This dissertation assumes single antenna at UEs. It is important to generalize this analysis to the case where mobile users have multiple antennas. This adds another dimension to system design and it is important to understand how to best use the additional degrees of freedom. In the HetNet MIMO system considered in the first contribution, the channel distribution will change if UEs have multiple antennas. Hence, the optimal association rules and cell selection biases may change in presence of multi-antenna UEs. For the multi-operator mmWave systems considered in last two contributions, the UE antennas will create further directionality in the transmission. This decreases the inter-operator interference further favoring spectrum sharing even more. This effect need to be characterized to accurately evaluate the gain from spectrum sharing.

6.2.2 Impact of Multi-user MIMO on Spectrum Sharing

It is worth investigating how multi-antenna techniques such as multiplexing multiple users affect the insights about uncoordinated license sharing and restricted secondary licensing. For example, if we schedule more users in single resource block using any multi-user multiplexing, the interference at typical user will increase. In addition, it will be difficult to form non-overlapping directional beams as the probability of users being close to each other will increase. Hence, it is important to see how many users can be scheduled in a single block without hurting the system performance. Using the analysis in [128], we can derive expressions for the rate coverage for multi-operator mmWave systems with multiuser MIMO and characterize the gains of spectrum sharing for these systems.

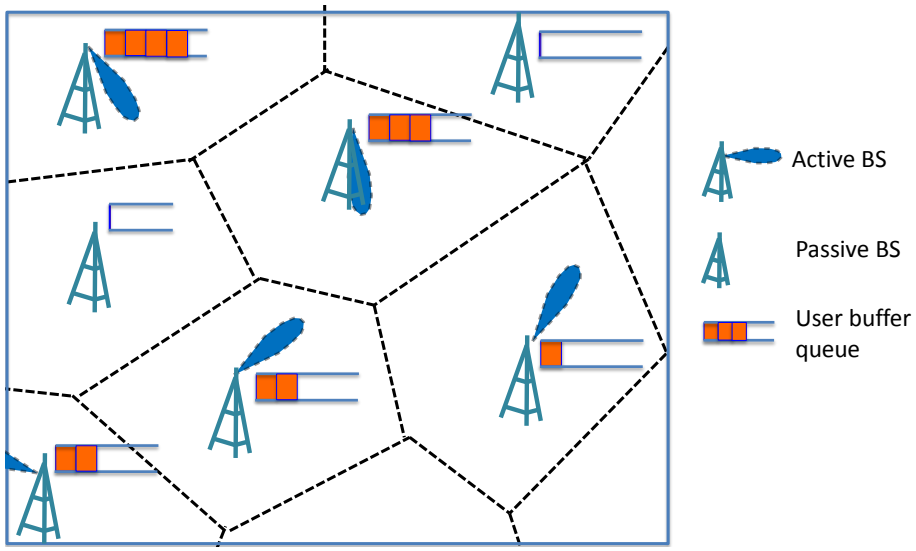

Figure 6.1: A mmWave cellular system with buffers to keep track of users. The BSs with empty buffer can be switched off to reduce the interference.

6.2.3 Considering File Traffic Models

If the user density is small, there is a chance that some BSs may not have any users associated to them. In this case, such BSs can be switched off which further reduces the interference. In the third contribution of this dissertation, we model this scenario using an independent on-off model where each BS is either active or idle according to an indicator which is independent to other BSs. In real systems, the BSs use buffers to keep track of their users and to schedule them. The interference from other BSs reduces the average data throughput and hence, elongates the user buffer. This creates a correlation among buffer sizes of neighboring BSs. One way to model this impact is using a file transfer protocol model. It is worth exploring how temporal variations in the traffic demands for the operators impact the network performance to derive more accurate quantitative performance. Such an analysis is in general non-tractable, however, there has been some recent work which proposes approximate approaches to handle it [129–131].

6.2.4 Infrastructure Sharing

In the dissertation, we showed that multi-operator mmWave cellular system even with co-located BSs can achieve significant performance gain from spectrum license sharing in terms of median rate. This result indicates that multiple operators can also share site infrastructure (such as macrocell towers, as is common practice today) while also sharing their spectrum licenses. It is interesting to understand how other essential infrastructure including backhaul can be shared among networks reducing the cost further, especially in the case of co-located BSs.

6.2.5 Modeling Partial Co-location Among Cellular Operators

In our dissertation, we have assumed independence for BS deployment among operators and modeled the BSs locations using superposition of multiple independent PPPs. In practical cases, there is some correlation among different operator owing to various geographical constraints and user requirements. To include the impact of correlation among deployments of operators, we also considered a co-located deployment where site locations are defined by a single PPP and each operator has one BS at each site. This is the other extreme case of BSs deployment when compared to the independent PPPs' superposition case. A practical deployment with some co-location and some unique sites will lie between these two extremes of independent and fully co-located BS locations. Therefore, it is important to carefully model this partial co-location among operators to accurately characterize the gains from spectrum sharing for mmWave cellular systems.

6.2.6 Economical Perspective of Spectrum Sharing

In this dissertation, it was shown that spectrum sharing is beneficial for mmWave cellular operators from technical perspective. However, technological gains may not be directly proportional to economic benefits for operators and users. Cellular markets provide coverage and networks services to users which are network based good. When there is a network based good, there is an extra buying incentive proportional to the network size for users [132]. Due to sharing, the network size increases for all operators, providing some extra gain to users. However, sharing also can affect competition among operators. Consider the case when there are two operators pro-

viding different level of quality in services and having different level of prices. Now, when the operators share some resources, they may be able to provide higher quality of service for the same level of price. This will cause some customers of the operator with higher quality and price to move to the other operator as they can now get the same service at lower price. This will negatively affect the profit of the higher quality operator and may stop it from sharing its resources. Such a model was studied recently in [126] for systems with open access and full sharing and it was shown that the leading service provider in a duopoly market prefers to share resources only when sharing gains are small or the market is highly segmented so that lower operators can get only small advantage from sharing and can not affect its own market segment. The same approach can also be applied to closed access systems with full spectrum sharing and co-located deployments to understand the economical gains of spectrum sharing.

Appendices

Appendix A

Stochastic Geometry

In this appendix, we will discuss some basic concept of PPP and stochastic geometry. A more detailed tutorial discussing stochastic geometry and its application to wireless networks can be found in [120].

Point processes (PP) are the central concept of stochastic geometry. A PP $\Phi = \{\mathbf{x}_i, i \in \mathbb{N}\}$ is a random collection of points residing in a Euclidean space $\mathbb{R}^d$. The expectation measure of a point process is a function which maps a set $\mathcal{A}$ to the mean number of points in it and is given as

$$\Lambda(\mathcal{A}) = \mathbb{E}\left[\#\text{ points in } \mathcal{A}\right]. \tag{A.1}$$

The point process widely used in cellular analysis is Poisson point process (PPP). A PPP is a point process with expectation measure $\Lambda(\cdot)$ such that

1. The number of points in $\mathcal{A}$ is Poisson distributed with mean $\Lambda(\mathcal{A})$ for every set $\mathcal{A}$.

2. For any m disjoint sets $\mathcal{A}_1, \cdots, \mathcal{A}_m$, the number of points in these sets are independent.

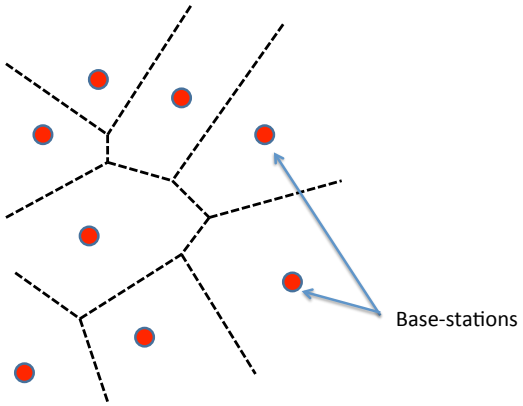

Figure A.1: Random spatial model for cellular networks. BSs locations are modeled by a PPP and the cell area of each BS is determined by the Voronoi tessellation.

Let $\mathcal{B}(r)$ denote a ball of radius r and center at the origin. The intensity (or density) of an isotropic PPP is defined as

$$\lambda(r) = \frac{1}{2\pi r}\frac{\mathrm{d}}{\mathrm{d}r}\Lambda(\mathcal{B}(r)). \tag{A.2}$$

PPPs can be categorized into homogenous or non-homogeneous PPPs. The homogeneous PPP is a PPP with uniform intensity λ. An important property of a homogeneous PPP is that conditioned on the number of points in A, all the points are independently and uniformly distributed in A. Similarly, the non-homogeneous PPP is a PPP with non-uniform intensity $\lambda(r)$.

For a distance dependent function $y = f(\|\mathbf{x}\|)$, the probability generating functional (PGFL) of a PP is defined as the mean of the product of the function's values at each point of the PP, *i.e.*

$$\mathcal{P}_{\Phi}(f) = \mathbb{E}\left[\prod_{\mathbf{x}_i \in \Phi} f(\|\mathbf{x}_i\|)\right]. \tag{A.3}$$

For an isotropic PPP, the PGFL is further simplified as

$$\mathcal{P}_{\Phi}(f) = \exp\left(-2\pi \int_0^{\infty} (1 - f(r))\lambda(r) r \mathrm{d}\mathbf{r}\right). \tag{A.4}$$

The PGFL is useful for converting an expectation of a product of the points in the PPP into a (hopefully computable) integral, primarily while computing the Laplace transform of the interference. We refer the reader to [120] for detailed treatment on how to compute the Laplace transform of the interference using PGFL.

While evaluating performance of a cellular system, we often are interested in the performance of a typical user. If the user distribution is stationary, this typical user can be taken at the origin without loss of generality.

Bibliography

[1] "3GPP TR 25.996: Spatial channel model for multiple input multiple output (MIMO) simulations (release 10)," Mar. 2011.

[2] A. D. Wyner, "Shannon-theoretic approach to a Gaussian cellular multi-access channel," *IEEE Trans. Inf. Theory*, vol. 40, no. 6, pp. 1713–1727, Nov. 1994.

[3] F. Baccelli and B. Błaszczyszyn, *Stochastic Geometry and Wireless Networks*, 2nd ed. NOW Publishers, 2009, vol. 1.

[4] Cisco, "Visual networking index," Feb. 2014, white paper at Cisco.com.

[5] J. Andrews, S. Buzzi, W. Choi, S. Hanly, A. Lozano, A. Soong, and J. Zhang, "What will 5G be?" *IEEE J. Sel. Areas Commun.*, vol. 32, no. 6, pp. 1065–1082, June 2014.

[6] Z. Pi and F. Khan, "An introduction to millimeter-wave mobile broadband systems," *IEEE Commun. Mag.*, vol. 49, no. 6, pp. 101–107, June 2011.

[7] T. Rappaport, S. Sun, R. Mayzus, H. Zhao, Y. Azar, K. Wang, G. Wong, J. Schulz, M. Samimi, and F. Gutierrez, "Millimeter wave mobile communications for 5G cellular: It will work!" *IEEE Access*, vol. 1, pp. 335–349, May 2013.

[8] T. Bai and R. W. Heath Jr., "Coverage and rate analysis for millimeter wave cellular networks," *IEEE Trans. Wireless Commun.*, vol. 14, no. 2, pp. 1100–1114, Feb. 2015.

[9] T. Bai, R. Vaze, and R. Heath, "Analysis of blockage effects on urban cellular networks," *IEEE Trans. Wireless Commun.*, vol. 13, no. 9, pp. 5070–5083, Sept. 2014.

[10] T. Marzetta, "Noncooperative cellular wireless with unlimited numbers of base station antennas," *IEEE Trans. Wireless Commun.*, vol. 9, no. 11, pp. 3590–3600, November 2010.

[11] A. Alkhateeb, J. Mo, N. Gonzalez-Prelcic, and R. W. Heath, "MIMO precoding and combining solutions for millimeter-wave systems," *IEEE Commun. Mag.*, vol. 52, no. 12, pp. 122–131, Dec. 2014.

[12] J. G. Andrews, F. Baccelli, and R. K. Ganti, "A tractable approach to coverage and rate in cellular networks," *IEEE Trans. Commun.*, vol. 59, no. 11, pp. 3122–3134, Nov. 2011.

[13] A. Ghosh, T. Thomas, M. Cudak, R. Ratasuk, P. Moorut, F. Vook, T. Rappaport, G. MacCartney, S. Sun, and S. Nie, "Millimeter-wave enhanced local area systems: A high-data-rate approach for future wireless networks," *IEEE J. Sel. Areas Commun.*, vol. 32, no. 6, pp. 1152–1163, June 2014.

[14] S. Singh, M. Kulkarni, A. Ghosh, and J. Andrews, "Tractable model for rate in

self-backhauled millimeter wave cellular networks," *IEEE J. Sel. Areas Commun.*, vol. PP, no. 99, pp. 1–1, 2015.

[15] "Further advancements for e-utra physical layer aspects (release 9)," Tech. Rep. 3GPP TR 36.814, Mar. 2010.

[16] H. S. Dhillon, R. K. Ganti, and J. G. Andrews, "A tractable framework for coverage and outage in heterogeneous cellular networks," in *Proc., Information Theory and its Applications (ITA)*, San Diego, CA, Feb. 2011.

[17] H. S. Dhillon, R. K. Ganti, F. Baccelli, and J. G. Andrews, "Modeling and analysis of K-tier downlink heterogeneous cellular networks," *IEEE J. Sel. Areas in Commun.*, vol. 30, no. 3, pp. 550 – 560, Apr. 2012.

[18] H.-S. Jo, Y. J. Sang, P. Xia, and J. G. Andrews, "Heterogeneous cellular networks with flexible cell association: A comprehensive downlink SINR analysis," *IEEE Trans. Wireless Commun.*, vol. 11, no. 10, pp. 3484 – 3495, Oct. 2012.

[19] P. Madhusudhanan, J. G. Restrepo, Y. Liu, T. X. Brown, and K. Baker, "Downlink performance analysis for a generalized shotgun cellular systems," *IEEE Trans. Wireless Commun.*, vol. 13, no. 12, pp. 6684–6696, Dec. 2014.

[20] S. Mukherjee, "Distribution of downlink SINR in heterogeneous cellular networks," *IEEE J. Sel. Areas in Commun.*, vol. 30, no. 3, pp. 575 – 585, Apr. 2012.

[21] H. S. Dhillon and J. G. Andrews, "Downlink rate distribution in heterogeneous cellular networks under generalized cell selection," *IEEE Wireless Commun. Lett.*, vol. 3, no. 1, pp. 42 – 45, Feb. 2014.

[22] H. S. Dhillon, M. Kountouris, and J. G. Andrews, "Downlink MIMO HetNets: Modeling, ordering results and performance analysis," *IEEE Trans. Wireless Commun.*, vol. 12, no. 10, pp. 5208 – 5222, Oct. 2013.

[23] T. Bai and R. W. Heath, "Analysis of self-body blocking effects in millimeter wave cellular networks," in *Proc. ASILOMAR*, Nov. 2014, pp. 1921–1925.

[24] K. Venugopal and R. W. Heath, "Millimeter wave networked wearables in dense indoor environments," *IEEE Access*, vol. 4, pp. 1205–1221, 2016.

[25] Y. Zhu, Q. Zhang, Z. Niu, and J. Zhu, "Leveraging multi-AP diversity for transmission resilience in wireless networks: architecture and performance analysis," *IEEE Trans. Wireless Commun.*, vol. 8, no. 10, pp. 5030–5040, Oct. 2009.

[26] X. Zhang, S. Zhou, X. Wang, Z. Niu, X. Lin, D. Zhu, and M. Lei, "Improving network throughput in 60GHz WLANs via multi-AP diversity," in *in Proc. ICC*, June 2012, pp. 4803–4807.

[27] J. Choi, "On the macro diversity with multiple BSs to mitigate blockage in millimeter-wave communications," *IEEE Commun. Lett.*, vol. 18, no. 9, pp. 1653–1656, Sept. 2014.

[28] J. G. Andrews, S. Singh, Q. Ye, X. Lin, and H. S. Dhillon, "An overview of load balancing in HetNets: Old myths and open problems," *IEEE Wireless Commun. Mag.*, vol. 21, no. 2, pp. 18 – 25, Apr. 2014.

[29] A. Jalali, "On cell breathing in CDMA networks," in *Proc. IEEE ICC*, vol. 2, June 1998, pp. 985–988.

[30] T. Togo, I. Yoshii, and R. Kohno, "Dynamic cell-size control according to geographical mobile distribution in a DS/CDMA cellular system," in *Proc. IEEE PIMRC*, vol. 2, Sept. 1998, pp. 677–681.

[31] N. S. Networks, "Aspects of pico node range extension,," *3GPP TSG RAN WG1 Meeting 61, R1-103824*, 2010, available: http://goo.gl/XDKXI.

[32] G. Li, T. Irnich, and C. Shi, "Coordination context-based spectrum sharing for 5G millimeter-wave networks," in *International Conference on Cognitive Radio Oriented Wireless Networks and Communications (CROWNCOM)*, June 2014, pp. 32–38.

[33] P. Karunakaran, T. Wagner, A. Scherb, and W. Gerstacker, "Sensing for spectrum sharing in cognitive LTE-A cellular networks," in *Proc. IEEE WCNC*, April 2014, pp. 565–570.

[34] C. Lima, M. Bennis, and M. Latva-aho, "Coordination mechanisms for self-organizing femtocells in two-tier coexistence scenarios," vol. 11, no. 6, pp. 2212–2223, June 2012.

[35] H. ElSawy and E. Hossain, "Two-tier HetNets with cognitive femtocells: Downlink performance modeling and analysis in a multichannel environment," *IEEE Trans. Mobile Computing*, vol. 13, no. 3, pp. 649–663, March 2014.

[36] J. G. Andrews, "Seven ways that HetNets are a cellular paradigm shift," *IEEE Commun. Mag.*, vol. 51, no. 3, pp. 136 – 144, Mar. 2013.

[37] Cisco, "Cisco visual networking index: Global mobile data traffic forecast update, 2011 - 2016," white paper, Feb. 2012.

[38] Qualcomm, "LTE advanced: heterogeneous networks," white paper, Jan. 2011.

[39] Q. Li, G. Li, W. Lee, M. Lee, D. Mazzarese, B. Clercks, and Z. Li, "MIMO techniques in WiMax and LTE: a feature overview," *IEEE Commun. Mag.*, vol. 48, no. 5, pp. 86–92, May. 2010.

[40] H. ElSawy, E. Hossain, and M. Haenggi, "Stochastic geometry for modeling, analysis, and design of multi-tier and cognitive cellular wireless networks: A survey," *IEEE Commun. Surveys and Tutorials*, vol. 15, no. 3, pp. 996 – 1019, 2013.

[41] A. K. Gupta, H. S. Dhillon, S. Vishwanath, and J. G. Andrews, "Downlink multi-antenna heterogeneous cellular network with load balancing," *IEEE Trans. Commun.*, vol. 62, pp. 4052–4067, Nov. 2014.

[42] ——, "Downlink coverage probability in MIMO HetNets with flexible cell selection," in *Proc. IEEE GLOBECOM*, 8-12 Dec. 2014, pp. 1534–1539.

[43] A. Damnjanovic, J. Montojo, Y. Wei, T. Ji, T. Luo, M. Vajapeyam, T. Yoo, O. Song, and D. Malladi, "A survey on 3GPP heterogeneous networks," *IEEE Wireless Commun. Mag.*, vol. 18, no. 3, pp. 10 – 21, Jun. 2011.

[44] S. V. Hanly, "An algorithm for combined cell-site selection and power control to maximize cellular spread spectrum capacity," *IEEE J. Sel. Areas Commun.*, vol. 13, no. 7, pp. 1332–1340, 1995.

[45] R. D. Yates and C. Y. Huang, "Integrated power control and base station assignment," *IEEE Trans. Veh. Technol.*, vol. 44, no. 3, 1995.

[46] M. Hong and Z. Luo, "Distributed linear precoder optimization and base station selection for an uplink heterogeneous network," *IEEE Trans. Signal Proc.*, vol. 61, no. 12, pp. 3214–3228, June 2013.

[47] Q. Kuang, J. Speidel, and H. Droste, "Joint base-station association, channel assignment, beamforming and power control in heterogeneous networks," *Proc. IEEE 75th Veh. Technol. Conf. (VTC Spring)*, 2012.

[48] H. S. Dhillon, M. Kountouris, and J. G. Andrews, "Downlink coverage probability in MIMO HetNets," in *Proc., IEEE Asilomar*, Pacific Grove, CA, Nov. 2012.

[49] R. W. Heath, Jr., M. Kountouris, and T. Bai, "Modeling heterogeneous network interference using Poisson point processes," *IEEE Trans. Signal Proc.*, vol. 61, no. 16, pp. 4114 – 4126, Aug. 2013.

[50] V. Chandrasekhar, M. Kountouris, and J. G. Andrews, "Coverage in multi-antenna two-tier networks," *IEEE Trans. Wireless Commun.*, vol. 8, no. 10, pp. 5314–5327, Oct. 2009.

[51] S. Park, W. Seo, Y. Kim, S. Lim, and D. Hong, "Beam subset selection strategy for interference reduction in two-tier femtocell networks," *IEEE Trans. Wireless Commun.*, vol. 9, no. 11, pp. 3440–3449, Nov. 2010.

[52] S. Park, W. Seo, S. Choi, and D. Hong, "A beamforming codebook restriction for cross-tier interference coordination in two-tier femtocell networks," *IEEE Trans. Veh. Technol.*, vol. 60, no. 4, pp. 1651–1663, May 2011.

[53] S. Akoum, M. Kountouris, and R. W. Heath Jr., "On imperfect CSI for the downlink of a two-tier network," in *Proc., IEEE Intl. Symposium on Information Theory*, Saint Petersburg, Russia, Jul.-Aug. 2011.

[54] A. Hunter, J. G. Andrews, and S. Weber, "Transmission capacity of ad hoc networks with spatial diversity," *IEEE Trans. Wireless Commun.*, vol. 7, no. 12, pp. 5058–5071, Dec. 2008.

[55] R. H. Y. Louie, M. R. McKay, and I. B. Collings, "Open-loop spatial multiplexing and diversity communications in ad hoc networks," *IEEE Trans. Info. Theory*, vol. 57, no. 1, pp. 317 – 344, Jan. 2011.

[56] R. Vaze and R. W. Heath Jr., "Transmission capacity of ad-hoc networks with multiple antennas using transmit stream adaptation and interference cancellation," *IEEE Trans. Info. Theory*, vol. 58, no. 2, pp. 780 – 792, Feb. 2012.

[57] H. S. Dhillon, R. K. Ganti, and J. G. Andrews, "Load-aware modeling and analysis of heterogeneous cellular networks," *IEEE Trans. Wireless Commun.*, vol. 12, no. 4, pp. 1666 – 1677, Apr. 2013.

[58] S. Singh, H. S. Dhillon, and J. G. Andrews, "Offloading in heterogeneous networks: Modeling, analysis and design insights," *IEEE Trans. Wireless Commun.*, vol. 12, no. 5, pp. 2484 – 2497, May 2013.

[59] Q. Ye, B. Rong, Y. Chen, M. Al-Shalash, C. Caramanis, and J. G. Andrews, "User association for load balancing in heterogeneous cellular networks," *IEEE Trans. Wireless Commun.*, vol. 12, pp. 2706–2716, June 2013.

[60] D. B. Taylor, H. S. Dhillon, T. D. Novlan, and J. G. Andrews, "Pairwise interaction processes for modeling cellular network topology," in *Proc., IEEE Globecom*, Anaheim, CA, Dec. 2012.

[61] B. Blaszczyszyn, M. K. Karray, and H.-P. Keeler, "Using Poisson processes to model lattice cellular networks," available online: arxiv.org/abs/1207.7208.

[62] H. S. Dhillon, R. K. Ganti, and J. G. Andrews, "Modeling non-uniform UE distributions in downlink cellular networks," *IEEE Wireless Commun. Lett.*, vol. 2, no. 3, pp. 339 – 342, Jun. 2013.

[63] D. Stoyan, W. S. Kendall, and J. Mecke, *Stochastic Geometry and Its Applications*, 2nd ed. Chichester: John Wiley and Sons, 1995.

[64] M. Shaked and J. G. Shanthikumar, *Stochastic Orders*. Springer, 2007.

[65] T. Bai, A. Alkhateeb, and R. W. Heath Jr, "Coverage and capacity of millimeter wave cellular networks," *IEEE Commun. Mag.*, vol. 52, no. 9, pp. 70–77, Sept. 2014.

[66] T. Bai, R. Vaze, and R. W. Heath, "Using random shape theory to model blockage in random cellular networks," in *Proc. SPCOM*, July 2012, pp. 1–5.

[67] R. Cowan, "Objects arranged randomly in space: an accessible theory," *Advances in Applied Probability*, vol. 21, pp. 543–569, Sep. 1989.

[68] P. Parker and R. Cowan, "Some properties of line segment processes," *Advances in Applied Probability*, vol. 13, pp. 96–107, Mar. 1976.

[69] A. Penrrinen and D. Stoyan, "Statistical analysis for a class of line segment processes," *Scandinavian Journal of Statistics*, vol. 16, pp. 153–168, 1989.

[70] Z. Genc, U. H. Rizvi, E. Onur, and I. Niemegeers, "Robust 60 GHz indoor connectivity: Is it possible with reflections?" in *in Proc. IEEE VTC.*, May 2010, pp. 1–5.

[71] X. An, C. S. Sum, R. V. Prasad, J. Wang, Z. Lan, J. Wang, R. Hekmat, H. Harada, and I. Niemegeers, "Beam switching support to resolve link-blockage problem in 60 GHz WPANs," in *in Proc. IEEE PIMRC*, Sept. 2009, pp. 390–394.

[72] S. Singh, F. Ziliotto, U. Madhow, E. M. Belding, and M. Rodwell, "Blockage and directivity in 60 GHz wireless personal area networks: From cross-layer

model to multi hop MAC design," *IEEE J. Sel. Areas Commun.*, vol. 27, no. 8, pp. 1400–1413, Oct. 2009.

[73] Y. Niu, Y. Li, D. Jin, L. Su, and D. Wu, "Blockage robust and efficient scheduling for directional mmWave WPANs," *IEEE Trans. Veh. Technol.*, vol. 64, no. 2, pp. 728–742, Feb. 2015.

[74] P. Shankar, "Analysis of microdiversity and dual channel macrodiversity in shadowed fading channels using a compound fading model," *AEU Int J. Electron Commun.*, vol. 62, no. 6, pp. 445–449, 2008.

[75] S. Mukherjee and D. Avidor, "Effect of microdiversity and correlated macrodiversity on outages in a cellular system," *IEEE Trans Wireless Technol.*, vol. 2, no. 1, pp. 50–59, 2003.

[76] N. Lee, D. Morales-Jimenez, A. Lozano, and R. W. Heath, "Spectral efficiency of dynamic coordinated beamforming: A stochastic geometry approach," *IEEE Trans. Wireless Commun.*, vol. 14, no. 1, pp. 230–241, Jan 2015.

[77] I. Hwang, C. B. Chae, J. Lee, and J. R. W. Heath, "Multicell cooperative systems with multiple receive antennas," *IEEE Wireless Commun.*, vol. 20, no. 1, pp. 50–58, Feb. 2013.

[78] K. Venugopal, M. C. Valenti, and R. W. Heath, "Analysis of millimeter wave networked wearables in crowded environments," in *Proc. ASILOMAR*, Nov. 2015, pp. 872–876.

[79] W. Roh, J.-Y. Seol, J. Park, B. Lee, J. Lee, Y. Kim, J. Cho, K. Cheun, and F. Aryanfar, "Millimeter-wave beamforming as an enabling technology for 5G cellular communications: Theoretical feasibility and prototype results," *IEEE Commun. Mag.*, vol. 52, no. 2, pp. 106–113, Feb. 2014.

[80] M. Akdeniz, Y. Liu, M. Samimi, S. Sun, S. Rangan, T. Rappaport, and E. Erkip, "Millimeter wave channel modeling and cellular capacity evaluation," *IEEE J. Sel. Areas Commun.*, vol. 32, no. 6, pp. 1164–1179, June 2014.

[81] S. Larew, T. Thomas, M. Cudak, and A. Ghosh, "Air interface design and ray tracing study for 5G millimeter wave communications," in *Proc. IEEE GLOBECOM Workshops*, Dec. 2013, pp. 117–122.

[82] M. Abouelseoud and G. Charlton, "System level performance of millimeter-wave access link for outdoor coverage," in *Proc. IEEE WCNC*, April 2013, pp. 4146–4151.

[83] A. K. Gupta, J. G. Andrews, and R. W. Heath Jr, "On the feasibility of sharing spectrum licenses in mmWave cellular systems," *IEEE Trans. Commun.*, vol. 64, no. 9, pp. 3981–3995, Sept. 2016.

[84] ——, "Can operators simply share millimeter wave spectrum licenses?" in *Proc. ITA*, San Diego, CA, Feb. 2016.

[85] FCC, "Spectrum policy task force," *ET Docket 02-135*, Nov. 2002.

[86] S. Haykin, "Cognitive radio: Brain-empowered wireless communications," *IEEE J. Sel. Areas Commun.*, vol. 23, no. 2, pp. 201–220, Feb. 2005.

[87] X. Kang, Y.-C. Liang, H. Garg, and L. Zhang, "Sensing-based spectrum sharing in cognitive radio networks," *IEEE Trans. Veh. Technol.*, vol. 58, no. 8, pp. 4649–4654, Oct. 2009.

[88] C. Stevenson, G. Chouinard, Z. Lei, W. Hu, S. Shellhammer, and W. Caldwell, "IEEE 802.22: The first cognitive radio wireless regional area network standard," *IEEE Commun. Mag.*, vol. 47, no. 1, pp. 130–138, Jan. 2009.

[89] I. F. Akyildiz, W.-Y. Lee, M. C. Vuran, and S. Mohanty, "NeXt generation/dynamic spectrum access/cognitive radio wireless networks: A survey," *Computer Networks*, pp. 2127–2159, 2006.

[90] S. Stotas and A. Nallanathan, "Enhancing the capacity of spectrum sharing cognitive radio networks," *IEEE Trans. Veh. Technol.*, vol. 60, no. 8, pp. 3768–3779, Oct 2011.

[91] H. Kamal, M. Coupechoux, and P. Godlewski, "Inter-operator spectrum sharing for cellular networks using game theory," in *Proc. IEEE PIMRC*, Sept. 2009, pp. 425–429.

[92] X. Lin, J. Andrews, and A. Ghosh, "Spectrum sharing for device-to-device communication in cellular networks," *IEEE Trans. Wireless Commun.*, vol. 13, no. 12, pp. 6727–6740, Dec 2014.

[93] A. Alsohaily and E. Sousa, "Performance gains of spectrum sharing in multi-operator LTE-Advanced systems," in *Proc. IEEE VTC Fall*, Sept. 2013, pp. 1–5.

[94] E. Dahlman, S. Parkvall, and J. Skold, *4G: LTE/LTE-Advanced for mobile broadband*. Elsevier Science, 2013.

[95] "ECC report 205, Licensed shared access," Feb. 2014.

[96] M. Mueck, I. Karls, R. Arefi, T. Haustein, and W. Keusgen, "Licensed shared access for mmWave cellular broadband communications," in *Proc. International Workshop on Cognitive Cellular Systems (CCS)*, Sept. 2014, pp. 1–5.

[97] M. Matinmikko, M. Palola, H. Saarnisaari, M. Heikkila, J. Prokkola, T. Kippola, T. Hanninen, M. Jokinen, and S. Yrjola, "Cognitive radio trial environment: First live authorized shared access-based spectrum sharing demonstration," *IEEE Veh. Technol. Mag.*, vol. 8, no. 3, pp. 30–37, Sept. 2013.

[98] J. Khun-Jush, P. Bender, B. Deschamps, and M. Gundlach, "Licensed shared access as complementary approach to meet spectrum demands: Benefits for next generation cellular systems," in *Proc. ETSI Workshop Reconfigurable Radio Syst.*, Cannes, France, Dec 2013, pp. 1–7.

[99] H. Elsawy and E. Hossain, "On cognitive small cells in two-tier heterogeneous networks," in *Proc. WiOpt*, May 2013, pp. 75–82.

[100] H. Elsawy, E. Hossain, and D. I. Kim, "Hetnets with cognitive small cells: user offloading and distributed channel access techniques," *IEEE Commun. Mag.*, vol. 51, no. 6, pp. 28–36, June 2013.

[101] "Federal communications commission- notice of inquiry: FCC 14-154," Oct. 2014.

[102] S. Akoum, O. El Ayach, and R. Heath, "Coverage and capacity in mmWave cellular systems," in *Proc. ASILOMAR*, Nov. 2012, pp. 688–692.

[103] T. Bai and R. Heath, "Coverage analysis for millimeter wave cellular networks with blockage effects," in *Proc. GlobalSIP*, Dec 2013, pp. 727–730.

[104] M. Kulkarni, S. Singh, and J. Andrews, "Coverage and rate trends in dense urban mmWave cellular networks," in *Proc. IEEE GLOBECOM*, Dec. 2014.

[105] M. Di Renzo, "Stochastic geometry modeling and analysis of multi-tier millimeter wave cellular networks," *IEEE Trans. Wireless Commun.*, vol. 14, no. 9, pp. 5038–5057, Sept. 2015.

[106] J. Lee, J. Andrews, and D. Hong, "Spectrum-sharing transmission capacity," *IEEE Trans. Wireless Commun.*, vol. 10, no. 9, pp. 3053–3063, Sept. 2011.

[107] T. V. Nguyen and F. Baccelli, "A probabilistic model of carrier sensing based cognitive radio," in *Proc. IEEE Symposium on New Frontiers in Dynamic Spectrum*, April 2010, pp. 1–12.

[108] J. Kibilda, P. D. Francesco, F. Malandrino, and L. A. DaSilva, "Infrastructure and spectrum sharing tradeoffs in mobile networks," in *Proc. IEEE DySPAN*, Stockholm, Sweden, Sept. 2015.

[109] A. Guo and M. Haenggi, "Asymptotic deployment gain: A simple approach to characterize the SINR distribution in general cellular networks," *IEEE Trans. Commun.*, vol. 63, pp. 962–976, Mar. 2015.

[110] R. K. Ganti and M. Haenggi, "Asymptotics and approximation of the SIR distribution in general cellular networks," [Online]. Available: http://arxiv.org/pdf/1505.02310v1.pdf.

[111] J. Kibilda, B. Galkin, and L. A. DaSilva, "Modelling multi-operator base station deployment patterns in cellular networks," *IEEE Trans. Mobile Computing*, 2016.

[112] T. Bai and R. Heath, "Asymptotic SINR for millimeter wave massive MIMO cellular networks," in *Proc. IEEE International Workshop on SPAWC*, June 2015, pp. 620–624.

[113] E. Larsson, O. Edfors, F. Tufvesson, and T. Marzetta, "Massive MIMO for next generation wireless systems," *IEEE Commun. Mag.*, vol. 52, no. 2, pp. 186–195, Feb. 2014.

[114] A. K. Gupta, A. Alkhateeb, J. G. Andrews, and R. W. Heath, "Gains of restricted secondary licensing in millimeter wave cellular systems," *IEEE J. Sel. Areas in Commun.*, vol. 34, no. 11, pp. 2935–2950, Nov. 2016.

[115] ——, "Restricted secondary licensing for mmwave cellular: How much gain can be obtained?" in *Proc. IEEE GLOBECOM*, Dec. 2016.

[116] M. Khoshkholgh, K. Navaie, and H. Yanikomeroglu, "Outage performance of the primary service in spectrum sharing networks," *IEEE Trans. Mobile Computing*, vol. 12, no. 10, pp. 1955–1971, Oct. 2013.

[117] T. V. Nguyen and F. Baccelli, "A stochastic geometry model for cognitive radio networks," *The Computer Journal*, vol. 55, no. 5, pp. 534–552, 2012.

[118] J. Bae, E. Beigman, R. Berry, M. L. Honig, H. Shen, R. Vohra, and H. Zhou, "Spectrum markets for wireless services," in *Proc. IEEE DySPAN*, Oct 2008, pp. 1–10.

[119] A. M. Hunter, J. G. Andrews, and S. Weber, "Transmission capacity of ad hoc networks with spatial diversity," *IEEE Trans. Wireless Commun.*, vol. 7, no. 12, pp. 5058–5071, December 2008.

[120] J. G. Andrews, A. K. Gupta, and H. S. Dhillon, "A primer on cellular network analysis using stochastic geometry," *arXiv preprint arXiv:1604.03183*, 2016.

[121] H. L. Van Trees, "Optimum array processing (detection, estimation, and modulation theory, part iv)," *Wiley-Interscience, Mar*, no. 50, p. 100, 2002.

[122] A. Adhikary, H. S. Dhillon, and G. Caire, "Massive-MIMO meets HetNet: Interference coordination through spatial blanking," *IEEE J. Sel. Areas Commun.*, vol. 33, no. 6, pp. 1171–1186, June 2015.

[123] Y. Xu and S. Mao, "User association in massive MIMO HetNets," *IEEE Systems Journal*, vol. PP, no. 99, pp. 1–1, 2015.

[124] C. Li, J. Zhang, J. G. Andrews, and K. B. Letaief, "Success probability and area spectral efficiency in multiuser MIMO HetNets," *IEEE Trans. Commun.*, vol. 64, no. 4, pp. 1544–1556, April 2016.

[125] M. Rebato, M. Mezzavilla, S. Rangan, and M. Zorzi, "Resource sharing in 5G mmWave cellular networks," *arXiv preprint arXiv:1603.02651*, Mar. 2016.

[126] F. Fund, S. Shahsavari, S. S. Panwar, E. Erkip, and S. Rangan, "Spectrum and infrastructure sharing in millimeter wave cellular networks: An economic perspective," *arXiv preprint arXiv:1605.04602*, 2016.

[127] J. Kibilda, N. J. Kaminski, and L. A. DaSilva, "Radio access network and spectrum sharing in mobile networks: A stochastic geometry perspective," *arXiv preprint arXiv:1604.06588*, 2016.

[128] M. N. Kulkarni, A. Ghosh, and J. G. Andrews, "A comparison of MIMO techniques in downlink millimeter wave cellular networks with hybrid beamforming," *IEEE Trans. Commun.*, vol. 64, no. 5, pp. 1952–1967, May 2016.

[129] H. T. Nguyen, I. Z. Kovacs, Y. Wang, and K. I. Pedersen, "Downlink performance of a multi-carrier MIMO system in a bursty traffic cellular network," in *Proc. IEEE ICC*, June 2011, pp. 1–6.

[130] M. K. Karray and M. Jovanovic, "A queueing theoretic approach to the dimensioning of wireless cellular networks serving variable-bit-rate calls," *IEEE Trans. Vehi. Technol.*, vol. 62, no. 6, pp. 2713–2723, July 2013.

[131] B. Blaszczyszyn, M. Jovanovic, and M. K. Karray, "How user throughput depends on the traffic demand in large cellular networks," in *Proc. WiOpt/SpaSWiN*, 2014.

[132] N. Economides and C. P. Himmelberg, "Critical mass and network size with application to the US fax market," *NYU Stern School of Business EC-95-11*, 1995.

Vita

Abhishek K. Gupta received the B.Tech. and M.Tech. degrees in Electrical Engineering from IIT Kanpur, India, in 2010. He is currently a Ph.D. candidate in Electrical and Computer Engineering at The University of Texas at Austin, where his research has focused on 5G cellular networks, stochastic geometry and its applications in wireless communication. His other research interests include multiuser MIMO systems and optimization. He was recipient of GE-FS Leadership Award by General Electric (GE) Foundation and Institute of International Education in 2009. He has held summer internships at Nokia Networks, IL, Huawei Technologies, NJ, and Cranfield University, UK. He is author of the books *MATLAB by Examples* (Finch, 2010) and *Numerical methods using MATLAB* (Springer, 2014).

Permanent email: *g.kr.abhishek@utexas.edu*

This dissertation was typeset with LaTeX[†] by the author.

[†]LaTeX is a document preparation system developed by Leslie Lamport as a special version of Donald Knuth's TeX Program.